Analysis of Laser Shock Peening on Aluminium Alloy 7075 with Different Types of Sacrificial Coatings

Mayurkumar Mistry

Student number: 359124
Supervisor: Prof. Claudia Polese







science & innovation
Department:
Science and Innovation
REPUBLIC OF SOUTH AFRICA

A dissertation submitted to the Faculty of Engineering and the Built Environment, University of the Witwatersrand, Johannesburg, in fulfilment of the requirements for the degree of Master of Science in Engineering.

Johannesburg, November 2020

University of the Witwatersrand, Johannesburg
School of Mechanical, Industrial & Aeronautical Engineering

DECLARATION

I, the undersigned, am registered for the course **MSc (Mechanical Engineering)** in the year 2020. I herewith submit the following task "**Analysis of Laser Shock Peening on Aluminium Alloy 7075 with Different Types of Sacrificial Coatings**" in partial fulfilment of the requirements of the above course.

I hereby declare the following:

- I am aware that plagiarism (the use of someone else's work without their permission and / or without acknowledging the original source) is wrong;
- I confirm that the work submitted herewith for assessment in the above course is my own unaided work except where I have explicitly stated otherwise;
- This task has not been submitted before. either individually or jointly, for any course requirement, examination or degree at this or any other tertiary educational institution;
- I have followed the required conventions in referencing the thoughts and ideas of others;
- I understand that the University of the Witwatersrand may take disciplinary action against me if it can be shown that this task is not my own unaided work or that I my failed to acknowledge the sources of the ideas or words in my writing in this task.

Signed this 24th day of November 2020



Mayurkumar Mistry 359124

Acknowledgements

I would like to thank the following individuals for their support throughout the duration of this research project:

- Prof. Claudia Polese of the University of the Witwatersrand, my supervisor for her patience, availability, wisdom and guidance throughout the duration of this project.
- Dr Daniel Glaser of the CSIR for his guidance and assistance with the set up and use of the laser peening system and with the L-XRD Machine.
- Prof. Joao Nobre of the University of the Witwatersrand for his guidance with incremental hole drilling.
- Mrs Marina Labuschagne of the Centre of Excellence in Strong Materials, for her assistance with regards to procuring essential research consumables and equipment.
- Mrs Jacqui Jacobs of the Centre of Excellence in Strong Materials, for her dedication and assistance.
- Mr Shaun Riekert and workshop staff of the University of the Witwatersrand, Northwest engineering building for their assistance with this project.
- Mr N. Brayner Nelwalani and Mrs Petra Dinham of the University of the Witwatersrand for their assistance with the the Scanning Electron Microscope.
- Mr Rodney Genga of the University of the Witwatersrand for his assistance with the surface roughness testing.
- Mr Pieter le Roux of the University of Johannesburg for his assistance in operating the surface roughness testing machine.
- Mr Constantin Schulte-Brader, Mr Laveshan Nayager, Mr Nicholas Stiekema and Mr Tristan Strydom, my colleagues at the University of the Witwatersrand, for their support, help and assistance throughout this project.
- Mr Kgothatso Monnanyana, Mr Ndamulelo J. Mudau, Mr Titus T. Ndlovu, Honour's level students at the University of the Witwatersrand, who assisted with this project.

- My friends and family for their support throughout the project.

I would like to acknowledge the following institutions for their generous financial support:

- The DSI-NRF Centre of Excellence in Strong Materials (CoE-SM).
- The South African Centre for Scientific and Industrial Research National Laser Centre (CSIR NLC) Rental Pool Program (RPP), funded by the Department of Science and Innovation (DSI).

The opinions, findings and conclusions or recommendations expressed in this work are those of the author and are not necessarily to be attributed to the CoE-SM or to the NRF.

Abstract

This research project was aimed at the advancement of the Laser Shock Peening (LSP) process, by using 11 different ablative/sacrificial media (mainly adhesive tapes) on 7075-T651 aluminium alloy for the aeronautical industry. The LSP process is a surface enhancement treatment that induces compressive residual stresses into the material. The research carried out in this document focuses on studying the effect that the different ablative tapes have on the surface integrity and the residual stress profile of the treated samples by using four different laser power intensities. The surface integrity of the treated samples was investigated using optical microscopy, scanning electron microscopy (SEM) and by using two types of surface roughness testing. While the compressive residual stresses were mainly evaluated using Incremental Hole Drilling (IHD) and then by Laboratory X-Ray Diffraction (L-XRD) for comparative purposes for near surface residual stresses. The results obtained were favourable, the sacrificial tapes each provided unique results, but the samples coated using the tape backed with the vinyl material showed the highest compatibly with the LSP process. It was found that, not only does the ablative layer influence the LSP results, but the thickness of the ablative material itself changes the outcome of LSP. An additional study was conducted by changing the laser coverage density using the vinyl backed tape while keeping the other laser parameters constant. The results from both studies showed a clear trend in the surface characteristics of the peened sample and the induced residual stress depth profiles, the results also compared well to the finding outlined in literature. Some experiments were restricted due to the availability of apparatus, equipment, labour and cost. Therefore, additional samples and tests are recommended for any future projects. The work conducted from this study will contribute to the LSP database for various alloys that can be used for industrial engineering processes and for the development of Finite Element tools for LSP.

Contents

Declaration i

Acknowledgements ii

Abstract iv

Contents v

List of Figures xi

List of Tables xx

List of Symbols xxi

List of Acronyms xxii

1 Introduction 1

1.1 Background and Motivation 2

2 Literature Survey 5

2.1 The Laser Shock Peening Process 5

2.1.1 The Laser Shock Peening Process Parameters 6

2.1.1.1 The Laser System Parameters 7

2.1.1.2 The Control System Parameters 7
2.1.1.3 The Interaction Parameters 8
2.1.2 Laser Shock Peening Systems 9
2.1.2.1 Laser Systems 9
2.1.2.2 Laser Beam Delivery 10
2.1.2.3 Confinement Media 11
2.1.2.4 LSP with and without an Ablative Coating 12
2.2 The Effect of Laser Shock Peening on Material Properties 13
2.2.1 The Effect of Using an Ablative Coating for LSP 13
2.2.2 The Effect of LSP on Surface Integrity 15
2.2.2.1 Effect of LSP on Surface Roughness 18
2.2.3 The Effect of LSP on Microstructure 20
2.2.4 The Effect of LSP on Microhardness 22
2.2.5 The Effect of LSP on Fatigue Behaviour 24
2.2.6 The Effect of LSP on Residual Stress 27
2.2.7 The Effect of Varying LSP Parameters on the Residual Stress 28
2.2.7.1 Effect of Changing Laser Power Intensity 28
2.2.7.2 Effect of Changing Laser Spot Size 30
2.2.7.3 Effect of Changing the Coverage Ratio 31
2.2.7.4 Summary 32
2.3 Measurement Techniques 33
2.3.1 Surface and Microscopic Analysis 33
2.3.2 Surface Roughness Testing 33

2.3.3 Microhardness Testing . . . 34
2.3.4 Residual Stress . . . 35
2.3.4.1 The Incremental Hole Drilling Method . . . 37
2.3.4.2 X-Ray Diffraction . . . 38
2.4 Material Specifications . . . 39
2.4.1 Aluminium Alloys . . . 39
2.4.1.1 7075-T651 Aluminium Alloy . . . 39

3 Research Objectives **40**

4 Experimental Activity **43**

4.1 Experimental Methodology . . . 45
4.1.1 Sample Preparation . . . 46
4.1.2 Cutting Apparatus . . . 47
4.1.3 Ablative Coatings: Adhesive Tapes . . . 47
4.2 Laser Shock Peening . . . 48
4.2.1 LSP Apparatus and Equipment . . . 48
4.2.2 LSP Experimental Set-up . . . 49
4.2.3 Experiment Procedure . . . 50
4.2.4 Naming Convention for Samples . . . 51
4.3 Microscopic Surface Analysis . . . 53
4.3.1 Procedure . . . 54
4.3.1.1 Precautions . . . 54
4.4 Surface Roughness Testing . . . 55
4.4.1 Surface Roughness Testing Using Portable SRT-6210 Unit . . . 55

4.4.2 Procedure . . . 55
4.4.2.1 Precautions . . . 56
4.4.3 Surface Roughness Testing Using Stationary HOMMEL-ETAMIC T8000 Unit . . . 56
4.4.4 Procedure . . . 57
4.4.4.1 Precautions . . . 58
4.5 Scanning Electron Microscopy . . . 58
4.5.1 Procedure . . . 59
4.5.1.1 Precautions . . . 59
4.6 Microhardness Testing . . . 60
4.6.1 Procedure . . . 61
4.6.1.1 Precautions . . . 61
4.7 Incremental Hole Drilling Testing . . . 62
4.7.1 Procedure . . . 64
4.7.1.1 Precautions . . . 65
4.8 LXRD Testing . . . 66

5 Phase I - Surface Analysis **67**

5.1 Unpeened Base Sample . . . 67
5.2 No Tape (LSPwC) . . . 68
5.3 Aluminium Foil Tape (1436 3M) . . . 72
5.4 Clear Box Sealing Tape (313 Scotch 3M) . . . 77
5.5 Duct Tape (1900 3M) . . . 81
5.6 Vinyl Tape (471 3M) . . . 85
5.7 Flame-Retardant Tape with Polyester Film (1350-1 3M) . . . 90

5.8 Duct Cloth Fibre Tape (2903 3M) . . . 94
5.9 Vinyl Tape (Super 88 Scotch 3M) . . . 97
5.10 PVC Insulation Tape (21 Nitto) . . . 102
5.11 Micron Copper Foil Shielding Tape (AT525 35) . . . 106
5.12 Vinyl Tape (472 3M) . . . 111
5.13 Polymide Tape (HB830 Hi-Bond) . . . 116
5.14 SEM Results . . . 120
5.15 Microhardness . . . 123
5.16 Concluding Remarks . . . 126
5.17 Conclusions . . . 127
5.18 Recommendations . . . 128

6 Phase I - Residual Stress Analysis **129**

6.1 Incremental Hole Drilling Results . . . 129
6.2 Laboratory XRD . . . 135
6.3 Concluding Remarks . . . 136
6.4 Conclusions . . . 137
6.5 Recommendations . . . 138

7 Phase II Analysis **139**

7.1 Surface Observations and Results . . . 140
7.2 No Tape(LSPwC) Samples . . . 140
7.3 Vinyl 471 Tape Samples . . . 143
7.4 Concluding Remarks . . . 149
7.5 Conclusions . . . 149

7.6 Recommendations 150

8 Concluding Remarks **151**

9 Contribution to Community **155**

A Supplementary Experimental Details **160**

A.1 Sample Preparation 161

A.1.1 Cutting Procedure of Test Pieces 161

A.1.1.1 Precautions 161

A.2 Grinding and Polishing 164

A.2.1 Apparatus and Instrumentation 164

A.2.2 Grinding Procedure 165

A.2.2.1 Precautions 166

A.2.3 Polishing Procedure 166

A.2.3.1 Precautions 167

B Results and Data **169**

C Material Details **173**

List of Figures

2.1 Schematic of Traditional Laser Shock Peening[1]. 5

2.2 Raster Peening Pattern[5]. 8

2.3 Mirror and Fibre Delivery Systems[8]. 10

2.4 CNC Stage. 10

2.5 Various Confinement Modes. 11

2.6 Plasma and Cavitation Bubble Formation[9]. 12

2.7 Shock Wave Signal[1]. 12

2.8 RS Profile for Two Ablative Coatings[4]. 14

2.9 Aluminium Foil Surface and its Thickness Post LSP[11]. 15

2.10 Pits and Notches Defects on Peened Surface[11]. 16

2.11 Surface Defects on Aluminium Foil[11]. 16

2.12 Topography Profile of AISI 4140 Peened with 50% Coverage[12]. 17

2.13 6061-T6 Al sample Processed with and without an Ablative Coating[13]. . . . 17

2.14 Roughness and Waviness Profile[15]. 18

2.15 Arithmetical Mean Roughness Parameter Ra[16]. 19

2.16 Average Peak-to-Valley Roughness Parameter Rz[16]. 19

2.17 Optical Microscope Image of LSP Al 6061-T6[17]. 20

2.18 SEM Image of an Al 7075 Cross Section Surface[18]. 20

2.19 SEM and Optical Microscopy Images of LSP Titanium[19]. 21

2.20 Microhardness of Al 5083 Sample Before and After LSP Treatment[20]. 22

2.21 Surface Hardness of Al 5083[20]. 23

2.22 Cross-sectional Micro-hardness Profiles of Al 6061-T6[21]. 23

2.23 LSP - Cyclic Deformation Fatigue Behaviour of AISI 304[22]. 24

2.24 Crack Lengths as a Function of Fatigue for the Laser-Peened and Unpeened 2024-T3 Al[23]. 25

2.25 Comparison of Bending Fatigue of Untreated, Shot Peened and LSP Al 7075-T7351[24]. 25

2.26 Crack Length vs Load Cycles for Unpeened and LSP Specimens[25]. 26

2.27 RS Profiles for 2034 Al[1]. 27

2.28 RS Profiles for 7075 Al[1]. 27

2.29 RS Profile induced by LSP and SP[1]. 27

2.30 Residual Stresses in A356 Alloy Peened with Different Power Intensities[26]. . 28

2.31 Residual Stresses in 7049 T73 Al Peened with Different Power Intensities[27]. . 29

2.32 Peak Plasma Pressures as a Function of Laser Power Density[1]. 29

2.33 Effect of Changing Spot Size at Different Coverage Ratios[6]. 30

2.34 Effect of Changing Spot Size on Residual Stress[28]. 30

2.35 Effect of Changing Coverage Ratios with Different Spot Sizes[6]. 31

2.36 Effect of Changing Coverage Ratios[29]. 31

2.37 Roughness Testing Method. 33

2.38 Hardness Testing Method. 34

2.39 Depth Range for various Measurement Techniques[31]. 36

2.40 IHD Testing. 37

2.41 Strain Gauge. 37

2.42 Bragg's Law of Diffraction[33]. 38

4.1 Flow Chart for Experimental Activity. 44

4.2 Sample 60 *mm* x 60 *mm*. 46

4.3 Sample 40 *mm* x 40 *mm*. 46

4.4 LSP System at the NLC CSIR. 48

4.5 LSP Schematic. 48

4.6 LSP Schematic. 49

4.7 LSP Schematic and Naming Convention. 51

4.8 Nikon Zoom Stereo Microscope (Nikon SMZ1500). 53

4.9 SRT-6210 Surface Roughness Tester. 55

4.10 HOMMEL-ETAMIC T8000 R120-400 Surface Roughness Tester. 57

4.11 Zeiss Sigma SEM System. 58

4.12 INNOVATEST Falcon 500 Hardness Testing Machine. 60

4.13 IHD System Configuration. 62

4.14 Apparatus used to Apply Strain Gauge. 63

4.15 Strain Gauge. 63

4.16 Strain Gauge Properties. 63

4.17 Proto iXRD Machine and Apparatus. 66

5.1 Microscopic Image and 3-D Roughness Map and Data for Unpeened Sample. . 67

5.2 Surface Images for Sample: N1-No-Tape-P1.5. 68

5.3 Surface Images for Sample: N2-No-Tape-P2. 68

5.4 Surface Images for Sample: N3-No-Tape-P3. 68

5.5 Surface Images for Sample: N4-No-Tape-P4. 69

5.6 Surface Roughness Results for the LSPwC samples. 69

5.7 3-D Surface Map for Samples: M1-No-Tape-P1.5 and M1-No-Tape-P2. 70

5.8 3-D Surface Map for Samples: M3-No-Tape-P3 and M4-No-Tape-P4. 71

5.9 Surface Images for Sample: A1-AL-Foil-P1.5. 72

5.10 Surface Images for Sample: A2-AL-Foil-P2. 72

5.11 Surface Images for Sample: A3-AL-Foil-P3. 73

5.12 Surface Images for Sample: A4-AL-Foil-P4. 73

5.13 Surface Roughness Results for Aluminium Foil Tape Samples. 75

5.14 3-D Surface Map for Samples: A3-AL-Foil-P3 and A4-AL-Foil-P4. 76

5.15 Surface Images for Sample: C1-Clear-P1.5. 77

5.16 Surface images for Sample: C2-Clear-P2. 77

5.17 Surface images for Sample: C3-Clear-P3. 78

5.18 Surface images for Sample: C4-Clear-P4. 78

5.19 Surface Roughness Results for Clear Box Sealing Tape Samples. 80

5.20 Surface Images for Sample: D1-Duct-P1.5. 81

5.21 Surface Images for Sample: D2-Duct-P2. 81

5.22 Surface Images for Sample: D3-Duct-P3. 82

5.23 Surface Images for Sample: D4-Duct-P4. 82

5.24 Surface Roughness Results for Duct Tape Samples. 84

5.25 Surface Images for Sample: E1-Vinyl471-P1.5. 85

5.26 Surface Images for Sample: E2-Vinyl471-P2. 85

5.27 Surface Images for Sample: E3-Vinyl471-P3. 86

5.28 Surface Images for Sample: E4-Vinyl471-P4. 86

5.29 Surface Roughness Results for Vinyl Tape 471 Samples. 88

5.30 3-D Surface Map for Samples: E1-Vinyl471-P1.5 and E2-Vinyl471-P2. 89

5.31 3-D Surface Map for Samples: E3-Vinyl471-P3 and E4-Vinyl471-P4. 89

5.32 Surface Images for Sample: F1-Polyster-P1.5. 90

5.33 Surface Images for Sample: F2-Polyster-P2. 90

5.34 Surface Images for Sample: F3-Polyster-P3. 91

5.35 Surface Images for Sample: F4-Polyster-P4. 91

5.36 Surface Roughness Results for Polyester Tape Samples. 92

5.37 3-D Surface Roughness Results for Polyester Tape Samples. 93

5.38 Surface Images for Sample: G1-Fiber-P1.5. 94

5.39 Surface Images for Sample: G2-Fiber-P2. 94

5.40 Surface Images for Sample: G3-Fiber-P3. 95

5.41 Surface Images for Sample: G4-Fiber-P4. 95

5.42 Surface Roughness Results for the Cloth Fibre Tape Samples. 96

5.43 Surface Images for Sample: H1-Vinyl88-P1.5. 97

5.44 Surface Images for Sample: H2-Vinyl88-P2. 97

5.45 Surface Images for Sample: H3-Vinyl88-P3. 98

5.46 Surface Images for Sample: H4-Vinyl88-P4. 98

5.47 Surface Roughness Results for Vinyl 88 Tape Samples. 99

5.48 3-D Surface Map for Samples: H1-Vinyl88-P1.5 and H2-Vinyl88-P2. 101

5.49 3-D Surface Map for Samples: H3-Vinyl88-P3 and H4-Vinyl88-P4. 101

5.50 Surface Images for Sample: I1-PVC-P1.5. 102

5.51 Surface Images for Sample: I2-PVC-P2. 102

5.52 Surface Images for Sample: I3-PVC-P3. 103

5.53 Surface Images for Sample: I4-PVC-P4. 103

5.54 Surface Roughness Results for the PVC Tape Samples. 104

5.55 3-D Surface Map for the PVC Samples. 105

5.56 Surface Images for Sample: J1-Cu-P1.5. 106

5.57 Surface Images for Sample: J2-Cu-P2. 106

5.58 Surface Images for Sample: J3-Cu-P3. 107

5.59 Surface Images for Sample: J4-Cu-P4. 107

5.60 Surface Roughness Results for the Copper Tape Samples. 109

5.61 3-D Surface Map for Samples: J1-Cu-P1.5 and J2-Cu-P2. 110

5.62 3-D Surface Map for Samples: J3-Cu-P3 and J4-Cu-P4. 110

5.63 Surface Images for Sample: K1-Vinyl472-P1. 111

5.64 Surface Images for Sample: K2-Vinyl472-P2. 111

5.65 Surface Images for Sample: K3-Vinyl472-P3. 112

5.66 Surface Images for Sample: K4-Vinyl472-P4. 112

5.67 Surface Roughness Results for the Vinyl Tape 472 Samples. 114

5.68 3-D Surface Map for Samples: K3-Vinyl472-P3 and K4-Vinyl472-P4. 115

5.69 Surface Images for Sample: L1-Polymide-P1. 116

5.70 Surface Images for Sample: L2-Polymide-P2. 116

5.71 Surface Images for Sample: L3-Polymide-P3. 117

5.72 Surface Images for Sample: L4-Polymide-P4. 117

5.73 Surface Roughness Results for the Polymide Tape Samples. 118

5.74 3-D Surface Map for Samples: L3-Polymide-P3 and L4-Polymide-P4. 119

5.75 SEM Images. 120

5.76 SEM Images for Samples Peened using Metallic Ablative Tapes. 121

5.77 SEM Images for Samples Peened using Non-Metallic Ablative Tapes. 122

5.78 Microhardness Results for LSPwC Samples. 123

5.79 Microhardness Results for Vinyl 88 Samples. 124

5.80 Microhardness Results for Samples Peened using 3 GW/cm^2. 124

5.81 Microhardness Results for Vinyl Tape Samples. 125

6.1 Residual Stress vs Depth for Samples Peened with PI = 3 GW/cm^2. 130

6.2 Residual Stress vs Depth for Samples Peened with PI = 4 GW/cm^2. 132

6.3 Residual Stress vs Depth for Samples Peened with PI = 2 GW/cm^2. 133

6.4 Residual Stress vs Depth for Samples Peened using the Vinyl Coating. 134

6.5 Residual Stress vs Depth for Samples Peened using the Vinyl 471 at Different PI. 135

6.6 IHD and L-XRD Residual Stress vs Depth Results. 136

7.1 Unpeened Base Sample. 139

7.2 Surface Images for Sample: n1-No-Tape-30. 140

7.3 Surface Images for Sample: n2-No-Tape-40. 140

7.4 Surface Images for Sample: n3-No-Tape-50. 140

7.5 Surface Images for Sample: n4-No-Tape-60. 141

7.6 Surface Images for Sample: n5-No-Tape-70. 141

7.7 Surface Images for Sample: n6-No-Tape-80. 141

7.8 Surface Images for Sample: n7-No-Tape-90. 141

7.9 Surface Roughness Results for LSPwC Samples 142

7.10 Surface Images for Sample: a1-Vinyl471-30. 143

7.11 Surface Images for Sample: a2-Vinyl471-40. 143

7.12 Surface Images for Sample: a3-Vinyl471-50. 144

7.13 Surface Images for Sample: a4-Vinyl471-60. 144

7.14 Surface Images for Sample: a5-Vinyl471-70. 145

7.15 Surface Images for Sample: a6-Vinyl471-80. 145

7.16 Surface Images for Sample: a7-Vinyl471-90. 146

7.17 Surface Roughness Results for Vinyl 471 Tape Samples. 147

7.18 SEM results for Samples: a1-Vinyl471-30, a3-Vinyl471-50 and a5-Vinyl471-70. 148

7.19 Residual Stress vs Depth for Vinyl Tape Samples. 148

A.1 Startrite Band Saw. 160

A.2 Grinding and Polishing Table. 164

B.1 Microhardness Results for Aluminium Tape Samples. 169

B.2 Microhardness Results for Clear Box Sealing Tape Samples. 169

B.3 Microhardness Results for Copper Tape Samples. 170

B.4 Microhardness Results for Duct Tape Samples. 170

B.5 Microhardness Results for Duct Cloth Fibre Tape Samples. 170

B.6 Microhardness Results for Polyester Tape Samples. 171

B.7 Microhardness Results for Polymide Tape Samples. 171

B.8 Microhardness Results for PVC Tape Samples. 171

B.9 Microhardness Results for Vinyl 471 Tape Samples. 172

B.10 Microhardness Results for Vinyl 472 Tape Samples. 172

List of Tables

2.1 Laser Institutions and Laboratories. 10

2.2 Effects of LSP Parameters on Residual Stress. 32

2.3 Chemical Composition of 7075 Aluminium Alloy. 39

4.1 Material Properties for Aluminium Alloy 7075-T651. 46

4.2 Quanta-Ray Pro Laser Specifications. 49

4.3 Sample Naming Convention and LSP Parameters for Phase 1 of Experiment. 52

4.4 Sample Naming Convention and LSP Parameters for Phase 2 of Experiment. 53

4.5 Proto iXRD Specifications. 66

A.1 Startrite Band Saw: Machine Specifications. 160

A.2 Nikon Zoom SMZ1500 Stereo-microscope Specifications[37]. 162

A.3 SRT-6210 Roughness Tester Specifications[38]. 162

A.4 JENOPTIK waveline HOMMEL-ETAMIC T8000 Roughness Testing Machine[39].163

A.5 Grinding and Polishing Apparatus and Consumables. 167

A.6 IHD Apparatus and Consumables. 168

A.7 Falcon 500 Series Hardness Testing Machine[42]. 168

List of Symbols

θ - Diffraction Angle [^{o}].

ν - Poisson's Ratio.

λ - Wavelength [nm].

σ_x - Stress in x-direction [MPa].

σ_y - Stress in y-direction [MPa].

ϵ - Strain.

%Overlap - Percentage Overlap [%].

Cv - Coverage [spots].

d_s - Laser Spot Diameter [mm].

E - Beam Energy [J].

E - Young's Modulus [MPa].

I_0 - Power Intensity [GW/cm^2].

RS - Residual Stresses [MPa].

R_a - Surface Roughness Value [μm].

Ra_{mean} - Average Surface Roughness Value [μm].

R_z - The Linear Distance between the Top Peak and the Valley Base [μm].

R_p - Peak Surface Roughness Value [μm].

SS - Spot Size [mm].

List of Acronyms

BSD - Back Scatter Detector.

Cv - Coverage.

%Cv - Coverage Ratio.

CRS - Compressive Residual Stresses.

CSIR - Council for Scientific and Industrial Research.

IHD - Incremental Hole Drilling.

L-XRD - Laboratory X-Ray Diffraction.

LSP - Laser Shock Peening.

LSPwC - Laser Shock peening without coating.

NLC - National Laser Centre.

Np - Pulse Density.

PI or I_0 - Power Intensity $[GW/cm^2]$.

R - stress ratio

R_a - Surface Roughness Value$[\mu m]$.

SCC - Stress Corrosion Cracking.

SE2 - Secondary Detector.

SEM - Scanning Electron Microscope.

SS - Spot Size $[mm]$.

SP - Shot Peening.

XRD - X-Ray Diffraction.

1 Introduction

Due to an increasingly large trend to utilize specially engineered materials to operate in extreme environments for the numerous fields of engineering and manufacturing, several methods have since been developed and successfully applied. Likewise, improvements to a materials surface and resistance to extreme environments is an essential part for the engineering industry. The surfaces are often subjected to different treatment processes to achieve certain criteria or qualities that cannot be achieved from the primary manufacturing process[1],[2].

The enhancement process is conducted for various reasons which includes the performance of the material, altering material dimensions and improving properties such as the mechanical, metallurgical, corrosion resistance and fatigue resistance. A diverse range of surface enhancement technologies have been developed in the past few decades to vastly modify and improve surface characteristics[1].

Since the turn of the century, advances in laser technology and its use in material science has been greatly increased. Laser technology is now endorsed in many fields and processes such as; laser drilling, cutting, welding, polishing and shock peening[1],[2].

Laser Shock Peening or "LSP" is a surface enhancement technique that significantly modifies the properties of a metallic alloy and is useful in numerous engineering applications as it introduces beneficial residual stresses into an alloy[1][2]. In short, the LSP treatment converts tensile residual stresses into compressive residual stresses by irradiating laser pulses under an aqueous environment on to the surface of metallic alloys[1],[2].

The current research program aims to investigate the potential of using LSP to treat aluminium alloy 7075 with various types of sacrificial coatings with the goal of optimising the LSP parameters in order to achieve optimum performance. Therefore, the objectives are to use locally sourced materials (where possible) to treat the alloy with LSP and to analyse and characterise the surface integrity of the peened alloys, and also to measure the LSP induced residual stresses and finally, to optimise the LSP parameters for specific requirements.

The surface integrity of the samples will be analysed and studied using optical microscopy, surface roughness testing and microhardness testing. For this research programme it will be

vital to accurately measure the residual stresses near the surface of the material and through the depth of the material. These accurate measurements can only be achieved by using methods such as Incremental Hole Drilling (IHD) and laboratory X-Ray Diffraction (XRD). XRD is used for taking stress measurements near the surface of an alloy whereas IHD is used for taking stress measurements through the depth of the material. The only restriction of IHD is that there is a minimum sample thickness (as set by the ASTM standard) in which the stresses can be measured, therefore these restrictions will not allow for in depth measurements for samples thinner than what is stipulated in the standard. Therefore, the samples used for the research programme will have a higher thickness so that the IHD testing can be conducted according to the ASTM standard. Once the data for the various sample are collected, only then can the optimising process be performed.

1.1 Background and Motivation

The concept of using high energy based lasers to generate shock waves to induce compressive residual stresses in a material was first explored in the early 1960s[1],[2]. The LSP process has been studied intensively over the past few decades due to the various benefits provided by this surface enhancement treatment. LSP was initially developed and used extensively for the aerospace industry as a method to improve the performance against fatigue cracking of highly stressed metallic parts[1].

The research conducted using LSP generated multiple patents and journal articles over the last two decades and due to the overall benefits provided by the LSP treatment a strong interest in the need for commercialisation was generated. LSP was seen as a direct replacement method for conventional surface enhancement methods such as shot peening (SP)[1]. Even though the conventional processes are cheaper and readily available, the benefits and advantages provided by the LSP process are far greater. LSP produces a significantly higher depth penetration for the compressive residual stresses and a significantly higher increase in the fatigue life of material when compared to traditional surface enhancement methods[1],[2].

The one disadvantage of LSP is that it requires the use of high density lasers which are highly expensive and large in size and thus LSP can only be performed in a closed controlled environment. LSP is a relatively quick process, the preparation time for the material is however large using traditional LSP, generally the surface of the material is prepared with a type of absorbent/sacrificial layer to protect the surface of the material prior to laser irradiation[1],[3]. However, depending on the laser system, the laser parameters used and the type of ablative layer used the efficiency of the process can be increased.

There two main types of LSP methods used, namely laser shock peening without coating (LSPwC) and laser shock peening with coating (traditional LSP)[3]. The two different processes that are available for use are described in detail below:

- Traditional LSP makes use of an ablative layer that prevents the surface of the material against damage and surface melting. This process traditionally makes use of a Nd:glass type laser that operates at a higher laser density and a high pulse duration[1].

  The type of coating that is traditionally applied to the surface of the alloy prior to laser irradiation is black paint or aluminium foil, the coating is generally removed after the LSP process[1],[3].

  The disadvantage of the traditional LSP process is that it is a very time costly process.

- LSPwC was first researched and implemented successfully in 1995 Japan as a maintenance method against stress corrosion cracking (SCC) in a nuclear power facility[3].

  The process does require an ablative layer and make use of a compact Nd:YAG type laser that operates at lower laser energies, higher coverage ratios, smaller spot sizes with much shorter pulse durations.

  The disadvantage of the method is that the surface integrity of the material changes significantly after laser irradiation[3].

The Nd:YAG laser system used for the LSP process is both compact and commercially available thus gives an opportunity to conduct LSP on site in harsh and remote environments. The advantage of using the Nd:YAG laser system is that it can be used to conduct both LSPwC and traditional LSP, therefore has the potential to be commercialised and replace existing methods. The operating cost involved in using the Nd:YAG laser is significantly lower than that of the Nd:glass laser system. The present paper outlines the process and research parameters for traditional LSP using the Nd:YAG laser system with adhesive tapes as the ablative medium.

LSP is still a relatively new and unknown surface enhancement technique in South Africa and thus significant research is still required for further development. In recent times there is significantly higher demand for products to meet high performance standards and operate in harsh environments, therefore continuous monitoring, checking and evaluating of the components is required for the manufacturing process and operating process. The quality control implemented in certain environments adhere to strict regulations, an important aspect in these regulations regards the measurement of surface features such as surface roughness and microhardness.

Surface roughness is difficult to evaluate during the manufacturing process and during the operating process due to the uncertainties involved. Surface roughness is both a desired and undesired material characteristic, in certain applications it is not desired and thus adds additional cost to the manufacturing process when the need for control is required. Thus as a result a trade-off occur between the manufacturing cost and the performance of the component.

The research of LSP and LSPwC has extensive applications in modern engineering. Thus this document primarily focuses on the surface integrity of the processed material and also studies the compressive residual stresses. The Al 7075 samples will be covered with 10 different types of ablative coatings (adhesive tapes, each unique with different backing materials and adhesive). The samples will be treated with 4 different types of laser power intensities on a 20 mm x 20 mm area using the same spot size and coverage ratio.

The overview objective of the research experiment is to select an ideal ablative coating to improve the LSP process parameters whilst allowing a robust and efficient process. The experiments were carried out at the University of Witwatersrand North West Engineering Barloworld Laboratory, the Council for Scientific and Industrial Research (South Africa's national research organisation), the University of Johannesburg and at other facilities of the University of Witwatersrand.

2 | Literature Survey

2.1 The Laser Shock Peening Process

Laser Shock Peening with and without coating (LSP or LSPwC) is a surface enhancement process that generates high compressive residual stresses in a material by using a high powered laser. After the LSP treatment the fatigue properties of the metallic alloy can be significantly increased due to the presence of the compressive residual stresses[1],[3],[4]. The generation of these compressive residual stresses (CRS) is achieved by firing a focused laser beam with certain characteristics and intensity onto the surface of the target material as illustrated in Figure 2.1.

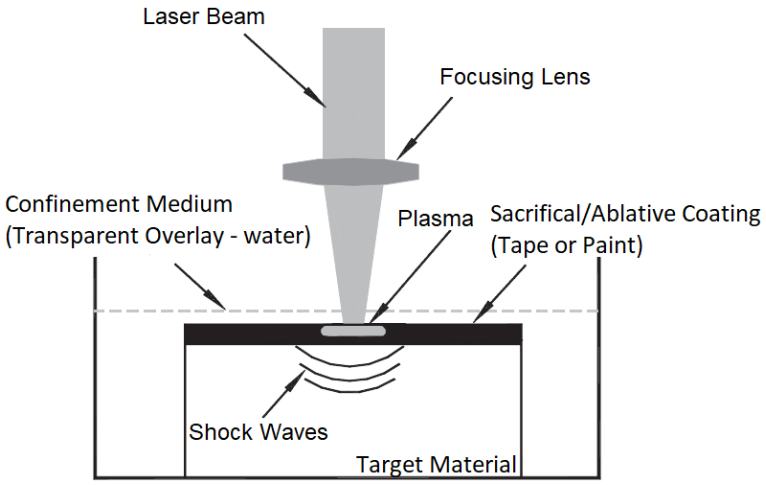


Figure 2.1: Schematic of Traditional Laser Shock Peening[1].

The laser pulse causes a thin layer of the surface to instantaneously vaporise through ablative interaction. The water overlay confines this evaporating vapour which is then immediately ionised to form plasma by inverse braking radiation and thus driving the resulting energy into the surface[1]–[4]. The plasma absorbs energy to generate a dominant high pressure heat-sustained shock wave, which immediately impinges on the surface of the material. The generated shock wave which has an intensity of several giga-pascals (GPa) far exceed the dynamic yield strength of the alloy[1]–[4]. The shock wave propagates through the alloy

while losing energy and compresses the material directly under the treated area to create a permanent strain in the material[1]−[4]. (Note: 'direct ablation' is defined as the interaction between the plasma and the metal surface without a coating).

Once the flow of the shock wave has completely propagated through the plastically deformed area, the shocked subsurface becomes plastically stressed and wants to expand and stretch, whereas the surrounding un-shocked area which is elastically responding to restrain the stretching[1]−[4]. Therefore, the interaction between these two areas results in the generation of the compressive residual stresses. These high CRS are confined to the shallow surface layer while balancing low tensile residual stress which are spread out much deeper within the cross-section of the material thus contributing to the improvement of the hardness and yield strength of the laser peened material[1]−[4].

The main effect of LSP is the merging or fusing of the dislocations and the generation of CRS[1],[3]. In general, depending on the processing conditions and material properties a penetration depth between 0.5 - 1 mm can be attained for the induced stresses[2].

LSP has been used in countless application due to the numerous benefits and the flexibility provided by the process. LSP has been successfully implemented to treat aircraft components, turbine blades, nuclear reactor shrouds, automotive components and various metallic components that operate in a high stressed environment[1],[3].

2.1.1 The Laser Shock Peening Process Parameters

The various LSP parameters introduced in this section directly influence the characteristics of the induced shock wave, the depth of penetration of the shock wave, and the performance of the resulting peened material. The peening process can be precisely controlled using a wide range of parameters. Therefore, it is important to understand the basics of each parameter and the effect these individual parameters has on the peening process.

These parameters can be classified into 3 categories, these are as follows: the laser system parameters, the control system parameters and the interaction parameters. These subcategories are summarised in detail in this section.

Due to the vast ranges available for these process parameters, emphasis must be placed on these to ensure that the parameters chosen give the optimal peening result for the material. It is important to note that the laser parameters have the largest influence on the characteristics of the resulting residual stresses[5].

2.1.1.1 The Laser System Parameters

The following parameters that are listed below are determined by the laser system that is used to conduct the processing. The parameters are as follows:

- Laser Type: The type of laser can be divided according to the type of material used for light amplification. The most commonly used laser for LSP are the Nd:YAG and the Nd:glass laser types (Further discussed in section 2.1.2).
- Laser Wavelength: This is the wavelength that laser operates in, it is important to note that different plasma peak pressures are developed using different wavelengths[5]. The wavelength is measured in micrometers [μm].
- Laser Pulse Length: The pulse length is the length of time of a single laser pulse which is generally in the nanosecond range [ns].
- Laser Pulse Frequency: It is the frequency with which the laser pulses is fired from the laser, the rate of fire is generally between 10-100 Hz range.
- Laser Spot Shape: This is the profile of the laser spot it can either be circular or square, measured in millimetres [mm].

2.1.1.2 The Control System Parameters

These following parameters can be changed in order to control and influence the LSP treatment:

- Laser Energy: This is the energy output of the laser that can be varied by using an attenuator. The output laser energy is measured in Joules [J].
- Spot Size (SS): This is either the diameter or the width of the laser spot. It can be varied by either changing the focal distance of the laser beam from the sample or by moving sample along the laser beam path. The spot size is measured in mm.
- Laser Pulse Density (Np) : It is the number of spot per unit area, measured as [$spots/mm^2$]. This can be varied by changing the scan speed of the laser across the sample.
- Ablative Medium: An external coating applied to protect the surface from thermal damage.
- The Peening Strategy: This refers to the scanning pattern that is used to apply laser spots on the sample. The peening strategy is programmed and controlled using a CNC, the following patterns can be used: a helix pattern, a raster pattern and a random pattern. Figure 2.2 shows an illustration of the raster pattern.

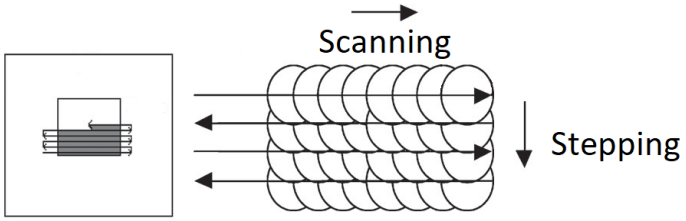


Figure 2.2: Raster Peening Pattern[5].

2.1.1.3 The Interaction Parameters

The following interaction parameters are the input variables for the control parameters, these parameters give an indication for the laser power and coverage for the LSP process:

- Laser Power Intensity (I_0): This is the intensity of the laser when fired upon a sample, it is measured in $[GW/cm^2]$ and is also referred to as Power Density $[PI]$ The power intensity of the laser beam can be calculated using Equation 2.1.

$$I_0 = \frac{400 \cdot E}{\pi \tau d_s^2} \tag{2.1}$$

  Where: I_0 is the Laser power intensity (GW/cm^2), E is the Laser energy (mJ), τ is the Pulse duration (ns), d_s is the Spot diameter (cm).

- Coverage (Cv): This implies how much of the treated area on the sample is covered by laser spot, it is measured in $[spots]$.The coverage can be calculated by using Equation 2.2

$$Cv = Np \times \frac{\pi}{4} SS^2 \tag{2.2}$$

  Where: Np is the Laser Pulse Density $(spots/mm^2)$, SS is the Spot Size (mm),

- The Coverage Ratio $(\%Cv)$: This is the percentage of each laser spot that is covered or overlapped by the neighbouring laser spot, it is also referred to as the overlapping ratio and is calculated using Equation 2.3 as follows:

$$\%Cv = 1 - \frac{SS}{\sqrt{N_p}} \tag{2.3}$$

Remarks: The most significant parameters for conducting LSP are the interaction parameters namely the power intensity, coverage ratio and the spot size of the laser system. It is important to understand the effect these parameters have on the final peening process and the residual stresses. The effect of using these parameters will be studied and the effect it has on 7075 aluminuim alloy this is part of the development process for the University of Witwatersrand and the CSIR LSP department.

2.1.2 Laser Shock Peening Systems

LSP can be applied and performed in a variety of ways. This sections aims to outline the different types of lasers that are used for LSP, the way in which the laser beam is delivered to the target surface, the confinement method used to confine the laser pulse and the protective ablative (sacrificial) coatings used to protect the surface from thermal damage[1],[5].

These parameters have a direct influence on the characteristics of the induced shock wave, the depth of penetration of the residual stress, the surface integrity of the material and the final mechanical performance of the peened material[1],[5].

Many authors make use of different laser systems with different settings and configurations for conducting LSP thus it is important to understand the basics of each component and the effect they have on the peening process. Therefore, emphasis must be placed on the laser system, beam delivery, confinement media and ablative coatings.

2.1.2.1 Laser Systems

A specialised laser system is required to conduct LSP. These laser systems require a power level output ranging from several hundreds watts for smaller units to kilowatts for larger units, a laser pulse energy in the range of 40 mJ - 100 J and a suitable pulse duration between the range of 8 - 100 ns operating at a relatively high repetition rate and reasonable wavelength[1].

There are currently two types of laser systems that are mainly used to perform LSP, the neodymium-doped glass (Nd-glass) laser and the yttrium aluminium garnet (Nd:YAG) laser[1]. The differences between the two laser systems are highlighted below.

The Nd-glass laser system developed in 1974 is a large and powerful laser system, it operates at slow repetitions rates due to the high recharge time. The laser system can produce larger spot sizes and can deliver laser pulse energies in the ranges of 25 - 100 J[1]. An ablative coating is required for the peening of the materials in order to prevent significant surface damage.

The Nd:YAG laser system is a much smaller and compact laser system, it operates at lower pulse energies, but with high repetitions rates and much smaller spot sizes using a laser pulse duration in the ranges of 10-100 ns[1],[3]. This laser system is the most suitable to shock peen materials with and without coating.

Selecting a suitable laser system for the LSP does not only require the physical characteristics of the laser, but other factors such as efficiency, cost and maintenance also need to be taken into account. The aforementioned factors will aid in fully commercialising the process in the future. The Nd:YAG laser is the most suitable laser for the application of LSP as it is able

to operate at near infra-red wavelength of 1064 μm with continuous pulses[1]. The operating wavelength of the laser system is an important parameter because it controls the interaction between the laser beam and the material surface[1].

Table 2.1 outlines a few types of laser systems and laboratories that are available for LSP around the world.

Institution	Laser System	Laser Wavelength $[nm]$	Pulse Duration $[ns]$	Laser Energy$[J]$	Spot shape	Spot size $[mm]$
Toshiba, Japan[3]	Nd:YAG	532	$\leqslant$ 10	0.04-0.25	◯	0.4-0.7
CSIR, RSA	Nd:YAG	532 & 1064	$\leqslant$ 10	0.2-1.5	◯	0.4-4
UPM, Spain[5]	Nd:YAG	1064	$\leqslant$ 10	2.8	◯	1.5
HZG, Germany[6]	Nd:YAG	1064	$\leqslant$ 10-20	3-5	□	1x1, 3x3, 5x5
MIC, USA[7]	Nd:glass	1064	18	5.8-15.2	□	5x5 - 8x8

Table 2.1: Laser Institutions and Laboratories.

The aforementioned institutions and laboratories that specialise in LSP each have different characteristics and operate at using different parameters and thus produce different and unique results when performing LSP. These parameters include different laser settings and specifics such as laser pulse duration, type of spot shape and the method in which LSP is applied the material, thus these factors influence the application of LSP for each laser system.

2.1.2.2 Laser Beam Delivery

The laser beam can be delivered to the surface of the material in numerous ways. It can be delivered by using complex robots to control either the path of laser beam or the movement of the work piece. The beam can also be delivered by using fibre optics or mirrors as illustrated in Figure 2.3[3],[8].

The movement of the water confinement medium can also be configured using complex robots. Using complex robots allows LSP to be conducted on highly complex geometries, however laboratories generally make use of simple systems, this system commonly make use of a fixed laser beam path by using mirrors and a flexible water delivery system whereas the work piece is mounted on either a XY or XYZ CNC stage as shown in Figure 2.4.

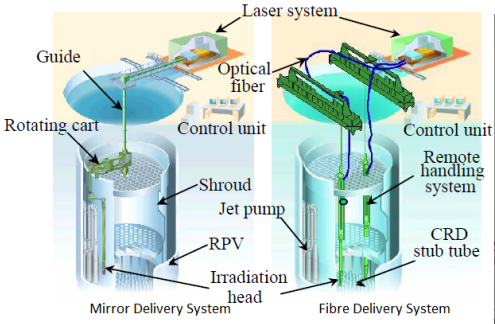


Figure 2.3: Mirror and Fibre Delivery Systems[8].

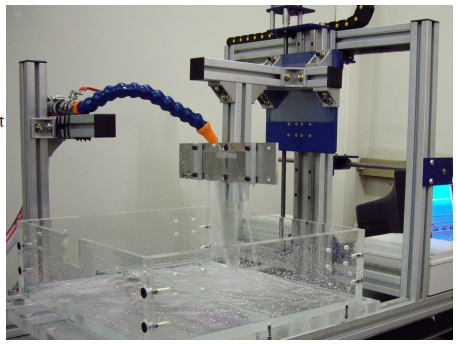


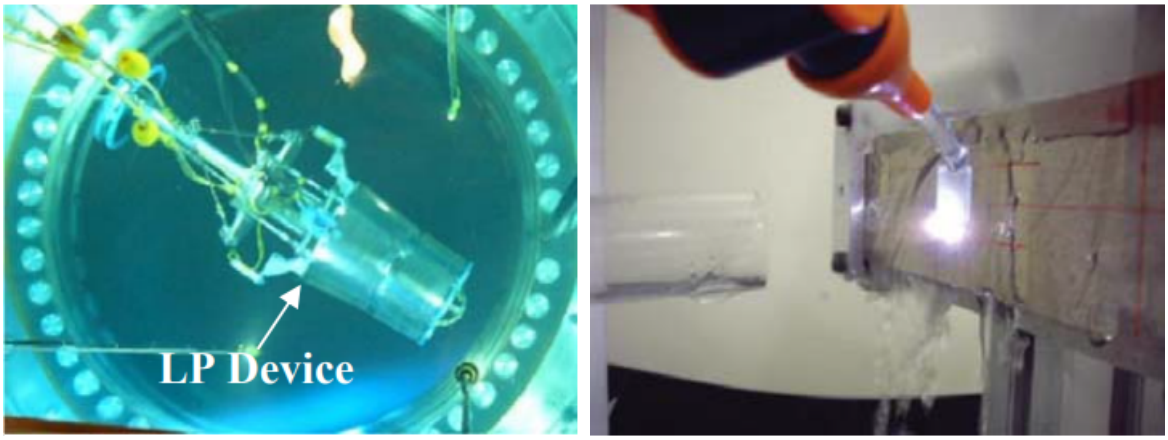
Figure 2.4: CNC Stage.

2.1.2.3 Confinement Media

With the development of the laser, it was soon recognised that a higher amplitude of the shock wave could be achieved by confining the generated plasma at the surface of the material by using a laser beam with a pulse duration in the nanosecond range. Initial experiments found that the pressure applied due to plasma formation could be significantly increased if the generated plasma was confined by using a confinement medium. The physics and mechanisms of the induced shock wave has been intensively investigated[1].

In early experiments the material was placed in a vacuum and the generated plasma expanded freely, further experiments included using glass as the confinement medium[1]. Eventually, it was found that using either deionised water or regular tap water yielded the best peak pressure results for confining the plasma[1].

Modern LSP typically makes use of water as the confining medium as it has a higher threshold and can be easily applied using different types of configurations. The material can be submerged entirely in water as shown in Figure 2.5a to perform underwater peening[8] or a stream of water can be flowing over the material as indicated in Figure 2.5b. The method of using a nozzle to deliver the water is often used by most LSP systems.



(a) Submerged Confinement[8]. (b) Flowing Water Confinement.

Figure 2.5: Various Confinement Modes.

It has been observed that if the layer of water confining the plasma is sufficiently thick, a cavitation bubble may form as a result the plasma cloud collapses as shown in Figure 2.6 this results in the formation of a second shock wave as shown by the shock wave signal in Figure 2.7, which leads to the peening in being more effective[9].

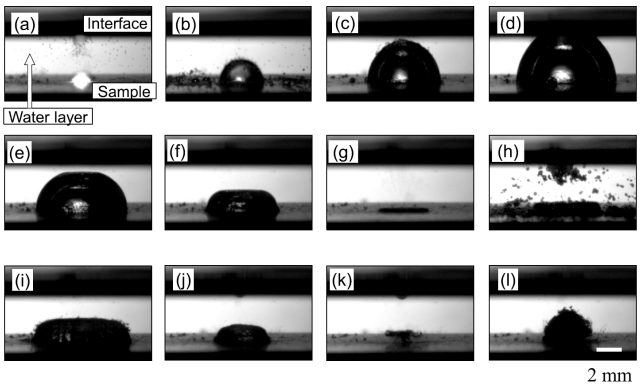


Figure 2.6: Plasma and Cavitation Bubble Formation[9].

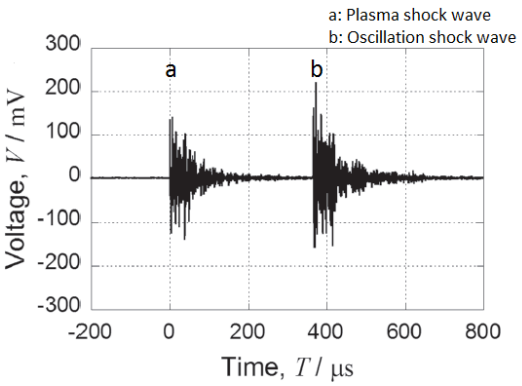


Figure 2.7: Shock Wave Signal[1].

2.1.2.4 LSP with and without an Ablative Coating

During the early development of LSP process, the process was initially performed by using a protective coating that was applied to the surface of the material before processing, this was done to protect it against the high thermal effects that were being introduced during the LSP process. Since then various types of ablative coatings have been used such as aluminium tape[1],[4], vinyl adhesive tape[4], black paint[1], etc.

The LSP results obtained using the different coating varied depending on the ablative coating used, each result was unique thus showed the importance of selecting and using the correct ablative coating for LSP[4]. Due to time and cost involved in applying an ablative coating a method of performing LSP without coating was investigated and later optimised.

LSP without using an ablative coating is generally referred to as Laser Shock Peening without Coating or LSPwC. LSPwC is generally performed using low laser energies with high coverage ratios, the only drawback in using LSPwC on a sample is that the process results in an increased surface roughness.

Although the process reduces time and cost, certain application still require the use of LSP with an ablative coating. The benefits provided by using a sacrificial layer with LSP are much higher when compared to using LSPwC, as it provides a better surface finish but with a slightly lower residual stress depth penetration.

Thus for this dissertation only traditional LSP will be used, and as for the ablative coating a variety of adhesive tapes will be used as they can be easily applied and removed. These adhesive tapes are readily available and easy to procure.

2.2 The Effect of Laser Shock Peening on Material Properties

The theory and related mechanisms for LSP have been introduced in the previous section, it is important to note that much effort is directed into the development of the LSP process. LSP is a surface enhancement technique that irradiates the surface of the treated sample with a pressure that far exceeds the yield strength of the material. This results in strain hardening and plastic deformation to occur and thus establishes a residual stress field around the treated area which in turn alters the surface morphology of the material[1]. Therefore, a positive change occurs when conducting LSP as it changes the fatigue properties and the corrosion properties of the material, due to these beneficial effects imparted by the LSP process there is a high demand for industrial application and research based projects. The effect of LSP on the material properties will be discussed in this section.

2.2.1 The Effect of Using an Ablative Coating for LSP

There are two basic methods for LSP that were introduced, direct ablation (LSPwC) and indirect ablation (traditional LSP)[1],[5]. The ablative or sacrificial layer has the main function of protecting the surface of the material since the direct method exposes the surface of the material to high temperature plasma which can produce surface damage and can also increase the base surface roughness. The major difference between the two methods lies in the fact that when no coating is used, the only way to minimise the surface damage is to use lower laser power intensities coupled with low laser spot sizes and increased coverage ratios.

Since the development of LSP, a large number of ablative coatings have been investigated, from the use of these coatings it has been found that not only do the coatings protect the metal surface from laser ablation and melting but also to aid in increasing the shock wave intensity [1]. Metallic coatings such as aluminium, copper and zinc and other non metallic coating such as paint and tape have been found to be beneficial and necessary in protecting the surface of a material when conducting LSP. Black paint as a coating has been found to be practical and effective when compared to other coatings [1]. This is further explained later in this section.

When the laser pulse irradiates a specimen with an ablative coating through a transparent overlay, the ablative layer vaporises and forms plasma, due to the very short energy deposition, as a result the diffusion of the thermal energy is limited to a few micrometers away from the interaction zone and is generally less than the thickness of the ablative coating to maintain protection[1]. This is especially important for aluminium alloys because the surface ablation process without coating can detrimentally affect the fatigue life[1]. The plasma will continue to absorb laser energy up until the end of energy deposition[1].

It was found that the mechanical effects of the stress wave induced by peening depends significantly on whether the treated area is covered by an ablative coating. The thermal effects only occur in the coating layer whereas the shock waves penetrate into the material to create a mechanical effect to induce a compressive residual stress field[1]. The coating can be metallic, organic or adhesives; these coatings not only protect the surface from radiation but also enhances the induced plasma thus the coating could play a fundamental role in plasma pressure and properties[1]. A high shock wave pressure can be generated by using a combination of a transparent overlay and an ablative coating. An uncoated treated area can lead to high tensile stress and severe surface melting even when a transparent overlay is used. In order to achieve the effective peening results for different types of metallic materials the optimisation of LSP parameters, including the transparent overlay and the ablative coating is very important[1].

In a separate experiment that investigated the effects of using adhesive tapes and black paint as a ablative medium, it was observed that black PVC tape was more effective sacrificial medium when compared to the other media[10]. Three different types of alloys were used for the experiment, these were Ti6Al4V alloy, SAE 9260 spring steel and DIN X20Cr13 martensitic stainless steel, these material were treated using black paint and black PVC tape. It was also observed that using black PVC tape instead of black paint as the coating media provided a lower surface roughness post LSP processing[10]. It was also concluded that by using the black PVC tape there was no surface melting and that the surface was more smooth rather when using black paint. There was minimal change in the surface roughness using black PVC tape, and the compressive residual stress also penetrated deeper layers. Tape in general is easily available and when compared to using black paint, tape facilitates for a much quicker application and also reduces the overall post processing time[10].

A similar experiment was conducted, this experiment investigated the effect two different types of tape have on the residual stress of the material when peening with the same conditions. Figure 2.8 shows that black vinyl tape perform better as it allows for a higher magnitude of stress near the surface and performs better when compared to the metallic aluminium tape[4].

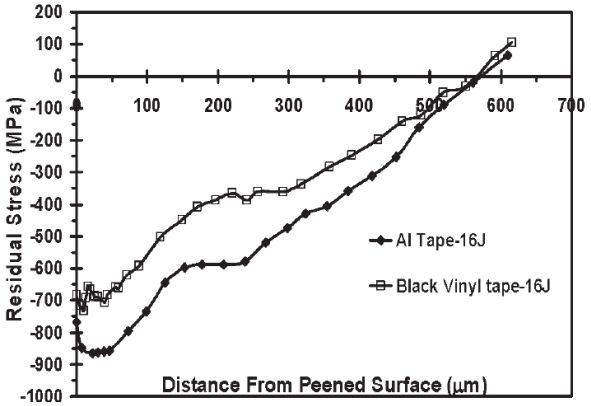


Figure 2.8: RS Profile for Two Ablative Coatings[4].

2.2.2 The Effect of LSP on Surface Integrity

Due to the nature of the LSP process it is important to study the effects that the process has on the surface integrity and the surface roughness of the treated material. Because LSP is applied to the surface of the material, the process tends to change the surface integrity of the material[3],[4]. The use of an ablative coating protects the surface of the material against melting while providing a pure mechanical effect and has a lower impact on the surface integrity whereas using direct ablation tends to have a higher impact on the surface integrity as there is no medium to protect the surface from thermal damage[3],[4]. These changes in the surface are microscopic but can impact the performance of the material. Various authors have investigated the changes in the surface integrity in detail, the details of their finding are outlined below.

An experiment was conducted to find the surface defects produced by LSP using Aluminium foil as the ablative coating on TC17 titanium alloy[11]. The experiment was carried out with a Q-switch Nd: glass pulse laser system with pulse duration of 30 ns and pulse frequency of 0.1 Hz with a square laser spot of 4x4 mm using a laser pulse energy of 50 J. The thickness of the foil was 120 μm[11]. The surface of the foil and the material were studied after the LSP process was conducted. Figure 2.9 depicts the surface of the aluminium foil and its thickness post LSP processing. Due to the fact that the foil was used as an ablative medium , the foil when processed with LSP instantaneously evaporated and ionized to produce plasma which resulted in a decrease of the foil thickness by about 10 μm[11]. Figure 2.9c, d, e shows the cross-section thickness of aluminium foil corresponding regions labeled in Figure 2.9a. From the original thickness of about 120 μm, and this value decreased to 80, 55 and 25 μm from one laser impact (Figure 2.9c), two laser impacts (Figure 2.9d) and four laser impacts (Figure 2.9e) respectively[11].

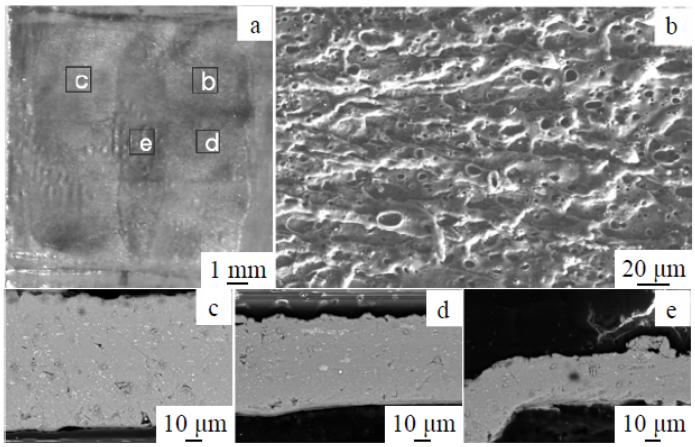


Figure 2.9: Aluminium Foil Surface and its Thickness Post LSP[11].

These findings show that the ablative thickness decreases with increasing laser impacts or coverage. The image also shows the change in the surface state after LSP processing.

The surface was further investigated to observe the micro impression defects that were found after ablative layer had been removed. Typical micro impression defects were detected by use of white light interference method as shown in Figure 2.10[11].

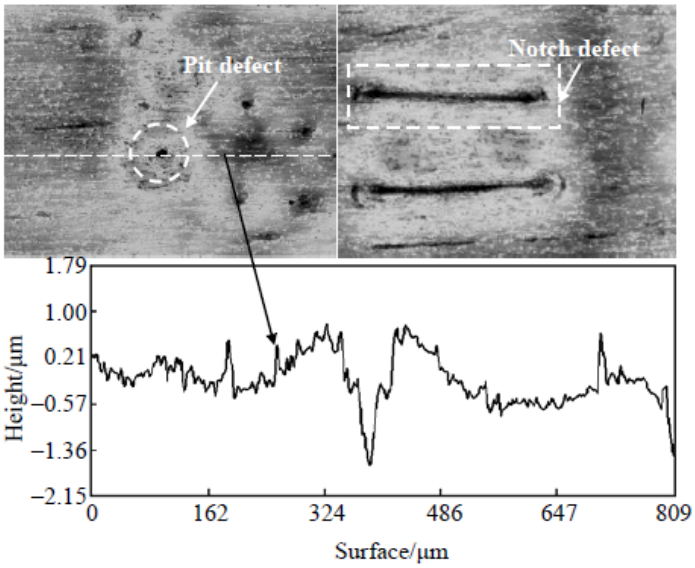


Figure 2.10: Pits and Notches Defects on Peened Surface[11].

From Figure 2.10 number of tiny pits and notches can be observed on peened surface. The average size of these pit defects is around 100 μm, whereas the size of the notch defects is in the range of several micrometers to a millimetre. The depth of these defects is in the range of 1-2 μm, thus it was found that the material surface around these defects is either elevated or depressed. Thus, these micro impressions tend to deteriorate the surface roughness post LSP, and also initiate fatigue cracks around the defect area because of the stress concentration[11]. This type of defects are difficult to locate when using black vinyl tape or black paint as the ablative medium[11]. Similar defect patterns were also observed in the foil as shown in Figure 2.11

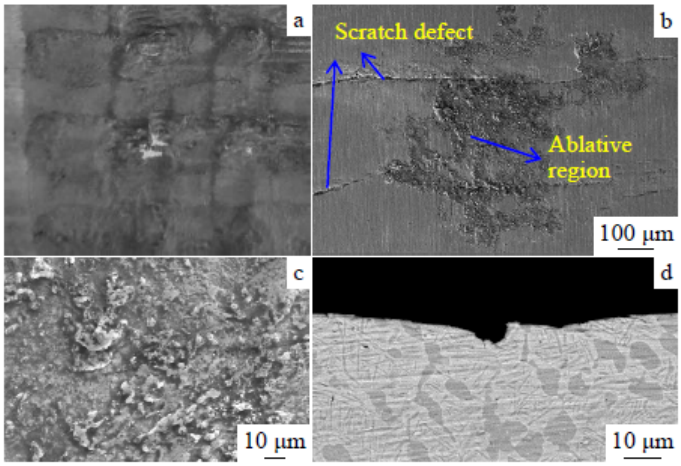


Figure 2.11: Surface Defects on Aluminium Foil[11].

In a separate experiment that investigated the surface characteristics of LSP and shot peening (SP) for AISI 4140, it was found that the LSP treatment on a material does have an adverse effect on the surface topography and roughness of the material, the treatment created periodic wave like features or defects on the surface of the material as shown in Figure 2.12.

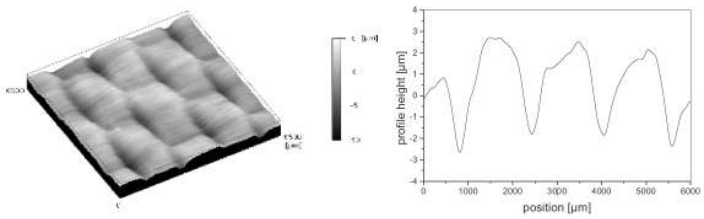


Figure 2.12: Topography Profile of AISI 4140 Peened with 50% Coverage[12].

Figure 2.12 illustrates the observations found for the surface topography for high tensile steel AISI 4140, the material was laser peened using a Nd:glass laser system with a 50% coverage ratio, laser energy of 25 J and with a square laser spot of 3.5 x 3.5 mm over a 6.5 x 6.5 mm surface area[12]. The image shows recurrent notches which are 5 μm with a distance of about 1.7 mm, which is half of the laser spot size[12]. The mean surface roughness (R_a) was measured to be 2.8 μm and increased to 8.1 μm when shot peening was used[12]. It was found that when compared to the base material, not only does the surface roughness of the peened samples increase but the residual stresses are also influenced by the overlapping of laser pulses[12].

The surface integrity of the material, which includes factors such as the surface roughness among others can either encourage or reduce the surface crack initiation and thus influence the overall fatigue life of shocked material. In general, all metallic surfaces are inherently rough, but the degree of surface roughness changes according to the manufacturing process and machining techniques that are used. The problem presented by LSP process on the surface roughness is that the surface does not retain its original properties when compared to the base material. Initially all metallic surfaces have some degree of roughness but after applying any surface enhancement or modification technique such as LSP, the material's surface state tend to change on a macro and microscopic level[1],[12]. Therefore, the changes in the surface state is important because it affects the overall performance of the peened material.

LSPwC dramatically changes the surface finish when compared to LSP using an ablative medium, the differences observed between the two techniques is illustrated in Figure 2.13[13].

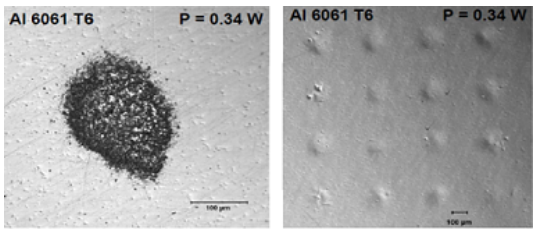


Figure 2.13: 6061-T6 Al sample Processed with and without an Ablative Coating[13].

Figure 2.13 shows 6061-T6 Al sample that is processed with and without an ablative coating, it can been seen that the LSPwC process dramatically changes the surface integrity of the material when compared to sample processed using an ablative coating. The surface results show clearly that the specimen peened without coating has a degraded surface finish and is most likely to have a higher surface roughness parameter when compared to the specimen peened with an ablative coating.

2.2.2.1 Effect of LSP on Surface Roughness

The surface roughness (Ra) induced on the surface by the LSP process can be seen as wavy irregularities which makes up the surface texture of the material. As illustrated in Figure 2.14 the surface finish or surface texture of a material is made up of 3 individual parameters: lay, surface roughness and the waviness. The surface finish compares the small, local deviations of a surface from the perfectly flat ideal. The lay is defined as the repetitive pattern that is generated on the surface by either the machining or the manufacturing process. Whereas, the waviness of the surface is the measure of irregularities which has a spacing that is higher than surface roughness of the material. The waviness pattern generally occur due to vibrations during the machining process. The surface roughness of a material is the measure of the unevenness in the surface texture which results from any type of surface treatment or a manufacturing process.

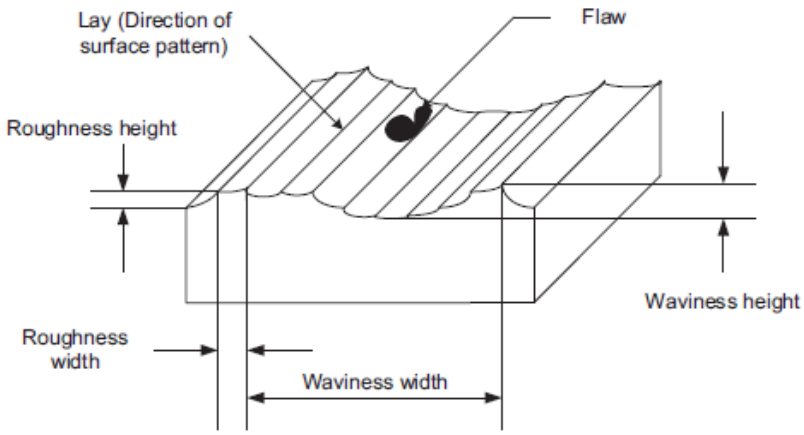


Figure 2.14: Roughness and Waviness Profile[15].

Due to the numerous irregularities and waviness of the surface, it becomes difficult to evaluate and measure these values. Therefore, these characteristics are generally represented using either of the following roughness parameters: the arithmetical mean roughness parameter (Ra) and the average peak-to-valley roughness parameter (Rz) (Note: advanced roughness parameters are not considered)[15],[16]. The surface roughness measurements are generally given by the arithmetical mean roughness value (Ra) because it represents the average of the absolute value of the roughness profile as shown in Figure 2.15. Ra is one of the most effective surface roughness parameter and is commonly adopted in general practice because it gives a

good description of the height variations of the materials surface whereas (Rz) is determined from the average height values of the peaks and valleys as illustrated in Figure 2.16.

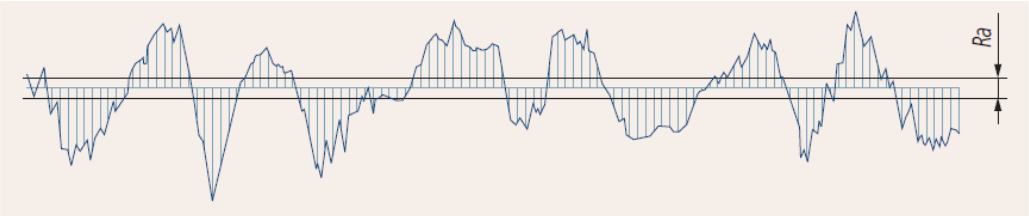


Figure 2.15: Arithmetical Mean Roughness Parameter Ra[16].

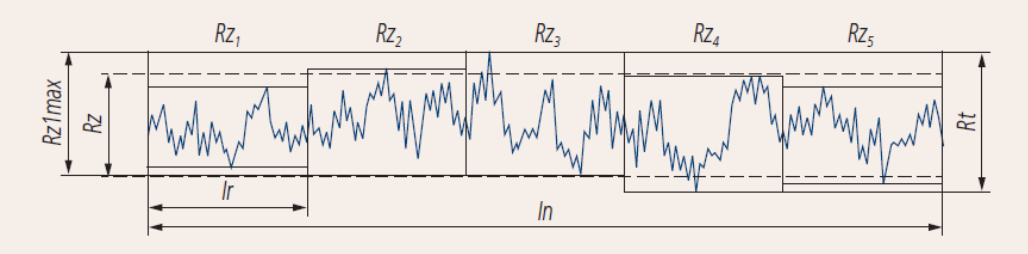


Figure 2.16: Average Peak-to-Valley Roughness Parameter Rz[16].

From previous investigations LSP does indeed effect the surface roughness of the material, the degree of changes in surfaace roughness vary according to the peening parameters and with material properties. For example a material that has a low surface roughness post machining processes will show a noticeable increase in surface roughness after the LSP treatment has been applied[1]. The opposite is also true for a material that has a higher surface roughness (i.e. not machined) will show a negligible change in surface roughness after the LSP treatment has been applied[1].

Generally, LSP using an ablative coating is able to achieve relatively finer surface qualities[1]. From a previous study that investigated the surface roughness measurement of polished and etched titanium Ti (RT15) specimens before and after LSP was applied[14]. It was found that there was a significant increase in surface roughness for the polished samples (increase from Ra= 0.4 μm to Ra= 1.2 μm) and a slight increase in surface roughness for the etched samples (increase from Ra= 3.7 μm to Ra= 3.9 μm)[14].

From the results obtained it is clear that materials with an initial low surface roughness tend to show a larger increase in roughness post LSP whereas the material with moderately low roughness remain either unchanged or experience a slight increase in roughness post LSP.

2.2.3 The Effect of LSP on Microstructure

To investigate the effects of LSP on the microstructure, a number of microscopes can be used that reveal different features at different magnifications. The following investigations represents Al 6061-T6 samples that have been treated by LSP and the microstructure analysed using an optical microscopy.

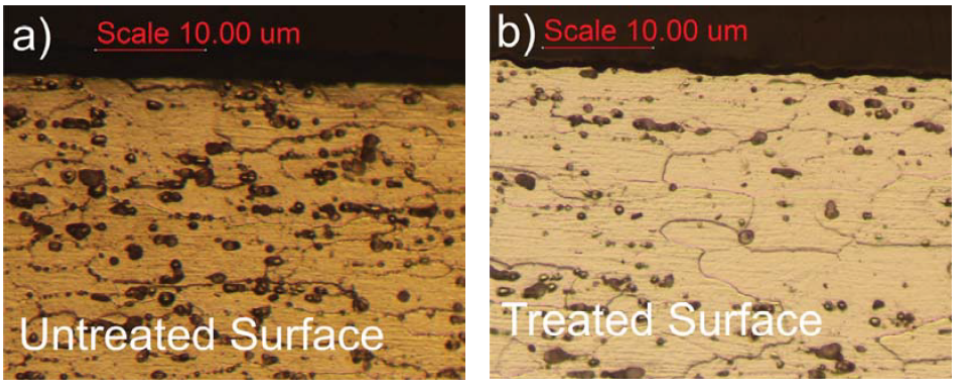


Figure 2.17: Optical Microscope Image of LSP Al 6061-T6[17].

Figure 2.17 shows an optical microscope image of the cross-section taken at high magnification. There are minor visible change in the microstructure following LSP, however the surface is considerably roughened[17].

Figure 2.18 shows SEM micrograph image of the cross-section for Al 7075. The sample was processed using LSPwC at the same laser energy but using different coverage ratios. The polished unpeened surface of the cross section appeared relatively smooth as shown in Figure 2.18a[18]. The sample peened using 10 $pulse/mm^2$ as shown in Figure 2.18b as compared to the sample peened using 100 $pulse/mm^2$ shown in Figure 2.18c appeared differently[18]. This can be attributed to the increase in ablative interaction and thermal impact on the surfaces when there is an increase in the coverage ratio. As the laser pulse density is increased the resulting indentations becomes deeper and wider[18].

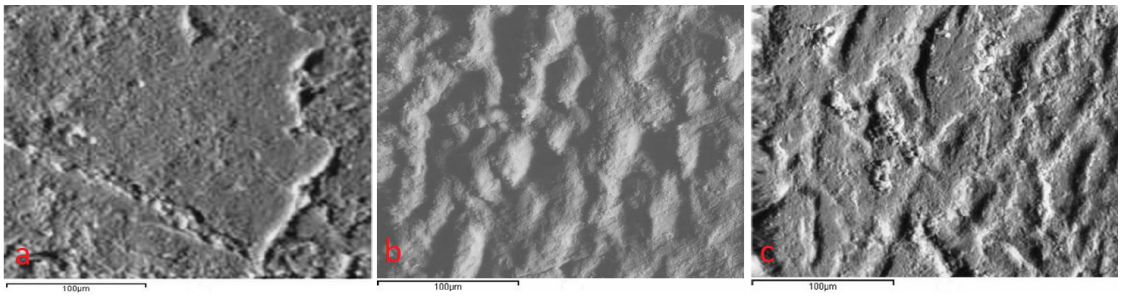


Figure 2.18: SEM Image of an Al 7075 Cross Section Surface[18].

Figure 2.19 shows the surface structure and cross-sectional structure as captured using SEM imaging and optical microscopy for titanium samples peened with a power of 6 GW/cm^2, without coating and using PVC tape coating of 2 mm thickness[19]. When the surface was analysed using SEM represented by Figure 2.19a and Figure 2.19b, the sample treated without coating showed surface melting and subtle changes in dislocation density when compared to the sample treated using the PVC coating[19].

Similarly, the cross-section was observed using optical microscopy represented by Figure 2.19c and Figure 2.19d, it was noticed that there the sample treated without coating had small variations when compared to the sample treated using an ablative coating[19].

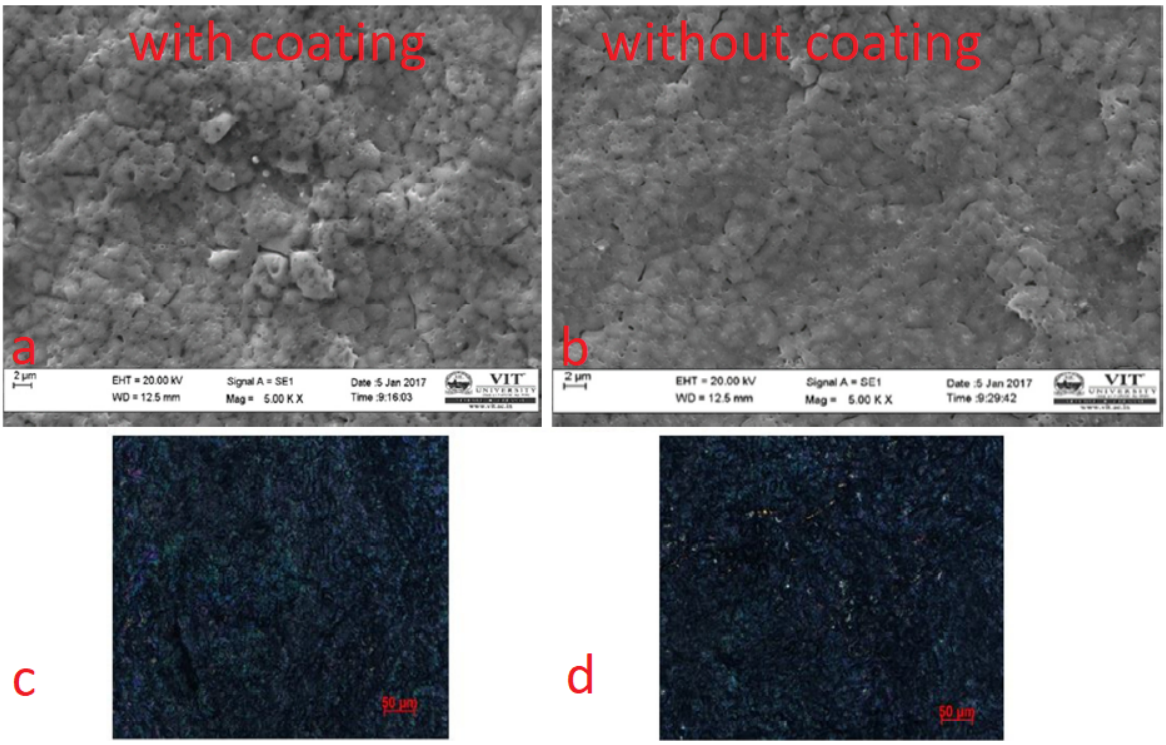


Figure 2.19: SEM and Optical Microscopy Images of LSP Titanium[19].

Compared to the untreated sample the dislocation density increased in general for the sample treated with both LSP with coating and LSPwC[19].

2.2.4 The Effect of LSP on Microhardness

The hardness of a material is defined as the materials ability to resist indentation, and is determined by measuring the permanent depth of the indentation made on the material[1]. The indentation hardness value is found by measuring the depth or the area of the indentation, it is generally evaluated using the Vickers hardness testing method. This method is based on an optical measurement system and makes use of diamond tipped indenter with loads ranging from a few grams to kilograms.

Figure 2.19 shows microhardness results obtained for Al 5083 that was treated with a laser intensity of 8.14 GW/cm^2 and a 50% coverage ratio[20]. The variation in the microhardness profile along the cross section of the samples were observed up to a depth of $1.2mm$. the hardness profile for the treated sample gradually decreases from the peened surface, this is due to the shockwave pressure induced by LSP on the surface of the material[20]. The hardness of the material decreases along the cross section until the hardness reaches the base hardness of the untreated material. LSP does increase the hardness near the surface of the material[20].

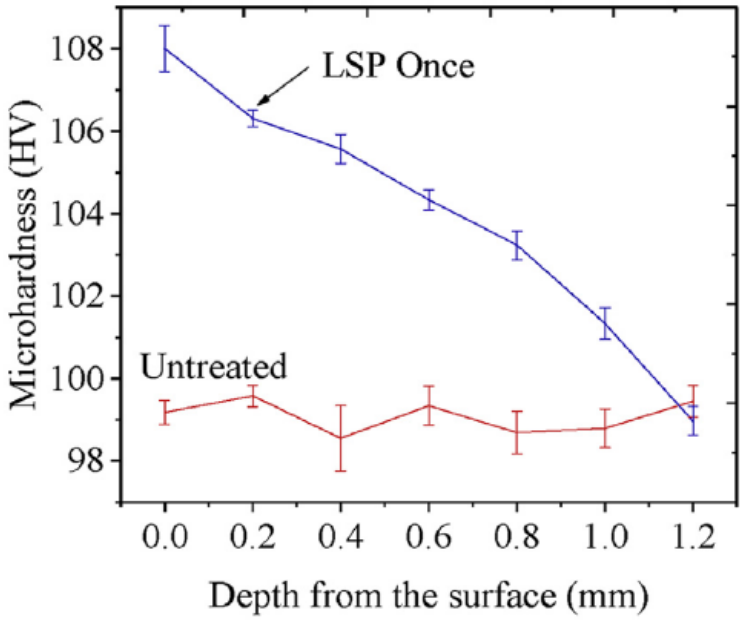


Figure 2.20: Microhardness of Al 5083 Sample Before and After LSP Treatment[20].

Figure 2.19 illustrates the surface hardness trend observed for the samples treated with different LSP impacts. After LSP treatment was applied with 1 impact, 3 impacts and 5 impacts, the hardness of Al 5083 increased to 104 HV, 107 HV and 111 HV from the 96 HV observed for the untreated sample[20]. The hardness increased by 8.14%, 11.56% and 15.96%, respectively[20]. From obtained observations and results, it could be said that the hardness increases with increasing laser impacts or coverage ratios[20].

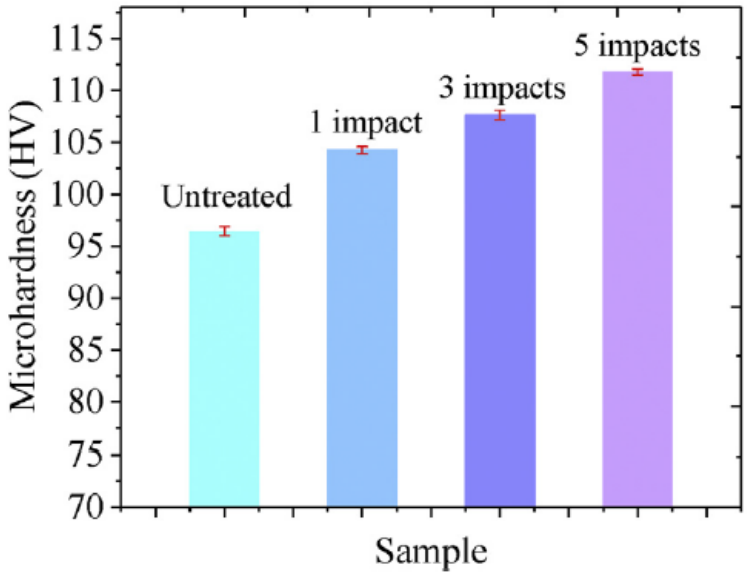


Figure 2.21: Surface Hardness of Al 5083[20].

In a different experiment that was performed on 6061-T6 aluminium alloy using a laser energy of 1.2 J with 3 different coverages; 900, 2500 and 5000 $pulses/cm^2$ [21]. Illustrated in Figure 2.22 below are the results obtained from the micro-hardness test. The highest micro-hardness values for the peened materials were found to be 105.4 HV and 94.4 HV. The average micro-hardness values for the untreated materials was 83 HV. From Figure 2.22 it is clear that with a higher pulse density there is deeper penetration and with this there is a greater hardened region[21].

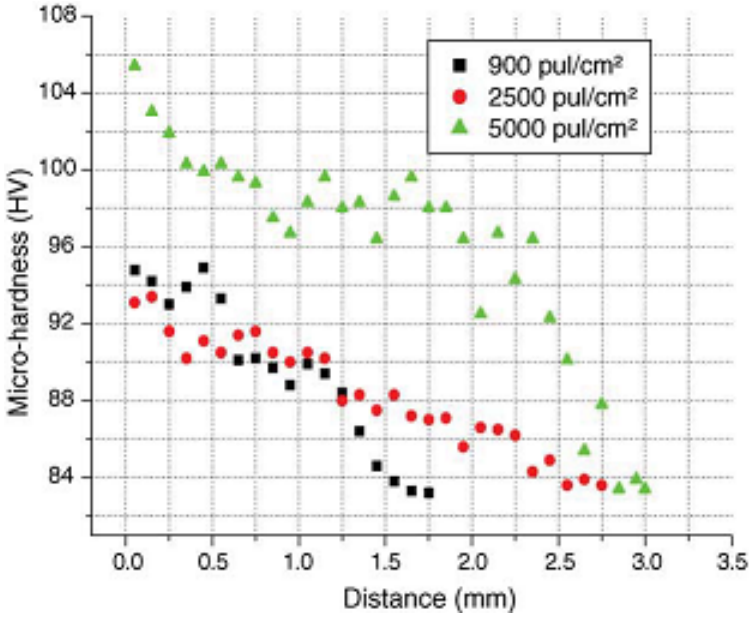


Figure 2.22: Cross-sectional Micro-hardness Profiles of Al 6061-T6[21].

2.2.5 The Effect of LSP on Fatigue Behaviour

A investigation was carried out to compare the fatigue behaviour and residual stress stability of laser-shock peened and deep rolled stainless steel AISI 304 in the temperature range 25 - 600 deg C. The investigations were carried out on samples with a diameter of 7 mm and a gauge length of 10 mm. LSP was carried out using a coverage of 200%, a power density of 10 GW/cm^2 with a square spot size of 2.5 x 2.5 mm. The residual stress measurements were performed by a standard X-ray diffraction technique. Isothermal fatigue experiments were conducted under loads in tension - compression on a standard servo-hydraulic testing machine using a stress ratio (R) of -1 with a frequency of 5 Hz and in temperatures of 25 - 600 deg C. The fatigue results are as follows:

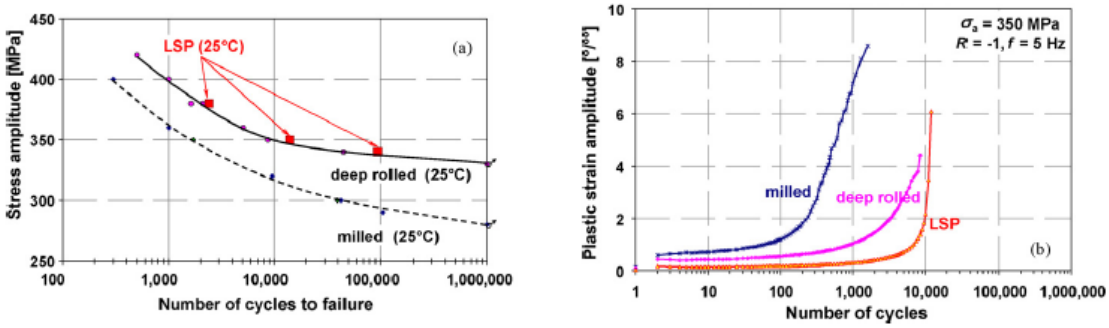
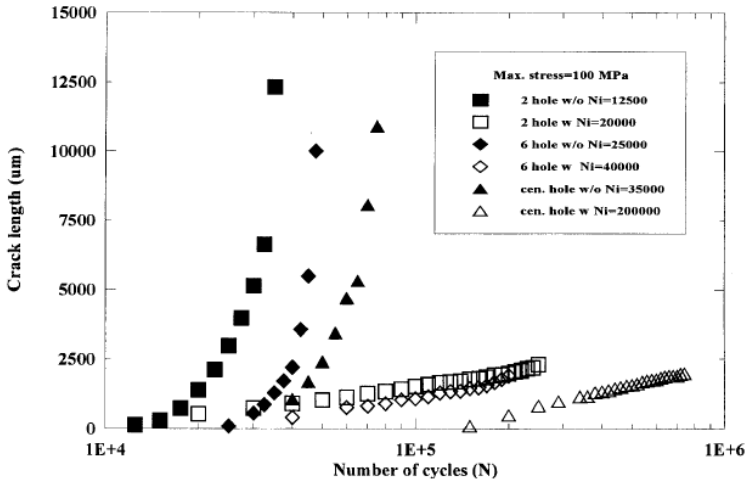


Figure 2.23: LSP - Cyclic Deformation Fatigue Behaviour of AISI 304[22].

Figure 2.23a shows S-N curves for untreated, shock peened and deep rolled conditions. The two types of mechanical surface treatments significantly improve the fatigue behaviour in the low and high cycle fatigue regime[22]. Fatigue lifetimes of the peened samples are slightly higher than that of the deep rolled sample. This higher fatigue lifetime is due to smaller strain amplitudes during fatigue tests as compared to the initial state shown in Figure 2.30b. At high applied stress amplitudes the cyclic deformation behaviour is characterized by cyclic softening until failure for untreated sample and for both surface treated conditions[22]. At low applied stress amplitudes the cyclic softening is followed by cyclic hardening[22]. The two types of mechanical surface treatments enhances the fatigue behaviour of the material by more than 15%[22].

The fatigue crack lengths as a function of fatigue cycles for the laser-peened and unpeened 2024-T3 Al alloys with a fastener hole and stop holes are depicted in Figure 2.24[23]. The results are obtained for an experiment that was conducted using a Nd:glass laser, spot size of 10 mm, laser power intensity of 5 GW/cm^2 with a black paint ablative coating[23]. The fatigue behaviour of the peened samples were conducted under a tension - tension mode at room temperature with a stress ratio R = 0.1 with a frequency of 10 Hz and a maximum stress of 100 MPa[23].



Specimen	Crack initiation life (cycle)		Fatigue life (cycle)	
	Unpeened	Laser-peened	Unpeened	Laser-peened
Center hole	35 000	200 000	70 000	>800 000
One crack stop-hole	12 500	20 000	32 000	>300 000
Three in-line crack stop-holes	25 000	40 000	41 000	>300 000

Figure 2.24: Crack Lengths as a Function of Fatigue for the Laser-Peened and Unpeened 2024-T3 Al[23].

Many interesting points can be drawn from the results depicted in Figure 2.24. First, both the fatigue crack initiation life and fatigue life of the unpeened sample are strongly affected by the geometry of the fastener hole[23]. It was noticed that the fatigue crack initiation life and fatigue life of the unpeened Al alloy decreases as the stress concentration factor for the fastener holes increases[23]. The results also show that three in-line holes at each end of the crack is significantly more effective for stress reduction and crack stopping than the one crack hole at each end of a fatigue crack[23]. Second, it is clear that LSP has a significant effect on the fatigue behaviour of the material. As shown in Figure 2.24 the fatigue crack initiation life and fatigue life for the peened material is significantly higher than that of the unpeened material[23].

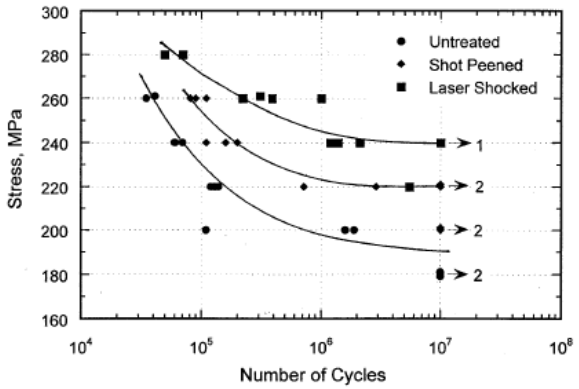


Figure 2.25: Comparison of Bending Fatigue of Untreated, Shot Peened and LSP Al 7075-T7351[24].

Figure 2.25 shows bending fatigue results obtained for Al 7075-T7351 alloy. The LSP was conducted using a Nd:glass laser system. The specimens were tested in bending using a stress ratio of R = 0.1 and the results obtained are shown in Figure 2.25. Form the results obtained it was found that shot peening provided an 11 percent increase in the run-out stress whereas laser shock peening provided a 22 percent increase[24]. Overall the fatigue life of the laser peened sample is higher than that of the shot peened and untreated samples.

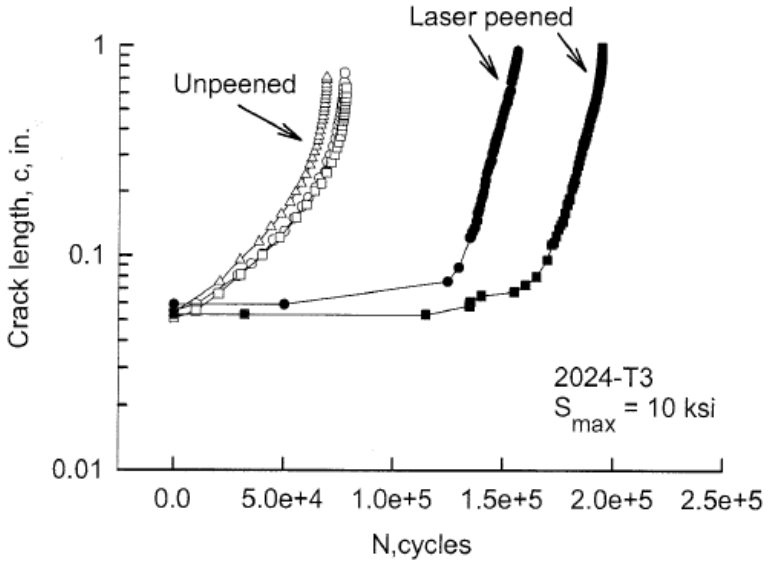


Figure 2.26: Crack Length vs Load Cycles for Unpeened and LSP Specimens[25].

The effect of LSP on crack growth length is shown in Figure 2.26. The Al 2024-T3 alloy was processed using a laser energy output of 100 J/cm^2[25]. The fatigue test were conducted using stress ratio of R = 0.1 with a maximum loading of 10 ksi[25]. The crack growth life for the laser peening samples showed less scatter than those conducted with shot peening tests. It was found that the crack growth life for the LSP test was increased by a factor of 1.8 from the unpeened test[25]. The results showed that after peening the crack growth rates were noticeably slower when the cracks were fairly short for both the shot and laser peened samples resulting in general a greater crack growth life[25].

2.2.6 The Effect of LSP on Residual Stress

The effect of LSP on residual stresses were studied through experiments. Figure 2.27 shows the residual stress profile for 2024-T3 aluminium alloy before and after LSP processing. The compressive residual stress induced by LSP is higher when compared to the untreated material, having maximum stress of -53 MPa when compared to -8 MPa of the untreated material. The treated material shows that the depth of penetration reaches over 1 mm. The general trend for LSP induced stresses is that the compressive residual stress is usually highest near the surface and gradually decreases with depth across the cross section of material.

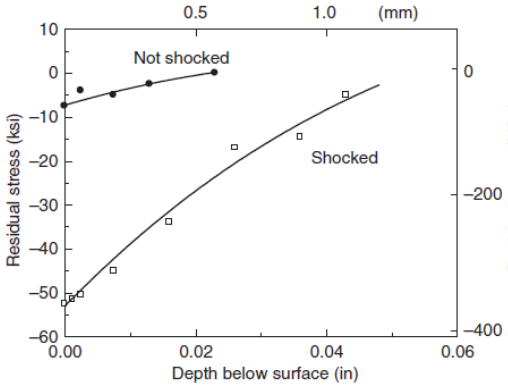


Figure 2.27: RS Profiles for 2034 Al[1].

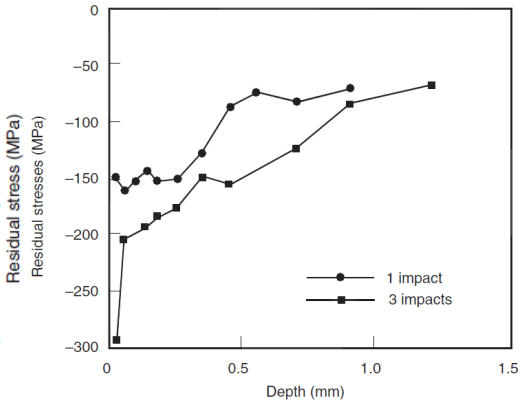


Figure 2.28: RS Profiles for 7075 Al[1].

Figure 2.28 shows that the depth of penetration of residual stress is dependent on the LSP parameters and it increases with multiple LSP. The magnitude of the surface residual stress also increases with increasing laser spot impacts[1].

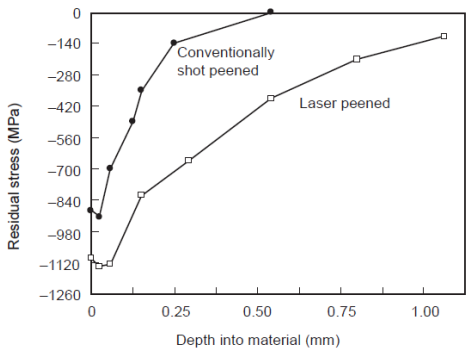


Figure 2.29: RS Profile induced by LSP and SP[1].

Figure 2.29 shows a similar residual stress depth profile induced by LSP and by SP on Inconel 718. The residual stresses induced by LSP has a maximum value of around -1120 MPa at a depth of around 0.1 mm. Thereafter, the residual stress becomes less compressive with increasing depth and reaching zero after a depth of 1 mm[1]. The residual stresses induced by LSP are significantly more compressive when compared to the stresses induced by SP. The shape of the depth profiles and the residual stress gradient are typical of those induced by surface enhancement techniques[1].

2.2.7 The Effect of Varying LSP Parameters on the Residual Stress

In the previous sections it was shown that the residual stress profile induced by LSP has a significant impact on the performance and properties of the treated samples. Due to this reason, an important part of characterising the LSP process is the study of the induced residual stresses. Because LSP can be influenced by controlling a variety of parameters (as mentioned in section 2.1.2), it is thus important to study the effect that these parameters individually have on the induced residual stresses. This section aims to highlight the main parameters authors use to conduct LSP, these parameters are the laser power intensity, laser spot size and coverage ratio. The following is some of the previous work that was found in literature.

2.2.7.1 Effect of Changing Laser Power Intensity

Figure 2.30 shows the IHD residual stress results for A356 Cast Alloy Samples. The samples were treated with LSP using a LALP pulsed Nd-glass prototype laser with a 50% Overlap using laser power intensities of values of 0.9 GW/cm^2, 1.5 GW/cm^2 and 3.0 GW/cm^2[26].

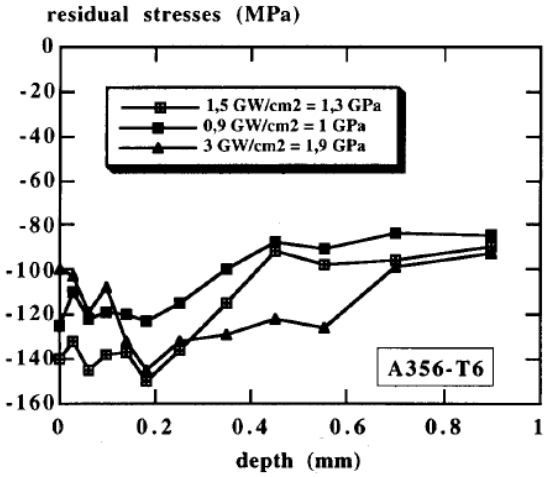


Figure 2.30: Residual Stresses in A356 Alloy Peened with Different Power Intensities[26].

The effect of increasing power intensity is that the residual stresses were more compressive through the depth of the material, but also the residual became more tensile near the surface of the material. The location of the peak residual stress occurred at a deeper depth within the sample and the depth at which the residual stresses were compressive was also increased with increasing power intensity. From Figure 2.30 it can be observed that the surface stresses increase up to -145 MPa for 1.5 GW/cm^2, but further increase in power intensity to 3.0 GW/cm^2 tend to reduce the stress level to about -100 MPa, whereas the in-depth stress levels continue to increase[26].

Figure 2.31 below shows the residual stress results obtained for 7049 T73 aluminum alloy samples using the slitting method. The samples were treated with LSP using a novel Nd:glass, flash lamp pumped laser with a 10% Overlap using laser power intensities of values of 40 J/cm^2 and 60 J/cm^2[27]. The effect of increasing the PI resulted in a minor increase in the compressive residual stress through the entire depth[27].

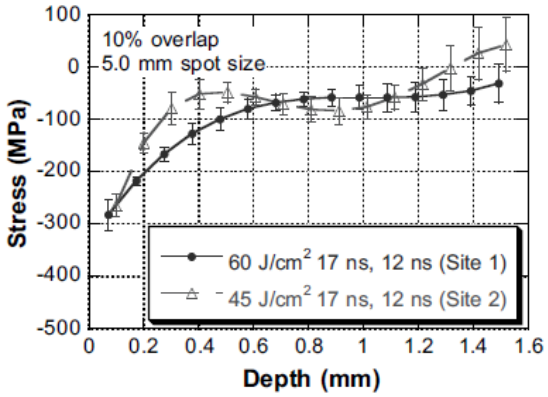


Figure 2.31: Residual Stresses in 7049 T73 Al Peened with Different Power Intensities[27].

The increase in compressive residual stresses through the depth of the material as the power intensity increases can be attributed to an increase in the shock wave pressure[1]. It has been shown that as the shock wave pressure increases with power intensity, at some point will achieve saturation as shown in Figure 2.32[1]. Therefore, this means that eventually the effect of PI on the residual stress will also saturate[1].

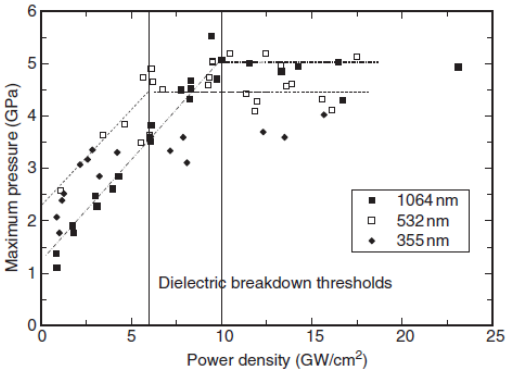


Figure 2.32: Peak Plasma Pressures as a Function of Laser Power Density[1].

The dielectric breakdown phenomenon illustrated in Figure 2.32 has been shown to occur at relatively high power intensity values. This phenomenon is the generation of plasma not on the material surface and thus also absorbs the incoming laser pulse resulting in limiting the energy to generate a shock wave and therefore drastically decreases the effectiveness of the LSP treatment[1]. The breakdown threshold which occurs after a certain critical PI value has been reached depends on the breakdown properties of the confinement media as well as the wavelength of the laser used[1]. Therefore, the breakdown threshold should be determined for the laser system used.

2.2.7.2 Effect of Changing Laser Spot Size

Figure 2.33 and Figure 2.35 shows the residual stress results obtained for an research experiment that conducted a parametric study of laser spot size and coverage on the LSP induced residual stress. LSP was performed on aluminium alloy 2024-T341 samples using a Nd:YAG laser using 0.3 mm and 0.4 mm spot size with 40% and 60% coverages ratios. The residual stress was measured using IHD method.

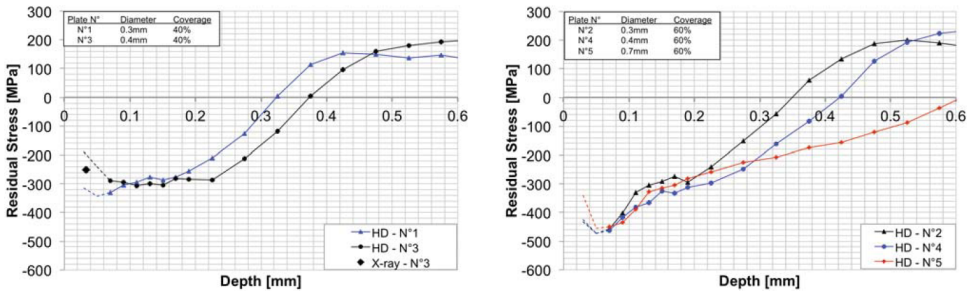


Figure 2.33: Effect of Changing Spot Size at Different Coverage Ratios[6].

Figure 2.33 shows two sets of results, where the coverage ratio for the LSP treatment was kept constant and the laser spot size was changed. The results obtained show that increasing the spot size caused an increase in the depth to which the residual stresses were compressive, but there was relatively no change in the maximum compressive value[6].

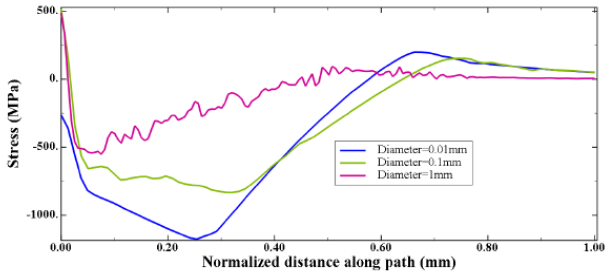


Figure 2.34: Effect of Changing Spot Size on Residual Stress[28].

Figure 2.34 shows results obtained for an experiment that was conducted using a laser energy of 3 J with 3 different spot sizes. The effect of spot size was studied to understand the variation of peak compressive stresses[28]. It should be noticed that from Figure 2.34 the peak compressive stress is high for the spot diameter of 0.01 mm and with increase in spot size, the peak compressive stress decreases due to relaxation of the induced shock wave[28]. Therefore, small beam diameter is beneficial to induced higher compressive residual stress, but this will increase overall processing time[28]. Note that near the surface, the larger spot size causes tensile residual stress to occur, but the depth to which the residual stresses are compressive was increased. Thus, the two studies outlined in this section show that the primary effect of increasing the spot size is to increase the depth at which the residual stresses are more compressive.

2.2.7.3 Effect of Changing the Coverage Ratio

Figure 2.35 below depicts two sets of plots where the spot size and power intensity were kept constant and only the coverage ratio was changed. The results show that increasing the coverage ratio caused an increase in the stresses near the surface of the material, but there was little to no change in the stresses through the depth of the sample. This increase in the compressive stress was accompanied by an increase in the tensile stress through the depth of the material.

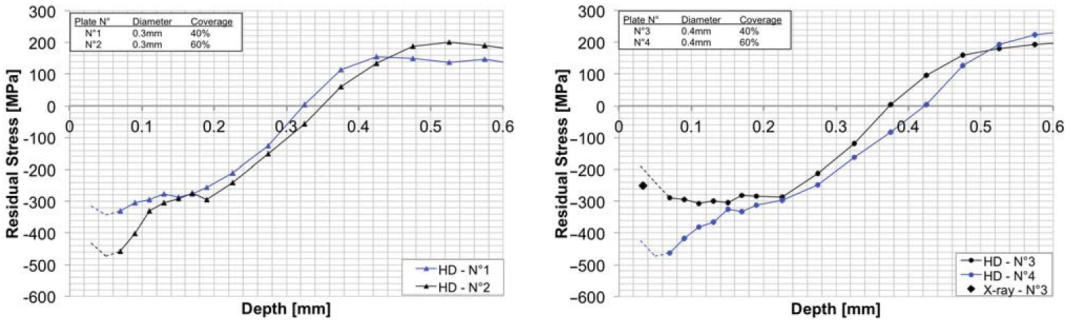


Figure 2.35: Effect of Changing Coverage Ratios with Different Spot Sizes[6].

Figure 2.36 shows the experimental depth profiles obtained for LSP induced residual stresses for three representative values of overlapping. The samples were processed using Nd:YAG laser source with a laser energy of 0.5 J with a 1.5 mm spot size[29]. From the graph depicted below it can be seen that there is an increase in the penetration depth and in the maximum compressive residual stress for the increasing density of laser pulses[29].

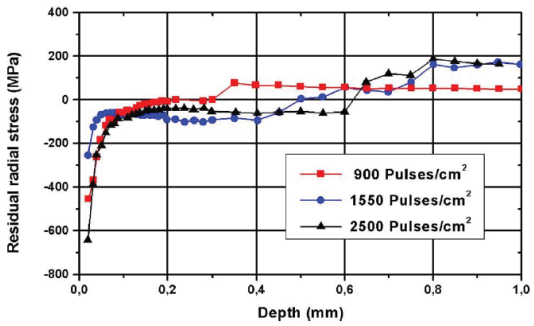


Figure 2.36: Effect of Changing Coverage Ratios[29].

The effect of increasing coverage ratio was to increase the compressive residual stress through the depth and near the surface. The position of the maximum remains unchanged and the depth to which the residual stresses were compressive was increased[6],[29]. The effect of the increased coverage is more pronounced near the surface of the sample[6],[29]. In cases presented above, it was shown that by increasing the coverage ratio leads to an increase in the amount of compression induced near to the surface, but significantly unchanged through the depth.

2.2.7.4 Summary

This subsection has shown that the various effects of certain LSP parameters on the compressive residual stress profile induced by LSP. Table 2.2 below provides a summary. Additional parameters are also included in the summary due to the dependent nature they have with each other (i.e. laser energy is directly related to the laser power density).

LSP Parameter	Effect on Residual stress
Spot Size	An increase in size causes an increase in the penetration depth, but not in the maximum compressive residual stress[6].
Coverage Density	An increase in coverage density causes an increase in the penetration depth and in the maximum compressive residual stress[6],[29].
Laser Energy	An increase in energy causes an increase in the penetration depth and in the maximum compressive residual stress [1],[26],[27].
Pulse Duration	An increase in pulse duration causes an increase in the penetration depth and in the maximum compressive residual stress [28].
Intensity	An increase in intensity causes an increase in penetration depth and in the maximum compressive stress [1],[26],[27].
Coverage Pattern	Residual stresses are more compressive in the longitudinal direction to the laser movement than in the transverse direction[28].

Table 2.2: Effects of LSP Parameters on Residual Stress.

These experiments outlined in this section were performed with different types of materials and with different LSP systems. It is therefore important to understand the effect that each of these parameters have on the specific alloy that were processed in different types environments.

2.3 Measurement Techniques

2.3.1 Surface and Microscopic Analysis

The microscopic details and the surface of the laser peened samples were studied at high magnification under an optical microscope. The optical microscope can be used to capture the finer details of the materials surface that is invisible to the naked eye. These surface features are important to study, because these features are a part of the materials property and thus can influence the materials performance and functionality for a given application. There are various instruments that can be used to observe points of interest at various magnification levels.

For this research programme optical microscopy and scanning electron microscopy (SEM) will be used to observe the peened samples. The SEM is a type of electron microscope that produces images of a sample by scanning the surface with a focused beam of electrons and very high magnifications whereas for optical microscopy is employed to closely view a surface through the magnification of a lens with visible light.

2.3.2 Surface Roughness Testing

The surface roughness can be measured by using two different methods, namely the contact and non-contact method. The contact method make use of a measurement stylus, the stylus is dragged across the surface to detect and record the texture of the surface. The non-contact method makes use of special types of optical instruments that record the surface texture by using advanced imaging techniques such as the atomic force microscope (AFM). The only disadvantage of using the contact method is that the stylus tip comes into physical contact with the surface of the material which can lead to undesired contamination of the material and data.

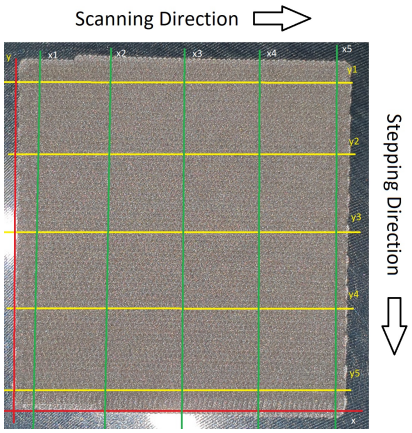


Figure 2.37: Roughness Testing Method.

For this research project the contact method will be used, by using the SRT 6210 surface roughness testing machine and the JENOPTIK waveline HOMMEL-ETAMIC T8000, both machines make use of a probe stylus which measures the surface roughness of the material. The surface roughness of the material will be tested along the stepping and scanning directions, five measurements will be taken in each direction as indicated in Figure 2.37. The measured surface roughness will be compared to that of the unpeened base sample.

2.3.3 Microhardness Testing

The hardness of a material is a characteristic and not a property of a material and thus is important to define the theory behind hardness testing. Hardness is defined as the materials resistance to permanent deformation such as indentation or wear[34]. The importance of hardness testing has to do with the relationship between the hardness and the other properties of a material. The hardness test is generally preferred over other tests because it is quick, simple and relatively non-destructive. There are various types of methods that can be used to determine the hardness of the material, but for this research programme the Vickers microhardness testing method will be used.

The Vickers hardness testing method consists of indenting the material with a diamond tipped indenter which is subjected to a loads of 1 to 100 kgf. The indenter is in the form of a pyramid-shaped diamond of 136° as shown in Figure 2.38 The full load is generally applied for 10 - 15 seconds[34]. The two diagonals of the indentation left on the surface after the removal of the load are measured using a microscope and their average calculated. The hardness value (HV) for the Vickers hardness testing process is calculated using Equation 2.4[34]:

$$HV = \frac{2Fsin\frac{136°}{2}}{D^2} \tag{2.4}$$

Where: F = Load (kgf), D= Arithmetic mean of the two diagonals (mm), HV= Vickers hardness

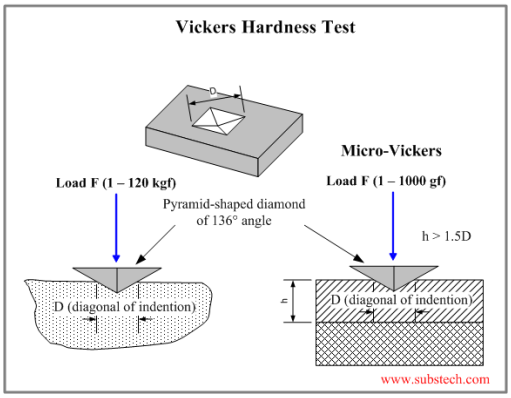


Figure 2.38: Hardness Testing Method.

2.3.4 Residual Stress

In the previous sections, it was conveyed that part of developing the LSP process was to characterise the effect of varying LSP parameters on the induced residual stresses. The residual stresses induced near the surface and maximum penetration depth is important in developing the LSP process. Therefore, a robust strategy is required in order to accurately measure and characterise these induced stresses at the various depths in the peened sample. This section will explore the methods that will be used to evaluate to residual stresses induced by the LSP process for the current research project.

Firstly, it is important to define the residual stress. A residual stress is a type of stress that exist inside a material in absence of any external force or thermal gradient that can be caused by plastic deformation[30]. Because the residual stress exists in an absence of any applied loading, they must therefore be globally balanced inside the material[30].

Residual stresses can be characterized by the scale in which they exist within a given material. Stresses that occur over long distances in a material are referred to as macro residual stresses whereas stresses that exist locally between grains or inside a grain are called micro residual stresses. In simpler term the residual stress is the stress that is present in an object or material in the absence of any external force or load.

Therefore, the total residual stress at a given location within a material is the sum total of all 3 types of stresses. The residual stress types are as follows:

- Type I Stresses: Macro residual stresses occurring over distances that involve many grains[30].
- Type II Stresses: Micro residual stresses caused by the differences in the microstructure of a material and will occur over distances comparable to the size of the grain. It can also occur in single-phase and multi-phase materials[30].
- Type III Stresses: Exist within a grain structure as a result of crystal imperfections[30].

There are two different techniques that can be used to evaluate the induced residual stress in a material. Namely, the mechanical residual stress measurement method and the diffraction residual stress measurement method.

The mechanical residual stress measurement method determine the residual stresses in a sample by mechanically releasing these stresses and strains embedded within a material. This can be done by performing a cut or by drilling a hole and measuring the effect of the stress or strains released.

There are various methods that can be used such as the incremental hole drilling method and the slitting method among others. Each of these techniques have there unique advantages,

the techniques mentioned before measure to different depths and resolutions. The methods can either be destructive or semi-destructive to a material as shown in Figure 2.39[31].

Figure 2.39 shows a comparison between the various stress measurement techniques for the depths and resolution that can be achieved. This shows that different measurement techniques can be used to fully describe the residual stresses at the at all depths within a sample. Therefore, different combination of the techniques can be used with each other to fully describe the residual stress profile.

The diffraction residual stress measurement method determine the stress within a sample by using the principle of diffraction to measure the distance between crystallographic planes (d-spacing)[30]. When the material is in tension the d-spacing increases and when under compression the d-spacing decreases. Stresses can be determined from measuring the d-spacing. X-rays diffract from crystalline materials at known angles 2θ according to Bragg's Law[30]. Some of these methods include: Laboratory X-Ray Diffraction (L-XRD), Synchrotron XRD and Neutron Diffraction (ND), etc. Each of these methods listed previously measure to different depths and resolutions however they are all non-destructive and each has its own advantages and disadvantages.

These methods outlined in this section can be easily integrated with each other and can be used for comparative analysis for measuring the stress at the different depths, as highlighted in Figure 2.39. For this research program the Incremental Hole Drilling method (IHD) and the Laboratory X-Ray Diffraction (L-XRD) will be used as it is readily available within the university. These details regarding these two methods will be outlined further.

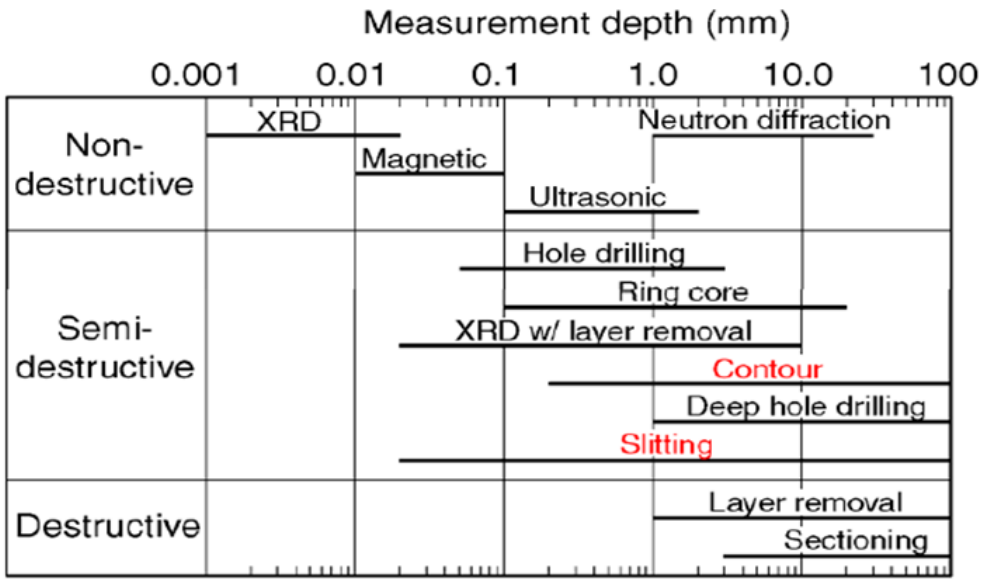


Figure 2.39: Depth Range for various Measurement Techniques[31].

2.3.4.1 The Incremental Hole Drilling Method

The Incremental Hole Drilling method (IHD) as depicted in Figure 2.40 is used to measure the residual stresses across the depth of the material by drilling a hole at the center of a strain gauge rosette shown in Figure 2.41 and then measuring the relaxed strains that are released by the drilling process.

The residual stresses are calculated using the relaxed strains, the materials elastic properties and the calibration coefficients that are tabulated in the ASTM E837 standard[32].

The IHD method can be considered as a semi-destructive method. The technique as described in the ASTM E837 recommended the depth steps, maximum depth as well as the limitations for different strain gauge rosettes.

By adhering to the recommendations and guidelines in the ASTM standard, the hole-drilling method can be applied easily, because no special expertise is required in gathering the measurements.

The hold-drilling method is described as a semi-destructive technique, because the small hole will not significantly affect the structural integrity of the tested material (the hole is generally in a region of 0.8 mm to 4.8 mm in both diameter and depth)[32].

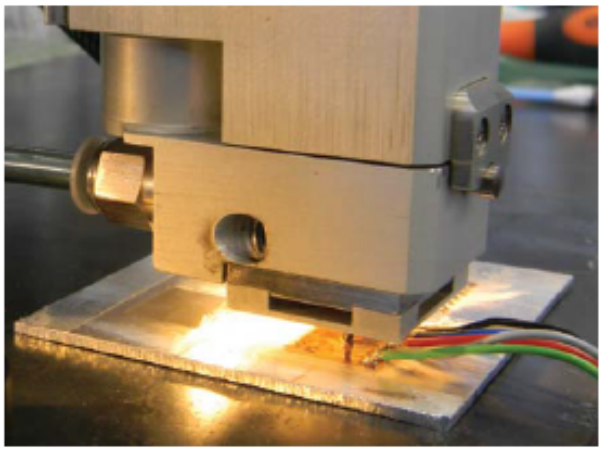


Figure 2.40: IHD Testing.

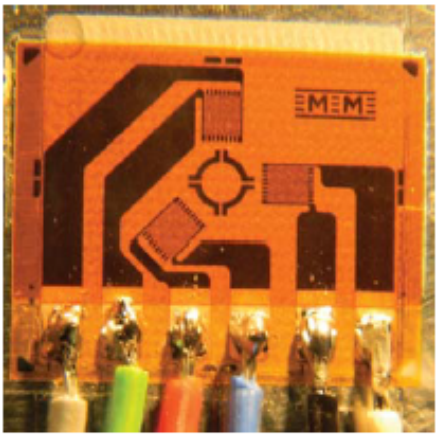


Figure 2.41: Strain Gauge.

The IHD technique is relatively costly as the components used for the testing are disposed after each test, this includes the strain gauge and the drill bit. It is therefore important that the steps outlined in the ASTM standard are strictly followed so that the test conducted remain successful and the rate of failure is kept to a minimum.

2.3.4.2 X-Ray Diffraction

X-Ray Diffraction (XRD) is a process of irradiating a test sample with X-rays and measuring the pattern that is created by the light after it has been diffracted by the crystal structure of the material. The diffraction pattern consists of a number of peaks at various angles and positions that are unique to the sample[30],[33]. Bragg's Law, represented by Equation 2.5 and in Figure 2.42 is used to determine the diffraction of X-rays from crystalline materials.

$$n\lambda = 2dsin\theta \tag{2.5}$$

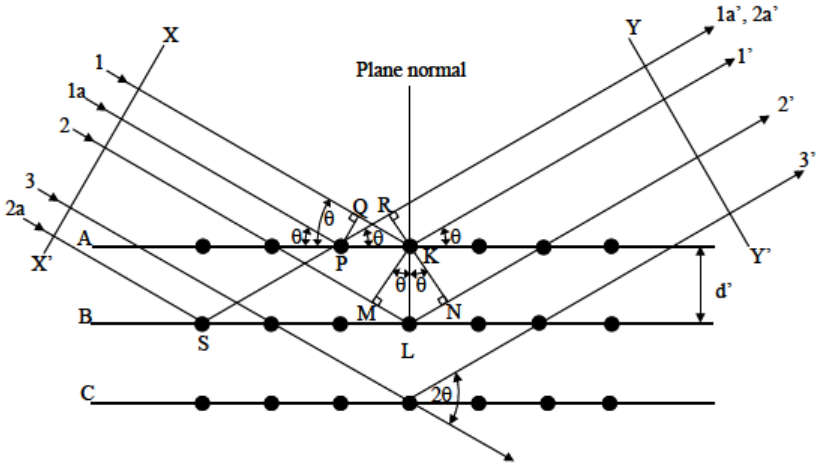


Figure 2.42: Bragg's Law of Diffraction[33].

To determine the residual stress, the lattice planes in the crystalline structure will be deformed from its original reference position which creates shifted diffraction peaks. This peak shift is used to calculate the residual strain and the residual stress of the material.

The penetration depth of XRD depends mainly on the intensity of the light used by the XRD instrument and the light absorption properties of the material[33]. Most laboratory XRD instruments can take depth measurements of approximately 8 μm for Aluminium alloys, However the synchrotron XRD instrument can take depth measurements between a range of 145 μm - 1000 μm, this range depends on the power of the synchrotron.

XRD can be used in conjunction with hole-drilling, since the residual stresses measured by XRD is closer to the surface and because it is a non-destructive method. Therefore, both methods can be used to compare residual stress values at a relative depth. XRD can also be used with electro-polishing to determine residual stresses at higher depths. Electro-polishing is a technique that removes material, so that deeper residual stress measurements can be taken. The polishing process changes the stress field and therefore has to be used with certain correction factors [33].

2.4 Material Specifications

2.4.1 Aluminium Alloys

Aluminium alloys have a wide range of properties and characteristics, due to this it is used extensively for various engineering applications and structures. Due to the wide range of properties available for aluminium alloy, a system is used to classify these alloys, this is done by using a number system (ANSI standard) or by using names that indicate the main alloy constituents (DIN and ISO standard).

To select the correct type of aluminium alloy for a given application requires the tensile strength, ductility, density, workability and corrosion resistance to be considered. Aluminium alloys have been used extensively in the aerospace industry due to the high strength-to-weight ratio provided by the alloy[35].

2.4.1.1 7075-T651 Aluminium Alloy

7075-T651 aluminium alloy is a high strength alloy which is solution heat treated, stress relieved and then artificially aged. It has excellent mechanical properties including high strength, toughness, exhibits good ductility, good resistance to fatigue and has good corrosion resistance. It is one of the most commonly used aluminium alloy for highly stressed environments, and has been generally been utilized in the aero space industry. The T651 temper helps increase the resistance against stress-corrosion cracking. The chemical composition of the 7075 alloy is given Table 2.3[35]:

Chemical Element	% Present	Chemical Element	% Present
Aluminium (Al)	87.1 - 91.4	Silicon (Si)	Max 0.4
Chromium (Cr)	0.18 - 0.28	Titanium (Ti)	Max 0.2
Copper (Cu)	1.2 - 2	Manganese (Mn)	Max 0.3
Zinc (Zn)	5.1 - 6.1	Other (Each)	Max 0.05
Magnesium (Mg)	2.1 - 2.9	Others (Total)	Max 0.15
Iron (Fe)	Max 0.5		

Table 2.3: Chemical Composition of 7075 Aluminium Alloy.

The 7075-T651 aluminium alloy is typically used for highly stressed applications, aircraft components, meter shafts and gears, missile parts, aerospace and defence applications[35].

3 | Research Objectives

From the extensive literature review performed for the field of Laser Shock Peening (LSP) in the previous section, a number of key opportunities have been identified to conduct further research and add to the already growing database of LSP in South Africa (SA). Most of the LSP based research in SA is conducted by University of the Witwatersrand in conjunction with the National Laser Centre (NLC) a laser based division of the South African Council for Scientific and Industrial Research (CSIR) located in Pretoria.

The laser system that will be used for this research programme is a mid range laser which is located at the CSIR, as outlined in subsection 2.1.1. The current research programme is part of on ongoing going initiative for LSP based research for aeronautical grade alloys (such as aluminium alloy 7075-T651) using different LSP parameters between the University of the Witwatersrand, the CSIR and the SA LSP Group.

LSP is a surface enhancement treatment that has various beneficial effects on a wide range of metallic alloys as identified in sections 2.2 - 2.5. The process improves the fatigue life, corrosion resistance and increases the hardness of the processed material. However, negative effects such as the increase in surface roughness, are somewhat negligible because this can be easily mitigated by using simple post-processing techniques if necessary. Overall the benefits brought by using LSP is higher and thus the field is worthwhile to conduct research and extend the current database for LSP. It was observed that the main reason for the beneficial effects induced by LSP, can be attributed to the compressive residual stress field imparted by the LSP process through the depth of the treated material.

From section 2.6, it was shown that variations in any of the LSP parameters has a significant impact on the final induced residual stress field. It is clear that an extensive amount of research has been done by numerous authors looking into the effect these variations in parameters have on the residual stress profile.

Authors mainly conducted experiments to study the LSP induced stresses by changing either the power intensity, spot size and the coverage ratio. They also characterised the effect that LSP has on the surface integrity, the surface roughness, the microhardness and the microstructure of the treated alloys. The authors conducted research on a variety of alloys while also

studying the effects of different LSP parameters have on the induced stress profiles. However, there was no study looking specifically at aluminium alloy 7075 using different adhesive tapes as the sacrificial coating and using different power intensities and coverage ratios. Therefore, this was identified as the key research area for the current research programme as this will contribute to the already growing LSP database and knowledge.

Section 2.7 showed that to measure the depth-resolved residual stress profile a variety of instruments and techniques can be used. The LSP induced can be measured using methods that have their individual strengths and weaknesses such as cost, time, availability, different depths measurement, use different resolutions and can either be destructive or non-destructive.

In order to study the effect of LSP on the residual stress profile, It is therefore important to develop a strategy to evaluate the stress profile using the appropriate techniques and comparing the results obtained against each other. Since no study in past literature had compared a vast range of stress profiles using different ablative media for Al 7075, this too can be identified as a research area in which a contribution to knowledge can be made.

Therefore, the research questions and objectives for this research programme are as follows:

Research Questions

1. What will be the effect of using LSP with tape on the surface integrity of the peened samples and will the different tapes provide better or comparable results than that of conventional LSP methods?
2. Can LSP using tapes as the sacrificial medium on aluminium provide better or comparable residual stress profiles than that of conventional LSP methods such as LSPwC ?

Research Objectives

1. To investigate and observe the interaction between the adhesive layer of the tape and the surface of the peened material using optical microscopy.
2. To study the damage induced on the tape by the LSP process using optical microscopy.
3. To study the surface integrity for the LSP processed samples using optical microscopy, scanning election microscopy, surface roughness testing and microhardness testing.
4. To characterise and measure the residual stress profiles near the surface of the material and the across depth of the material for the various LSP treatments using the different tape as the ablative medium.

5. To optimise the LSP parameters for samples peened with the various tapes, so that the residual stress profiles and surface integrity can be accurately engineered for specific requirements.

A range of LSP parameters (I_0, SS, $\%Cv$) have already been previously investigated for Aluminium alloy 7075-T651 using the LSP work cell at the CSIR by two MSc student from the University of the Witwatersrand and by the SA LSP Group. Therefore, there is large database that is available and could be used for comparative studies. The results that will be obtained for the samples peened with tape will be assessed against the results that have already been investigated. The results that will be obtained from the current research project will add to the already growing database in SA.

4 | Experimental Activity

The research project was divided into two phases: the first phase used the different ablative media with fixed LSP parameters to answer objectives 1 - 4, whereas the second phase was conducted with varying LSP parameters to answer the research objectives.

The experiments performed for the two parts were conducted with the same equipment and instruments, thus all experimental activities for these two phases are presented together in this chapter. The differences in how the two different experiment were performed will also be outlined in this chapter.

The following scheme represented by Figure 4.1 in block form will be implemented for the current research program:

The secondary aim for phase 1 is to select a suitable ablative tape that can be used for analysis the 2nd phase of the project. The 1st phase will also be used as a benchmark and if possible improvements will be made to the experiment design so that the results obtained have a higher degree of accuracy.

The outline of this chapter will be as follows: first to describe the steps used to prepare and process the samples for the two cases. It will then describe in detail the steps taken and the apparatus used for the various studies and measurements that were performed on the samples.

The apparatus used for the research project in this section are listed with descriptions. Further specification and serial numbers of the apparatus can be found in Appendix A. Each process will be listed in its own section with the precautions that were taken, this is done because of the lager number processes that have been used to conduct the research project.

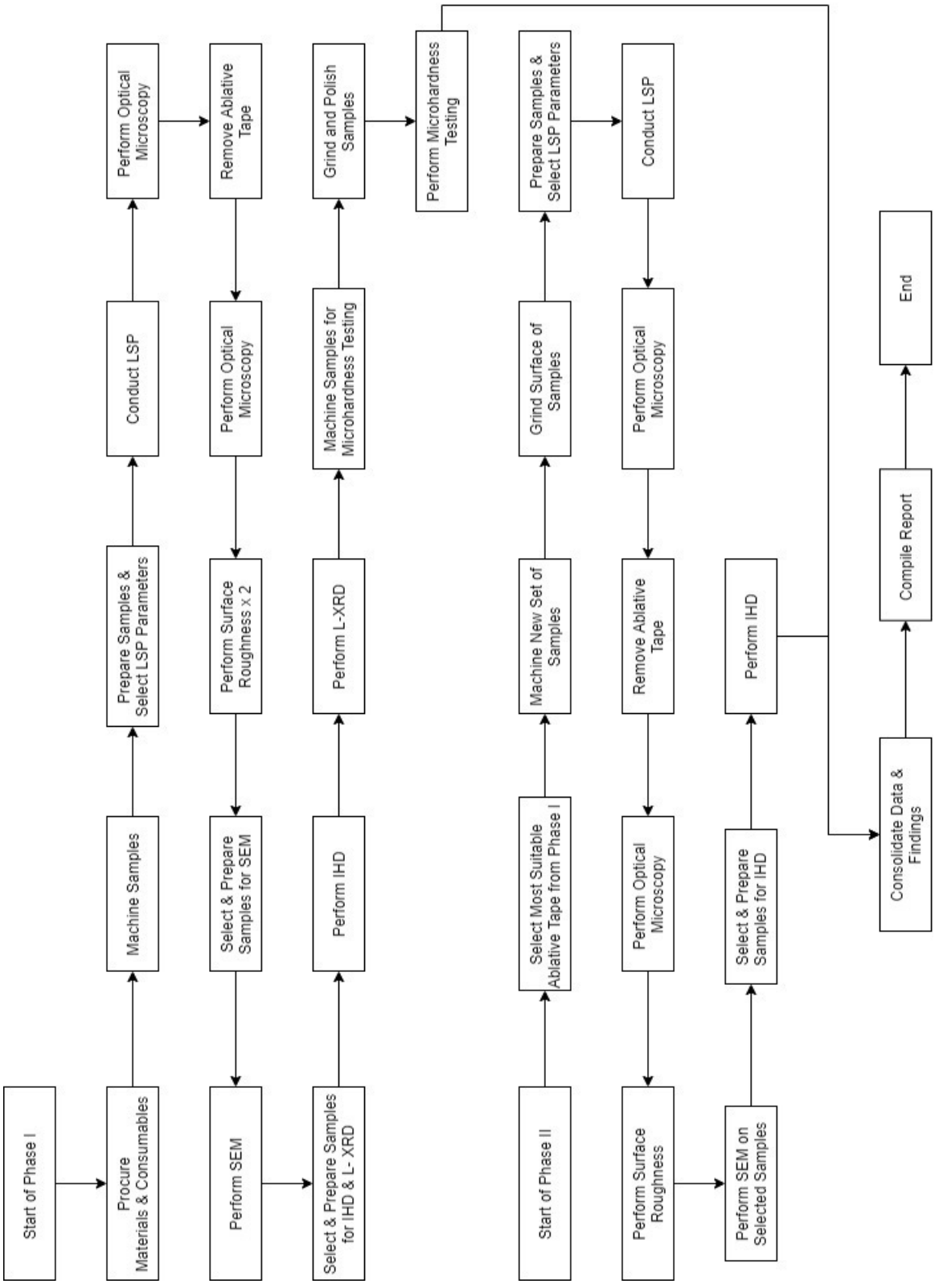


Figure 4.1: Flow Chart for Experimental Activity.

4.1 Experimental Methodology

Aluminium alloy 7075-T651 with a thickness of 15 mm was used for the first phase of the experiment. The plates were machined to a thickness of 14 mm and cut into square specimens measuring 60 mm x 60 mm by a CNC machine. These test pieces were then cleaned, and than coated with 11 different types of adhesive tape (ablative medium). A total of 48 samples were prepared for phase 1 of this research project. These samples were treated using LSP at the CSIR with the following LSP parameters, laser power intensities of 1.5 GW/cm^2, 2 GW/cm^2, 3 GW/cm^2, 4 GW/cm^2 using a laser spot size of 1 mm with a 70% coverage ratio. The peening area for the sample were 20 mm x 20 mm. These samples were then analysed, evaluated and studied using the following methods:

1. Optical microscopy at the University of the Witwatersrand, South Africa.
2. Surface roughness testing at the University of the Witwatersrand and at the University of Johannesburg, South Africa.
3. SEM analysis at the University of the Witwatersrand, South Africa.
4. Microhardness testing at the University of the Witwatersrand, South Africa.
5. IHD testing at the University of the Witwatersrand, South Africa.
6. L-XRD testing at the CSIR, South Africa.

For phase 2 of the experiment the samples were prepared from 10 mm thick Al 7075-T651 plate. The plates were machined to a thickness of 9 mm and cut into square specimens measuring 40 mm x 40 mm by a CNC machine. These samples were further processed by 3 stages of grinding and then by 3 stages of polishing to acquire a final surface finish in the range of of 0.05 - 0.1 μm. These test pieces were then cleaned, and than coated with adhesive tape (ablative medium). A total of 16 samples were prepared for phase 2 of this research project. These samples were treated using LSP at the CSIR with the following LSP parameters, laser power intensity of 4 GW/cm^2 using a laser spot size of 1 mm with the following coverage ratio 30%, 40%, 50%, 60%, 70%, 80%, 90%. The peening area for the sample were 15 mm x 15 mm. These samples were then analysed by the steps listed previously, and including the L-XRD analysis that was conducted at the CSIR, South Africa.

4.1.1 Sample Preparation

The 7075-T651 aluminium alloy that were used for the experiment arrived as 1000 *mm* wide, 990 *mm* long and 15 *mm* thick plate. This aluminium stock was than cut and machined to the desired dimensions of 60 *mm* x 60 *mm* x 14 *mm* as shown in Figure 4.2. A separate plate measuring 850 *mm* x220 *mm* x10 *mm* was also, this was machined and cut to the following dimensions 40 *mm* x 40 *mm* x 9 *mm* as shown in Figure 4.3

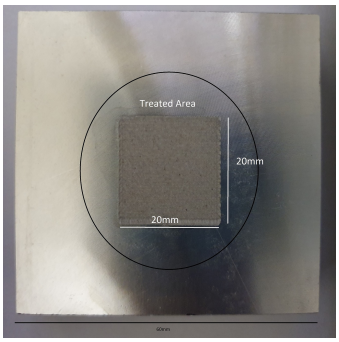


Figure 4.2: Sample 60 *mm* x 60 *mm*.



Figure 4.3: Sample 40 *mm* x 40 *mm*.

These test samples were coated using different tape ablative layers introduced in the next subsection. They were processed using 4 different power intensities using the same coverage ratio and laser spot size. The material inspection certificate can be found in Appendix A.

The 7075-T651 plate was supplied by NK Cuttings and the chemical composition is shown in Table 2.3 in subsection 2.8.1. The material properties of the alloy are shown in Table 4.1 below:

Table 4.1: Material Properties for Aluminium Alloy 7075-T651.

Material Property	Value
Tensile Strength [MPa]	540
Yield Strength [MPa]	460
Vicker's Hardness [HV]	175
Elogation %	8
Surface Finish	Uniform brushed
Modulus of Elasticity [GPa]	71.7
Poisson's Ratio	0.33

The samples were prepared and cut at the laboratory workshop at the School of Mechanical, Industrial and Aeronautical Engineering at the University of the Witwatersrand. The apparatus used to prepare these sample are outlined in the following subsection.

4.1.2 Cutting Apparatus

The following equipment and apparatus was used to cut the stock aluminium plate.

1. Startrite 30 RWH Bandsaw - This machine was used to cut both the big(60 mm x 60 mm) and small (40 mm x 40 mm) test samples from the stock plate. (see Table A.1 in Appendix A)
2. 30 cm ($\pm$ 0.5 mm) ruler - The ruler was used to measure and mark the lengths required for the cutting and mounting of the samples.
3. Vernier Calliper - The vernier was used to measure the thickness of the samples.

The procedure and precautions used to cut the Al 7075 plates can be found in Appendix A.

4.1.3 Ablative Coatings: Adhesive Tapes

Adhesive tapes generally refers to a combination of backing materials which is coated with a type of adhesive. For LSP the adhesive tape which can be used as a ablative medium that covers the peening surface to protect it against the thermal damage that is created during the peening process. From previous investigations tape has been found to be very effective in protection the surface integrity of the material when conducting LSP.

For conducting LSP, tape is readily available and using tape in general makes for quicker application as it reduces the overall processing time than compared other ablative media such as paint. The following are the ablative tape media that have been selected for the current research programme. The detailed description and properties for the tapes can be found in Appendix A[36].

- Aluminium Foil Tape (1436 3M)
- Duct Tape (1900 3M)
- Vinyl Tape (471 3M)
- Duct Cloth Tape (2903 3M)
- PVC Insulation Tape (21 Nitto)
- Vinyl Tape (472 3M)
- Polymide Tape (HB830 Hi-Bond)
- Clear Box Sealing Tape (313 Scotch 3M)
- Flame-Retardant Tape with Polyester Film (1350-1 3M)
- Vinyl Tape (Super 88 Scotch 3M)
- Micron Copper Foil Shielding Tape (AT525 35)

Note: Once the samples were processed and cleaned, the adhesive tape was applied over the targeted peening area. Finally the samples were labelled and stored in a sterile plastic packet.

4.2 Laser Shock Peening

The LSP for the two phases of the project were performed at different times but using the same apparatus and following the same procedures and precautions.

4.2.1 LSP Apparatus and Equipment

The LSP was performed at the National Laser Centre (NLC) at the CSIR in Pretoria, South Africa using a Quanta-Ray Pro Spectra Physics Nd:YAG laser. Access to the laser was granted through the Rental Pool Program of the NLC. The system is shown in Figure 4.4 and the specifications are listed in Table 4.2.

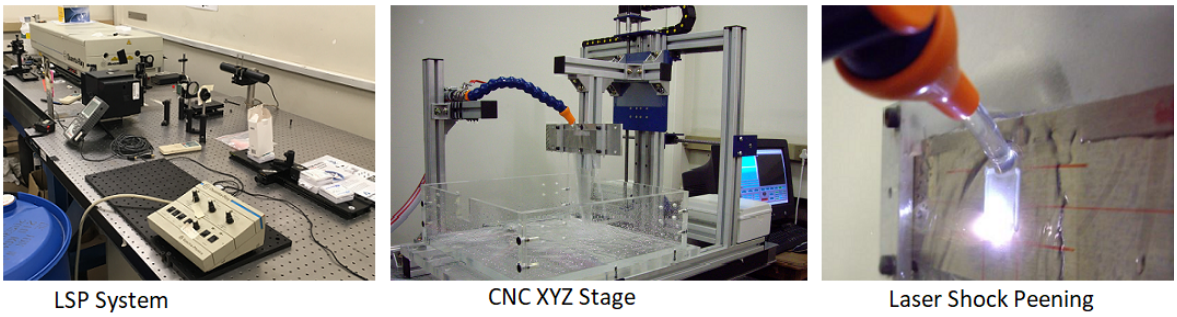


Figure 4.4: LSP System at the NLC CSIR.

Figure 4.5 illustrates the schematic of the LSP system used at the CSIR. The energy of the laser is controlled and set using the laser attenuator. The laser system is stationary and the laser pulse is fired at sample which is moved by the CNC XYZ Stage which control where the pulse will strike on the sample. A CNC code is used to automate the coverage pattern in which the LSP is performed. The spot size is achieved by changing the focal distance between the optical lens and the CNC XYZ stage (along the z-direction). The pulse density is controlled by changing the speed at which the CNC stage moves across the laser beam path (the laser pulses at a constant frequency), This is done by controlling the CNC motor speed inputs for the x and y-direction. Other laser parameters such as power intensity and coverage ratio are achieved by controlling the previously mentioned laser parameters.

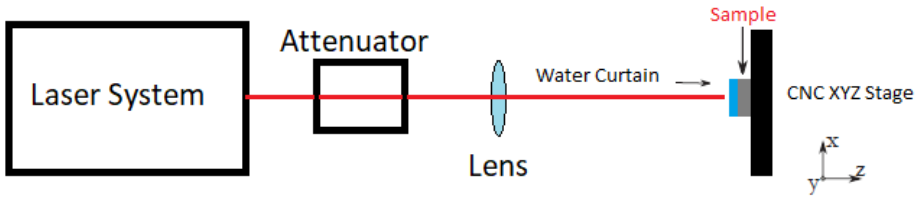


Figure 4.5: LSP Schematic.

Quanta-Ray Pro Spectra Physics	
Laser Type	Nd:YAG
Wavelength [nm]	1064
Pulse Frequency [Hz]	20
Energy Range [J]	0.2 - 1
Spot Shape	Circular
Spot Size Range [mm]	0.5 - 2.5

Table 4.2: Quanta-Ray Pro Laser Specifications.

4.2.2 LSP Experimental Set-up

Figure 4.6 illustrates the geometry of the LSP treatment area used for the research project. The samples were treated with LSP patches of 20 *mm* x 20 *mm* in size for phase 1 of the project and 15 *mm* x 15 *mm* in size for phase 2 of the project.

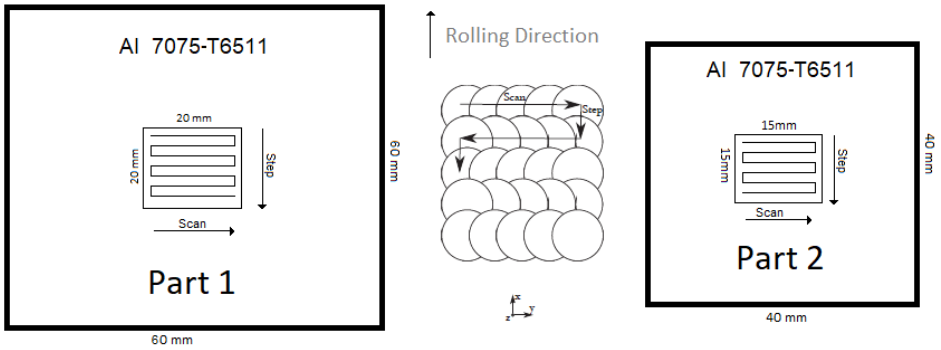


Figure 4.6: LSP Schematic.

All of the laser shock peening that was conducted, were done so by using the raster pattern, as illustrated in Figure 4.6. The samples were aligned such that the step direction was aligned with the x-direction (rolling direction) and the scanning direction was aligned with the y-direction.

Table 4.3 and Table 4.4 also illustrates the parameters that were used for the experiment. These parameters were selected based on previous research conducted by the South African LSP Group and the previous MSc students from the University of the Witwatersrand that worked with Al 7075 and other similar aluminium alloys. Four different power intensities were chosen to determine if the results were consistent for different ablative tape used for phase 1 of the project. The coverage ratio was varied for the 2nd phase of the project. The spot size was fixed at 1 *mm* for both experiments.

4.2.3 Experiment Procedure

The following are the experimental procedures for treating a sample with LSP:

1. Switch on the laser system, the cooling unit, the extractor then allow for at least 3 hours so that the laser can stabilise.
2. Obtain the laser spot size required for the experiment by changing the focal distance between the optical lens and the CNC XYZ stage.
3. Set the laser energy required for the experiment on the laser attenuator.
4. Mount the sample using bolts and washers to the CNC XYZ Stage.
5. Check that the CNC code has the correct parameters entered into it. Once checked load and build the code.
6. Set the laser to pulse and start the water flow and ensure that the water curtain is flowing smoothly over the sample.
7. Run the CNC code to start the peening process.
8. Once the CNC code is completed, turn the water and switch the laser pulse off then remove the sample.
9. Repeat steps 3-8 for each sample.
10. Switch off the laser system and corresponding instrumentation.

The following are the precautions that needs to be taken to ensure that the treatment is performed in a repeatable and safe manner.

- All the samples were processed on the same day to avoid fluctuations and variation in the performance of the laser system.
- The laser energy level was monitored and recorded before and during the test to ensure that optimal performance and minimal deviation in the LSP treatment for the various samples.
- The position of the sample before and after the treatment in the z-direction was always monitored to ensure that the spot size was correct.
- The water curtain and its position was also monitored to ensure that smooth constant flow over the sample. Distilled water was used for the experiment.
- The optical lens was monitored to ensure that they were clean from any water vapour.

- The CNC script was checked to ensure the correct parameters were used to conduct the peening.
- The samples were checked for alignment and orientation when mounting onto the CNC stage.

Note: It is essential that the appropriate PPE is worn at all times during the LSP processing. These include: the goggles which block the light of the correct wavelength, a face mask for the fumes released during the process and hearing protection due to the loud nature of the process. It is also important to ensure that there is no reflective equipment such as a watch or cellular device on a person during the processing.

4.2.4 Naming Convention for Samples

The samples were prepared from a 15 *mm* thick and 10 *mm* thick Aluminium alloy 7075-T651 rolled plate purchased from NK Cutting. A combined total of 64 (48 for phase 1 and 16 for phase 2 as mentioned in section 4.1) 7075 T651 aluminium specimens were experimented upon throughout the duration of the research project. Due to the extensive number of these samples a naming convention was established. The 64 samples were shock peened using the Nd:YAG laser system at the CSIR, South Africa.

The naming convention for the samples is shown by the schematic in Figure 4.7 and is also illustrated in Table 4.3 and Table 4.4. From these 64 samples, 48 were prepared using different coating and were processed under different laser parameters. These first 48 samples were processed separately from the other 16 samples, they were processed under different conditions and in a separate time frame.

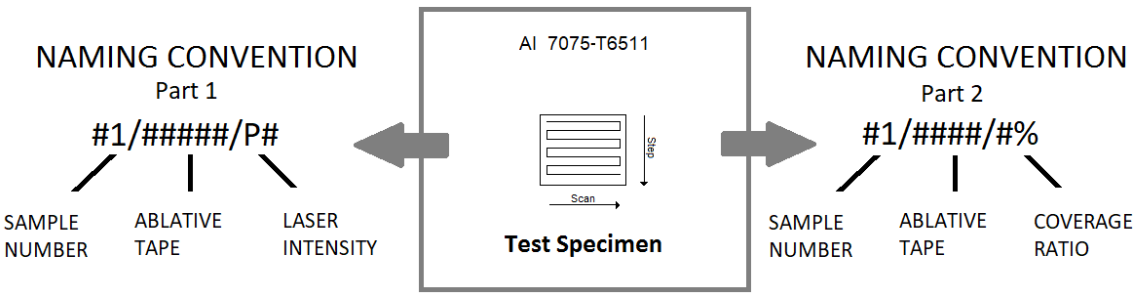


Figure 4.7: LSP Schematic and Naming Convention.

Table 4.3: Sample Naming Convention and LSP Parameters for Phase 1 of Experiment.

Sample No.	Sample Name	Description: Ablative Tape Layer	Laser IntensityGW/cm^2	Laser Energy (mJ)	Coverage %
1	N1-No-Tape-P1.5	No Tape (LSPwC)	1.5	100	70
2	N2-No-Tape-P2	No Tape (LSPwC)	2	135	70
3	N3-No-Tape-P3	No Tape (LSPwC)	3	200	70
4	N4-No-Tape-P4	No Tape (LSPwC)	4	300	70
5	A1-AL-Foil-P1.5	Aluminium Foil Tape	1.5	100	70
6	A2-AL-Foil-P2	Aluminium Foil Tape	2	135	70
7	A3-AL-Foil-P3	Aluminium Foil Tape	3	200	70
8	A4-AL-Foil-P4	Aluminium Foil Tape	4	300	70
9	C1-Clear-P1.5	Clear Box Sealing Tape	1.5	100	70
10	C2-Clear-P2	Clear Box Sealing Tape	2	135	70
11	C3-Clear-P3	Clear Box Sealing Tape	3	200	70
12	C4-Clear-P4	Clear Box Sealing Tape	4	300	70
13	D1-Duct-P1.5	Duct Tape	1.5	100	70
14	D2-Duct-P2	Duct Tape	2	135	70
15	D3-Duct-P3	Duct Tape	3	200	70
16	D4-Duct-P4	Duct Tape	4	300	70
17	E1-Vinyl471-P1.5	Vinyl Tape 471	1.5	100	70
18	E2-Vinyl471-P2	Vinyl Tape 471	2	135	70
19	E3-Vinyl471-P3	Vinyl Tape 471	3	200	70
20	E4-Vinyl471-P4	Vinyl Tape 471	4	300	70
21	F1-Polyster-P1.5	Flame-Retardant Tape with Polyester Film	1.5	100	70
22	F2-Polyster-P2	Flame-Retardant Tape with Polyester Film	2	135	70
23	F3-Polyster-P3	Flame-Retardant Tape with Polyester Film	3	200	70
24	F4-Polyster-P4	Flame-Retardant Tape with Polyester Film	4	300	70
25	G1-Fiber-P1.5	Duct Cloth Fiber Tape	1.5	100	70
26	G2-Fiber-P2	Duct Cloth Fiber Tape	2	135	70
27	G3-Fiber-P3	Duct Cloth Fiber Tape	3	200	70
28	G4-Fiber-P4	Duct Cloth Fiber Tape	4	300	70
29	H1-Vinyl88-P1.5	Vinyl Tape Super 88	1.5	100	70
30	H2-Vinyl88-P2	Vinyl Tape Super 88	2	135	70
31	H3-Vinyl88-P3	Vinyl Tape Super 88	3	200	70
32	H4-Vinyl88-P4	Vinyl Tape Super 88	4	300	70
33	I1-PVC-P1.5	PVC Insulation Tape	1.5	100	70
34	I2-PVC-P2	PVC Insulation Tape	2	135	70
35	I3-PVC-P3	PVC Insulation Tape	3	200	70
36	I4-PVC-P4	PVC Insulation Tape	4	300	70
37	J1-Cu-P1.5	Copper Foil Shielding Tape	1.5	100	70
38	J2-Cu-P2	Copper Foil Shielding Tape	2	135	70
39	J3-Cu-P3	Copper Foil Shielding Tape	3	200	70
40	J4-Cu-P4	Copper Foil Shielding Tape	4	300	70
41	K1-Vinyl472-P1.5	Vinyl Tape 472	1.5	100	70
42	K2-Vinyl472-P2	Vinyl Tape 472	2	135	70
43	K3-Vinyl472-P3	Vinyl Tape 472	3	200	70
44	K4-Vinyl472-P4	Vinyl Tape 472	4	300	70
45	L1-Polymide-P1.5	Polymide Tape	1.5	100	70
46	L2-Polymide-P2	Polymide Tape	2	135	70
47	L3-Polymide-P3	Polymide Tape	3	200	70
48	L4-Polymide-P4	Polymide Tape	4	300	70

Table 4.4: Sample Naming Convention and LSP Parameters for Phase 2 of Experiment.

Sample No.	Sample Name	Description: Abalative Tape Layer	Laser Intensity	Laser Energy (mJ)	Coverage %
49	n1-No-Tape-30	No Tape (LSPwC)	4	300	30
50	n2-No-Tape-40	No Tape (LSPwC)	4	300	40
51	n3-No-Tape-50	No Tape (LSPwC)	4	300	50
52	n4-No-Tape-60	No Tape (LSPwC)	4	300	60
53	n5-No-Tape-70	No Tape (LSPwC)	4	300	70
54	n6-No-Tape-80	No Tape (LSPwC)	4	300	80
55	n7-No-Tape-90	No Tape (LSPwC)	4	300	90
56	a1-Vinyl471-30	Vinyl Tape 471	4	300	30
57	a2-Vinyl471-40	Vinyl Tape 471	4	300	40
58	a3-Vinyl471-50	Vinyl Tape 471	4	300	50
59	a4-Vinyl471-60	Vinyl Tape 471	4	300	60
60	a5-Vinyl471-70	Vinyl Tape 471	4	300	70
61	a6-Vinyl471-80	Vinyl Tape 471	4	300	80
62	a7-Vinyl471-90	Vinyl Tape 471	4	300	90

4.3 Microscopic Surface Analysis

The study of the microscopic surface features of the processed samples were conducted at the materials laboratory at the School of Mechanical, Industrial and Aeronautical Engineering at the University of the Witwatersrand using the Nikon Zoom stereo-microscope (Nikon SMZ1500) shown in Figure 4.8.

The specifications of the instrument were listed in Table A.2 Appendix B[37]. The instrument is fitted with a digital camera that is used to capture the observed microscopic details.

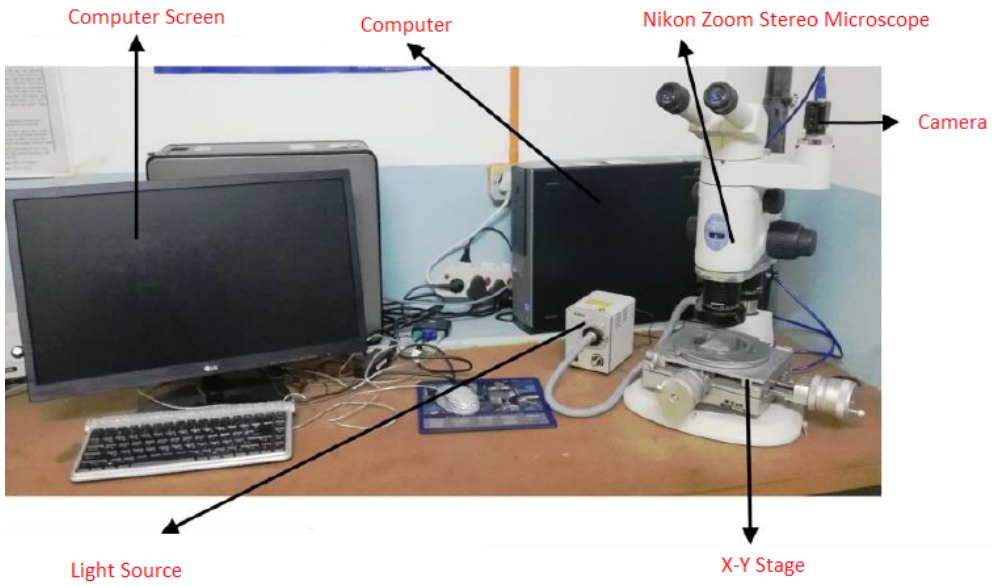


Figure 4.8: Nikon Zoom Stereo Microscope (Nikon SMZ1500).

4.3.1 Procedure

The following is the procedure that was adopted for capturing the surface images of the samples (with the attached ablative tape and after its removal).

1. Turn of the computer and the power supply to the light source and remove microscope cover.
2. Open and execute the NIS Elements imaging software.
3. calibrate the optical microscope to the least magnification level.
4. Place the sample in the middle of the X-Y stage and adjust the light source around the sample until it is adequate.
5. Set the magnification and the focus accordingly then double check the image using the live feed display from the NIS Elements imaging software.
6. If satisfied with the image quality and detailed that require study then proceed to capture a snapshot of the image using the software and save as required (label images as required).
7. Remove the ablative layer then repeat the previous step (if necessary).
8. Repeat the steps 5 to 7 for the remaining samples.
9. Once completed switch off the light source, exit the software, switch off the machine and cover the microscope.

4.3.1.1 Precautions

The following precautions should be taken:

- Ensure that lens, the eyepiece and the X-Y stage are clean.
- Ensure that the microscope is properly calibrated.
- Ensure that the images are labelled according to the sample captured.
- Cover on the microscope with the dust cover when done processing.
- Ensure that PPE is worn at all time (including gloves).

4.4 Surface Roughness Testing

The surface roughness testing was investigated by using two different instruments. They are as follows:

4.4.1 Surface Roughness Testing Using Portable SRT-6210 Unit

The portable (SRT-6210) roughness tester, shown in Figure 4.9 was used to study the surface roughness of the samples. The specification of the instrument are listed in Table A.3[38].

The test was conducted at the School of Mechanical, Industrial and Aeronautical Engineering at the University of the Witwatersrand.



Figure 4.9: SRT-6210 Surface Roughness Tester.

4.4.2 Procedure

The following is the procedure that was taken in analysing the surface roughness (only the arithmetic average roughness (Ra) was measured):

1. Turn on the machine and conduct the following checks:
   (a) Check the battery and charge if necessary.
   (b) Select the required cut-off length, profile filter and measuring units.
   (c) Select the roughness parameter to be measured.
2. Calibrate the tester accordingly.
3. Place the probe parallel to the laser scanning direction on the sample.
4. carefully align the sample with the probe stylus 2 mm from the edge of the peening area.

5. Take three measurement along the same position and record Ra the results.
6. Align the probe 6 mm from the peening edge and repeat step 5.
7. Align the probe 10 mm from the peening edge and repeat step 5.
8. Align the probe 14 mm from the peening edge and repeat step 5.
9. Align the probe 18 mm from the peening edge and repeat step 5.
10. Rotate the sample to measure the roughness along the stepping direction then repeat steps 4 to 9.
11. Repeat steps 3 to 10 for the remaining samples.
12. Switch off the tester and store in a closed environment.

4.4.2.1 Precautions

The following precautions should be taken:

- Do not touch the tip of the stylus probe or scratch it when changing or aligning samples.
- Ensure that the sample is correctly aligned and that the probe is placed correctly on the surface of the sample.
- When the tester is in operation, ensure that one does not touch either the sample or the tester as this could interfere with the results.
- Ensure that the probe stylus and the surface of the sample is free from dust and other contaminates.

4.4.3 Surface Roughness Testing Using Stationary HOMMEL-ETAMIC T8000 Unit

The Stationary HOMMEL-ETAMIC T8000 R120-400 roughness tester was used to study and 3-D map the surface features of the samples as shown in Figure 4.10. The specification of the instrument are listed in Table A.4[39] . The test was conducted at the School of Mechanical Engineering at the University of Johannesburg.

The surface of the peened area (6 mm x 6 mm centre area) was 3-D mapped using this machine. Due to the availability and long processing time required to process the samples, not all samples were 3-D mapped, only sample of interest were mapped. As a result, a total of 27 sample were processed using this method. The surface roughness testing was conducted with the aid of Mr. Pieter le Roux.

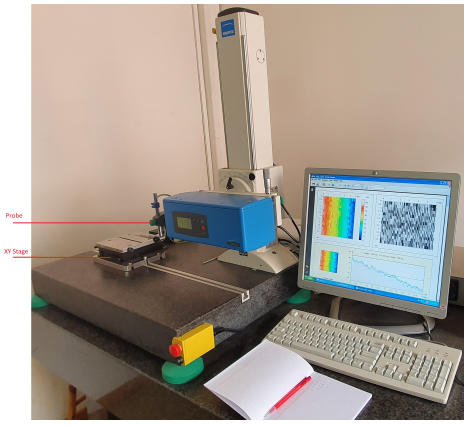


Figure 4.10: HOMMEL-ETAMIC T8000 R120-400 Surface Roughness Tester.

4.4.4 Procedure

The following is the procedure that was taken in analysing and mapping the surface roughness of the samples:

1. Switch on the roughness tester and the computer.
2. Install the probe stylus onto the machine.
3. Execute the TMess topography software and the HOMMEL MAP 3D topography analysis software.
4. Place the sample onto the XY stage.
5. Align the probe over the required scanning area.
6. Execute the calibration so that the probe can touch the scanning surface.
7. Input the required scanning area parameters.
8. Execute the program to start the scanning measurement.
9. Once completed save and label the collected data.
10. Export the data into the HOMMEL MAP 3D topography analysis software.
11. Extract the 3D profile, the 2D profiles and the surface roughness measurements from the raw data into a PDF document.
12. Save the PDF document and remove sample from XY stage.
13. Repeat steps 4 to 12 for the remaining samples.
14. Carefully remove the probe stylus and store in box then switch off the machine.
15. Close all software programs and switch off the machine.

4.4.4.1 Precautions

The following precautions should be taken:

- Do not touch the tip of the stylus probe.
- Ensure that the sample is correctly aligned on the XY stage.
- When the tester is in operation, ensure that one does not touch any part of the instrument as this could create vibrations and interfere with the data due to the high sensitivity of the machine.
- Ensure that the probe stylus and the surface of the sample is free from dust and other contaminates.

4.5 Scanning Electron Microscopy

The scanning electron microscope (SEM) was used to further study the surface and the cross-section of the sample under higher magnifications. This type of microscopy was used to further observe for any surface damage and any changes that occur in the microstructure. The analysis was conducted using the Zeiss Sigma SEM, shown below in Figure 4.11[40].

The machine is located at the School of Chemical and Metallurgical Engineering at the University of the Witwatersrand. The machine is equipped with three different detectors which are; the Secondary Detector (SE2) which captures topography images, the Back-Scatter Detector (BSD) which captures the composition of the material and the Oxford EDX Detector which captures the material characterisation.

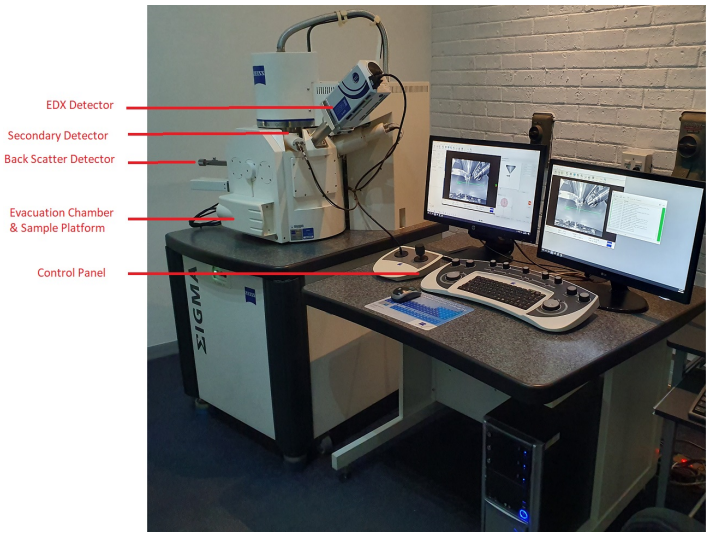


Figure 4.11: Zeiss Sigma SEM System.

4.5.1 Procedure

The following procedure was used to capture the images using the SEM:

1. Clean Sample using the spray degreaser.
2. Place the sample on to the sample platform and secure using aluminium tape then note the position and direction of the sample. (Note: The platform is marked for sample locations).
3. Place the sample platform into the evacuation chamber then evacuate the chamber.
4. Using the control panel, locate the surface of the sample.
5. Using the control panel, Zoom to the required magnification
6. Capture the required images at points of interests on the sample.
7. Save and label captured images accordingly.
8. Perform steps 4-7 for each of the samples on the platform.
9. Repeat steps 1-8 for remaining samples.

4.5.1.1 Precautions

The following precautions should be taken:

- Ensure that one is wearing gloves when handling the samples.
- Ensure that the sample platform is cleaned using a degreaser.
- Ensure that the samples are mounted correctly.
- Double check and note down the positions of the samples on the sample platform.
- Ensure that the surface of the samples are cleaned and do not have any contaminants.

4.6 Microhardness Testing

In order to conduct hardness testing, the samples have to first be cut and machined through the cross section. These samples then need to undergo three stages of grinding and polishing. The procedure to prepare the sample using the 3 stages of grinding and 3 stages of polishing for the hardness testing can be found in Appendix A. Strict quality control was applied to ensure that the sample were prepared to the required standard.

Note: The grinding process was also applied to the samples that were used for the second part of this research project.

The INNOVATEST Falcon 500 variable hardness testing machine, depicted in Figure 4.12 was used to measure the Vickers hardness number of the treated samples.

The hardness testing machine is equipped with a diamond tipped indenter and two optical microscopes with magnifications of 10x and 50x, full specification of the machine are listed in Table A.7[42]. The sample position can be controlled by using the two micrometer screw-gauges which have a resolution of 0.01 mm.

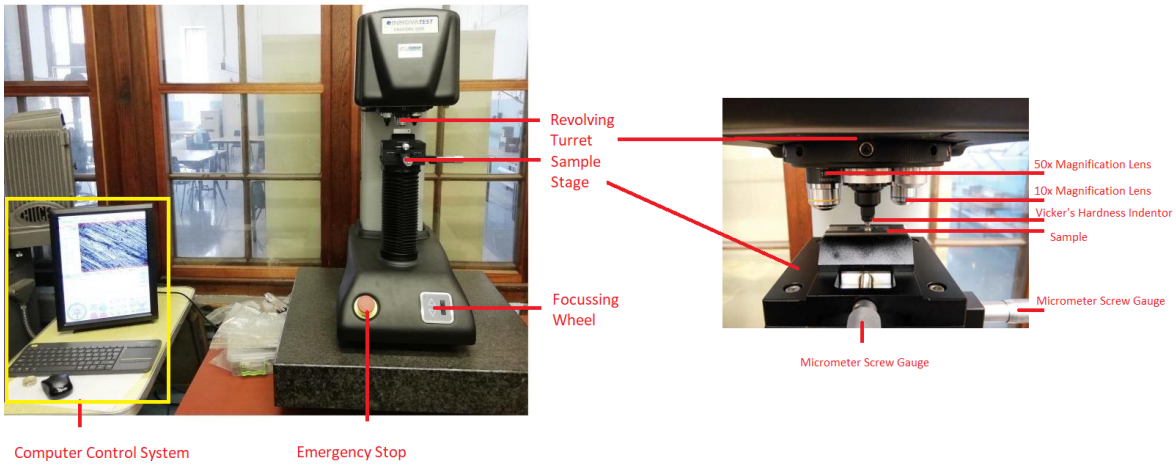


Figure 4.12: INNOVATEST Falcon 500 Hardness Testing Machine.

Once the samples were prepared using the three stages of grinding and polishing, only then can the samples be tested using the Falcon 500 variable hardness testing machine. The steps taken to conduct the test are outlined below.

4.6.1 Procedure

The following procedure was used to determine the microhardness of the treated samples:

1. Switch on the hardness machine, the monitor and allow the software to start up.
2. Ensure the stage is unobstructed when the during the startup sequence of the machine and wait for the green to flash.
3. Mount the X-Y stage on the sample platform.
4. In the software, set the indentation force to 100 gf and the dwelling time to 10 s.
5. Place the sample on the sample holder and secure it.
6. Adjust the Z-axis to get the surface of the sample in focus, use auto focus when necessary.
7. Perform the measurement 0.15 mm away from the peened surface the using increment of 0.15 mm until 0.9 mm then using increments of 0.2 mm until 1.7 mm away from the peened area.
8. Repeat steps 5 - 8 for all samples.
9. Shut down and switch off machine when done testing.

4.6.1.1 Precautions

The following precautions should be taken:

- Ensure the tested surface is polished to the required finish which satisfies the ASTM E384 standard.
- Do not touch or scratch the polished surface of the samples.
- Ensure that the sample is placed securely in the holder.
- Do not move the sample or the machine when the testing is in process.
- Ensure that the correct force is selected and applied during testing.
- Do not touch the probe stylus or the lens of microscope.

4.7 Incremental Hole Drilling Testing

Incremental hole-drilling was conducted to measure the stresses induced by LSP to an intermediate depth of 1.2 mm with good resolution. The testing was conducted using the equipment and apparatus at the materials laboratory at the School of Mechanical, Industrial and Aeronautical Engineering at the University of the Witwatersrand.

The IHD test was performed using the SINT Technology Restan MTS-3000 Automatic Hole Drilling Machine. A schematic of the IHD system set-up and the IHD machine is illustrated below by Figure 4.13[43].

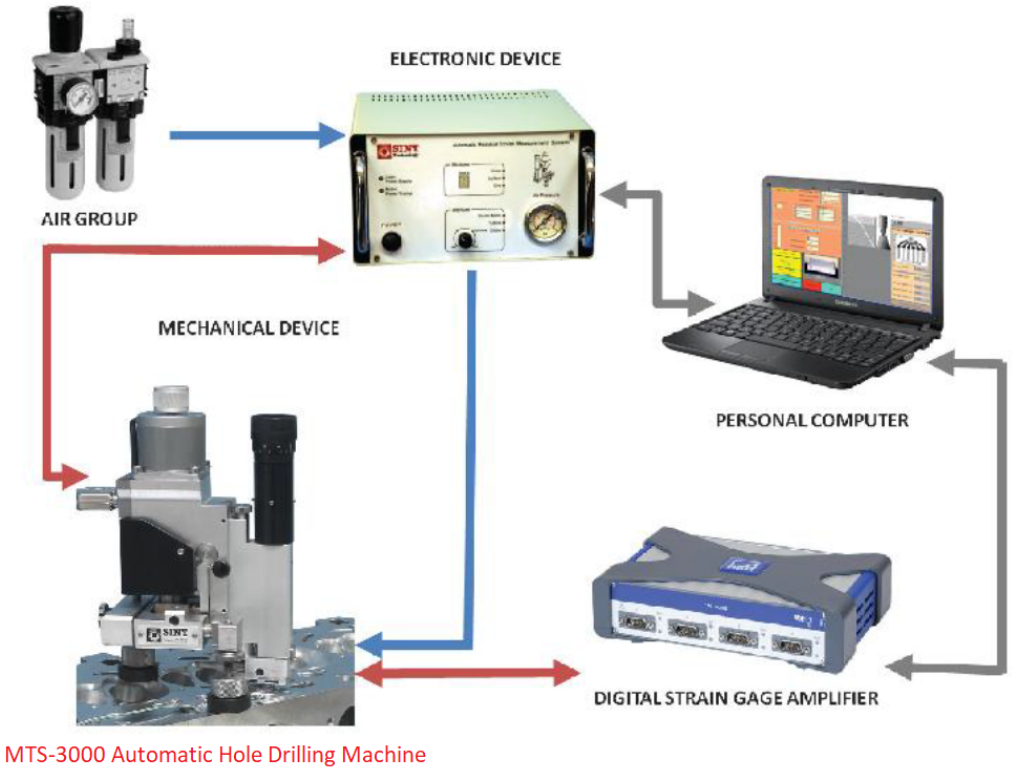


Figure 4.13: IHD System Configuration.

The apparatus used to apply the strain gauge rosette on the surface of the sample are shown in Figure 4.14. The specific details regarding these consumables and apparatus can be found in the appendix.

The strain gauge that was applied to the surface of the peened sample is depicted in Figure 4.15. The properties of the stain gauge is shown in Figure 4.16. For all the tests that were conducted, the strain gauge rosette were aligned such that gauge 1 was aligned along x-direction (scanning direction) and gauge 3 along the y direction (stepping direction), as shown in Figure 4.15.

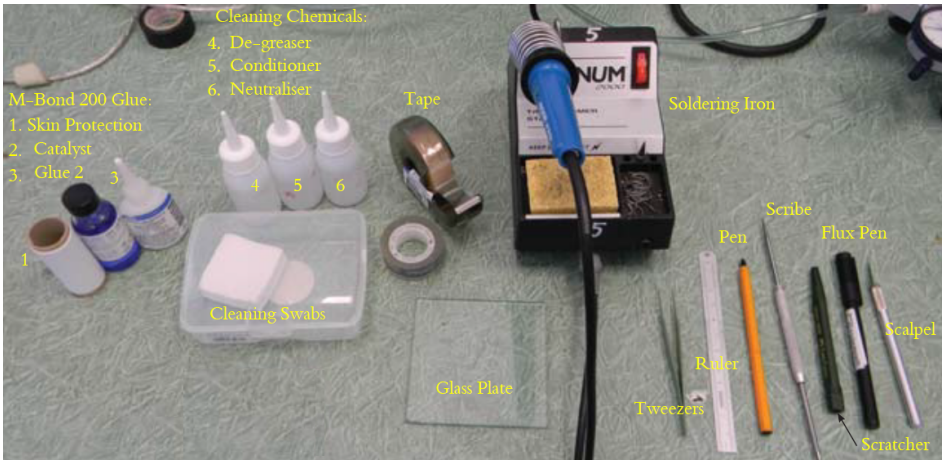


Figure 4.14: Apparatus used to Apply Strain Gauge.

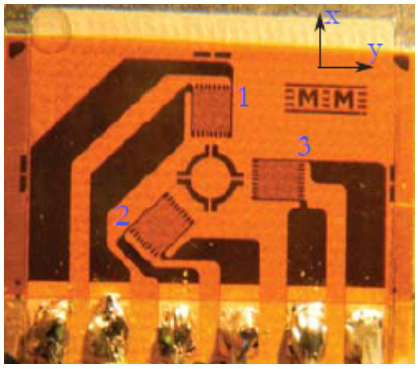


Figure 4.15: Strain Gauge.

Name	CEA-13-062UL-120
ASTM E837 Type	A
Rosette Diameter	5.13 mm
Nominal Hole Diameter	2 mm
Minimum Thickness	5.13 mm
Minimum Depth Step	0.02 mm
Drilling Depth	1.2 mm
Stress Calculation Depth	1 mm

Figure 4.16: Strain Gauge Properties.

The 2 mm diameter drill bits that were used for the process were manufactured by SS White. The samples were glued firmly to the laboratory work surface before testing. This was done to prevent the sample from moving during the test and to minimise any vibrational interference thus minimise any inaccuracies in the obtained result.

The hole was drilled at the centre of the strain gauge rosette so that the relieved strains can be measured, calibration coefficients are used to determine and calculate the residual stresses.

The hole drilling tests were performed in accordance with the ASTM E837 standard which contains the published calibration coefficients. The standard also defines the thickness of the test specimen, the placement of the strain gauge rosette and the hole diameter, it also defines the drilling depth and the eccentricity for the various strain gauges.

The EVAL software was used to process the data for the samples. The procedure to conducted to test is outlined in the next subsection.

4.7.1 Procedure

The following is the procedure that was used to apply the strain gauge and to conduct the IHD test:

1. Application of strain gauge rosette.
    (a) Wash hands and ensure the all equipment and surfaces are clean and have been degreased.
    (b) Mark the centre location required for the strain gauge on the sample by using a pencil and ruler.
    (c) Carefully place a strain gauge onto the glass plate by using the tweezers and firmly lay the clear tape over it.
    (d) Clean the surface of the sample first with the degreaser then conditioner to slightly etch the surface and then the neutraliser to neutralise the surface. Note: use a cleaning swab only once and always swipe in one direction as this prevents contaminants from returning to the clean area and make sure to not touch the cleaned surface.
    (e) Handling the tape, remove the rosette from the glass plate and carefully move it over to the sample and place the rosette in the correct marked position
    (f) Lift the tape again to expose the bottom surface of the rosette and apply a layer of catalyst on it then wait one minute.
    (g) Place the glue onto the marked position on the sample and carefully lower the rosette back into the sample and glue then apply pressure on the surface by using the skin protection paper and thumb then hold in position for at least three minutes.
    (h) Remove the overlaying tape and ensure that the rosette is bonded then either store away in a sterile packet or proceed to perform IHD testing (preparation).
2. IHD Testing (preparation).
    (a) Secure sample to workbench and solder wires from the digital strain gauge amplifier (DAQ) to the solder pads on the rosette.
    (b) Replace the drill bit if necessary then align the drill bit with the drilling point on the rosette (coarse alignment).
    (c) Level the IHD machine with the sample by using the bubble-level.
    (d) Using the microscope built in the IHD machine, align the cross-hairs of with the strain gauge rosette (fine alignment). Ensure that the cross hairs are perfectly aligned and that the dial gauges are set to zero.
    (e) Open the drill control software and home the Z-direction.
    (f) Open the compressed air-line.

(g) Connect the surface detection trigger wires from the electronic device to the IHD machine and the surface of the sample.

(h) Carefully position the end mill on to the surface of the rosette by visual inspection then run the command for the SINT built-in surface detection to find the true surface of the material.

3. Set up parameters on the software to run the test as follows:

   (a) Enter the strain gauge coefficients.

   (b) Set drilling depth and the drilling step as stipulated by Figure 4.16.

   (c) Set up save file details for the raw data to a new file and label accordingly.

   (d) Set the drill delay to 5 s and the acquisition delay to 15 s.

   (e) Zero the strain gauge readings.

4. Conduct the test, this includes the drilling one step length then waiting for the drill delay and then the stopping of the drill during the acquisition period in which the strain data is collected. The process then repeats itself for each drill step until the target depth is reached.

5. After the test is completed measure the drilled hole diameter by using the scope and the dial gauges on the IHD machine.

6. Process the data using the EVAL software.

4.7.1.1 Precautions

The following precautions should be taken:

- Ensure PPE is worn at all times.
- when handling the chemicals ensure that one is wearing safety glasses.
- Ensure that there is sufficient clearance around all moving parts.
- When the test is conducted ensure that hearing protection is worn.
- Ensure sample is firmly secured before conducting the test.

The author had access to the corresponding IHD apparatus during normal working hours. The time involved for a single residual stress measurement was about two hours, this includes the time involved in the sample preparation, drilling the hole and processing the corresponding data. The financial cost involved in performing a single measurement is estimated to be one thousand five hundred South African Rand.

4.8 LXRD Testing

L-XRD was performed using the Proto iXRD Portable Residual Stress and Retained Austenite Measurement Systems machine at the CSIR, South Africa. The LXRD machine shown below in Figure 4.17 is used for near-surface residual stress measurement which will serve to validate the results obtained from IHD.

Due to certain constraints the test was exclusively performed and executed by the technician at the CSIR, South Africa. The L-XRD was estimated to measure the stresses at a depth of 0.026 mm by using the corresponding Proto iXRD software. The specification of the apparatus can be found in Table 4.5[44].

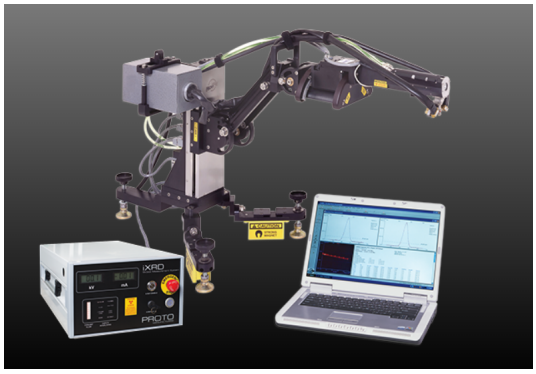


Figure 4.17: Proto iXRD Machine and Apparatus.

	iXRD	iXRD COMBO	iXRD MODULAR MAPPING	iXRD GANTRY
Dimensions (L x W x H)	400 x 300 x 200 mm 16 x 12 x 8 in	1600 x 1100 x 1800 mm 63 x 43 x 71 in	2500 x 1900 x 2000 mm 98 x 75 x 79 in	2700 x 1100 x 2600 m 106 x 43 x 102 in
Recommended Maximum Part Size	unlimited	500 mm 20 in	1000 mm 40 in	1000 mm 40 in
Goniometers	MG40, MGR40, MG30, MG15, MG15 axial		MG40	MGR40
Field Stands	FS2, FS4		FS2	tripod
HV Power	300 W			
Mapping Stages (X,Y)	FS4: 100 x 100 mm 4 x 4 in		200 x 200 mm 8 x 8 in	100 x 100 mm 4 x 4 in
Focusing Axis (Z)	FS2: 100 mm (optional 200 mm) FS4: 100 mm		400 mm 16 in	760 mm 30 in
Manual Stages (X,Y)	n/a			2100 x 650 mm 83 x 26 in
Phi Rotation Stage	MGR40 (0-360°), MG40 + C-Frame, portable table	optional integrated phi 500 mm (20 in) rotation stage (0-360°)	integrated phi 500 mm (20 in) rotation stage (0-360°)	MGR40 (0-360°)
Sample Table	n/a	1600 x 1100 mm 63 x 43 in	180 mm (7 in)	heavy-duty steel table 2700 x 1100 mm 106 x 43 in
Geometry	iso (omega), modified side inclination (psi)			
X-ray Tubes	fine focus 30 mm diameter metal ceramic			
X-ray Tube Cooling	integrated recirculating liquid-to-air heat exchanger			
X-ray Beam Apertures	round: 0.5, 1.0, 2.0, 3.0, 4.0 mm rectangular: 0.5x3, 1x3, 0.5x5, 1x5, 1.5x5, 2x5 mm			
X-ray Detectors	proprietary dual position sensitive scintillation detectors (PSSD)			
Detector Width (2θ)	standard 18.4°, wide 29.5°			
2θ Range	residual stress: 123°-171°, retained austenite: 70°-171°			
Focusing	manual, automated			
X-ray Filters	diffracted beam Kβ filters			
Safety	independent warning light beacons for "x-ray on" and "shutter open", emergency stop with lockout key, x-ray protective glass for zero x-ray emission from enclosure			
Computer	latest generation brand name desktop or laptop computer with each LXRD			
Software	powerful yet easy to use XRDWin 2.0			
Enclosure Features	enclosure light, fully interlocked, clear view windows, hand-held motion control pendant			
Operating Temperature Range	0°C to 35°C non-condensing humidity			
Power Requirements	90-240 VAC, 50/60 Hz, single phase			
System Compliance	ASTM E915, ANSI N43.2, CE			
Proto Manufacturing engages in continuous research and development, therefore specifications in this publication are subject to change. Please call for details. Various items and methods in this brochure are covered by patents or patents pending.				

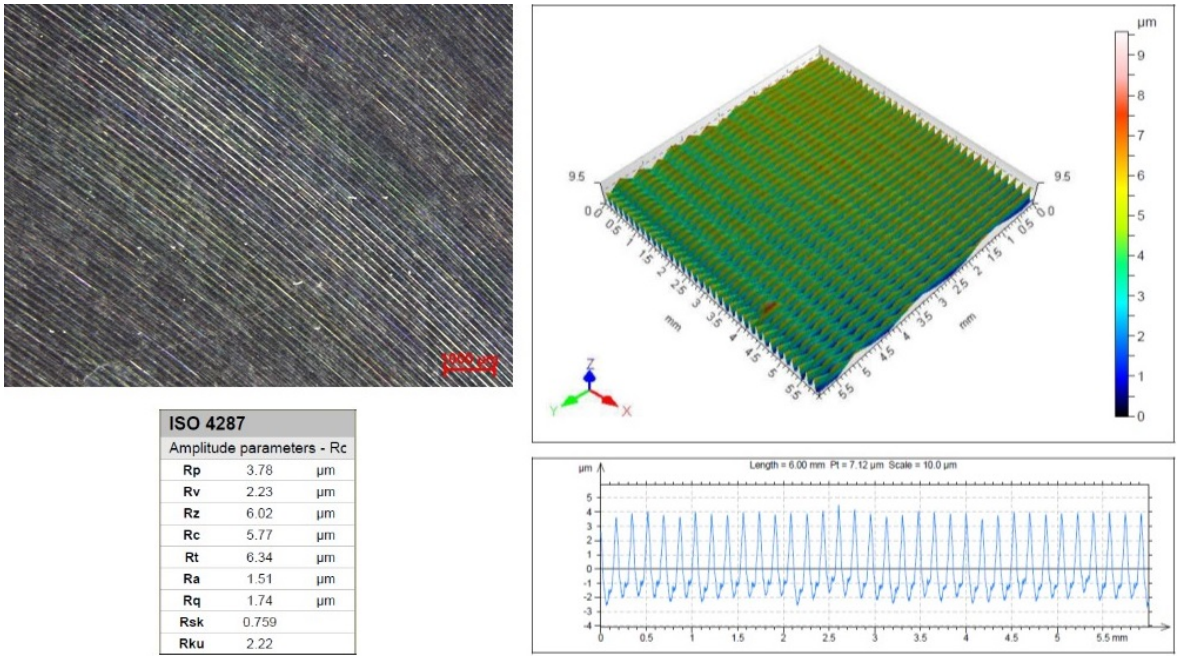
Table 4.5: Proto iXRD Specifications.

5 | Phase I - Surface Analysis

The following chapter illustrates the images and data obtained from the optical microscope, the surface roughness testing and the microhardness testing for each sample. The images depicted for the treated sample were taken before the removal of the ablative and after the removal of the ablative tape, these samples were cleaned using an alcohol solution after the removal of the tape. The microscopic images were taken at various locations on the treated area.

5.1 Unpeened Base Sample

Figure 5.1 shows and illustrates the microscopic image and roughness data obtained for the unpeened base sample. The shown data will be used for comparative studies with other samples.



ISO 4287		
Amplitude parameters - Rc		
Rp	3.78	µm
Rv	2.23	µm
Rz	6.02	µm
Rc	5.77	µm
Rt	6.34	µm
Ra	1.51	µm
Rq	1.74	µm
Rsk	0.759	
Rku	2.22	

Figure 5.1: Microscopic Image and 3-D Roughness Map and Data for Unpeened Sample.

5.2 No Tape (LSPwC)

The following are the microscopic images and data obtained for the samples peened without any type of ablative coating. The shown data will be used for comparative studies with the other peened samples.

Sample: M1-No-Tape-P1.5



Figure 5.2: Surface Images for Sample: N1-No-Tape-P1.5.

Sample: M2-No-Tape-P2



Figure 5.3: Surface Images for Sample: N2-No-Tape-P2.

Sample: M3-No-Tape-P3



Figure 5.4: Surface Images for Sample: N3-No-Tape-P3.

Sample: M4-No-Tape-P4

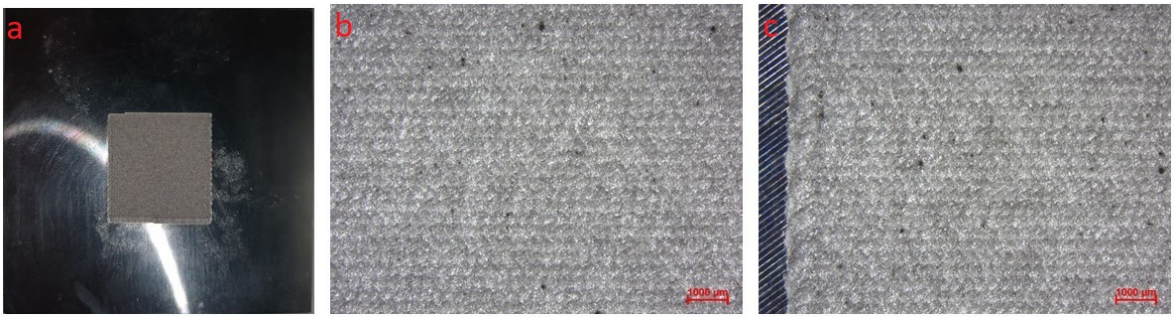


Figure 5.5: Surface Images for Sample: N4-No-Tape-P4.

Figure 5.2 to Figure 5.5 illustrate the peening results found for the samples peened without any ablative coating. The changes in the surface texture increase with the increase in the power intensity. Sample N1-No-Tape-P1.5 show a surface texture that has a slight amount of discolouration and the peening pattern is not clear visible when compared to other samples. The peening becomes visually clearer as the power intensity is increased. Sample N2-No-Tape-P2 shows a surface texture that is much cleaner and the laser spots and peening pattern can be seen in a uniform pattern. Similarly, sample N3-No-Tape-P3 and sample N4-No-Tape-P4 show a uniform surface texture that has experienced more surface ablation.

The surface texture that has been observed for these four samples will be used for comparative studies and will determine whether an ablative tape improves the surface texture in a positive or negative way. The samples were all peened on the same day using the same parameters to allow for this comparative study.

Surface Roughness Results

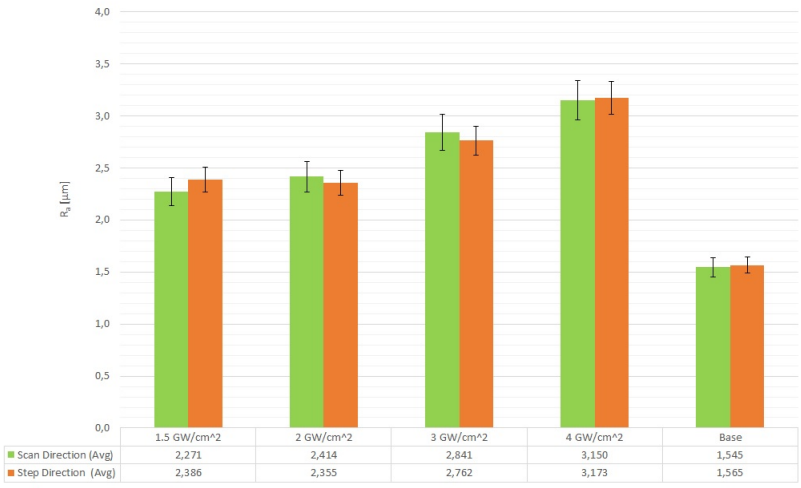


Figure 5.6: Surface Roughness Results for the LSPwC samples.

Figure 5.6 shows the results obtained for the surface roughness for the peened samples and the machined base sample using the portable SRT-6210 Unit. The results show that the surface roughness increases with the increase of the power intensity.

There is 49.9% increase in the mean surface roughness(R_a) for sample N1-No-Tape-P1.5 from the unpeened base sample. A 54.6% increase was found for sample N2-No-Tape-P2 and an increase of 80.3% sample N3-No-Tape-P3, whereas an increase of 103.4% was found for sample N4-No-Tape-P4 from the surface roughness of the unpeened base sample.

The linear increasing trend in the surface roughness along both the scanning and stepping direction can be observed for the samples peened with $2GW/cm^2$ to $4GW/cm^2$. The data shown in Figure 5.6 represents the average surface roughness over the entire peening area, multiple measurements were taken along both the scanning and stepping direction. The multiple measurements were taken to minimise the uncertainty and inaccuracies present when using this roughness testing machine. Overall the trend shown in the data conforms to the knowledge found in literature as outlined in subsection 2.2.3.

3-D Surface Maps for LSPwC Samples

Further surface analyses were conducted using the HOMMEL-ETAMIC T8000 R120-400 roughness testing machine to provide an accurate 3-D surface map and resulting surface roughness data. The results obtained for these samples are illustrated by Figure 5.7 and Figure 5.8.

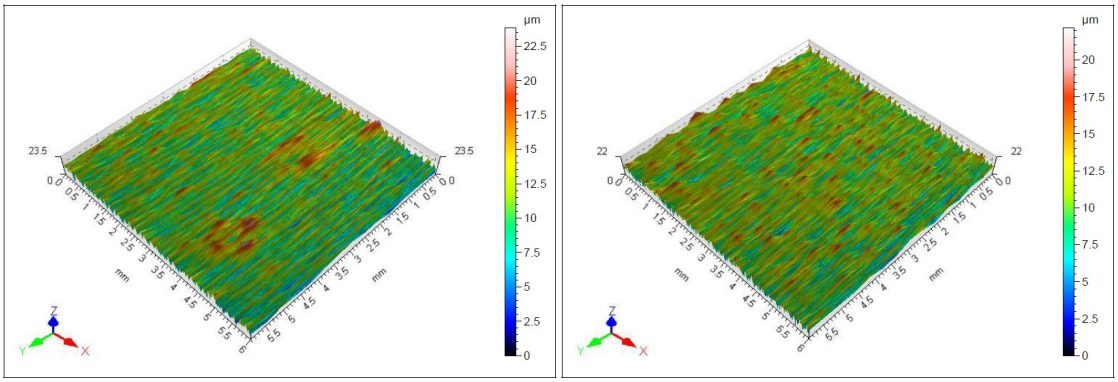
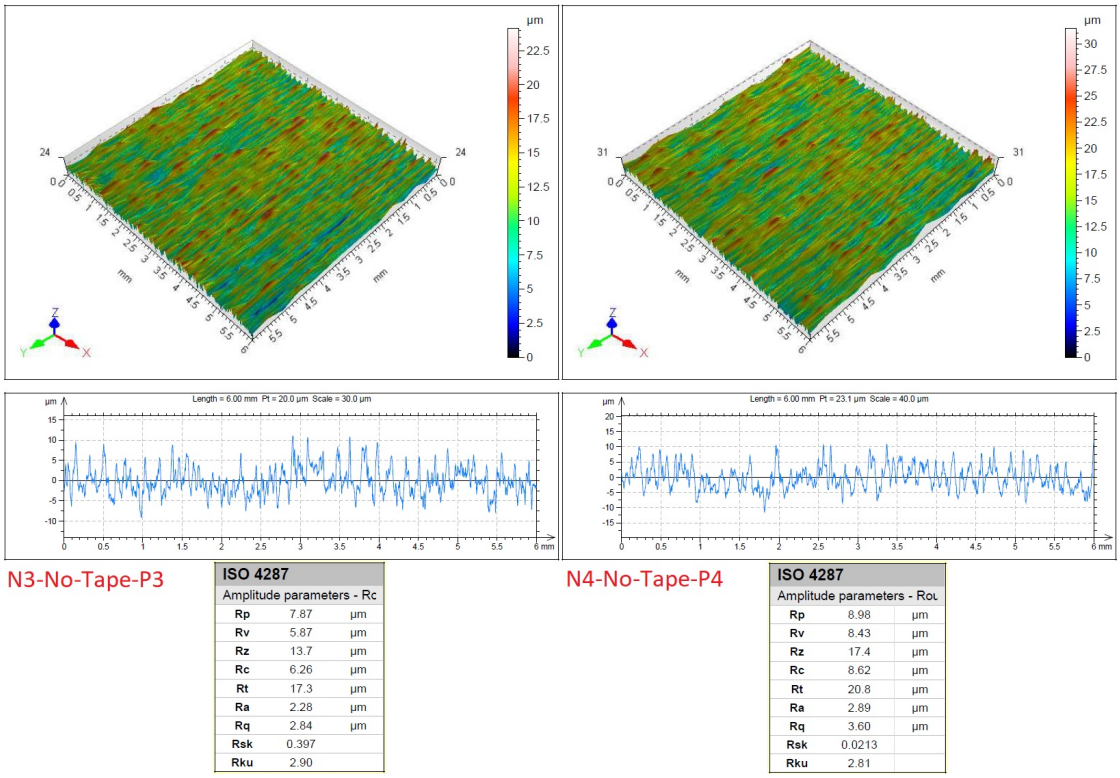


Figure 5.7: 3-D Surface Map for Samples: M1-No-Tape-P1.5 and M1-No-Tape-P2.



ISO 4287		
Amplitude parameters - Rc		
Rp	7.87	µm
Rv	5.87	µm
Rz	13.7	µm
Rc	6.26	µm
Rt	17.3	µm
Ra	2.28	µm
Rq	2.84	µm
Rsk	0.397	
Rku	2.90	

ISO 4287		
Amplitude parameters - Rou		
Rp	8.98	µm
Rv	8.43	µm
Rz	17.4	µm
Rc	8.62	µm
Rt	20.8	µm
Ra	2.89	µm
Rq	3.60	µm
Rsk	0.0213	
Rku	2.81	

Figure 5.8: 3-D Surface Map for Samples: M3-No-Tape-P3 and M4-No-Tape-P4.

The 3-D surface map shown for sample N1-No-Tape-P1.5 shows that the surface texture is uniform with the exception of two surface irregularities or defects that can been observed in Figure 5.7. These irregularities do skew the surface results obtained for this sample.

The changes in the surface texture with the increasing power intensity can be clearly seen in the images. A peak roughness (R_p) of 7.89 μm and 7.37 μm and the linear distance between the top peak and the valley base (R_z) of 14.3 μm and 13.3 μm was found for the two samples in Figure 5.7. While a peak roughness (R_p) of 7.87 μm and 8.98 μm and the linear distance between the top peak and the valley base (R_z) of 14.3 μm and 13.3 μm was observed 13.7 μm and 17.4 μm for the two samples in Figure 5.8.

The 2-D map provide a clearer representation of the surface and also show the variation in the surface texture to a higher degree. A sinusoidal type pattern can be observed in the graphs, this illustrates the effect that the peening has on the surface of the material.

The amount of noise that can be seen in the roughness map increases with the increase in the power intensity. The effect that the two defect have on the roughness are not visible in the 2-D plot as there is an observable pattern that is visible and that there is no sudden deviation in the plot.

Overall the nature of the peening without any ablative material and its effect on the surface texture is clearly illustrated in these two figure.

5.3 Aluminium Foil Tape (1436 3M)

The following are the microscopic images and data obtained for the samples peened using the aluminium foil tape as the ablative coating.

Sample: A1-AL-Foil-P1.5

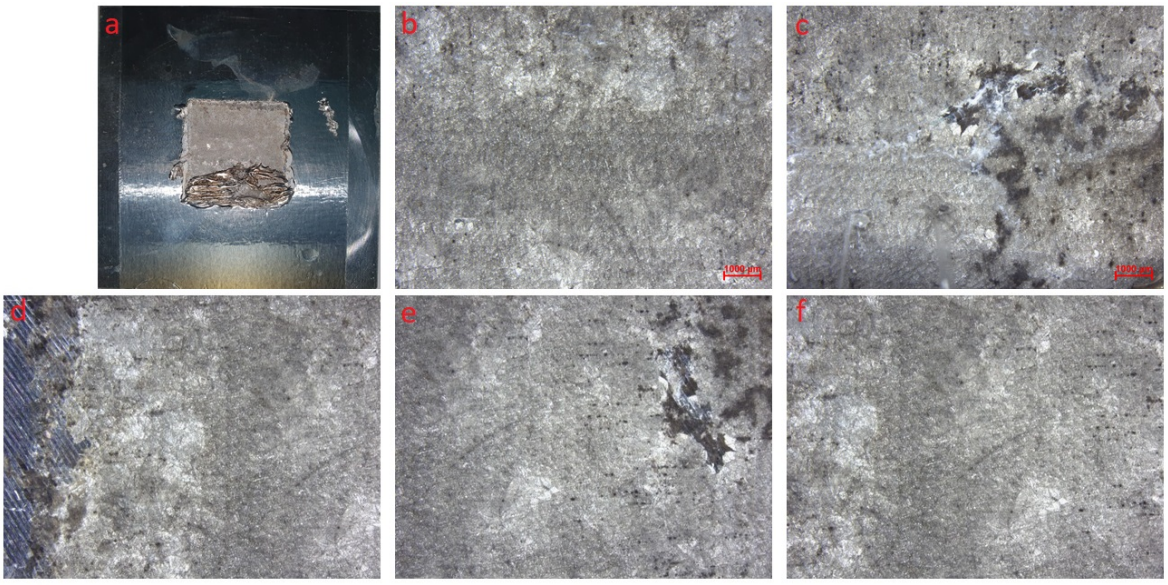


Figure 5.9: Surface Images for Sample: A1-AL-Foil-P1.5.

Sample: A2-AL-Foil-P2

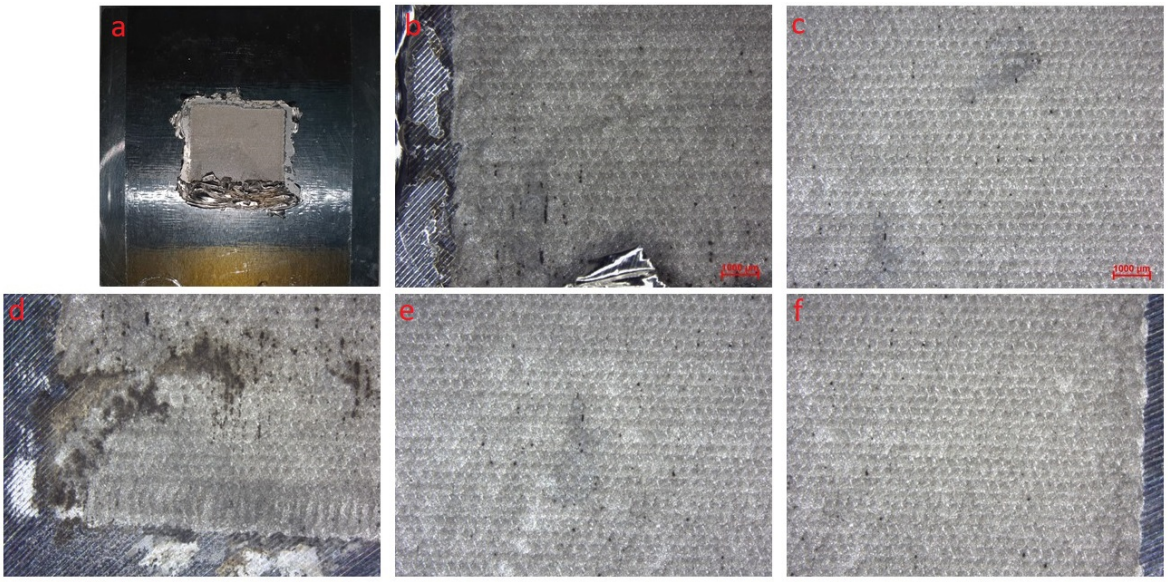


Figure 5.10: Surface Images for Sample: A2-AL-Foil-P2.

Sample: A3-AL-Foil-P3



Figure 5.11: Surface Images for Sample: A3-AL-Foil-P3.

Sample: A4-AL-Foil-P4

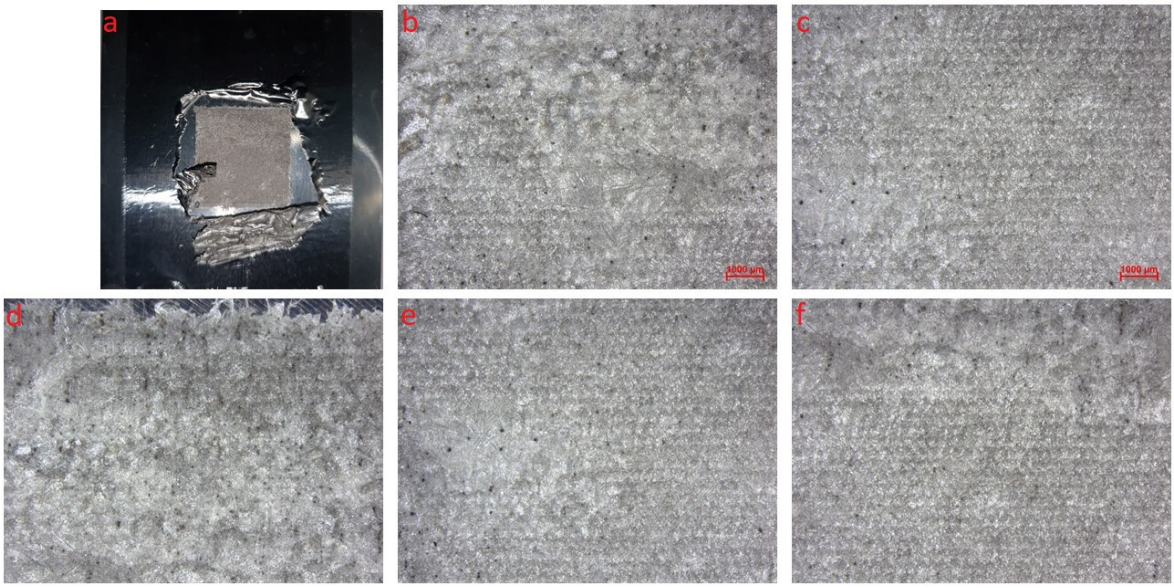


Figure 5.12: Surface Images for Sample: A4-AL-Foil-P4.

Sub-images (a-c) shown in Figure 5.9 to Figure 5.12 shows the surface state of the peened sample before the removal of the ablative tape whereas sub images (d-f) shows the surface state after the removal of the ablative tape, debris and contaminants.. The images for all samples clearly depict that the ablative layer failed to protect the surface of the sample during peening, at some point during the peening process the tape (film) and its adhesive failed thus leading to the uneven peening seen in the images.

The cause of the tape failure could be the result of the tape not having enough adhesive strength and under the aqueous environment and pressure from the water jet during the peening process the tape failed. Also, the force of the water overlay sprayed through the jet further increased the rate of failure for the ablative medium and thus exposing the surface to the oncoming laser pulse effectively making the laser peening occur without any coating in certain spots.

The ablative tape however did not completely fail, during the initial stages of the peening process the tape did ablate with its adhesive backing. However, further along the process in certain spots the rubber adhesive backing remained behind (not clearly visible in the images) thus suggesting that either the aluminium backing was ablated or the rubber adhesive melted and remained behind on the peened surface. Then the ablative medium failed and because of this failure the peening became irregular. During the peening process the laser beam did come into contact with the tape that was being self-removed and this interaction could also explain the regions that did not experience any peening which is clearly shown in Figure 5.9c, thus due to this all samples experienced this irregular type of peening. The uncertainties that were present during the peening process for this ablative tape medium is relatively unknown. Therefore, it is difficult to characterise and explain in detail the nature of peening experienced by the samples.

The tape itself only has a total thickness of 0.075 mm and uses soft an aluminium backing thus the tape is prone to failure. The thickness of the ablative layer does indeed affect the overall peening and performance of the ablative medium which will become more evident in the following sections. From the visual inspection conducted after the peening process the texture of the peening for this ablative medium is irregular, certain regions show surface melting and also discolouration.

The changes in the surface texture increases with power intensity, for the power intensity of 1.5 GW/cm^2 the surface state shown in Figure 5.9 has a high degree of surface texture irregularities. The same is true for the sample peened with 3 GW/cm^2 shown in Figure 5.11 which has medium degree of surface texture irregularities and surface melting with relativity large uniform peening patches. Similarly, the sample peened with 4 GW/cm^2 shown in Figure 5.12 has medium degree of surface texture irregularities and surface melting but with relativity large non-uniform peening patches. However, the sample peened with 2 GW/cm^2 shown in Figure 5.10 has low surface irregularities and surface melting. This shows that at a certain power intensity the ablative coating does protect the surface against surface melting but due to unpredictable nature of failure in the tape, it is highly unlikely that this ablative medium can fully protect the surface against LSP.

The images shown highlight the increase in surface damage with the increasing of the power intensity. The sample does get influenced by the peening and further experiments will provide better insight into using this specific type aluminium tape and the ablative material. It is important to note that the tape is commercially available and has not been engineering for

this specific purpose therefore slight changes in the properties of the tape could significantly influence the results because aluminium foil and aluminium tapes have been used in past for LSP experimentation.

Surface Roughness Results

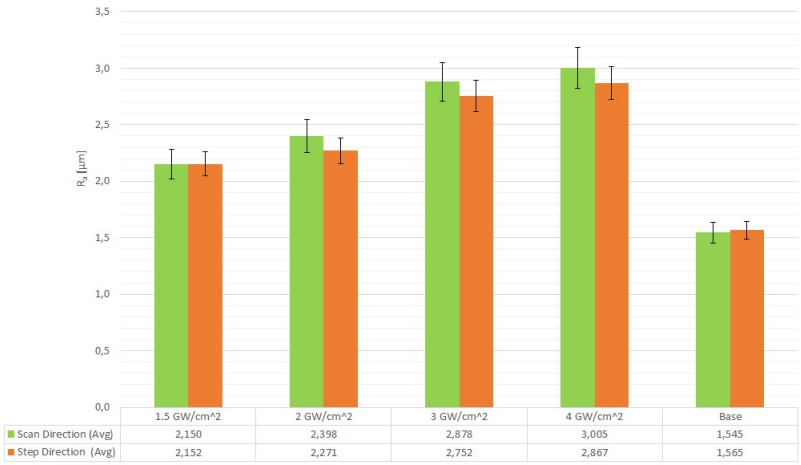


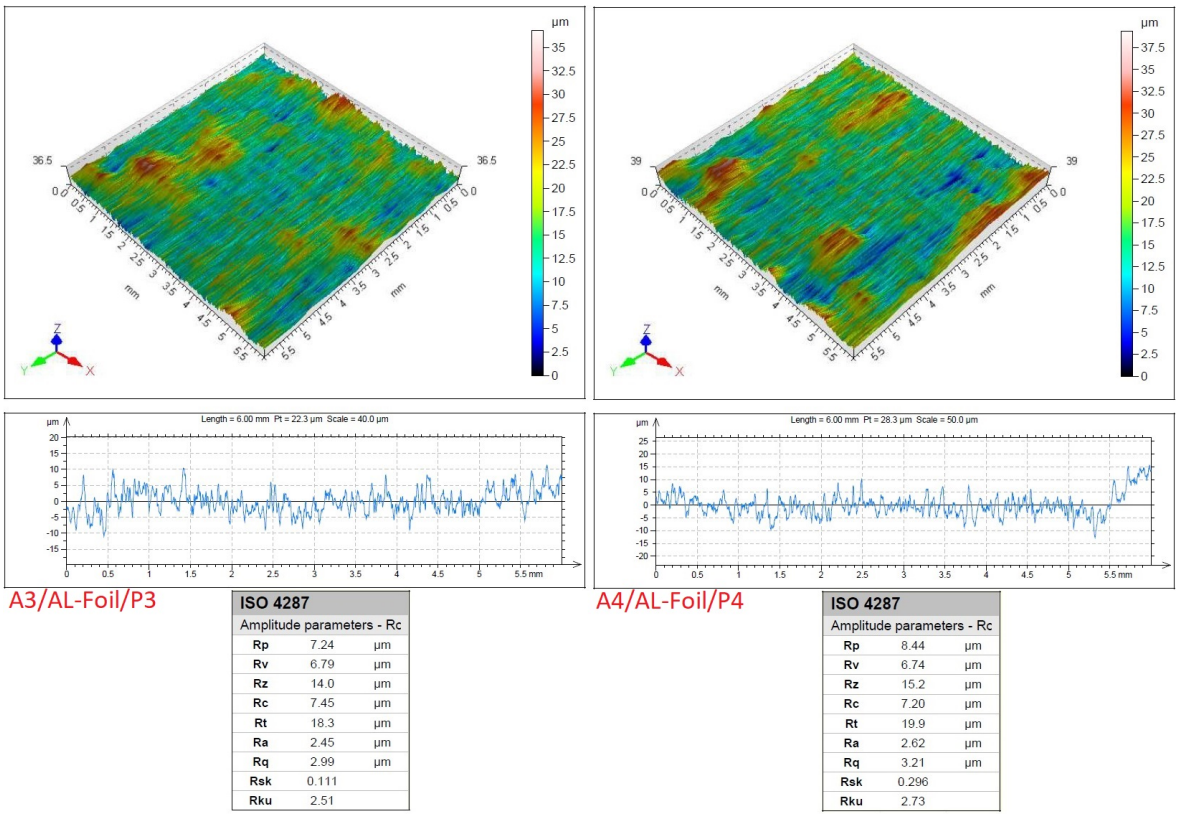
Figure 5.13: Surface Roughness Results for Aluminium Foil Tape Samples.

Figure 5.13 shows the results obtained for the surface roughness for the peened samples and the machined base sample using the portable SRT-6210 Unit. The surface roughness measurements were taken 3 times in 5 different location along both the longitudinal and transverse directions. The roughness data was tabulated and the average roughness was calculated which is represented in Figure 5.13. From Figure 5.13 an increasing trend can be seen for the roughness along both the scanning and stepping direction with the increasing power intensity.

A maximum mean surface roughness of 2.936 μm was obtained for specimen A4-AL-Foil-P4, while the minimum mean surface roughness of 2.151 μm was found for the LSP sample of A1-AL-Foil-P1.5 which was peened at a laser power intensity of 1.5 GW/cm^2. An increase of 38.29% was calculated for the average roughness for sample A1-AL-Foil-P1.5 from the surface roughness value of the unpeened base sample. While an increase of 50.12% was found for sample A2-AL-Foil-P2 and a 81% increase was observed for sample A3-AL-Foil-P3. The highest increase of 88.76% was found for sample A3-AL-Foil-P3.

The overall trend shown in Figure 5.13, is that there is a definite increase in surface roughness with the increasing of the laser intensity also an increasing gradient which is almost linear can be observed. The results also indicate that the surface roughness measured along the scanning direction is slightly higher, if not similar, to that measured along the stepping direction. The effect of using different ablative layers on surface roughness will be studied in the next section. The results obtained for these samples are similar to that found in literature, with increasing laser power at a constant coverage does increase the surface roughness of material[1].

3-D Surface Maps for Aluminium Foil Tape Samples



ISO 4287		
Amplitude parameters - Rc		
Rp	7.24	µm
Rv	6.79	µm
Rz	14.0	µm
Rc	7.45	µm
Rt	18.3	µm
Ra	2.45	µm
Rq	2.99	µm
Rsk	0.111	
Rku	2.51	

ISO 4287		
Amplitude parameters - Rc		
Rp	8.44	µm
Rv	6.74	µm
Rz	15.2	µm
Rc	7.20	µm
Rt	19.9	µm
Ra	2.62	µm
Rq	3.21	µm
Rsk	0.296	
Rku	2.73	

Figure 5.14: 3-D Surface Map for Samples: A3-AL-Foil-P3 and A4-AL-Foil-P4.

Figure 5.14 illustrates the 3-D surface that was obtained using the HOMMEL-ETAMIC T8000 R120-400 roughness testing machine for sample A3-AL-Foil-P3 and A4-AL-Foil-P4. The results show that peak roughness values of (R_p) 7.24 μm and 8.44 μm was obtained for the two samples. There is a definite change in the surface texture between the peened sample shown in Figure 5.14 when compared to the surface texture of the base sample shown in Figure 5.1.

The linear distance between the top peak and the valley base (R_z) of 15.2 μm for sample A4-AL-Foil-P4 is higher than that for sample A3-AL-Foil-P3 which has R_z= 14 μm. The same trend discussed for the results obtained in Figure 5.13 holds true, although the results obtained are highly accurate and have significantly lower uncertainties. The mean surface roughness for sample A3-AL-Foil-P3 was found to be R_a= 2.45 μm and R_a= 2.62 μm for sample A4-AL-Foil-P4.

The 2-D illustration of the peened surface roughness shows considerable change when compared to the uniform 2-D illustration shown in the base sample which shows the repetitive surface finish of the machining process and the LSPwC samples. There is a high degree of randomness which can be attributed to the failure of the ablative layer observed in the previous sub-section.

5.4 Clear Box Sealing Tape (313 Scotch 3M)

The following are the microscopic images and data obtained for the samples peened using clear box sealing tape as the ablative coating.

Sample: C1-Clear-P1.5

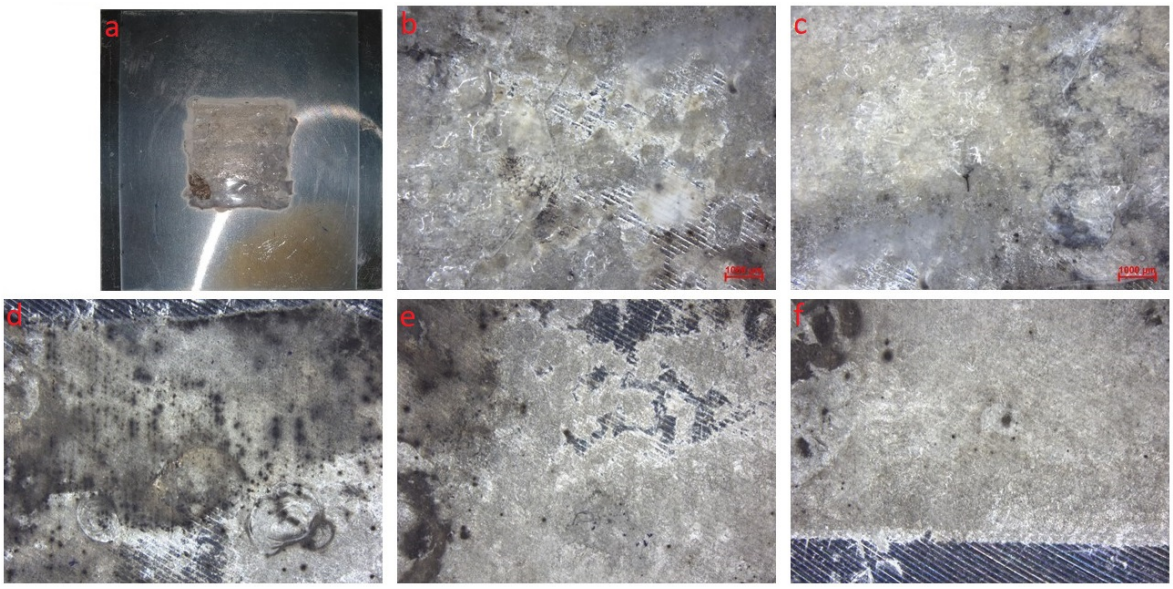


Figure 5.15: Surface Images for Sample: C1-Clear-P1.5.

Sample: C2-Clear-P2

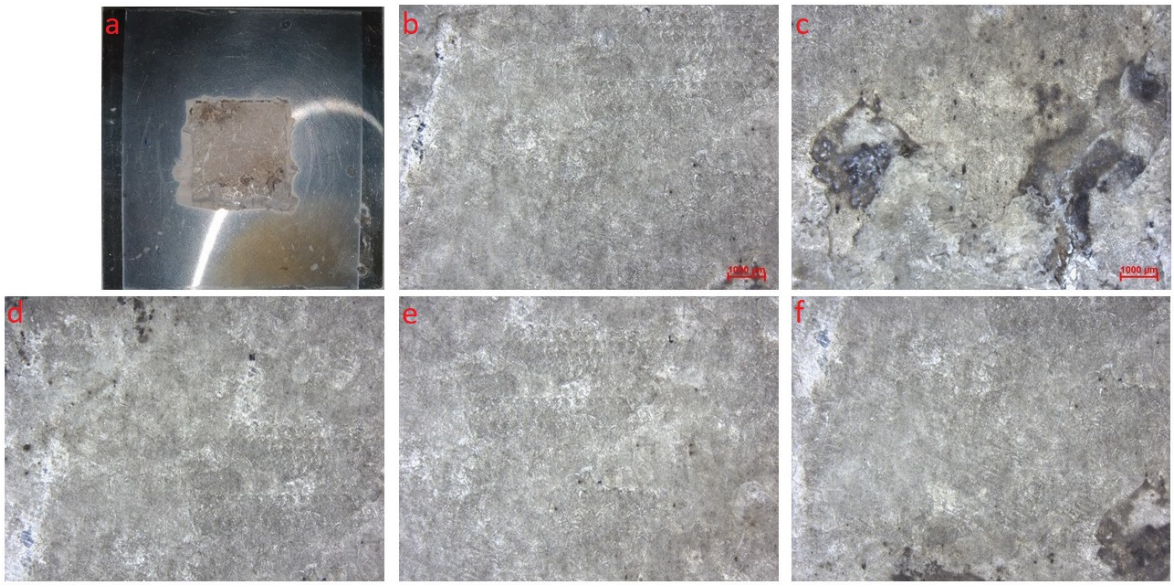


Figure 5.16: Surface images for Sample: C2-Clear-P2.

Sample: C3-Clear-P3

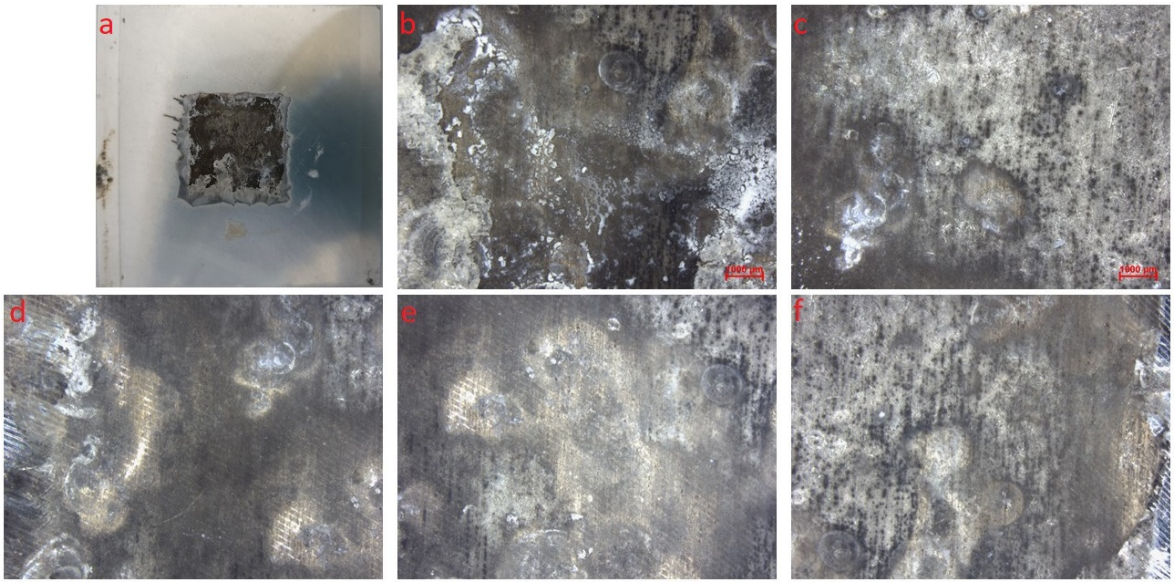


Figure 5.17: Surface images for Sample: C3-Clear-P3.

Sample: C4-Clear-P4

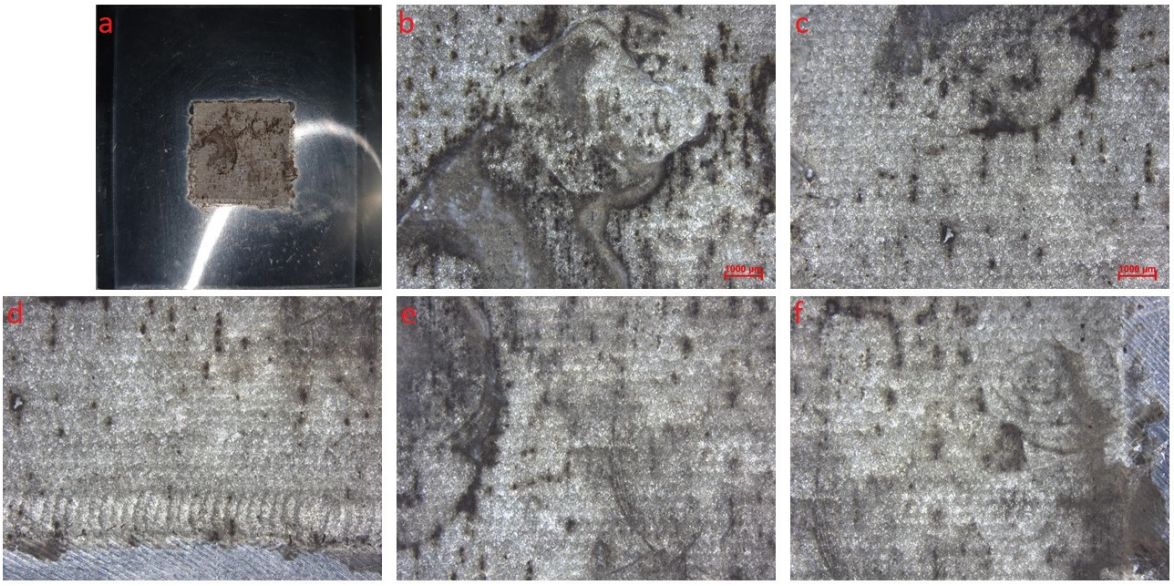


Figure 5.18: Surface images for Sample: C4-Clear-P4.

Sub-images (a-c) shown in Figure 5.15 to Figure 5.18 shows the surface state of the peened sample before the removal of the ablative tape whereas sub images (d-f) shows the surface state after the removal of the ablative tape, debris and contaminants. The degree of damage done by LSP on the ablative tape is illustrated in these images.

Figure 5.15a shows that the clear adhesive tape has been partially ablated under the power intensity of 1.5 GW/cm^2, the tape has been clearly melted during the peening process and due to this melting and the heat introduced by the laser, the tape in certain areas became thicker and thus resulted in irregular peening that can be observed in Figure 5.15. The melting of the tape also resulted in the discolouration of the peened surface.

Figure 5.16 shows the surface results obtained for the sample peened at 2 GW/cm^2. The tape for this instance has been ablated and there is minimal tape melting and tape residue that was left behind when compared to sample C1-Clear-P1.5. The surface texture however is irregular and displaying different peening textures.

Figure 5.17 however suggest a different contrast, the sample peened at 3 GW/cm^2 shows intense surface melting and discolouration, the clear tape was ablated by LSP but resulted in highly irregular peening. The observed surface texture shows high concentration of discolouration, surface melting and with small pockets of melted tape residue.

The images shown in Figure 5.18 when compared to Figure 5.17 is slightly different, although the sample was peened at a higher intensity the surface texture is unexpectedly less discoloured and shows a complete peening pattern and no tape residue thus suggesting that the clear tape was mostly ablated and vaporised during the peening process.

The clear tape which was made using polypropylene film and acrylic adhesive with a total thickness of 0.065 mm showed different results for each power intensity. At the low power intensity, the tape melted and remained behind on the surface after the peening process and as the power intensity increased the behaviour of the tape also changed, the tape experienced more melting with the increase in the intensity until it was completely ablated and vaporised at 4 GW/cm^2.

The performance of the clear tape as an ablative medium is erratic, the melting of the tape during the peening process introduces additional challenges, because the melting of tape changes the surrounding transparency and the physical properties of the tape that has yet to experience peening.

These samples also show that there was tape residue that was left behind during the peening process suggesting that there were some parts of the tape and its adhesive that did not fully ablate and could be the source of the discolouration that has been observed on the surface of the peened samples. The changes in the tape impact the overall performance of LSP, the melting and changes in the tape properties increase with the power intensity. Therefore, the changes that occur in real-time within the tape when peening impact the surface texture of the peened material.

Surface Roughness Results

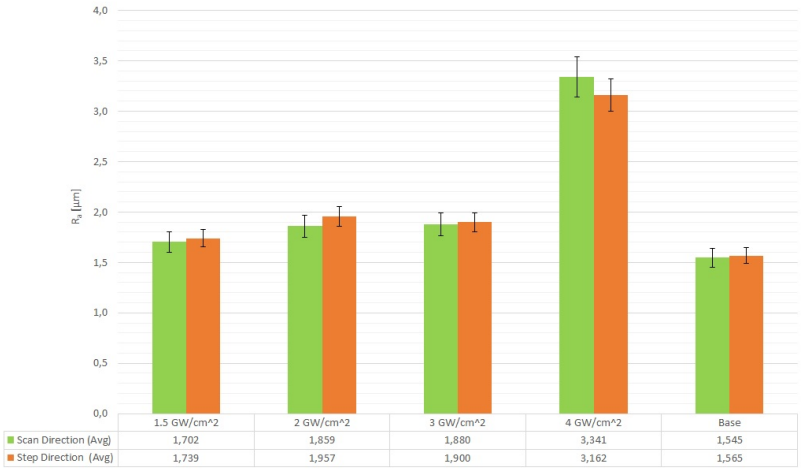


Figure 5.19: Surface Roughness Results for Clear Box Sealing Tape Samples.

Figure 5.19 illustrates the surface roughness data that was obtained for the peened samples using the portable SRT-6210 Unit. Due to the irregular peening that was observed from Figure 5.15 - Figure 5.18 the maximum mean surface roughness of 3.251 μm for sample C4-Clear-P4 whereas the minimum mean surface roughness of 1.721 μm was found for sample C1-Clear-P1.5. An increase of 10.66% in the mean surface roughness was calculated for sample C1-Clear-P1.5 and an increase of 22.69% and 21.53% was calculated for sample C2-Clear-P2 and C3-Clear-P3 respectively. However, a significant increase of 109.11% was calculated for sample C4-Clear-P4.

There is no clear trend that can be observed from Figure 5.19, due to the unseen behaviour of the clear tape during the peening process the overall results are skewed from expected results. The surface roughness result obtained for sample C3-Clear-P3 is a clear outlier, however during the roughness testing there were certain section that were found to have roughness values between 2.0 μm and 2.5 μm, the data found for this particular samples showed high degrees of variations. Therefore, the effect of changing power intensity for clear tape cannot be clearly defined thus showing that the tape itself is not a good ablative material and is not compatible for LSP.

5.5 Duct Tape (1900 3M)

The following are the microscopic images and data obtained for the samples peened using duct tape as the ablative coating.

Sample: D1-Duct-P1.5

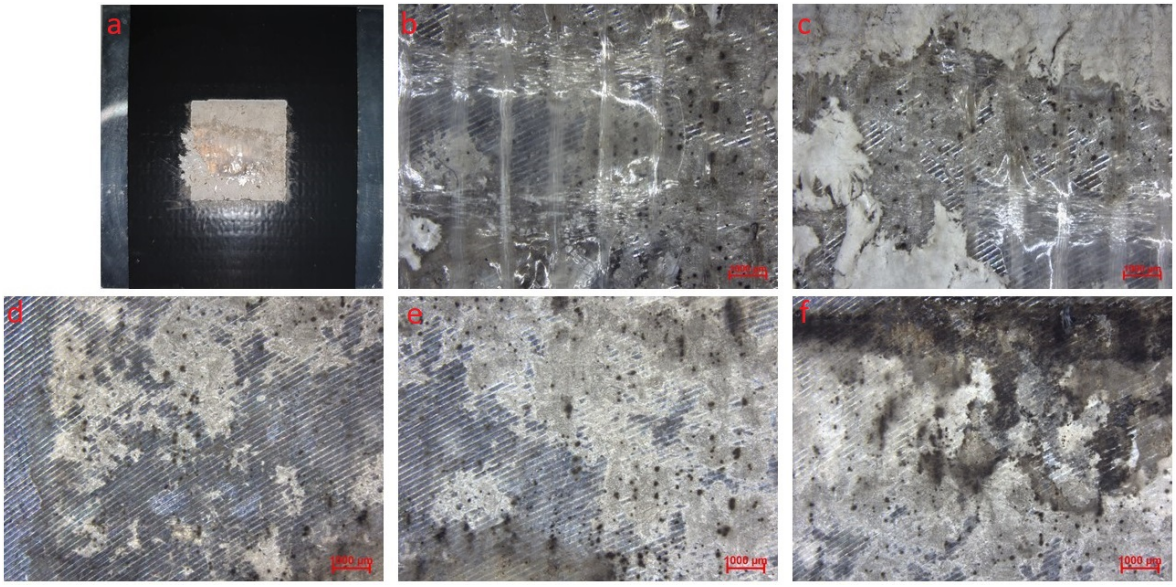


Figure 5.20: Surface Images for Sample: D1-Duct-P1.5.

Sample: D2-Duct-P2

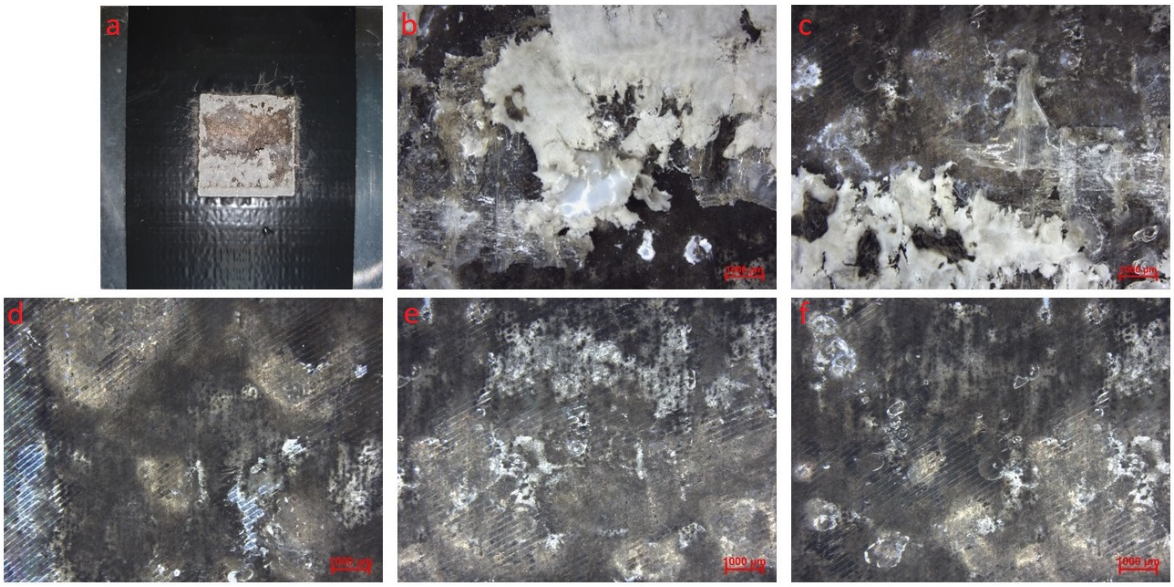


Figure 5.21: Surface Images for Sample: D2-Duct-P2.

Sample: D3-Duct-P3

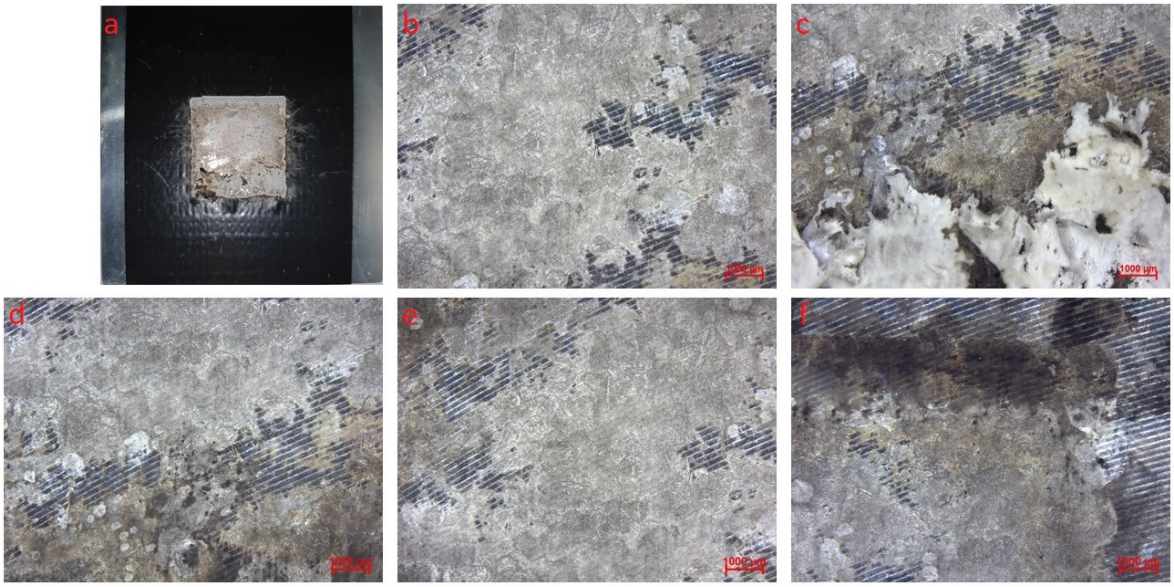


Figure 5.22: Surface Images for Sample: D3-Duct-P3.

Sample: D4-Duct-P4

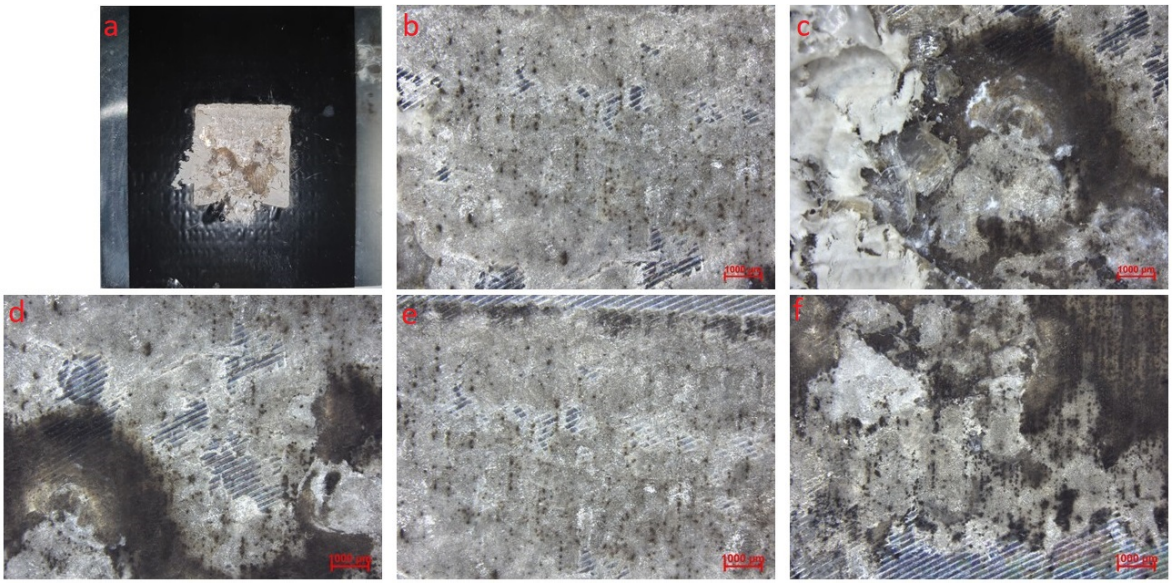


Figure 5.23: Surface Images for Sample: D4-Duct-P4.

Sub-images (a-c) shown in Figure 5.20 to Figure 5.23 shows the surface state of the peened sample before the complete removal of the ablative tape whereas sub images (d-f) shows the surface state after the removal of the ablative tape, debris and contaminants. The degree of damage done by LSP on the ablative tape is illustrated in these images.

The duct tape which consists of a combination of polyethylene film, cloth scrim and rubber adhesive interacts with LSP in a unique way. From Figure 5.20 it can be clearly seen that the tape experienced significant change when undergoing LSP, sub-image (b) clearly shows that that the polyethylene film is still intact however under the film a small amount of surface changes can be observed. At this low power intensity, the tape remained intact while no significant ablation can be observed. The cloth layer and its fibres do undergo changes and has been dislocated from the polyethylene film layer. The fibres of the cloth can be clearly seen and there is no major signs of surface melting. The surface texture of the peening is highly irregular with small patches of surface ablation.

The degree of damage that can be visually observed for the tape increases with the increasing in the laser power intensity. Figure 5.21 illustrates a higher degree of surface melting which resulted in the polyethylene film being ablated thus resulted in full penetration. The surface texture of the sample shows high degrees of surface melting and discolouration. The cloth fibre in this instance has been mostly ablated however the where the cloth fibres remained intact the underlying polyethylene film also remained intact thus resulting in uneven peening with high concentrations of discolouration.

Figure 5.22 shows the surface features for sample D3-Duct-P3, the tape experienced more ablation at this power intensity and as a result the surface is has a higher concentration of surface irregularities. The laser vaporised a larger portion of the tape thus resulting in a larger patch of surface ablation. The peening however is still not perfect as the ablative media nature is still erratic.

Figure 5.23 shows the surface state for sample D4-Duct-P4, the state of the tape in this instance is similar to sample D3-Duct-P3. The cloth and the polyethylene film has been mostly vaporised under the peening process. There is discolouration of the surface and this could be attributed to the melting of the tape. The surface texture is also similar to that of sample D3-Duct-P3, however there is a larger change in the texture of the surface when compared to the previous samples.

Overall the performance of tape became better with increasing power intensity. The configuration of the tape introduced additional challenges, at lower power intensities the film of the tape remained intact and as the power intensity increased the penetration of the laser also increased thus causing the film to ablate. The desired surface state using this tape as the ablative medium was not fully obtained.

Surface Roughness Results

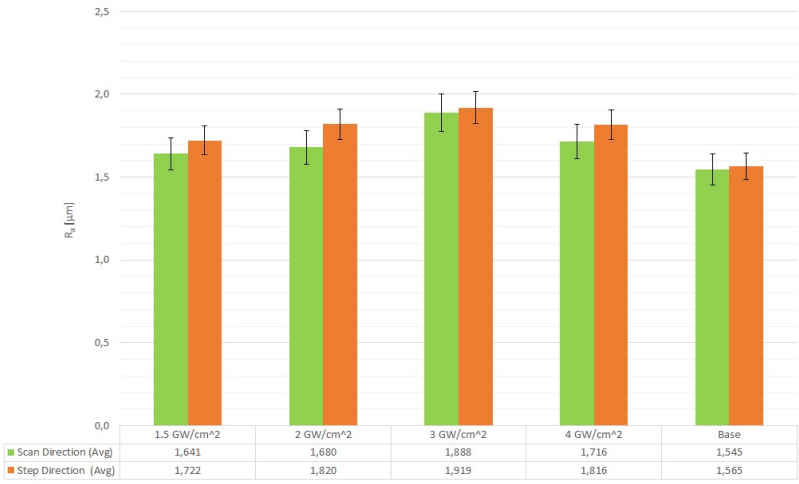


Figure 5.24: Surface Roughness Results for Duct Tape Samples.

Figure 5.24 shows the surface roughness results that were obtained for the sample peened using duct tape as the ablative layer. There is a 8.08% increase in the mean surface roughness for sample D1-Duct-P1.5 when compared to the unpeened base sample. A 12.5% increase in the mean surface roughness was calculated for sample D2-Duct-P2 and an increase of 22.4% was found for sample D3-Duct-P3. Sample D4-Duct-P4 peened with a power intensity of 4 GW/cm^2 saw an increase of 13.6% in the mean surface roughness.

The decrease in the roughness observed for sample D4-Duct-P4 from the mean surface roughness for D3-Duct-P3 can be attributed to the uneven peening that was conducted using this ablative material. The behaviour of the ablative medium in this case was erratic and did not conform to the findings that were observed in literature.

Overall from these finding it can be clearly seen from both the surface texture observed in the microscopic images and the surface roughness results that this ablative medium is not suitable for LSP as there are many factors within the tape that influence the final peening results.

5.6 Vinyl Tape (471 3M)

The following are the microscopic images and data obtained for the samples peened using vinyl tape 471 as the ablative coating.

Sample: E1-Vinyl471-P1.5

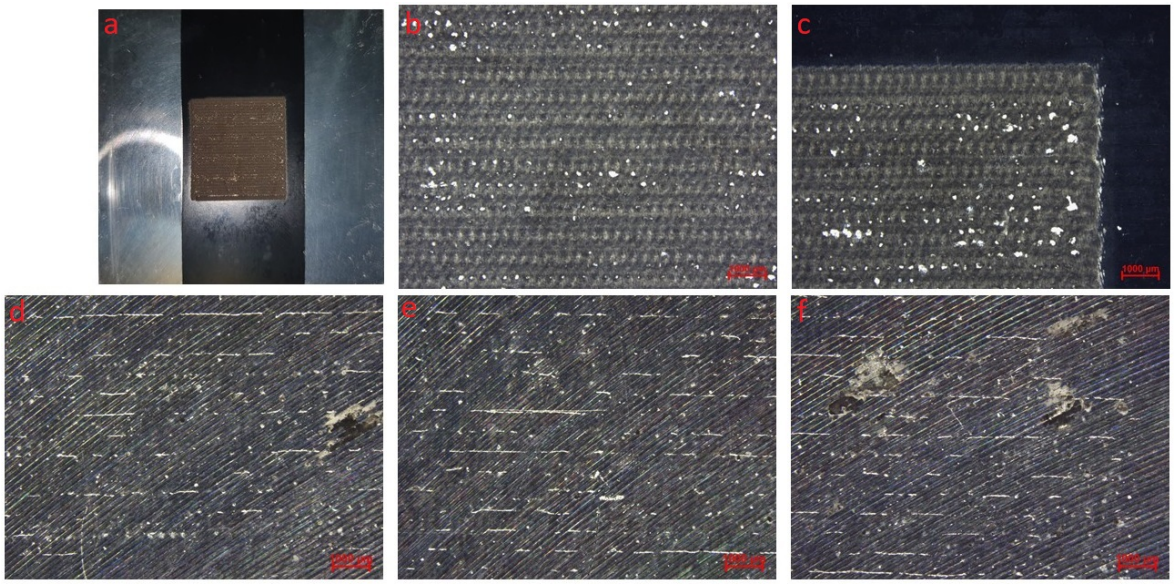


Figure 5.25: Surface Images for Sample: E1-Vinyl471-P1.5.

Sample: E2-Vinyl471-P2

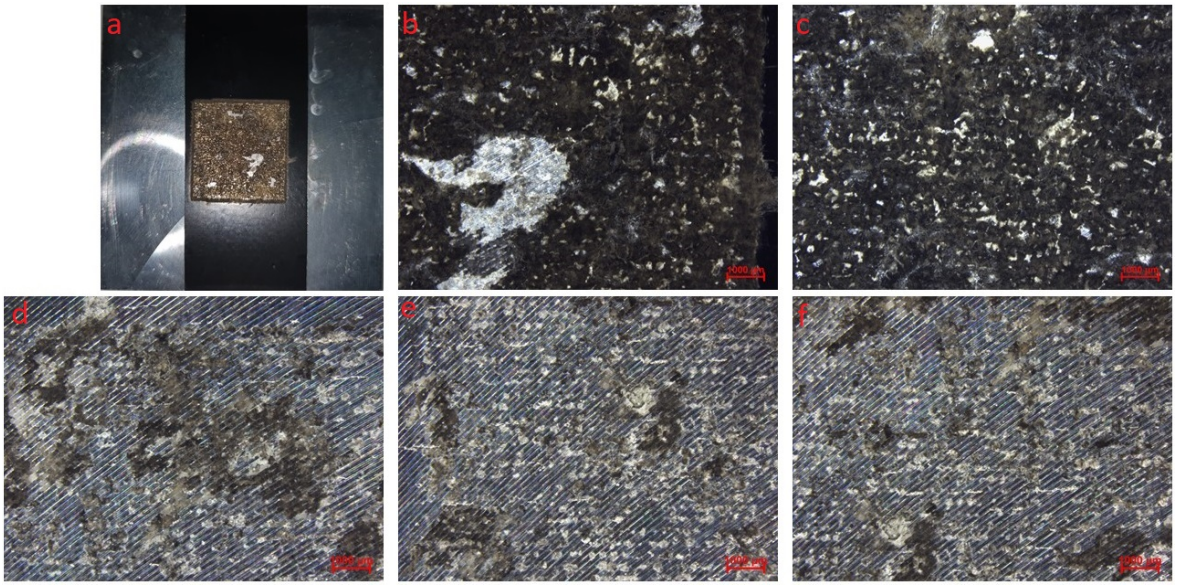


Figure 5.26: Surface Images for Sample: E2-Vinyl471-P2.

Sample: E3-Vinyl471-P3

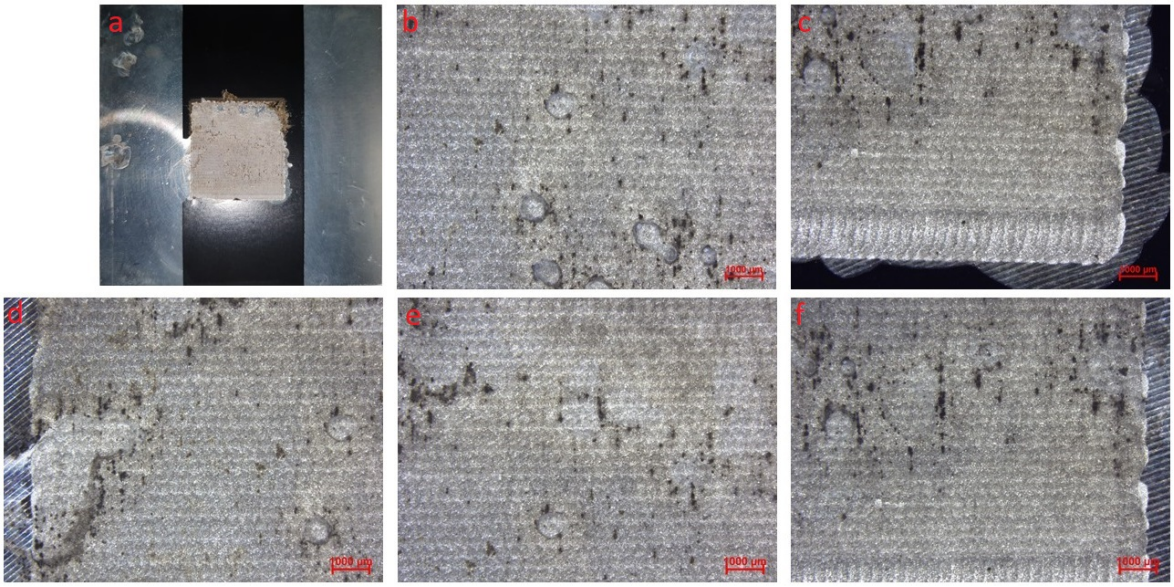


Figure 5.27: Surface Images for Sample: E3-Vinyl471-P3.

Sample: E4-Vinyl471-P4

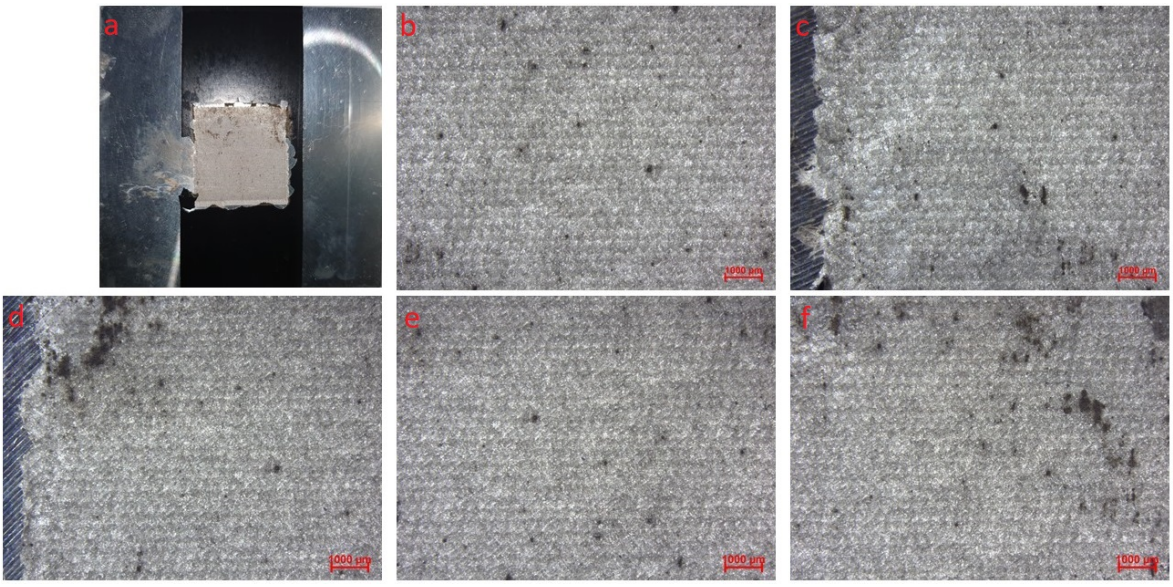


Figure 5.28: Surface Images for Sample: E4-Vinyl471-P4.

Sub-images (a-c) shown in Figure 5.25 to Figure 5.28 shows the surface state of the peened sample before the complete removal of the ablative tape whereas sub images (d-f) shows the surface state after the removal of the ablative tape, debris and contaminants. The degree of damage done by LSP on the ablative tape is illustrated in these images.

Figure 5.25 displays the peening results that were obtained using a power intensity of 1.5 GW/cm^2. The behaviour of the tape can be clearly seen, the tape has been partially ablated and the surface texture of peened sample can be clearly seen. The tape being intact shows that the power intensity was not enough to fully ablate and vaporise ablative material. There is no indication of surface discolouration and the machining marks is clearly visible. Overall the peening is as expected at this power intensity and using this tape. The tape remained in place and only been vaporised when compared to the previous ablative tapes that were studied.

Figure 5.26 shows the peening results conducted at 2 GW/cm^2. The surface texture of the tape indicated more tape has been ablated and vaporised at this power intensity. The final surface texture shows a change when compared to the sample Figure 5.25, there is more discolouration indicating that the tape experienced thermal damage. This result shows that with the higher power intensity more tape has been ablated.

The surface results obtained for sample E3-Vinyl471-P3 is shown in Figure 5.27. The surface texture is significantly better when compared to the previous two samples. The tape has been fully ablated, there is small amounts of surface discolouration but there is no tape residue left on the surface. The performance of the vinyl tape is considerable better when compared to sample that have been studied.

Figure 5.28 shows the peening results for the sample peened at 4 GW/cm^2. As shown in the figure the tape has been fully ablated and the surface texture is uniform with slight discolouration. The peening is considerably better, therefore the tape which is made with a vinyl backing and rubber adhesive is compatible with LSP provided that it is performed with the optimal laser parameters.

In conclusion, the peening using this type of backing material yields considerably better peening results when compared to the tape that have been analysed so far.

Surface Roughness Results

Figure 5.29 shows the surface roughness results that were obtained for the sample peened using vinyl tape 471 as the ablative layer using the portable SRT-6210 Unit.

There is a 6.40% decrease in the mean surface roughness for sample E1-Vinyl471-P1.5 when compared to mean surface roughness for the unpeened base sample. A 5.8% decrease in the mean surface roughness was calculated for sample E2-Vinyl471-P2 and a significant increase of 88.89% was found for sample E3-Vinyl471-P3. Whereas, for sample E4-Vinyl471-P4 peened with a power intensity of 4 GW/cm^2 saw an increase of 102.6% in the mean surface roughness.

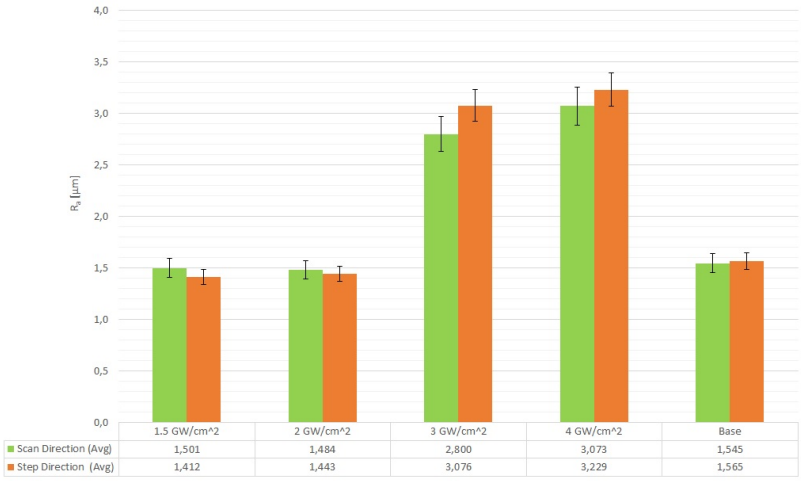


Figure 5.29: Surface Roughness Results for Vinyl Tape 471 Samples.

The changes found in the mean surface roughness for these show two distinct results, for the two sample where the tape remained intact the surface roughness was found to be lower than that of the machined unpeened sample. This indicates that the shock wave penetrated through the ablative material and peened the underlying material. This shows that at low power intensities the surface integrity of the material can be preserved and can introduce beneficial residual stresses into the material.

The second result that shows the increase in the mean surface roughness was found for the samples that had the ablative layer fully vaporised under LSP. The surface roughness of these two sample has been increased significantly.

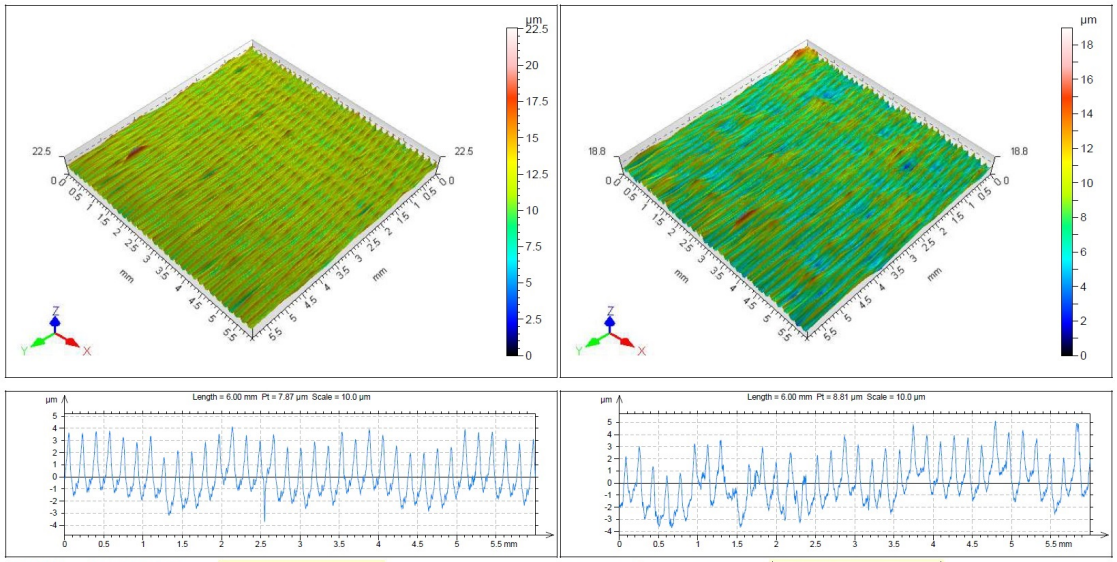
Overall the tape can be used as a medium to control the surface features of the peened material and can is quite compatible with LSP as a whole.

3-D Surface Maps for Vinyl Tape 471 Samples

Figure 5.30 and Figure 5.31 illustrates the 3-D surface maps of the samples. One can visually see the changes in the surface features as the power intensity is increased. The surface roughness values are represented more accurately and a clear trend can be seen.

The mean surface roughness (R_a) gradually increase from 1.27 μm for 1.5 GW/cm^2 to a maximum of 2.52 μm for 4 GW/cm^2. The changes in the 2-D map is also gradual, uniformity in the surface decreases after sample E3-Vinyl471-P3 and a significant amount of noise is present in the profile. The sinusoidal peening nature is represented in these images.

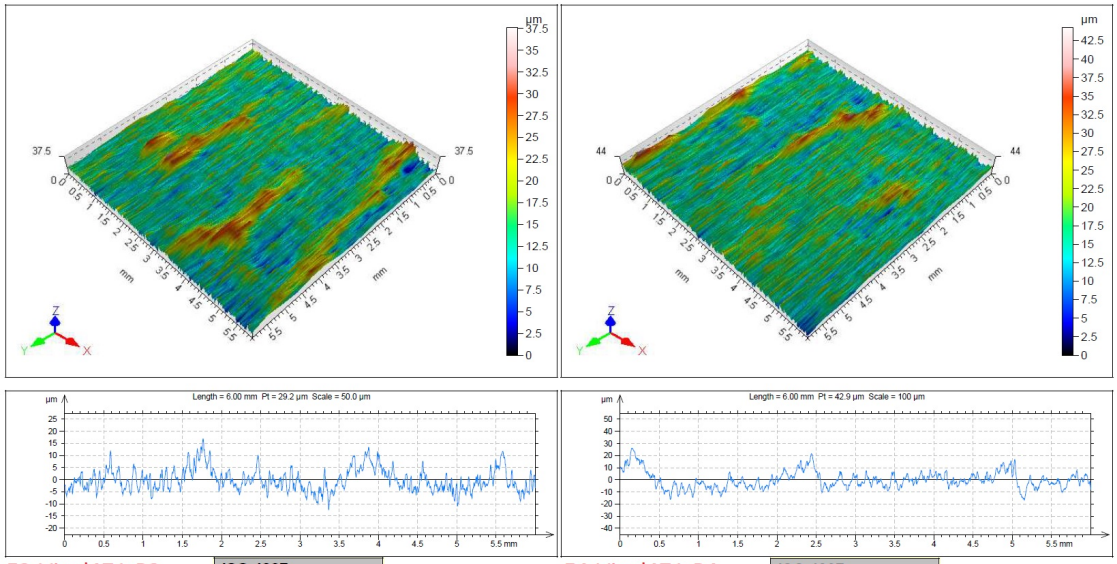
The changes in R_z and R_p only occur after the tape has been fully ablated which happen after the tape experience a power intensity of 3 GW/cm^2 and higher. Similar to the previous finding the surface roughness for 2 samples peened with 1.5 GW/cm^2 and 2 GW/cm^2 is lower than the unpeened base sample and the LSPwC samples.



ISO 4287		
Amplitude parameters - R		
Rp	4.48	µm
Rv	2.27	µm
Rz	6.74	µm
Rc	5.06	µm
Rt	12.9	µm
Ra	1.27	µm
Rq	1.59	µm
Rsk	1.01	
Rku	3.53	

ISO 4287		
Amplitude parameters - Rc		
Rp	3.78	µm
Rv	3.07	µm
Rz	6.85	µm
Rc	4.19	µm
Rt	9.37	µm
Ra	1.29	µm
Rq	1.56	µm
Rsk	0.379	
Rku	2.48	

Figure 5.30: 3-D Surface Map for Samples: E1-Vinyl471-P1.5 and E2-Vinyl471-P2.



ISO 4287		
Amplitude parameters - Rc		
Rp	8.74	µm
Rv	7.81	µm
Rz	16.6	µm
Rc	6.90	µm
Rt	20.7	µm
Ra	2.57	µm
Rq	3.26	µm
Rsk	0.159	
Rku	3.09	

ISO 4287		
Amplitude parameters - Rc		
Rp	7.68	µm
Rv	6.96	µm
Rz	14.6	µm
Rc	7.18	µm
Rt	20.0	µm
Ra	2.52	µm
Rq	3.13	µm
Rsk	0.320	
Rku	2.66	

Figure 5.31: 3-D Surface Map for Samples: E3-Vinyl471-P3 and E4-Vinyl471-P4.

5.7 Flame-Retardant Tape with Polyester Film (1350-1 3M)

The following are the microscopic images and data obtained for the samples peened using flame-retardant tape with a polyester film as the ablative coating.

Sample: F1-Polyster-P1.5

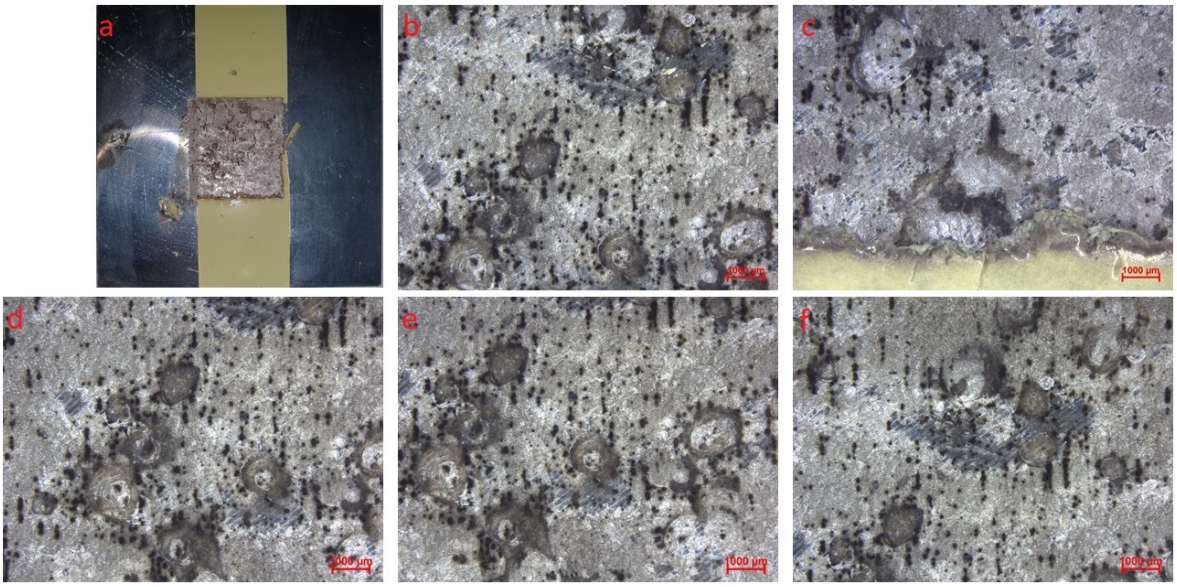


Figure 5.32: Surface Images for Sample: F1-Polyster-P1.5.

Sample: F2-Polyster-P2

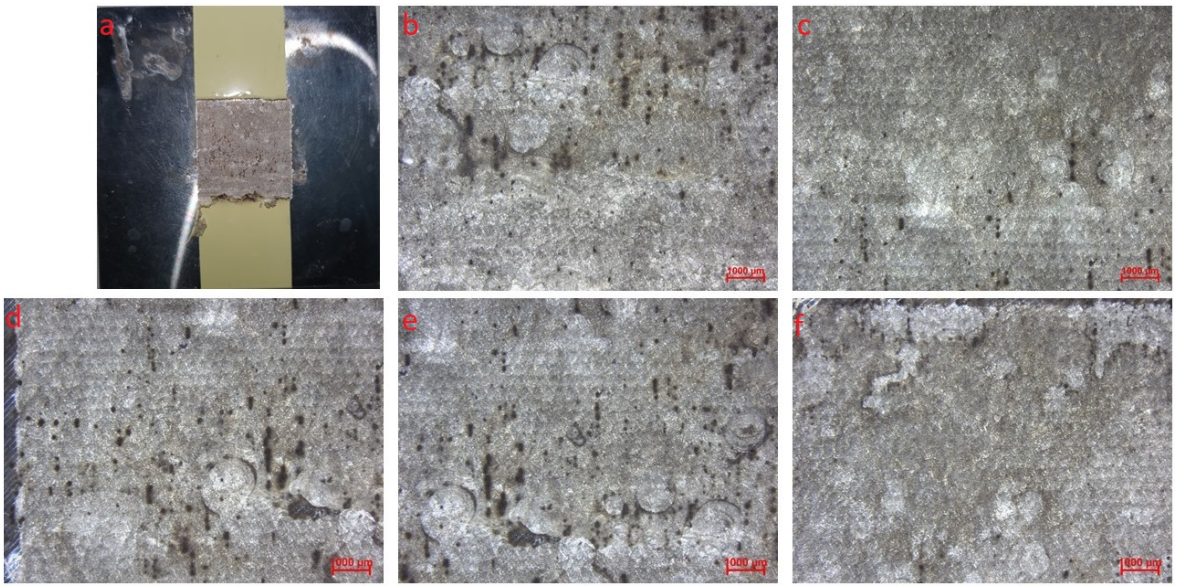


Figure 5.33: Surface Images for Sample: F2-Polyster-P2.

Sample: F3-Polyster-P3

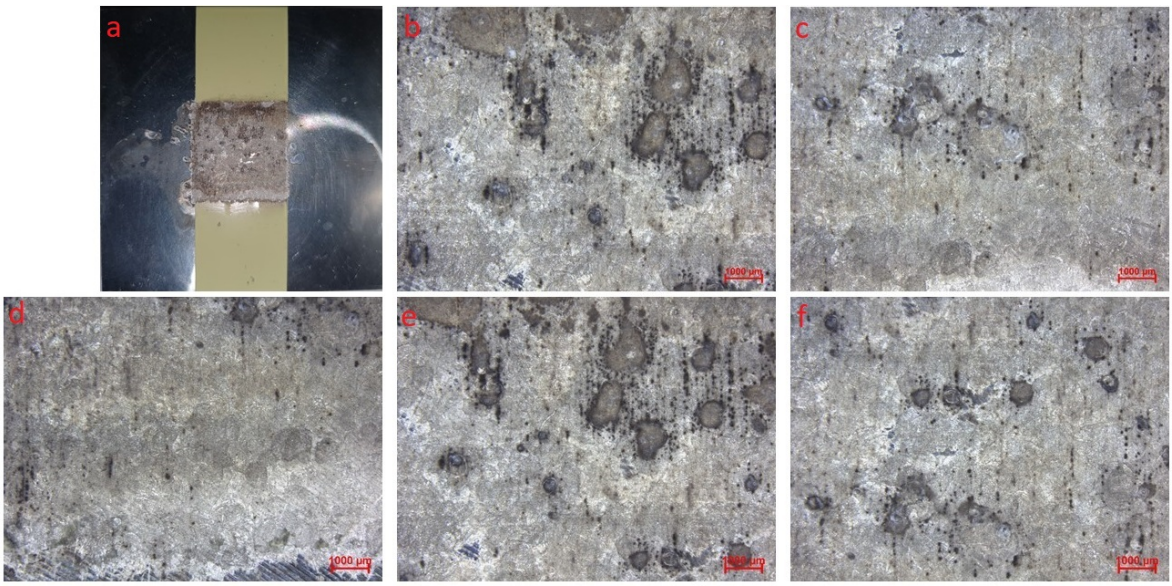


Figure 5.34: Surface Images for Sample: F3-Polyster-P3.

Sample: F4-Polyster-P4

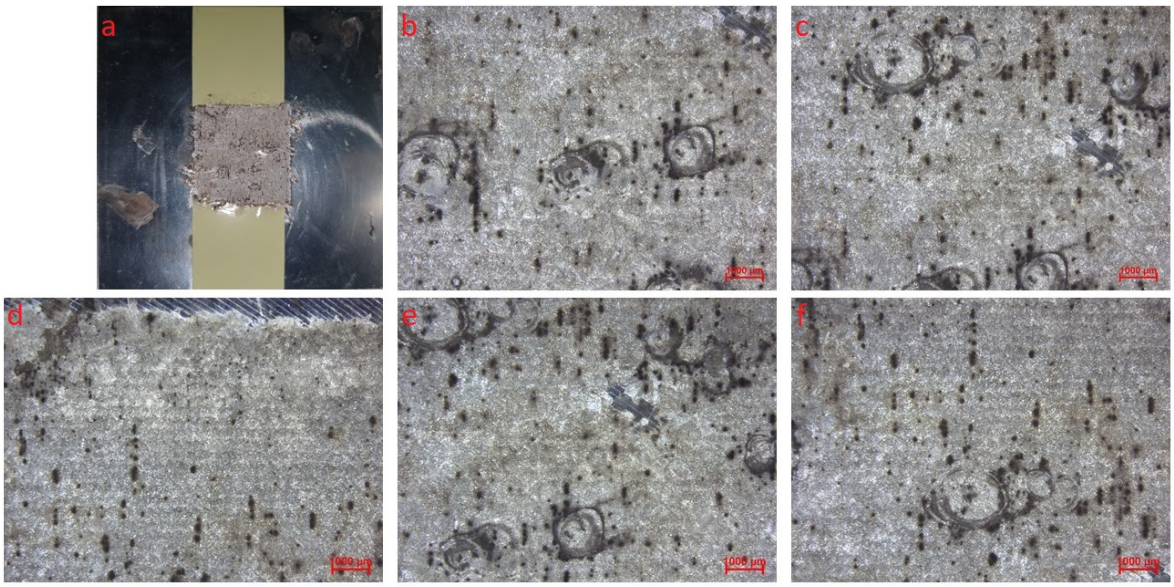


Figure 5.35: Surface Images for Sample: F4-Polyster-P4.

Sub-images (a-c) shown in Figure 5.32 to Figure 5.35 shows the surface state of the peened sample before the complete removal of the ablative tape whereas sub images (d-f) shows the surface state after the removal of the ablative tape, debris and contaminants. The degree of damage done by LSP on the ablative tape is illustrated in these images.

Figure 5.32 show the surface texture for sample F1-Polyster-P1.5, as illustrated in the figure the tape has been fully ablated. The result of the peening show that the surface texture is irregular with small sections that show an unpeened texture. There is also large amounts of discolouration and there is no observable peening pattern that can be seen on the sample. The tape itself has been fully ablated during the peening process.

The surface texture for sample F2-Polyster-P2 illustrated in Figure 5.33 shows a clearer peening pattern with small amount of surface discolouration and the tape itself has also been fully ablated. The surface texture for sample F3-Polyster-P3 and F4-Polyster-P4 shown in Figure 5.34 and Figure 5.34 show similar surface results. There is small amount of surface discolouration and small traces of surface smelting. The tape in both cases has also been ablated.

Overall the peening results found using this ablative tape is not excellent when compared to result found for the samples peened using vinyl tape.

Surface Roughness Results

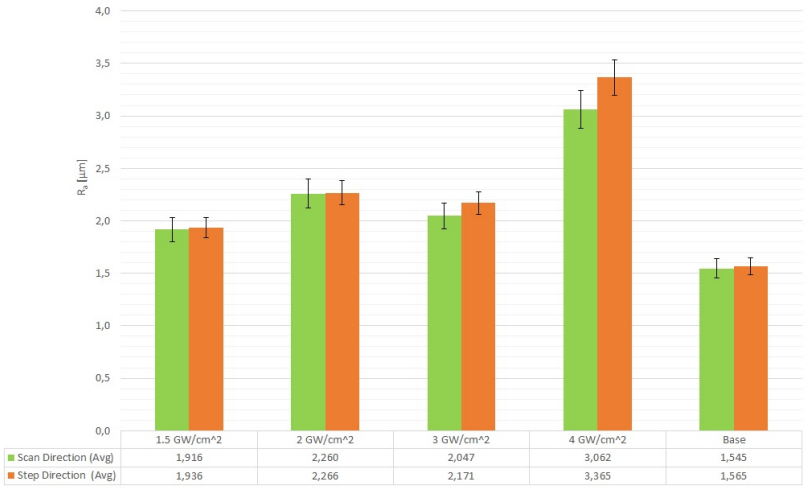


Figure 5.36: Surface Roughness Results for Polyester Tape Samples.

Figure 5.36 shows the surface roughness results that were obtained for the sample peened using the polyester tape as the ablative layer. The results show that tape achieved similar roughness results for the first three power intensities with the last power intensity showing a significant increase in the roughness.

There is a 23.9% increase in the mean surface roughness for sample F1-Polyster-P1.5 when compared to the unpeened base sample. A 45.5% increase in the mean surface roughness was calculated for sample F2-Polyster-P2 and a increase of 35.6% was found for sample F3-Polyster-P3. Sample F4-Polyster-P4 peened with a power intensity of 4 GW/cm^2 saw a high increase of 106.6% in the mean surface roughness from the unpeened base sample.

The increase in the roughness observed for sample F4-Polyster-P4 from the other samples can be attributed to the ablative not having enough influence in protecting the surface of the material during peening. The behaviour of the ablative medium in this case showed no clear trend, it influenced the surface texture of the material up until the peening intensity of 3 GW/cm^2.

Overall from these finding it can be clearly seen from both the surface texture observed in the microscopic images and the surface roughness results that this ablative medium is not suitable for LSP as it provides inconsistent results.

3-D Surface Maps for Polyester Tape Samples

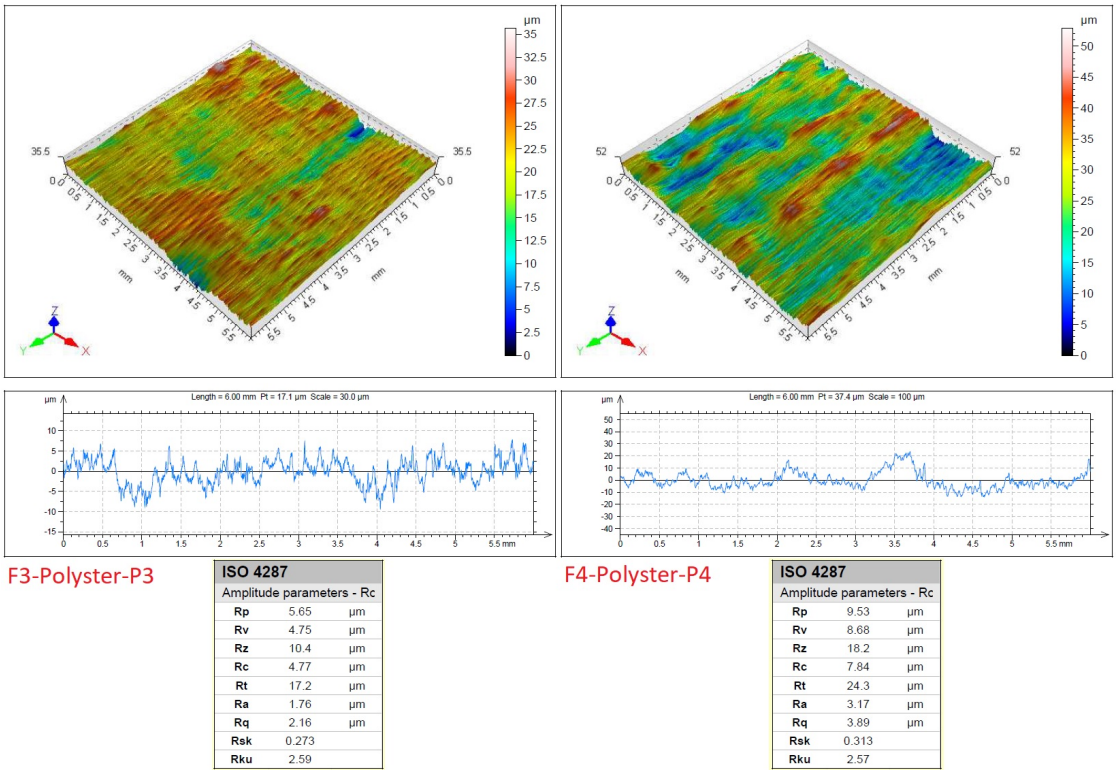


Figure 5.37: 3-D Surface Roughness Results for Polyester Tape Samples.

Figure 5.37 show the 3-D surface texture for samples F3-Polyster-P3 and F4-Polyster-P4. There is large difference in the surface textures that can be observed.

The results show that peak roughness values of (R_p) 5.85 μm and 9.53 μm was obtained for the two samples. The R_z value of 18.2 μm for sample F4-Polyster-P4 is higher than that for sample F3-Polyster-P3 which has R_z= 10.4 μm. The mean surface roughness for sample F3-Polyster-P3 was found to be 1.76 μm and 3.17 μm for sample F4-Polyster-P4.

The 2-D surface maps show no clear trend when compared to previous samples with high amounts of noise and randomness.

5.8 Duct Cloth Fibre Tape (2903 3M)

The following are the microscopic images and data obtained for the samples peened using duct cloth fibre tape as the ablative coating.

Sample: G1-Fiber-P1.5

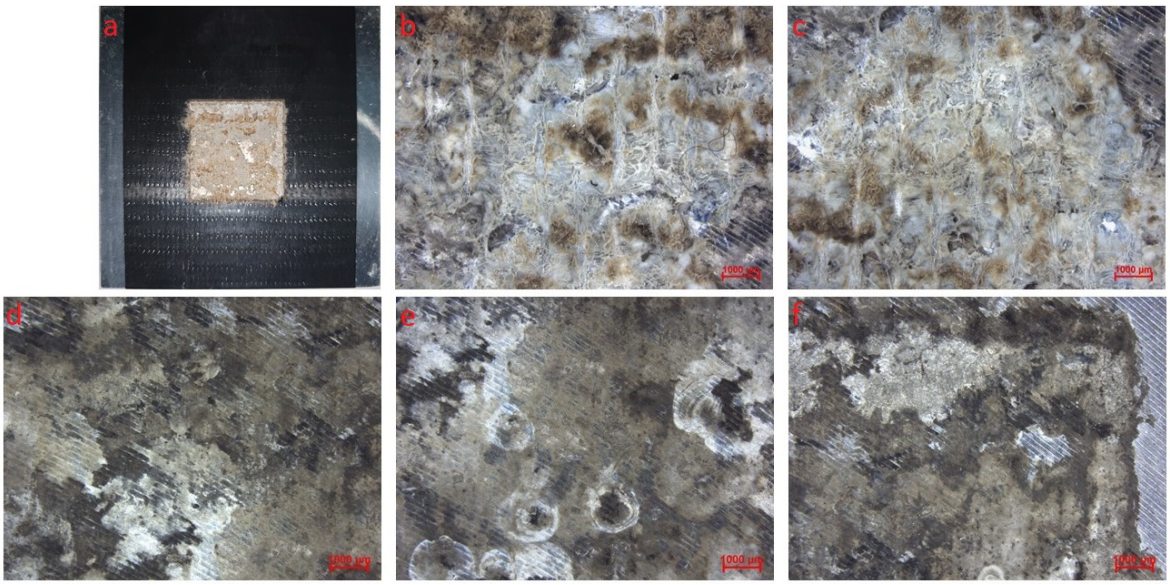


Figure 5.38: Surface Images for Sample: G1-Fiber-P1.5.

Sample: G2-Fiber-P2

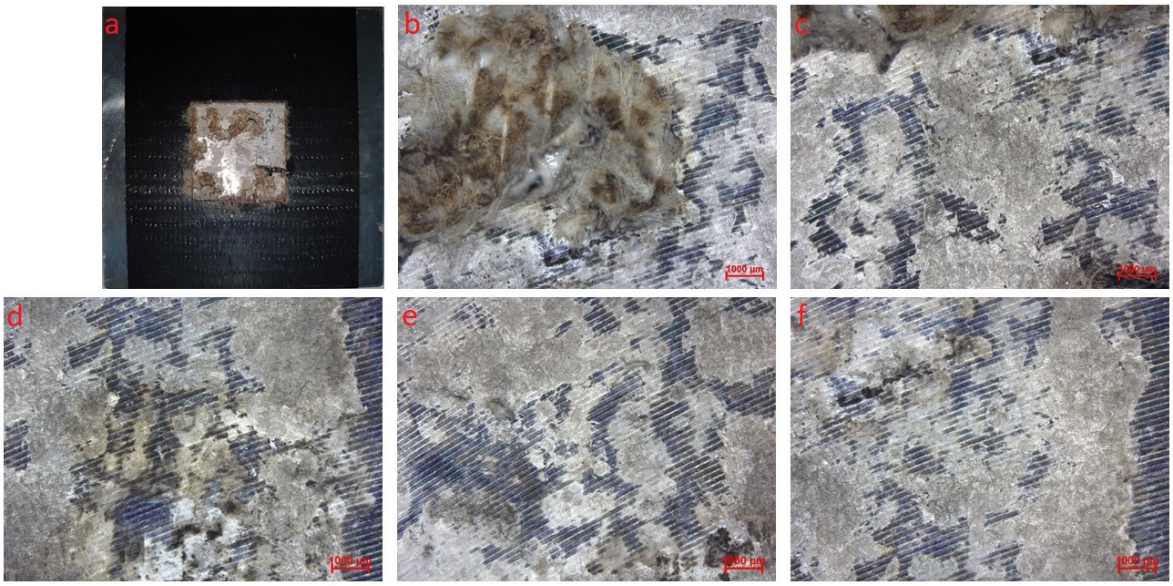


Figure 5.39: Surface Images for Sample: G2-Fiber-P2.

Sample: G3-Fiber-P3

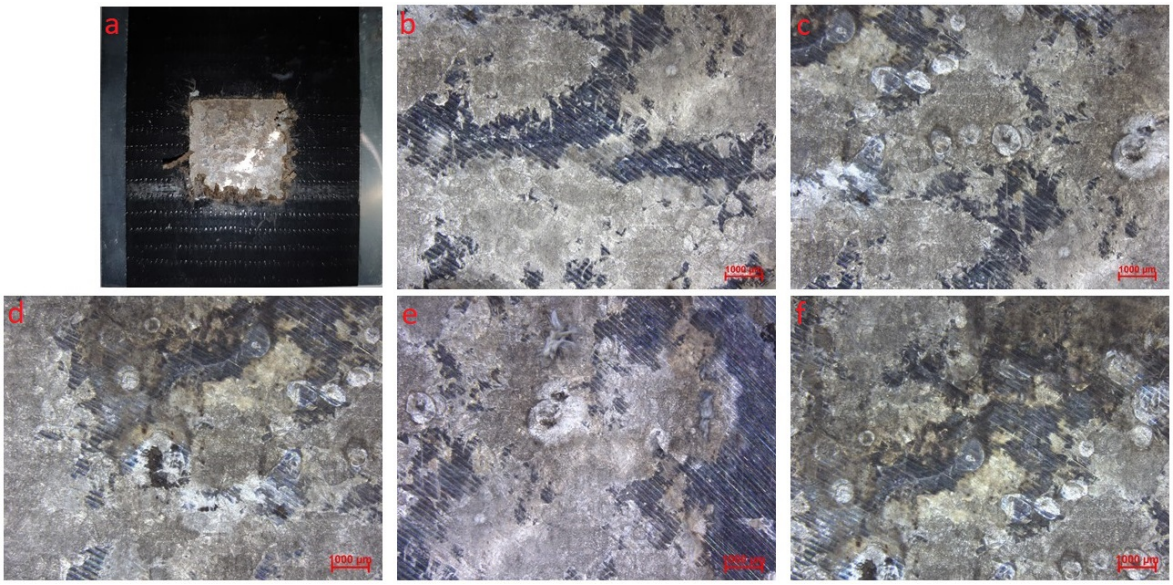


Figure 5.40: Surface Images for Sample: G3-Fiber-P3.

Sample: G4-Fiber-P4

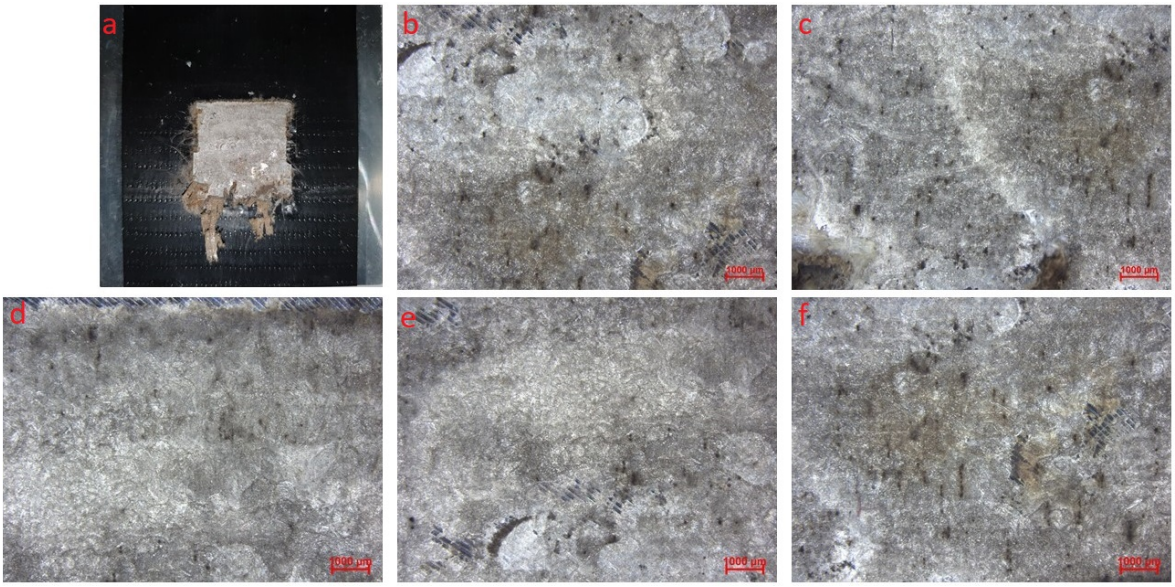


Figure 5.41: Surface Images for Sample: G4-Fiber-P4.

Sub-images (a-c) shown in Figure 5.38 to Figure 5.41 shows the surface state of the peened sample before the complete removal of the ablative tape whereas sub images (d-f) shows the surface state after the removal of the ablative tape, debris and contaminants. The degree of damage done by LSP on the ablative tape is illustrated in these images.

The results and behaviour found for the duct cloth fibre tape is quite similar to the results obtained for the samples peened using the duct tape in section 5.4. From Figure 5.38 the images show that most of the cloth fibre are intact and thus results in the uneven peening that can be observed in Figure 5.38 (d-f). There is high amounts of discolouration within the surface which is the result of the high temperatures that was experienced by the fibre tape during ablation.

Figure 5.39 show the surface results obtained for sample G2-Fiber-P2, there is less cloth fibres present on the sample after the peening. The peening is also irregular with small amounts of surface melting and discolouration. Figure 5.40 shows that the ablative material has been mostly ablated, there is trace of cloth fibres that are present at the edges of the peening area. Similar results can be observed for sample G4-Fiber-P4 shown in Figure 5.41. The surface texture has lower amounts of discolouration when compared to the previous samples.

Even though the performance of the cloth fibre tape is better than that of the duct tape outlined in section 5.4. Similarly like the duct tape, the fibre tape is not suitable for LSP as there is no consistency in the peening results when using this material as an ablative material.

Surface Roughness Results

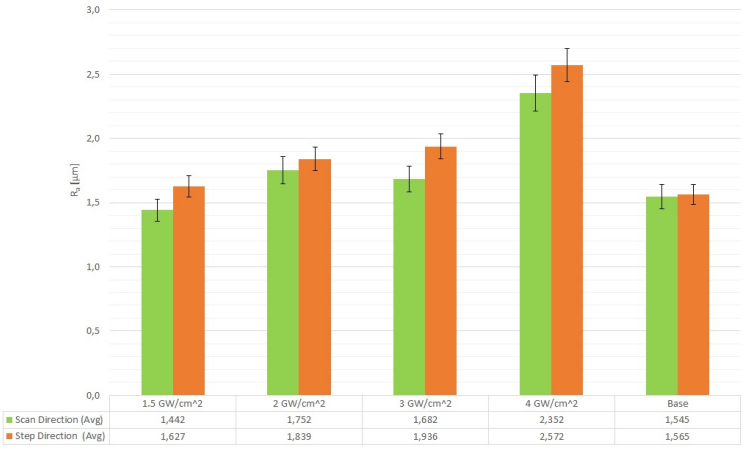


Figure 5.42: Surface Roughness Results for the Cloth Fibre Tape Samples.

Figure 5.42 shows the surface roughness results that were obtained for these peened samples. The results show that this ablative tape achieved similar roughness results for the first three power intensities with the last power intensity showing a significant increase in the roughness.

There is a 1.4% decrease in the mean surface roughness for sample G1-Fiber-P1.5 from the unpeened base same. A 15.4% increase was found in the mean surface roughness for sample G2-Fiber-P2, while an increase of 16.3% was found for sample G3-Fiber-P3 and whereas a significant increase of 58.3% for sample G4-Fiber-P4. The same trend is present as the changes in the surface roughness increases with the increasing power intensity. The inconsistency in the result show that the tape is not ideal as an ablative material.

5.9 Vinyl Tape (Super 88 Scotch 3M)

The following are the microscopic images and data obtained for the samples peened using vinyl tape super 88 as the ablative coating.

Sample: H1-Vinyl88-P1.5

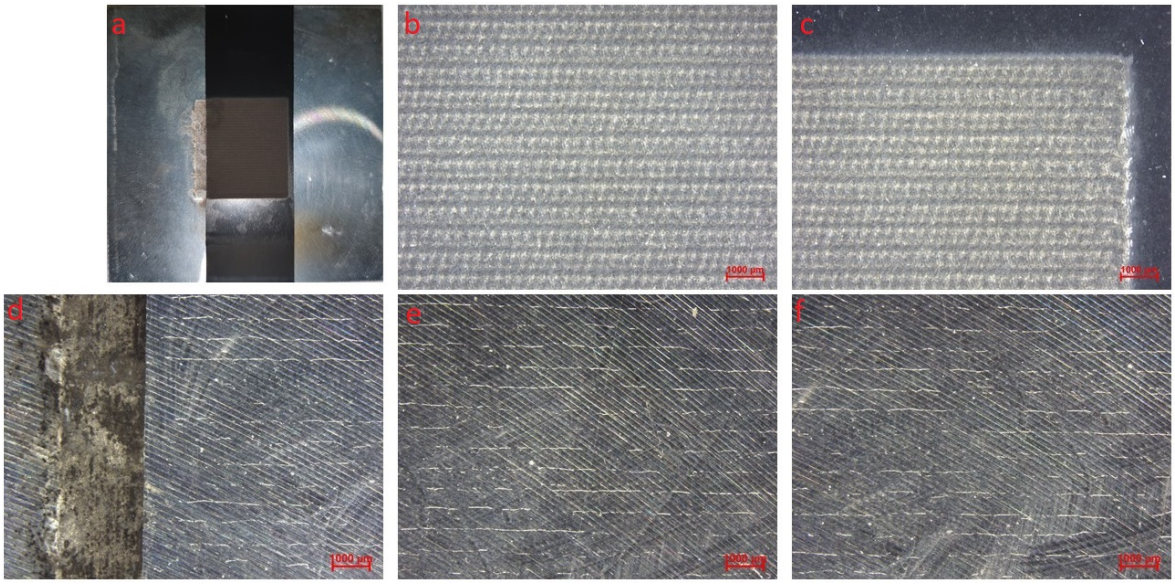


Figure 5.43: Surface Images for Sample: H1-Vinyl88-P1.5.

Sample: H2-Vinyl88-P2

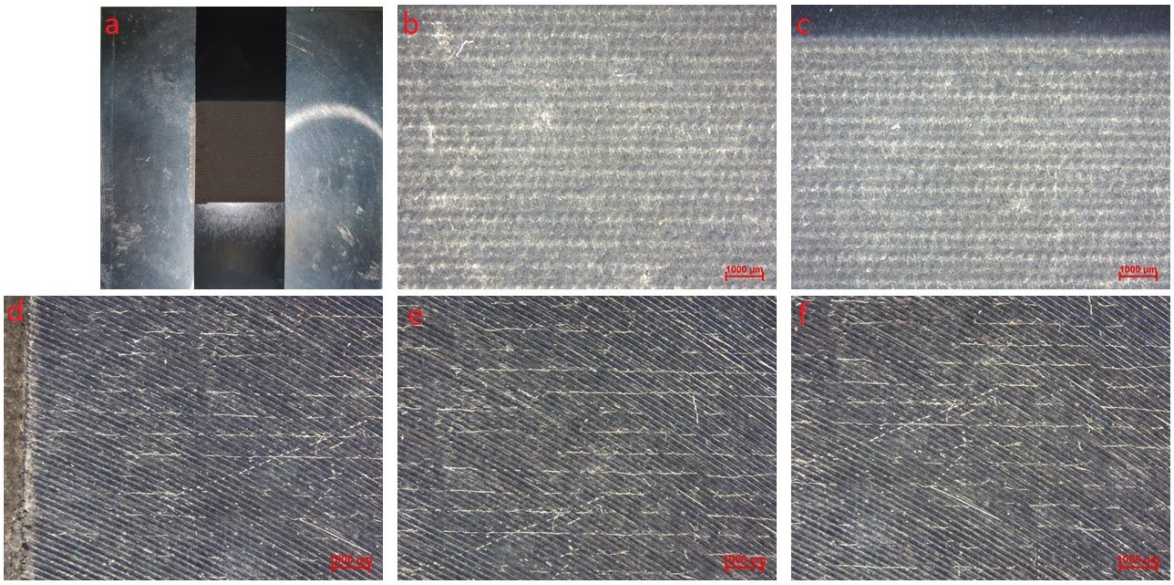


Figure 5.44: Surface Images for Sample: H2-Vinyl88-P2.

Sample: H3-Vinyl88-P3

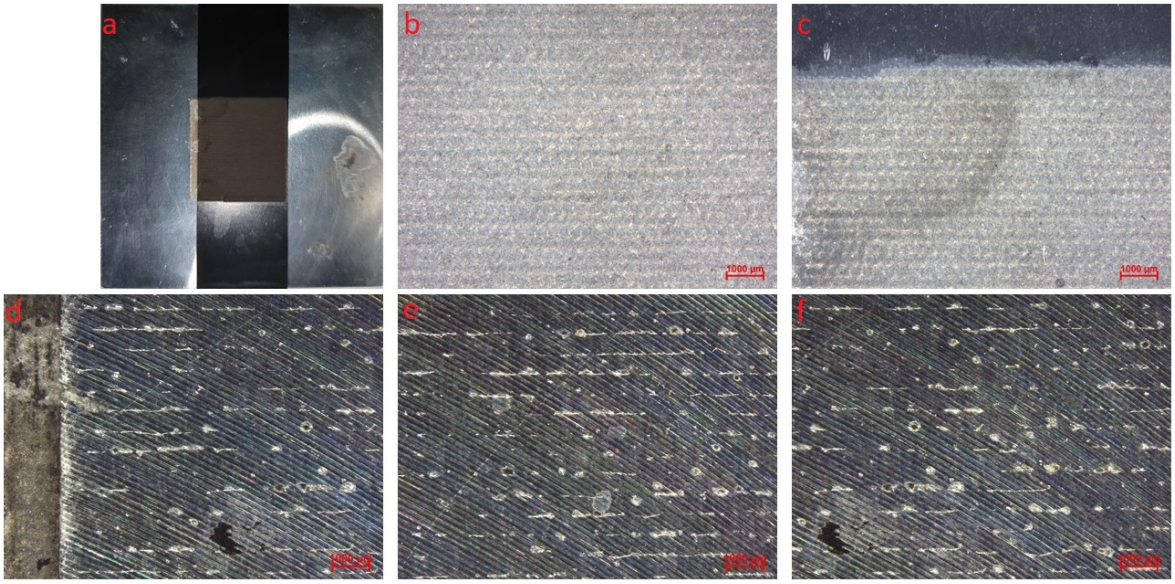


Figure 5.45: Surface Images for Sample: H3-Vinyl88-P3.

Sample: H4-Vinyl88-P4

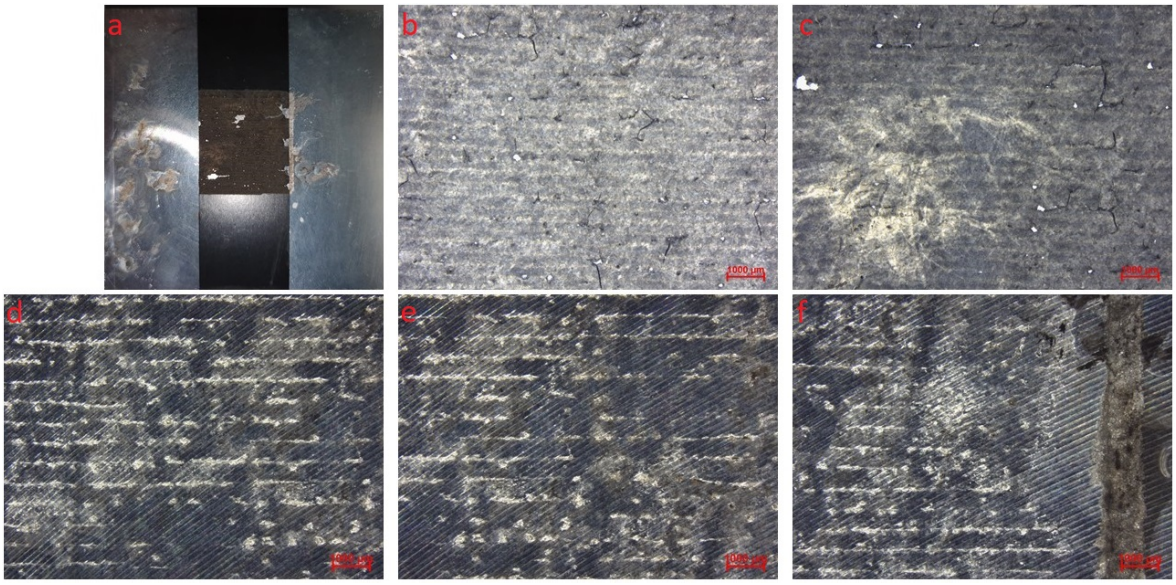


Figure 5.46: Surface Images for Sample: H4-Vinyl88-P4.

Sub-images (a-c) shown in Figure 5.43 to Figure 5.46 shows the surface state of the peened sample before the complete removal of the ablative tape whereas sub images (d-f) shows the surface state after the removal of the ablative tape, debris and contaminants. The degree of damage done by LSP on the ablative tape is illustrated in these images.

The peening results illustrated for the vinyl 88 tape have similar results to that obtained for vinyl 471 tape. The two tape have been manufactured by the same manufacturer with the only difference being that the thickness of the vinyl 88 is higher. The vinyl 471 tape has a total thickness of 0.14 mm whereas the vinyl 88 tape has a total thickness of 0.22 mm. The extra 8 mm of thickness has a significant influence on the peening results. The tape also has a higher breaking tensile strength when compared to the vinyl 471 tape. The vinyl 88 tape has a breaking tensile strength of 35 $N/10$ mm whereas the vinyl 471 tape has a breaking tensile strength of 27 $N/10$ mm. This difference in the breaking tensile strength has a large impact on the peening result.

Figure 5.43 shows the surface texture for sample H1-Vinyl88-P1.5. The surface texture of the peened tape shows no tape failure, the tape remains intact with small areas of penetrations which can be seen in Figure 5.43 (d-f). This result is similar to that obtained for sample E1-Vinyl471-P1. A similar result is also obtained for sample H2-Vinyl88-P2 and H3-Vinyl88-P3 illustrated in Figure 5.44 and Figure 5.45 the surface texture of peened tape is shows no signs of rupture and has remained intact at this power intensity. The surface texture remains uniform with small areas that have been penetrated. The surface of sample H3-Vinyl88-P3 has signs of discolouration which could be the result of the tape being exposed to high thermal damage. The surface texture shown in Figure 5.46 shows that under the higher power intensity higher amount of the tape has experienced ablation thus resulting in the surface texture experiencing more changes and damage as seen in Figure 5.46a. There are however higher amounts of surface discolouration and peening penetration.

Overall the surface results found for this ablative medium is suitable for LSP. The extra thickness of the tape allows for a wider range of LSP parameters.

Surface Roughness Results

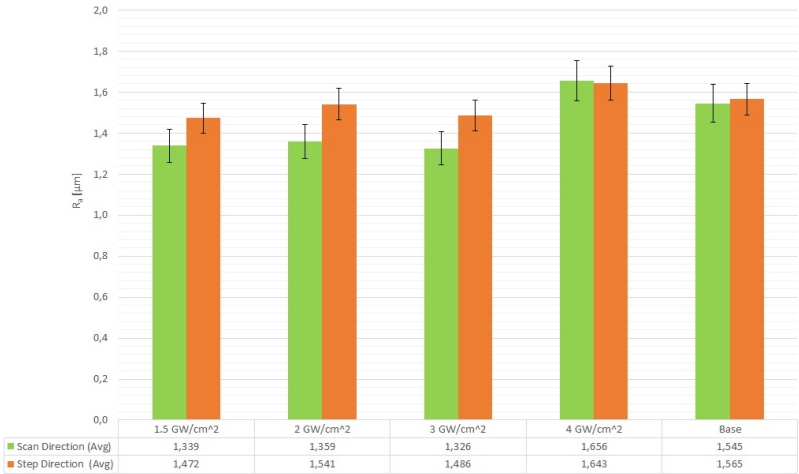


Figure 5.47: Surface Roughness Results for Vinyl 88 Tape Samples.

Figure 5.47 shows the surface roughness results that were obtained using the portable SRT-6210 Unit. From the results it can been observed that there is almost no changes in the surface roughness with the changing of the power intensity. There is 9.6% decrease in the mean surface roughness for sample H1-Vinyl88-P1.5 and a 6.8% decrease was found for sample H2-Vinyl88-P2 from the mean surface roughness of the unpeened base sample. Similarly, to the result obtained for sample H1-Vinyl88-P1, a 9.6% decrease was found for sample H3-Vinyl88-P3 whereas a 6.1% increase was found for sample H4-Vinyl88-P4.

The results found for the surface roughness show that the ablative tape successfully protected the surface of the material when conducting LSP. There is a consistency in the obtained results, the mean surface roughness does not change significantly when compared to the unpeened base sample.

At the lower power intensities, the ablative tape improves the surface of the material. The effect of the peening on the embedded stresses using this ablative tape will be studied in the next section.

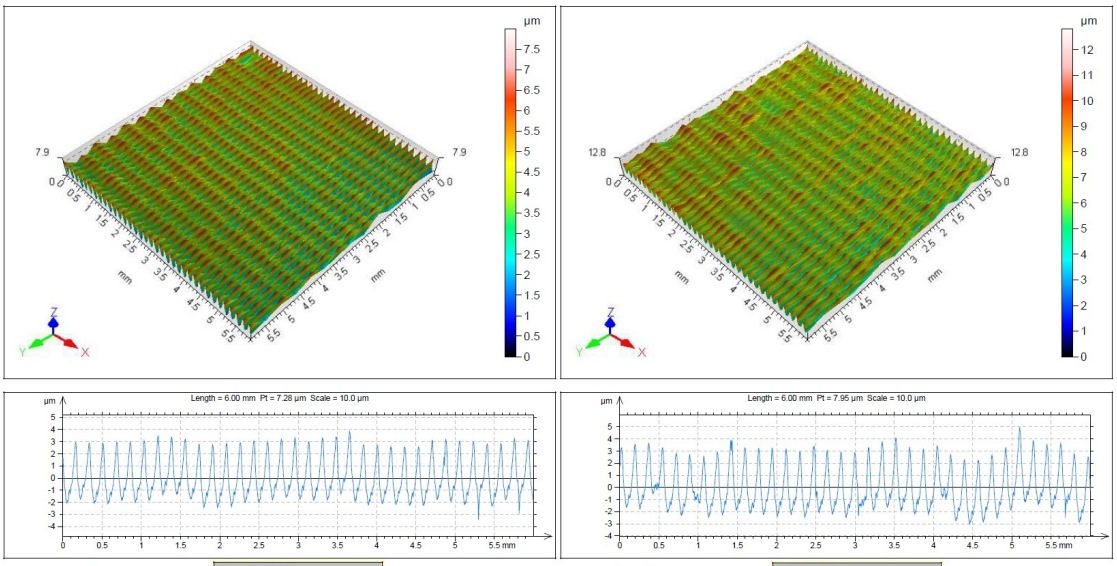
3-D Surface Maps for Vinyl 88 Tape Samples

The 3-D surface results show similar surface result that was obtained using the portable surface roughness tester.

All the samples have a mean surface roughness of around 1.4 μm with peak roughness values of around 3.5 μm for the first two samples and 5 μm for the last two samples. There is no significant changes in the surface texture between the samples, the texture is uniform as observed in Figure 5.48 and Figure 5.49.

The 2-D results also show a uniform sinusoidal pattern with relatively low amounts of noise present in the recorded data.

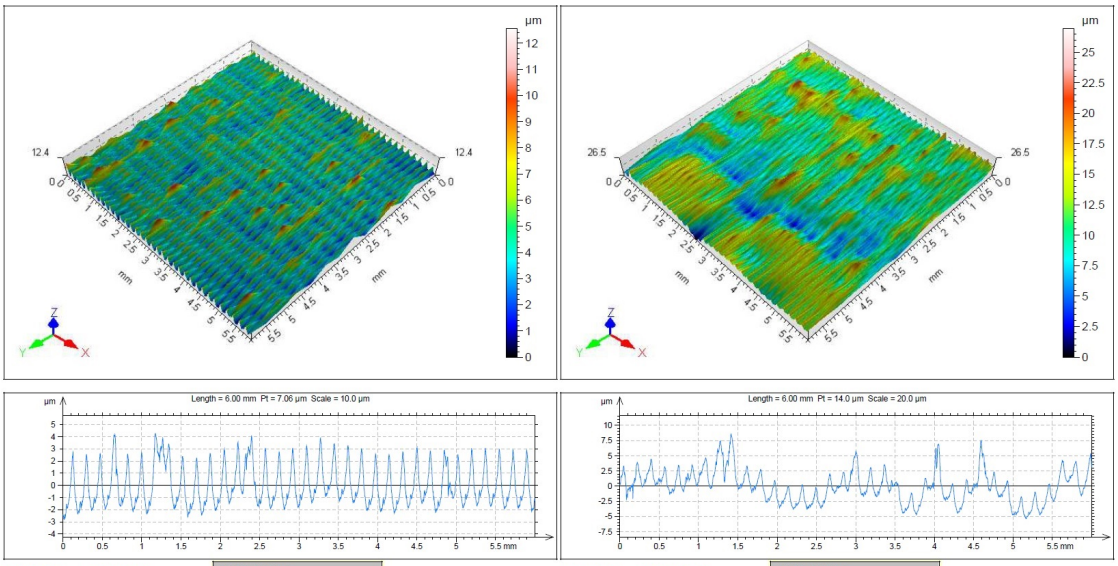
Overall the surface finish after LSP is excellent and acceptable for all power intensity. These finding show that the thickness of the ablative does indeed have a major influence on the outcome of the peening.



ISO 4287		
Amplitude parameters - Rc		
Rp	3.33	µm
Rv	2.19	µm
Rz	5.53	µm
Rc	5.16	µm
Rt	5.81	µm
Ra	1.39	µm
Rq	1.62	µm
Rsk	0.596	
Rku	2.06	

ISO 4287		
Amplitude parameters - Rc		
Rp	3.61	µm
Rv	2.55	µm
Rz	6.16	µm
Rc	5.55	µm
Rt	6.77	µm
Ra	1.47	µm
Rq	1.71	µm
Rsk	0.569	
Rku	2.08	

Figure 5.48: 3-D Surface Map for Samples: H1-Vinyl88-P1.5 and H2-Vinyl88-P2.



ISO 4287		
Amplitude parameters - Rc		
Rp	4.58	µm
Rv	2.19	µm
Rz	6.77	µm
Rc	5.23	µm
Rt	9.78	µm
Ra	1.40	µm
Rq	1.67	µm
Rsk	0.859	
Rku	2.83	

ISO 4287		
Amplitude parameters - Rc		
Rp	5.08	µm
Rv	2.83	µm
Rz	7.91	µm
Rc	4.32	µm
Rt	11.6	µm
Ra	1.43	µm
Rq	1.81	µm
Rsk	0.791	
Rku	3.25	

Figure 5.49: 3-D Surface Map for Samples: H3-Vinyl88-P3 and H4-Vinyl88-P4.

5.10 PVC Insulation Tape (21 Nitto)

The following are the microscopic images and data obtained for the samples peened using PVC insulation tape as the ablative coating.

Sample: I1-PVC-P1.5

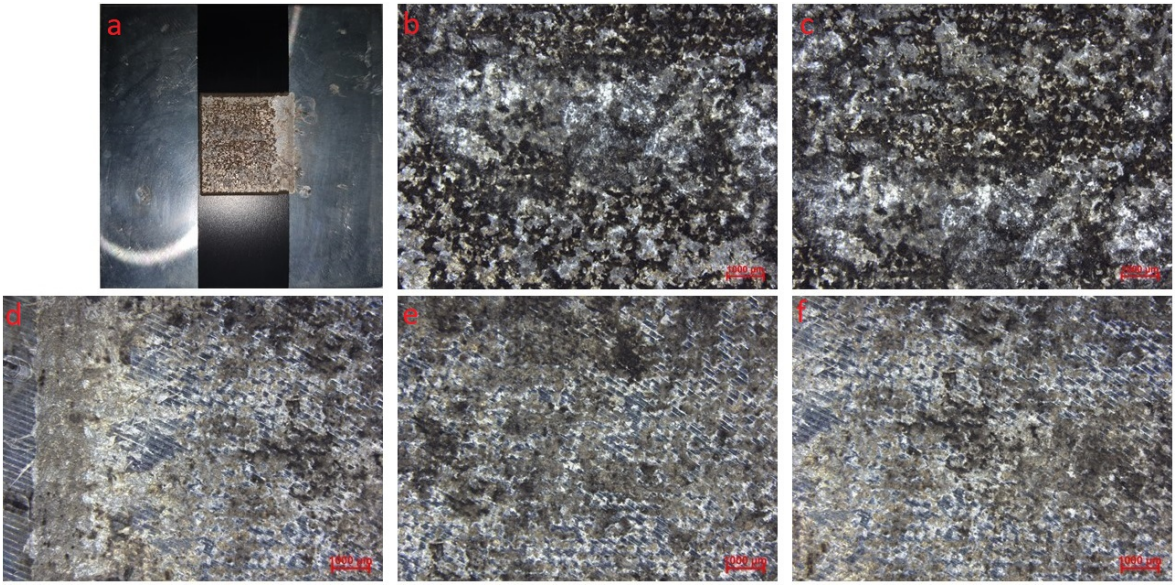


Figure 5.50: Surface Images for Sample: I1-PVC-P1.5.

Sample: I2-PVC-P2

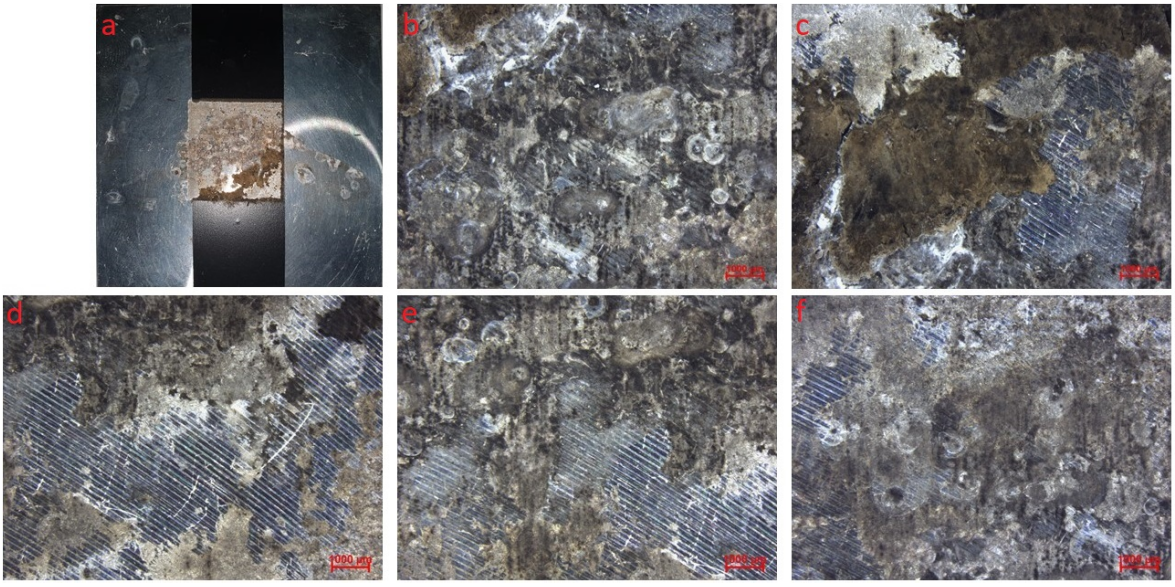


Figure 5.51: Surface Images for Sample: I2-PVC-P2.

Sample: I3-PVC-P3

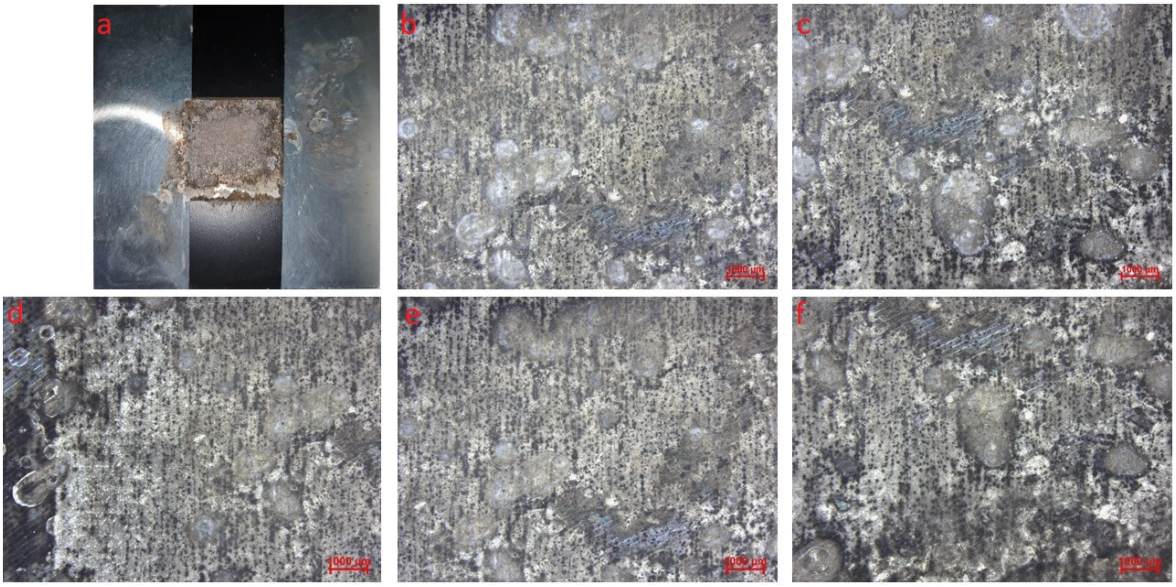


Figure 5.52: Surface Images for Sample: I3-PVC-P3.

Sample: I4-PVC-P4

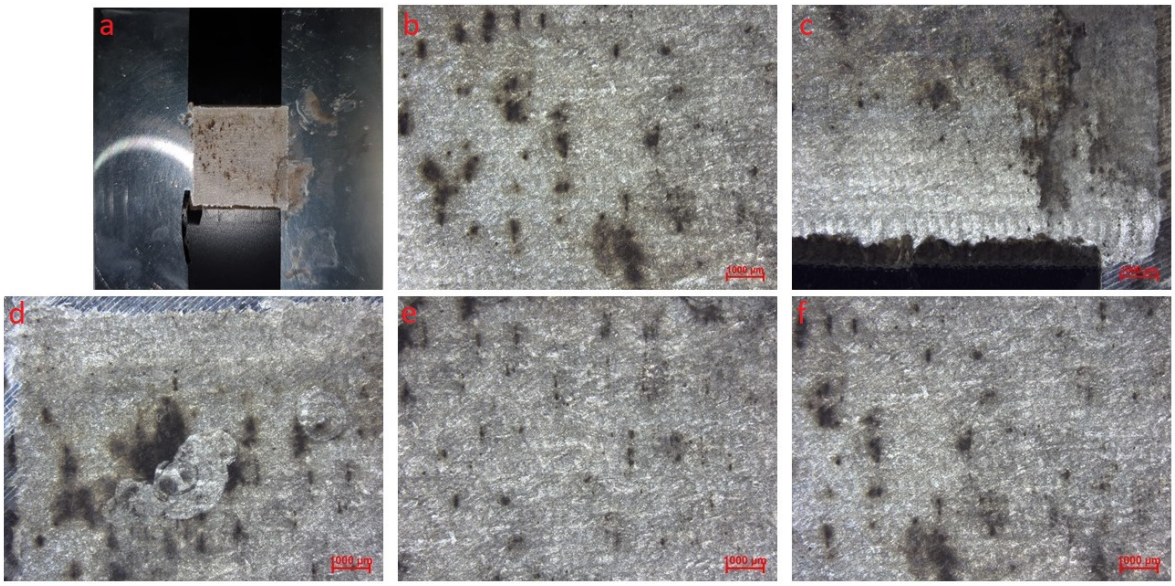


Figure 5.53: Surface Images for Sample: I4-PVC-P4.

Sub-images (a-c) shown in Figure 5.50 to Figure 5.53 shows the surface state of the peened sample before the complete removal of the ablative tape whereas sub images (d-f) shows the surface state after the removal of the ablative tape, debris and contaminants. The degree of damage done by LSP on the ablative tape and on the surface of the material is illustrated in these images.

The peening results illustrated for the PVC tape show a variety of different results. The PVC is polyvinyl chloride and a polymer of vinyl chloride, both the vinyl tape and the PVC tape are made from the same class of material yet have very contrasting results when used as an ablative material for LSP.

As shown in Figure 5.50, the ablative tape has been mostly vaporised under the peening however the remaining tape that did not vaporized remained adhered to the surface of the material thus resulting in the uneven peening that can observed after the tape and debris was removed. It can be seen that there is large amount of discolouration on the surface of the sample. Similarly, sample I2-PVC-P2 shown in Figure 5.51 also shows a surface texture that has experienced a high amount of discolouration with some tape debris and residue that has remained behind after the peening process.

Figure 5.52 shows the peening results obtained for sample I3-PVC-P3. The tape has been fully ablated and only leaving trace amount contaminants remaining behind. The surface texture has lower amounts of discolouration and is not uniform. Whereas sample I4-PVC-P4 shown in Figure 5.53 shows a uniform surface texture with the tape being fully ablated.

Even though the tape that has a thickness of 0.19 mm, which is greater than that the thickness of 0.14 mm of the vinyl 471. The ablative tape did not provide better surface result when compared to the vinyl 471 tape. Therefore, the properties of the backing material does not provide the same resistance to the thermal damage as the vinyl 471 tape.

Surface Roughness Results



Figure 5.54: Surface Roughness Results for the PVC Tape Samples.

Figure 5.54 shows the surface roughness results that were obtained using the portable SRT-6210 Unit. There is 4.5% increase in the mean surface roughness for sample I1-PVC-P1.5 and a 9.4% increase was found for sample I2-PVC-P2 from the mean surface roughness of the unpeened base sample. The result obtained for sample I3-PVC-P3 showed a 39.3% increase

in the mean surface roughness whereas an 83.8% increase in the mean roughness was found for sample I4-PVC-P4.

The results show that there are no significant changes in the surface roughness for the first two power intensities, whereas for the last two power intensities a significant change can be observed when compared to the roughness of the unpeened sample.

3-D Surface Maps for PVC Insulation Tape Samples

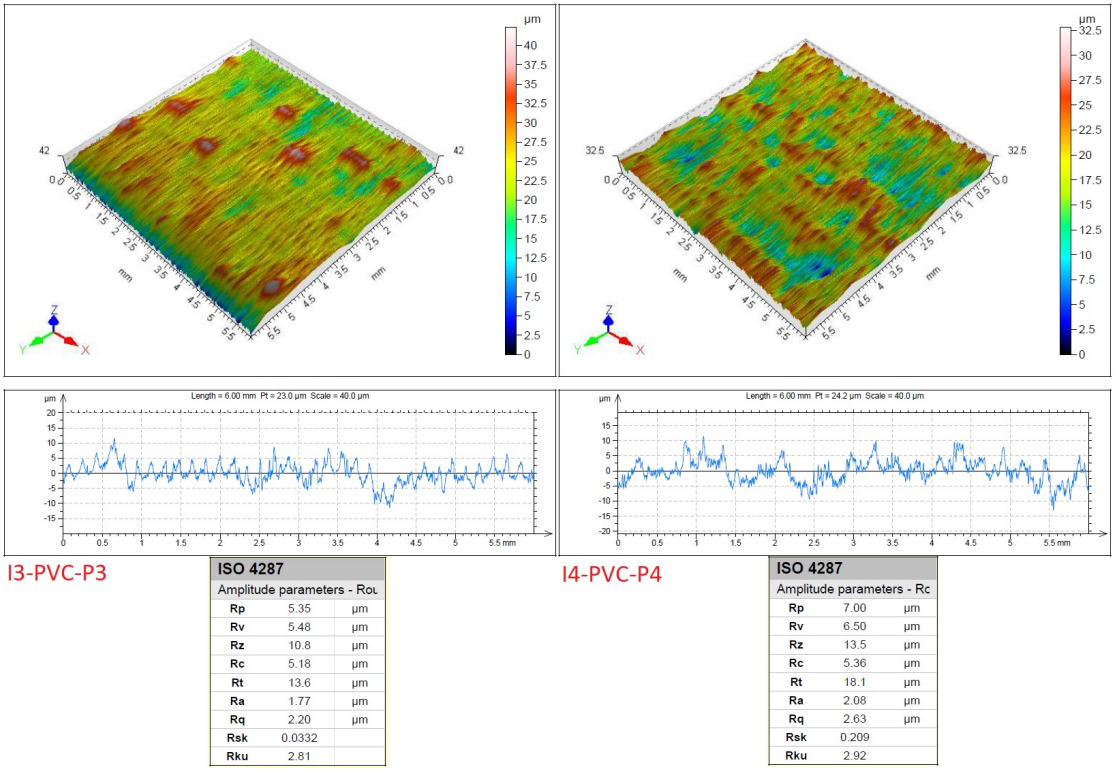


Figure 5.55: 3-D Surface Map for the PVC Samples.

The 3-D surface textures shown in Figure 5.55 for the sample I3-PVC-P3 and I4-PVC-P4. There is no uniformity in the surface texture and there is a degree of randomness present in the results. The peak roughness values of 5.35 μm and 7 μm were obtained for the two sample while R_z values of 10.8 μm and 13.5 μm were obtained for the two samples.

The 2-D results also have a degree of randomness to it. There is also a significant amount of noise present in the results shown in Figure 5.55.

5.11 Micron Copper Foil Shielding Tape (AT525 35)

The following are the microscopic images and data obtained for the samples peened using copper foil shielding tape as the ablative coating.

Sample: J1-Cu-P1.5

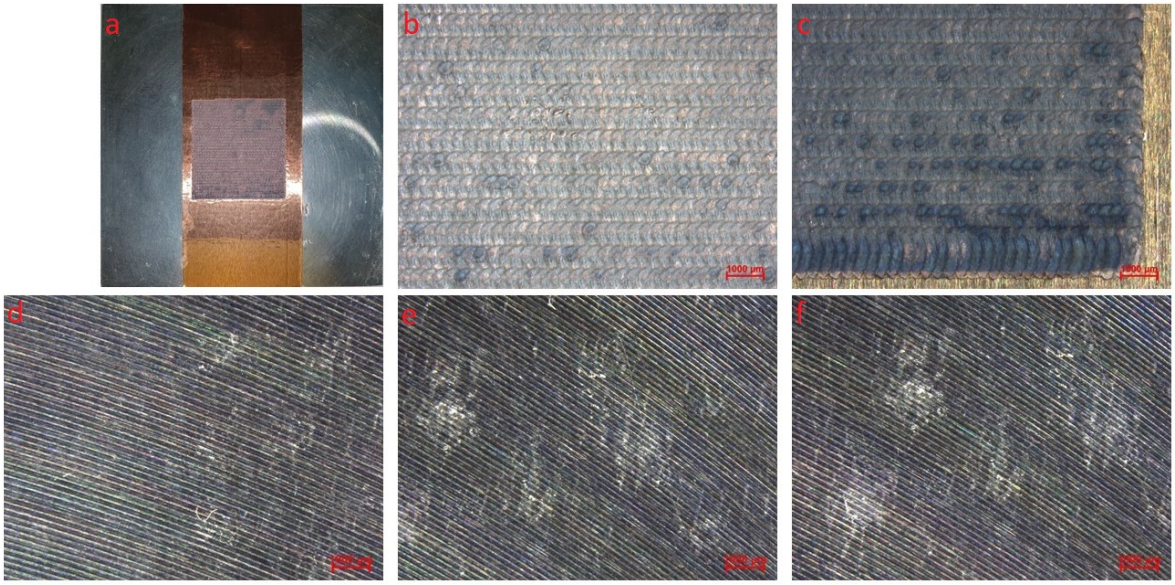


Figure 5.56: Surface Images for Sample: J1-Cu-P1.5.

Sample: J2-Cu-P2

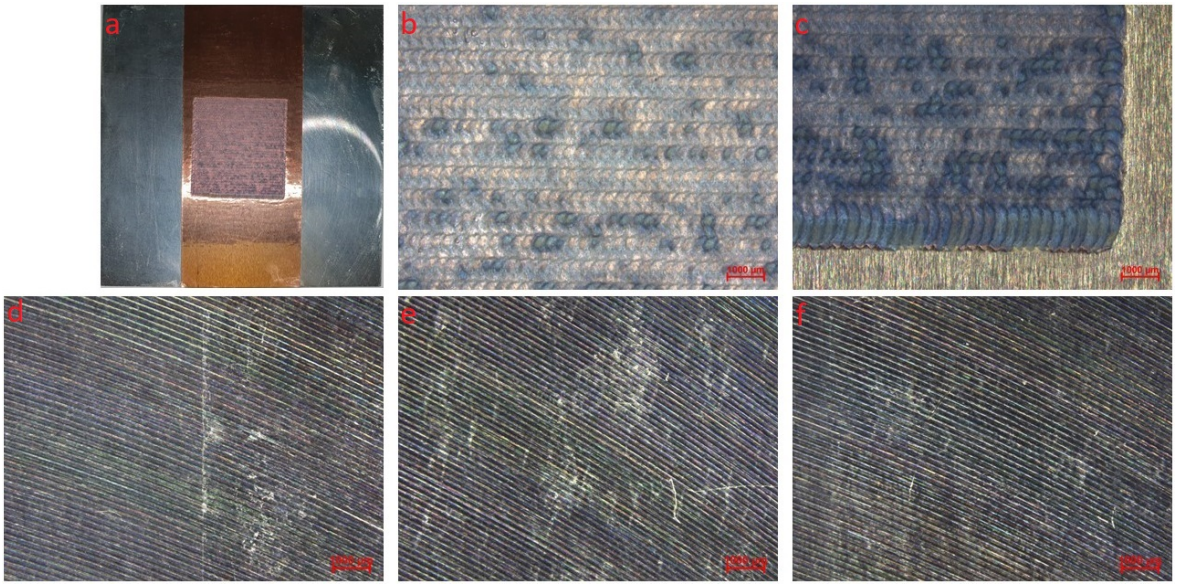


Figure 5.57: Surface Images for Sample: J2-Cu-P2.

Sample: J3-Cu-P3

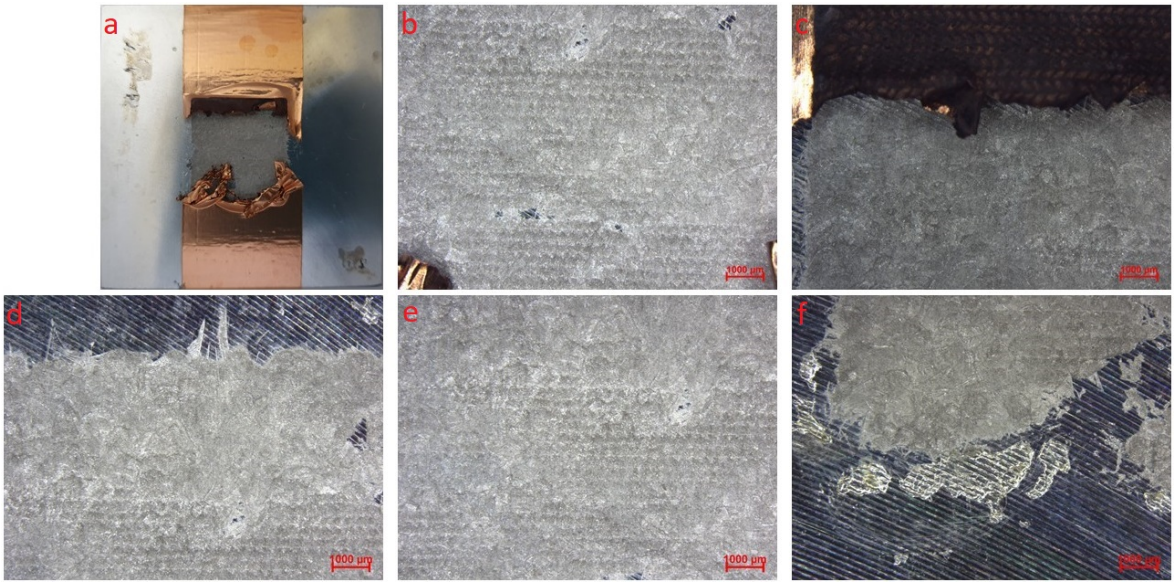


Figure 5.58: Surface Images for Sample: J3-Cu-P3.

Sample: J4-Cu-P4

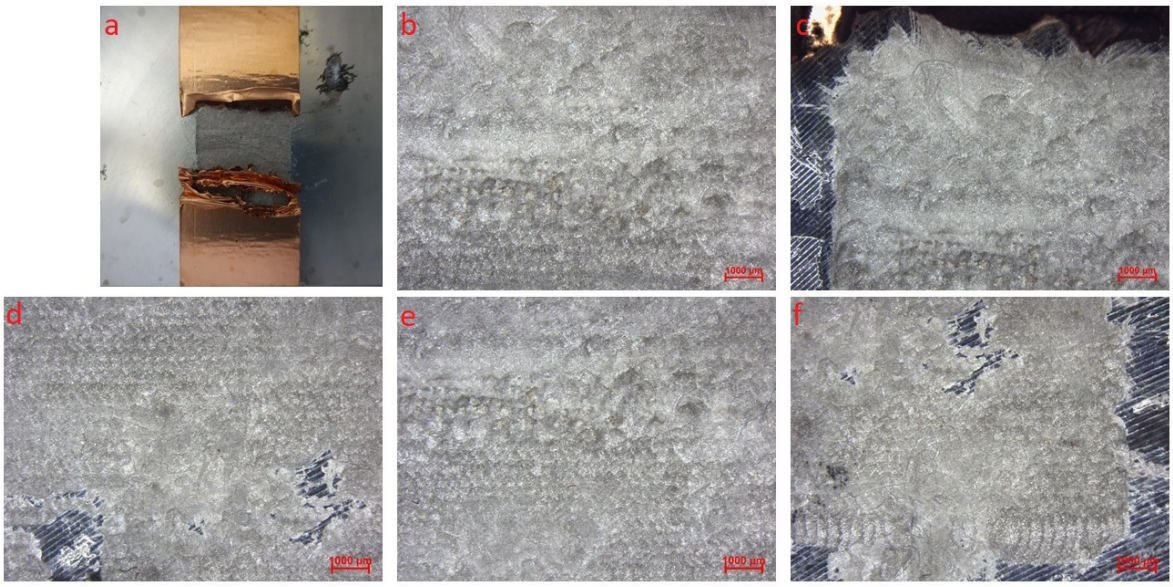


Figure 5.59: Surface Images for Sample: J4-Cu-P4.

Sub-images (a-c) shown in Figure 5.56 to Figure 5.59 shows the surface state of the peened sample before the complete removal of the ablative tape whereas sub images (d-f) shows the surface state after the removal of the ablative tape, debris and contaminants. The degree of damage done by LSP on the ablative tape and on the surface of the material is illustrated in these images.

The peening result found using for the copper tape show two contrasting results. The ablative tape remains in contact when peened with the two low power intensities but when peened with the last two power intensities the ablative tape fails at a certain point during the peening, which is similar to the results obtained for the samples peened using the aluminium tape.

Figure 5.56 shows the peening results found for sample J1-Cu-P1. The peening on the tape itself shows that areas that experienced slight surface melting, under the peening treatment the tape remained intact thus leaving the underlying surface texture to remain unchanged. The surface texture has areas that show the effect the of the peening however most of the peening and or damage was sustained by the ablative material.

Figure 5.57 displays the surface for sample J2-Cu-P2. Similarly, to the previous sample, the surface of the tape has experienced a slightly higher degree of thermal damage. The tape remains intact and only a slight layer of the ablative material has vaporised, the degree of surface damage is also higher when compared to the previous sample. The surface texture is also similar to the previous sample and signs of peening on the surface is visible.

A more pronounced surface texture result was obtained for sample J3-Cu-P3 shown in Figure 5.58. Firstly, the ablative tape failed in a similar way to that of the aluminium samples. The power intensity was sufficient enough to cause the tape to fail, as a result the underlying surface texture shows an irregular peening pattern. The adhesive layer has also remained behind as shown in Figure 5.58(f).

Sample J4-Cu-P4 shown in Figure 5.59, displays similar result to that shown in Figure 5.58. The ablative has experienced more damage and has failed earlier when compared to the previous sample. The surface texture shows a less variation in peening result but the surface irregularities still remain. The uniformity in the surface remains unchanged from the surface texture of the previous sample.

The tape which has a total thickness of 0.065 mm with a which is lower than that of the aluminium tape which has a total thickness of 0.075 mm has a higher tensile strength and can thus can withstand a higher degree of thermal damage. Therefore, not only does the thickness affect the peening but the material properties (mainly the tensile strength) does affect overall peening results. The copper backing material performs better when compared to the other metallic tape, but when compared to the results found for the non-metallic vinyl 88 tape the copper tape only performs well under low power intensities.

The unpredictability in the nature of the ablative tape when peening shows that the tape can only be used at low power intensity in order to keep surface integrity unchanged. Therefore, the ablative tape is only suitable for LSP at low power intensities.

Surface Roughness Results

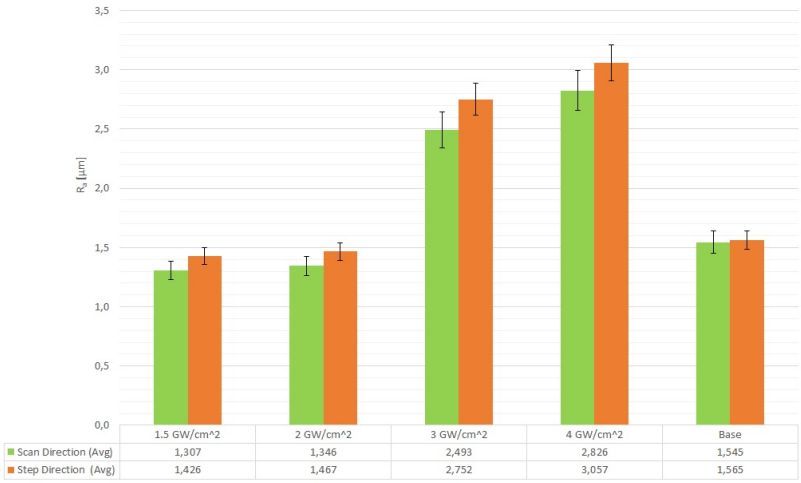


Figure 5.60: Surface Roughness Results for the Copper Tape Samples.

Figure 5.60 shows the surface roughness results found using the portable SRT-6210 Unit. The surface roughness results show a similar trend that was observed previously, two contrasting results can be seen. For the samples peened with the first two power intensities show a 12.1% and a 9.5% decrease in the mean surface roughness from the unpeened base sample. Whereas, the samples peened with the last two power intensities show a 68.6% and an 89.1% increase in the mean surface roughness from the unpeened base sample.

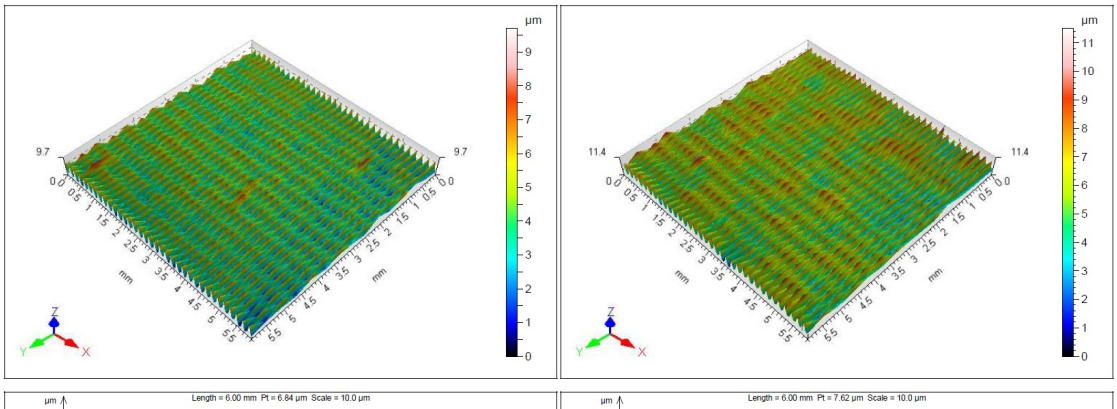
The surface roughness for the first two samples are significantly lower than the surface roughness of the last two samples. The high surface roughness values can be attributed to the failure of the ablative when LSP was conducted.

3-D Surface Maps for Copper Tape Samples

Further surface analyses was conducted using the using the HOMMEL-ETAMIC T8000 R120-400 roughness testing machine to provide an accurate 3-D surface map and resulting surface roughness data which are illustrated by Figure 5.61 and Figure 5.62.

The 3-D surface texture for the first two samples is uniform with R_z values of 5.92 μm and 6.86 μm and with R_p values of 3.62 μm and 4.29 μm. The 2-D map for the two samples shows a uniform sinusoidal structure with almost no surface variations and noise.

The surface textures for the last two samples is irregular with R_z values of 14.1 μm and 15.2 μm and with R_p values of 7.37 μm and 8.08 μm. The 2-D surface maps for these samples shows a structure that has no uniformity with significant amounts of noise and variations present in the data.



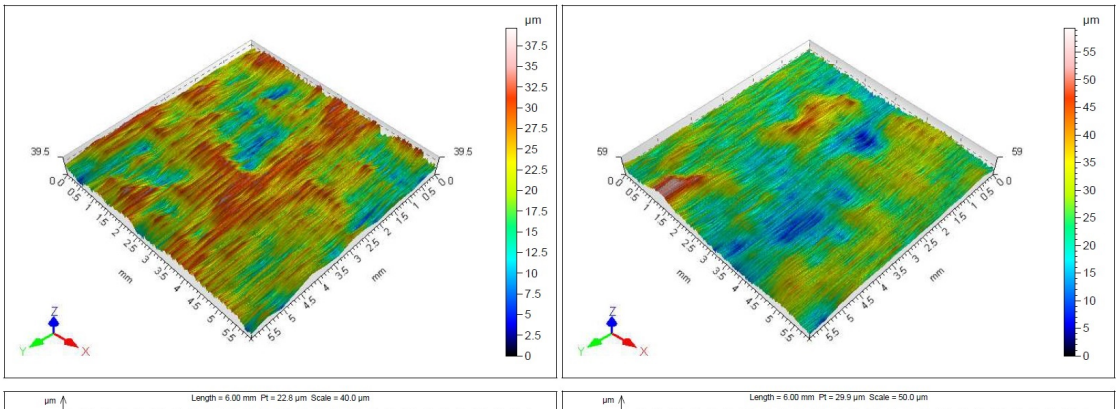
J1-Cu-P1.5

ISO 4287		
Amplitude parameters - Rc		
Rp	3.62	µm
Rv	2.31	µm
Rz	5.92	µm
Rc	5.49	µm
Rt	6.18	µm
Ra	1.42	µm
Rq	1.67	µm
Rsk	0.720	
Rku	2.22	

J2-Cu-P2

ISO 4287		
Amplitude parameters - Rc		
Rp	4.29	µm
Rv	2.57	µm
Rz	6.86	µm
Rc	5.33	µm
Rt	10.9	µm
Ra	1.36	µm
Rq	1.60	µm
Rsk	0.727	
Rku	2.45	

Figure 5.61: 3-D Surface Map for Samples: J1-Cu-P1.5 and J2-Cu-P2.



J3-Cu-P3

ISO 4287		
Amplitude parameters - Rou		
Rp	7.37	µm
Rv	6.75	µm
Rz	14.1	µm
Rc	6.74	µm
Rt	19.8	µm
Ra	2.48	µm
Rq	2.98	µm
Rsk	-0.0292	
Rku	2.51	

J4-Cu-P4

ISO 4287		
Amplitude parameters - Rc		
Rp	8.08	µm
Rv	7.07	µm
Rz	15.2	µm
Rc	6.74	µm
Rt	21.5	µm
Ra	2.49	µm
Rq	3.10	µm
Rsk	0.122	
Rku	2.90	

Figure 5.62: 3-D Surface Map for Samples: J3-Cu-P3 and J4-Cu-P4.

5.12 Vinyl Tape (472 3M)

The following are the microscopic images and data obtained for the samples peened using vinyl tape 472 as the ablative coating.

Sample: K1-Vinyl472-P1.5

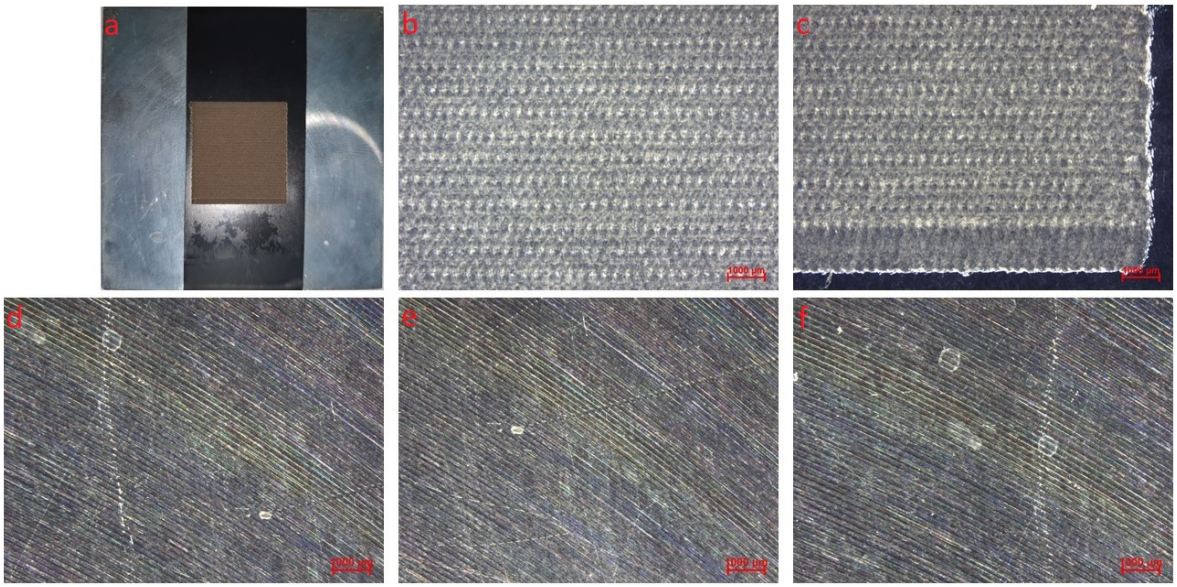


Figure 5.63: Surface Images for Sample: K1-Vinyl472-P1.

Sample: K2-Vinyl472-P2

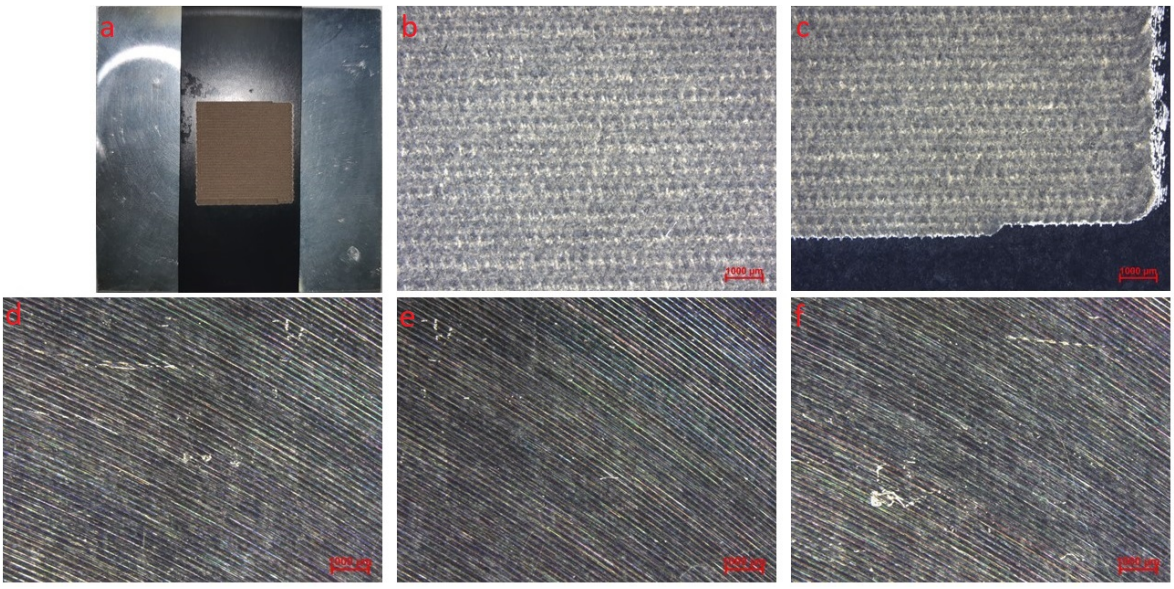


Figure 5.64: Surface Images for Sample: K2-Vinyl472-P2.

Sample: K3-Vinyl472-P3

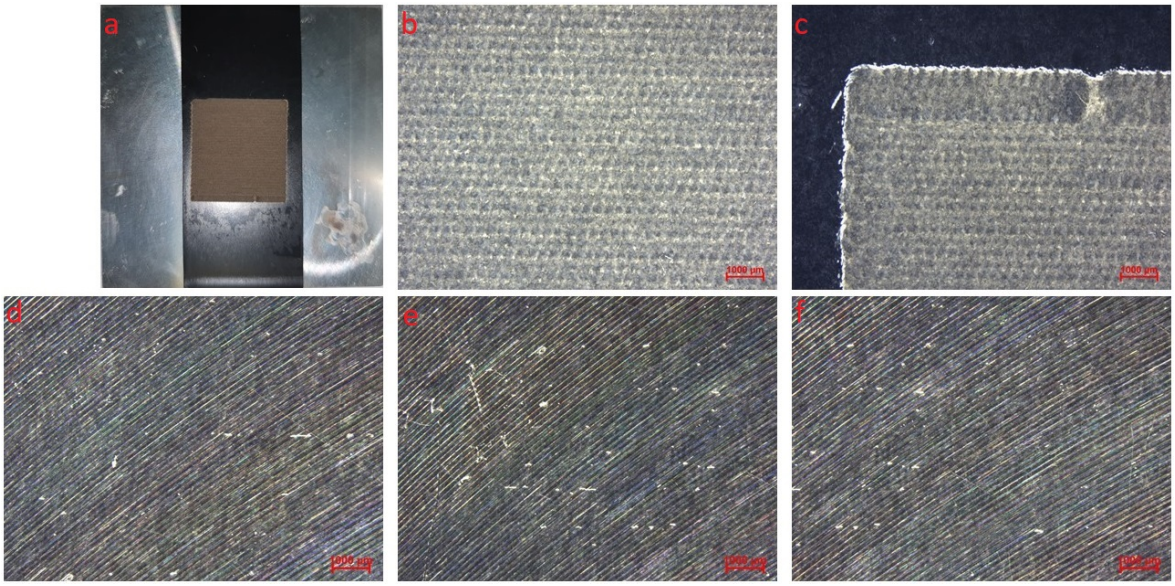


Figure 5.65: Surface Images for Sample: K3-Vinyl472-P3.

Sample: K4-Vinyl472-P4

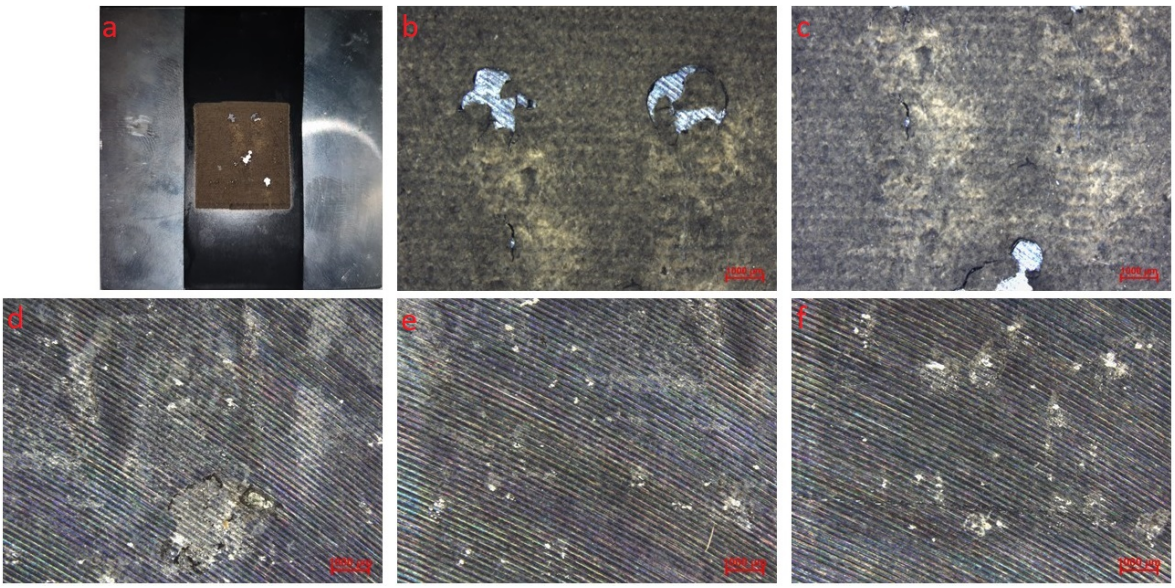


Figure 5.66: Surface Images for Sample: K4-Vinyl472-P4.

Sub-images (a-c) shown in Figure 5.63 to Figure 5.66 shows the surface state of the peened sample before the complete removal of the ablative tape whereas sub images (d-f) shows the surface state after the removal of the ablative tape, debris and contaminants. The degree of damage done by LSP on the ablative tape and on the surface of the material is illustrated in these images.

The peening results illustrated for the vinyl 472 tape have similar results to that obtained for vinyl 471 and vinyl 88 tape. The three tapes have been manufactured by the same manufacturer with the only difference being in the thickness. The vinyl 472 tape has a total tape thickness of 0.26 mm while the vinyl 88 tape has a total thickness of 0.22 mm whereas, the vinyl 471 tape has a total thickness of 0.14 mm which is the lowest between the three tapes. The extra thickness in the vinyl 472 tape has a significant influence on the peening results. The tape also has a higher breaking tensile strength when compared to the vinyl 471 tape and vinyl 88 tape. The vinyl 472 tape has a breaking tensile strength of 56 $N/10$ mm while the vinyl 88 tape has a breaking tensile strength of 35 $N/10$ mm and the vinyl 471 tape has a breaking tensile strength of 27 $N/10$ mm. This large increase in the breaking tensile strength has a significant influence on the final peening result.

Figure 5.63 shows the results obtained for sample K1-Vinyl472-P1.5. The results show uniform peening, the tape has remained intact and the underlying surface also remains unchanged. This indicates that there was no penetration through the ablative layer. The surface texture result at this low power intensity is better than that obtained for the samples H1-Vinyl88-P1.5 and E1-Vinyl471-P1.5.

Figure 5.64 shows the surface texture for sample K2-Vinyl472-P2. The results are similar to that obtained for the previous sample, the underlying surface remains the unchanged and the tape remains intact.

The results obtained for sample K3-Vinyl472-P3 shown in Figure 5.65, also shows results that are similar to the previous two samples. The surface texture remains uniform but signs of peening can be seen thus showing more ablative material has been vaporised during the peening process.

The results for sample K4-Vinyl472-P4 are shown in Figure 5.66. The damaged sustained by the tape is more clear, cracks can be identified in the tape thus indicates the thermal damage that was experienced by the tape. The surface texture is also uniform but there are minor irregularities that are present. The performance of this tape at this high power intensity is better than the samples tested so far, and because most of the surface integrity was maintained.

Overall the performance of the tape is excellent and is suitable to use as an ablative material for LSP. The tape remained intact and managed to protect the surface from thermal damage.

Surface Roughness Results

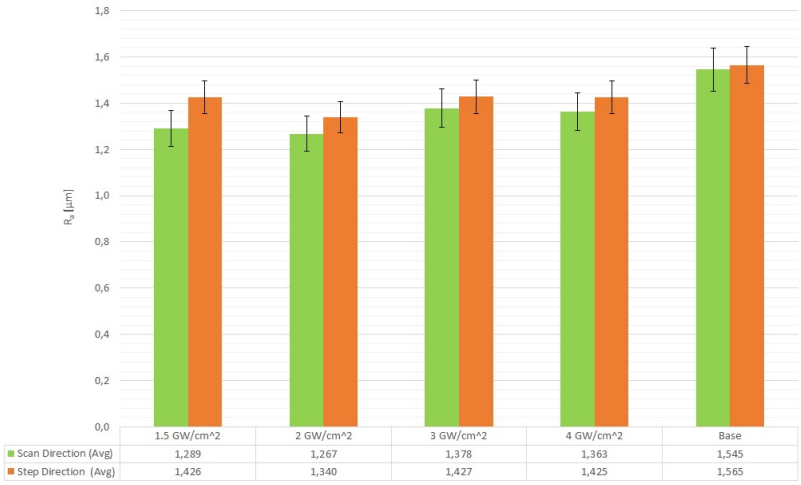


Figure 5.67: Surface Roughness Results for the Vinyl Tape 472 Samples.

Figure 5.67 shows the surface roughness results found using the portable SRT-6210 Unit. As illustrated in Figure 5.67 the surface roughness remains constant with the increasing power intensities. The surface roughness for the samples is lower than the unpeened base sample thus indicating that there is an improvement in the surface roughness when using this tape as the ablative material.

All the samples show a decrease in the mean surface roughness when compared to the unpeened base sample. Sample K1-Vinyl472-P1.5 shows a 12.7% decrease while sample K2-Vinyl472-P2 shows a 16.2% decrease in the mean roughness from the base sample. Sample K3-Vinyl472-P3 shows a 9.8% decrease in the roughness whereas sample K4-Vinyl472-P4 showed a 10.4% decrease in the mean roughness when compared to the unpeened sample.

The changes in the surface roughness between the peened samples is negligible with increasing power intensities. Overall there was an improvement in the roughness from the unpeened base sample.

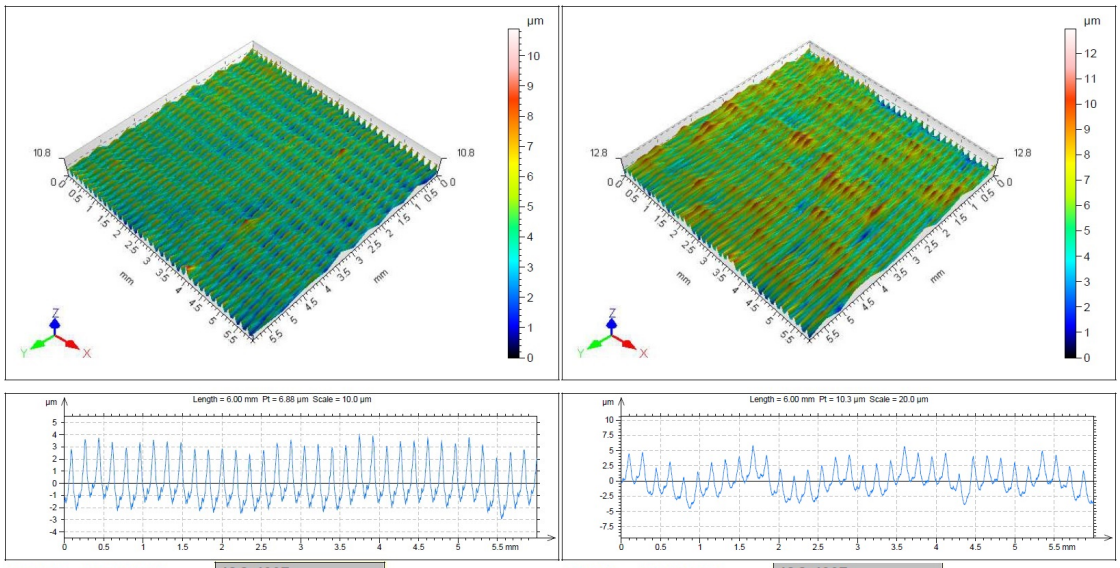
3-D Surface Maps for Vinyl 472 Tape Samples

Further surface analyses was conducted using the HOMMEL-ETAMIC T8000 R120-400 roughness testing machine which is shown in Figure 5.68

The figure shows the results that were obtained for sample K3-Vinyl472-P3 and sample K4-Vinyl472-P4. The surface texture shown for sample K3-Vinyl472-P3 is uniform with no irregular peaks, the surface is similar if not better than that of the base sample. The R_z of 5.16 μm and R_p of 3.18 μm was found for sample K3-Vinyl472-P3. when compared to the samples studied so far, the results obtained were significantly better at this particular power intensity. The 2-D plot is also uniform with almost no noise or variation in the data that is

presented. There is a clear sinusoidal trend that is visible, this trend indicates the nature of the peening that was experienced by the sample.

A positive surface result was obtained for sample K4-Vinyl472-P4. The surface texture is also uniform but shows a higher degree of peening that was experienced by the sample. There is not significant changes in the surface texture and unlike previous samples peened using this power intensity this sample shows no indication of high surface damage. The surface parameters are also similar if not better than the base sample, with R_z being 6.27 μm and R_p being 3.61 μm. The 2-D results also show uniformity with a slight increase in the amount of noise but the sinusoidal nature of the results is still present.



ISO 4287		
Amplitude parameters - Rc		
Rp	3.18	µm
Rv	1.99	µm
Rz	5.16	µm
Rc	4.81	µm
Rt	5.52	µm
Ra	1.23	µm
Rq	1.45	µm
Rsk	0.740	
Rku	2.27	

ISO 4287		
Amplitude parameters - Rc		
Rp	3.61	µm
Rv	2.65	µm
Rz	6.27	µm
Rc	5.09	µm
Rt	9.88	µm
Ra	1.34	µm
Rq	1.58	µm
Rsk	0.583	
Rku	2.23	

Figure 5.68: 3-D Surface Map for Samples: K3-Vinyl472-P3 and K4-Vinyl472-P4.

5.13 Polymide Tape (HB830 Hi-Bond)

The following are the microscopic images and data obtained for the samples peened using polymide tape as the ablative coating.

Sample: L1-Polymide-P1.5

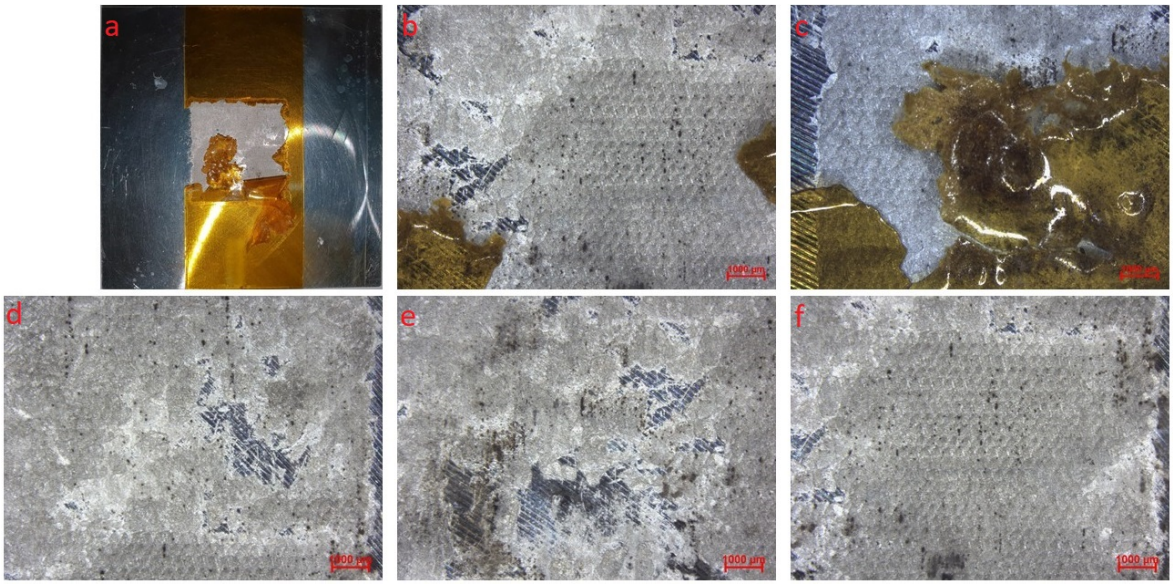


Figure 5.69: Surface Images for Sample: L1-Polymide-P1.

Sample: L2-Polymide-P2

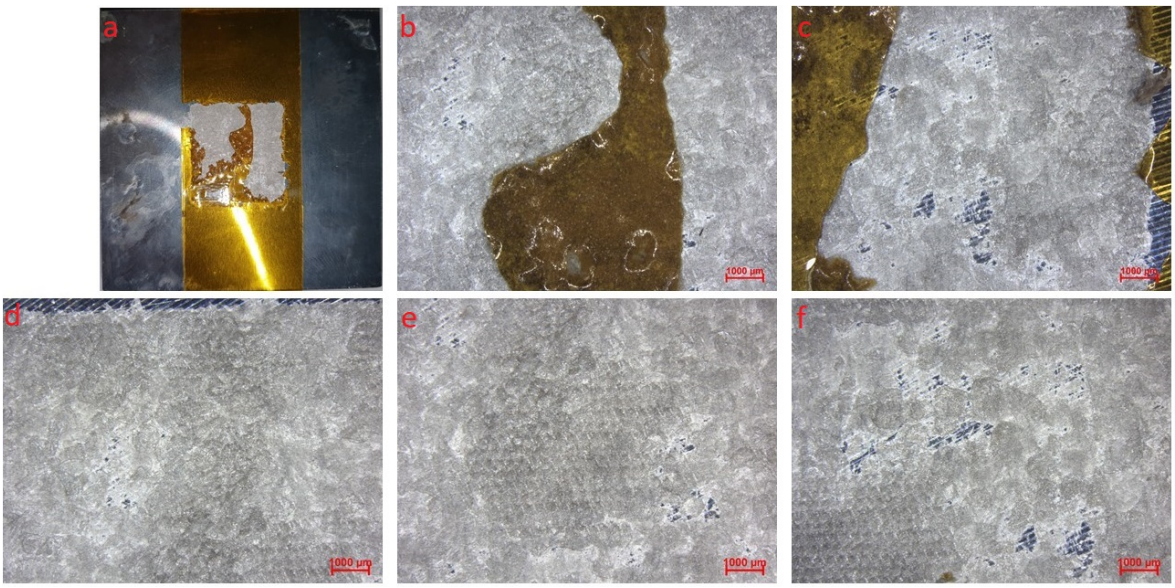


Figure 5.70: Surface Images for Sample: L2-Polymide-P2.

Sample: L3-Polymide-P3

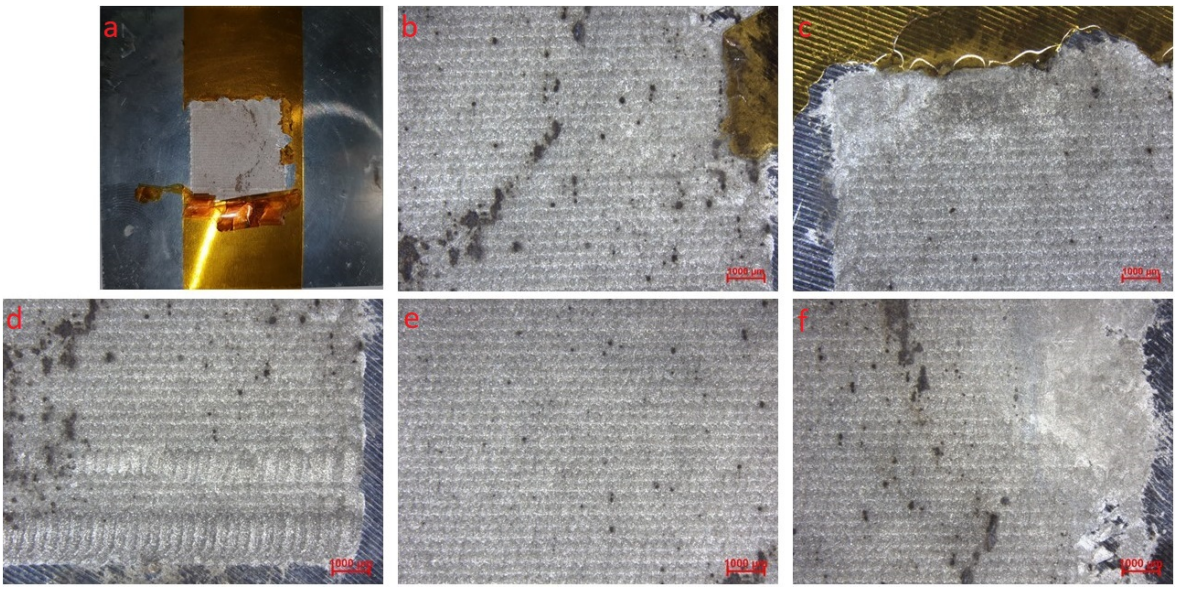


Figure 5.71: Surface Images for Sample: L3-Polymide-P3.

Sample: L4-Polymide-P4

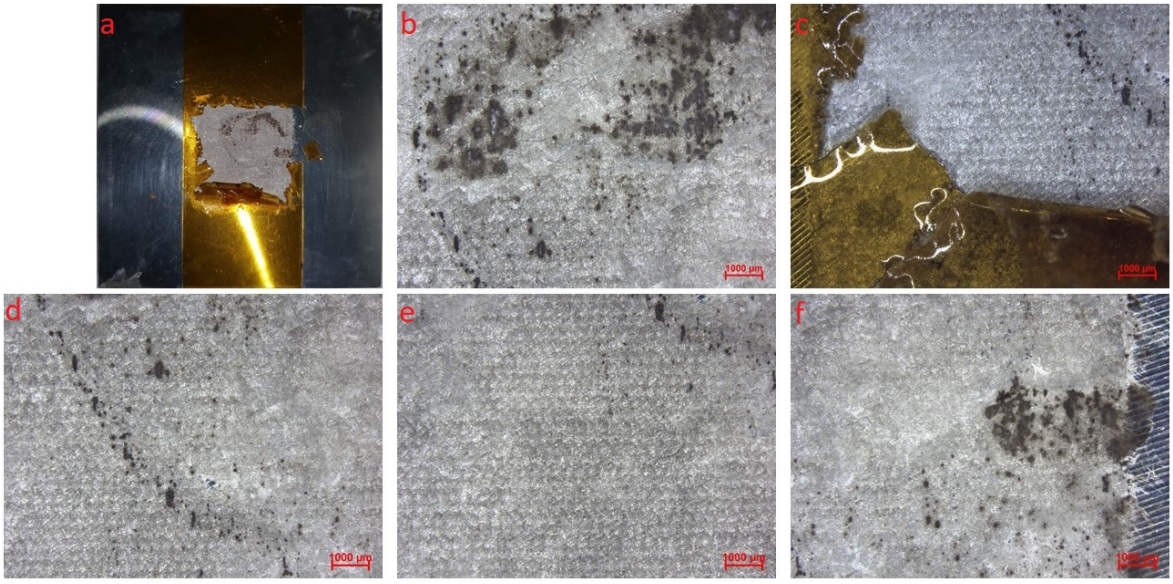


Figure 5.72: Surface Images for Sample: L4-Polymide-P4.

Sub-images (a-c) shown in Figure 5.69 to Figure 5.72 shows the surface state of the peened sample before the complete removal of the ablative tape whereas sub images (d-f) shows the surface state after the removal of the ablative tape, debris and contaminants. The degree of damage done by LSP on the ablative tape and on the surface of the material is illustrated in these images.

The peening conducted using this tape shows that the tape experienced high thermal damage, this is evident in the melting that was experienced in the tape as shown in the images. This tape which is generally used as electrical shielding and insulation is design to withstand high temperatures. This insulting properties can be clearly seen in the portions of tape that has remained behind on the surface after peening was conducted.

Figure 5.69 shows the surface results for sample L1-Polymide-P1.5. The peening is quite irregular, there is no consistency in the surface texture and portions of tape still remain. It was noticed that the tape de laminates easily from the surface of the material, the transparency of the tape also influences the results. The melting of the tape during the process also influence the final peening result. This is because the index of refraction changes when melting of the transparent tape occurs.

Figure 5.70 shows the surface results for sample L2-Polymide-P2. The surface texture is also irregular and with no peening structure. The melting of the tape is also evident. The results found for sample L3-Polymide-P3 show a much more uniform peening pattern but with slight discolouration as indicated in Figure 5.71. The peening results for sample L4-Polymide-P4 shown in Figure 5.72, the surface texture is similar to the previous sample but has a higher degree of discolouration and surface melting.

Overall, the tape in not quite suitable for LSP this is due to the unpredictability in the nature of the ablative tape when peening is conducted on it.

Surface Roughness Results

Figure 5.73 below shows the roughness results obtained for the peened samples and the machined base sample using the portable SRT-6210 Unit.

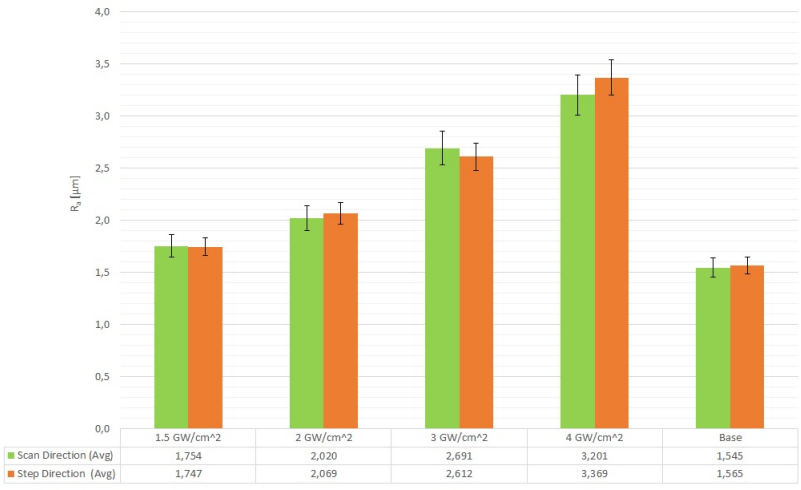
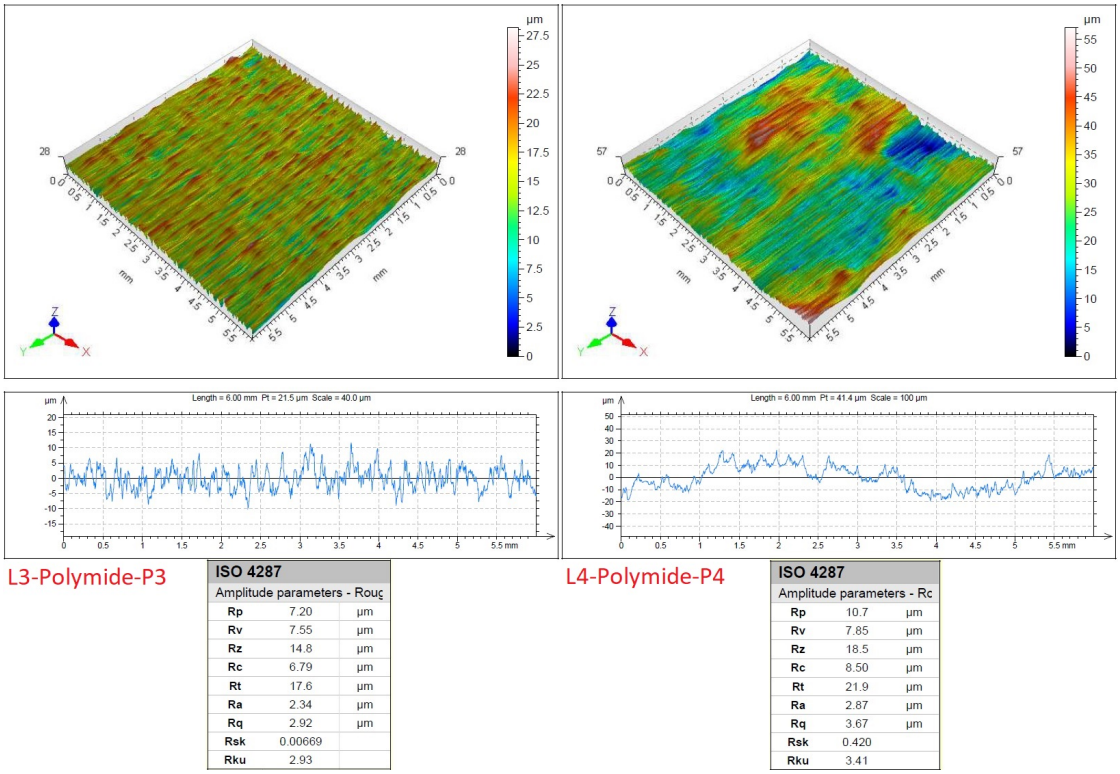


Figure 5.73: Surface Roughness Results for the Polymide Tape Samples.

The results show the typical increasing trend for the roughness with the increasing power intensity. There is almost linear increase in the surface roughness with the increasing power intensity. There is a 12.6% increase in the mean surface roughness for sample L1-Polymide-P1.5 and a 31.5% increase in the mean roughness for sample L2-Polymide-P2 from the mean roughness of the base sample. A 70.5% increase in the mean roughness was found for sample L3-Polymide-P3 and a 111.2% increase in the mean roughness was calculated for sample L4-Polymide-P4 from the mean roughness of the unpeened sample.

3-D Surface Maps for Polymide Tape Samples



ISO 4287		
Amplitude parameters - Rouç		
Rp	7.20	µm
Rv	7.55	µm
Rz	14.8	µm
Rc	6.79	µm
Rt	17.6	µm
Ra	2.34	µm
Rq	2.92	µm
Rsk	0.00669	
Rku	2.93	

ISO 4287		
Amplitude parameters - Rc		
Rp	10.7	µm
Rv	7.85	µm
Rz	18.5	µm
Rc	8.50	µm
Rt	21.9	µm
Ra	2.87	µm
Rq	3.67	µm
Rsk	0.420	
Rku	3.41	

Figure 5.74: 3-D Surface Map for Samples: L3-Polymide-P3 and L4-Polymide-P4.

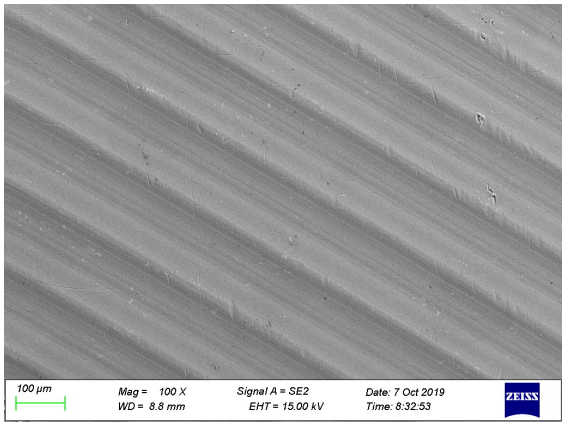
Figure 5.74 shows the results that were obtained for sample L3-Polymide-P3 and sample L4-Polymide-P4 by using the HOMMEL-ETAMIC testing machine.

The surface texture shown for sample L3-Polymide-P3 is slightly uniform with roughness parameters of $R_z = 14.8\ \mu m$ and $R_p = 7.2\ \mu m$ while 2-D results contains large amounts of noise. The 3-D texture for sample L4-Polymide-P4 is highly irregular with high roughness parameters of $R_z = 18.5\ \mu m$ and $R_p = 10.7\ \mu m$. The 2-D structure is highly staggered with small amounts of noise present.

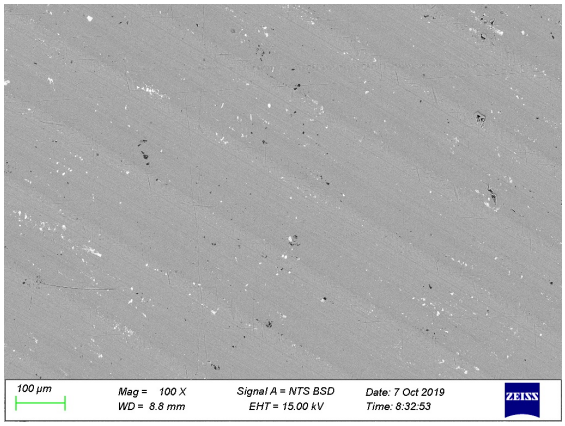
The changes in the texture between the two samples is large, indicating that under the influence of the higher power intensity and the nature of the ablative material more depth changes occur on the peened surface.

5.14 SEM Results

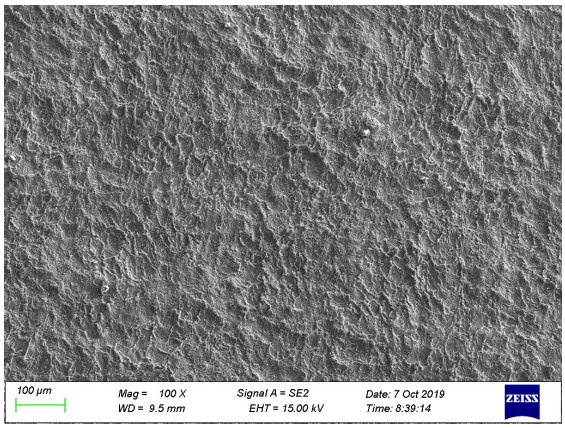
This section provides further analysis that was conducted into the surface of selected peened samples by obtaining SEM images under high magnification. Figure 5.75 shows the SE2 and BSD SEM images with a magnification of 100x for the unpeened base sample and the LSPwC sample which was peened using a power intensity of 3 GW/cm^2.



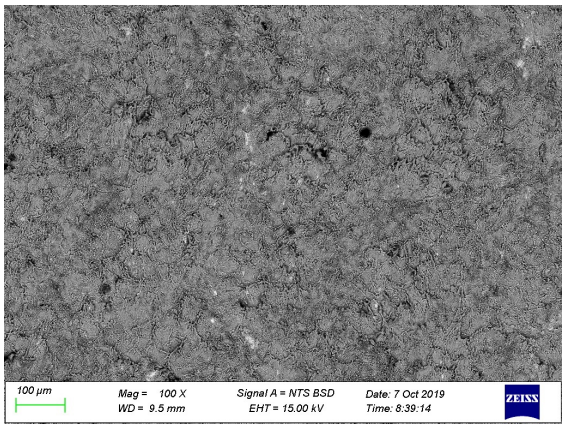
(a) SE2 - Unpeened Base



(b) BSD - Unpeened Base



(c) SE2 - LSPwC sample: M3-No-Tape-P3



(d) BSD - LSPwC sample: M3-No-Tape-P3

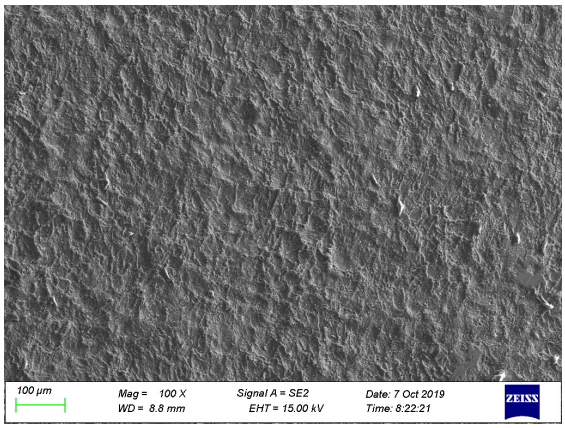
Figure 5.75: SEM Images.

The BSD surface image shown in Figure 5.75b and Figure 5.75d represent the chemical composition of the surface. The dark patches, which are visible in Figure 5.75d show that a change a chemical composition has occurred in the surface as a result of LSP. The SE2 surface images shown in Figure 5.75a and Figure 5.75c represent the topography of the surface, the effect of LSP on the surface is clearly indicated in Figure 5.75c. The surface shows areas that experienced remelting and deformation due to LSP.

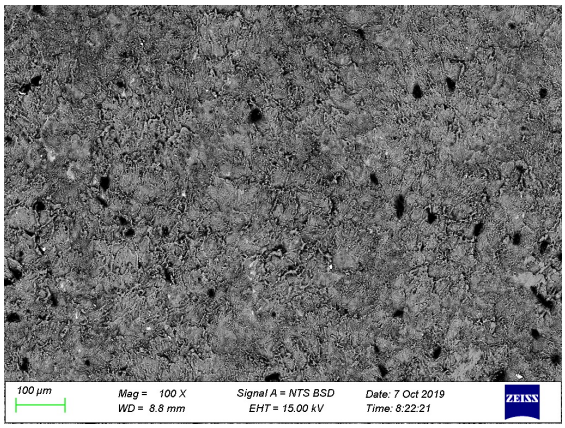
The machining of the surface is visible and a clear transition in the surface topography can be seen when LSP is applied. The LSP was performed without a ablative coating, thus showing the direct interaction between the laser and the surface of the sample. Because the LSP process generates a high temperature plasma on the surface, the high temperature gradient

causes a change in the chemical composition of the surface as observed in the SEM images. The result obtained are similar to the results reported from literature in subsection 2.3.

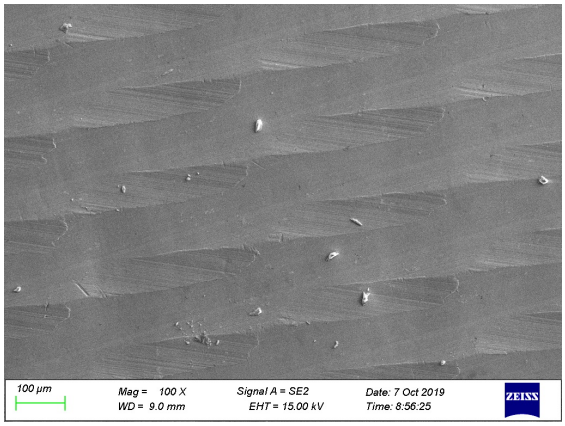
The remelting of the surface is a product of the interaction of the plasma, additional surface results reported in literature include surface micro-cracks which are the result of quick melting and solidification of the surface. Despite these effects, the residual stresses remains compressive near the surface, this is because the high pressure shock wave penetrates through the surface thus overcoming the thermal effects that are present at the surface.



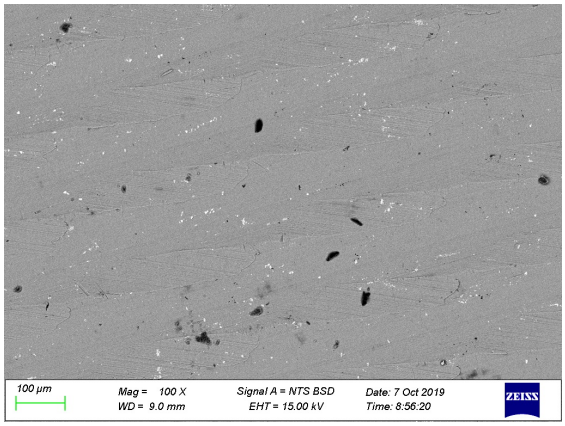
(a) SE2 - Al sample: A3/AL-Foil/P3



(b) BSD - Al sample: A3/AL-Foil/P3



(c) SE2 - Cu sample: J3-Cu-P3



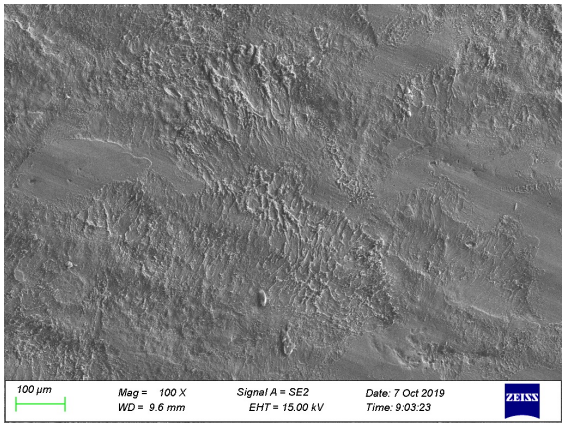
(d) BSD - Cu sample: J3-Cu-P3

Figure 5.76: SEM Images for Samples Peened using Metallic Ablative Tapes.

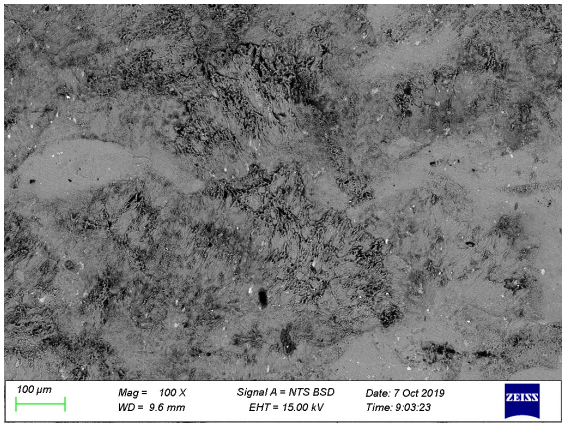
Figure 5.76 shows the SEM results found for the samples peened using the aluminium and copper tapes. The results for the aluminium tape sample shows a high degree of chemical change in the surface which resulted in a significant change in the surface topography. The resulting peened surface shows that the ablative tape failed in protecting the surface of the material thus showing similar results to that found for the sample peened without an ablative coating.

The results for the sample peened using the copper ablative tape shows very small changes in the surface chemical composition represented by the black dark patches in Figure 5.76d. Because there are hardly any changes in the chemical composition thus resulting in a unchanged

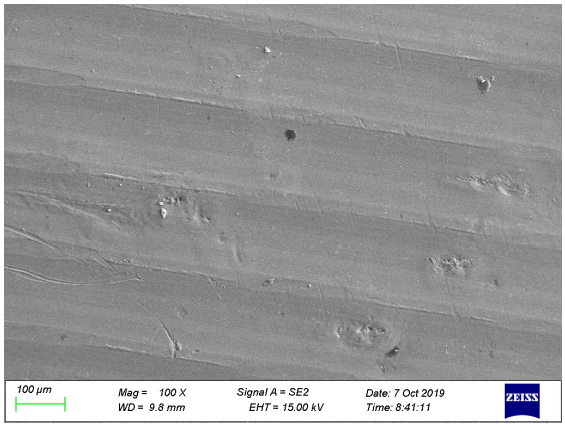
surface topography. This shows that the ablative tape did manage to protect the surface of the material prior to the failure of the tape. Even though there are no observable changes in the surface topography, the residual stresses will still compressive near the surface because the LSP generated shock wave has penetrated through the material.



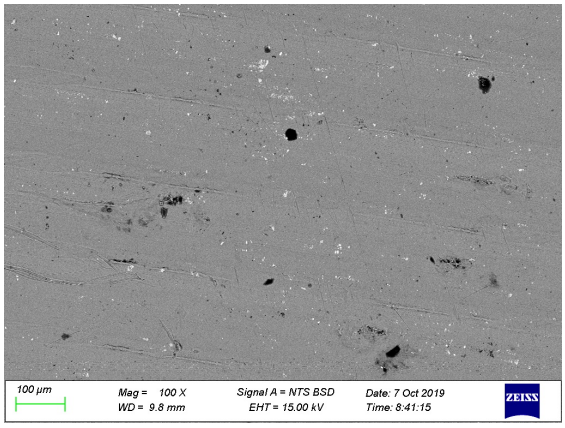
(a) SE2 - V471 sample: E3-Vinyl471-P3.



(b) BSD - V471 sample: E3-Vinyl471-P3.



(c) SE2 - V88 sample: H3-Vinyl88-P3.



(d) BSD - V88 sample: H3-Vinyl88-P3.

Figure 5.77: SEM Images for Samples Peened using Non-Metallic Ablative Tapes.

Figure 5.76 shows the SEM results found for the samples peened using the vinyl 471 and vinyl 88 tapes. The result found for the vinyl 471 sample shows that the changes in the chemical composition of the surface is distributed evenly with no major dark patches, this results in a small change in the surface topography. A brief reminder, the ablative did not fully ablate and remained behind on the surface after peening. Thus, the small patches that have not experienced any chemical change represent the areas where the tape remained behind and is represented clearly in the image. The results found for the sample peened using the vinyl 88 tape show almost no changes in the surface chemical composition and show a unchanged surface topography. However, evidence of peening is present in the surface which is represented by the small dent like changes shown in Figure 5.77c.

5.15 Microhardness

The microhardness of the samples were taken using the Falcon 500 testing machine using force of 100g. Figure 5.78 and Figure 5.79 shows the microhardness vs depth results for the samples peened with different power intensities. The results for each individual sample shows a similar trend, that is, a maximium increase is reached in microhardness near the treated surface, which is then followed by a gradual decrease in the microhardness through the depth of the material.

The microhardness result for the base sample also shows a similar trend, even though the sample did not experience peening, the machining that was conducted on it changed the grain structure near the surface thus resulting in a change in the hardness of the material. Therefore, the machining process does have an influence on the accuracy of peened results.

The effect of using an ablative medium shows the same trend, however with the increase in the power intensity, a increases in the hardness near the surface can be observed. Referring to Figure 5.78 there was a 9% increase in the hardness from the hardness of the base sample when a power intensity of 4 GW/cm^2 was applied while an increase of 6%, 4.5% and 3.2% was found for corresponding power intensities of 3 GW/cm^2 , 2 GW/cm^2 and 1.5 GW/cm^2. Although their was an observable increase in the hardness for the peened sample, the increase is not substantial, as the result falls within the allowable error.

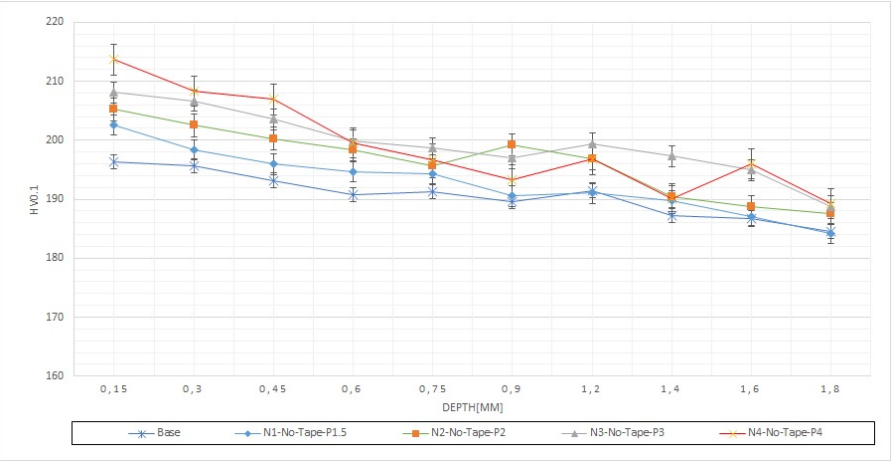


Figure 5.78: Microhardness Results for LSPwC Samples.

Similarly, referring to Figure 5.79 for the sample peened using the vinyl 88 tape, there was a 7% increase in the hardness from the hardness of the base sample when a power intensity of 4 GW/cm^2 was applied while an increase of 5.2%, 1.9% and 1% was found for corresponding power intensities of 3 GW/cm^2 , 2 GW/cm^2 and 1.5 GW/cm^2. Note: The % results listed previously were taken near the surface.

The result for the various ablative tapes shows a similar trend, with there results falling within the error bars, there was no substantial change in the behaviour of these results and thus can be found in Appendix B.

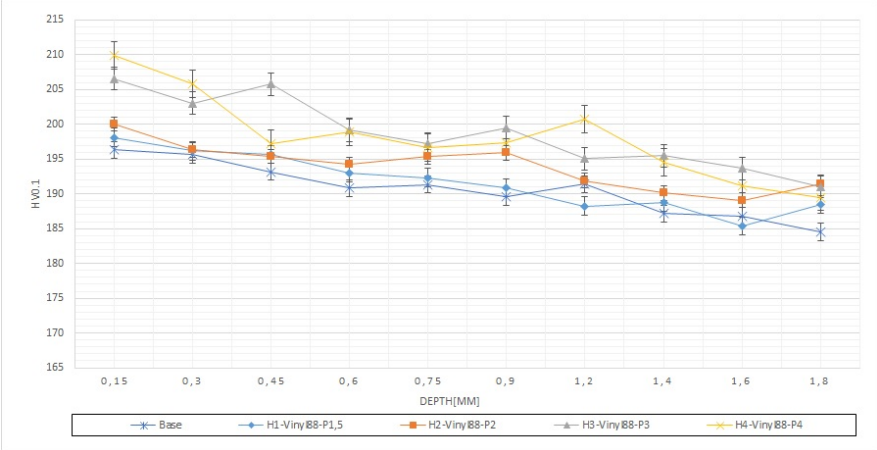


Figure 5.79: Microhardness Results for Vinyl 88 Samples.

Figure 5.80 shows the micrhardness vs depth results for the different samples peened using an power intensity 3 GW/cm^2. The results show that the using an ablative medium for LSP does indeed influence the final hardness of the material. The trend in the data with increasing depth does confer well with the finding in literature (see subsection 2.2). In general, the increase in microhardness is attributed to an increase in the dislocation density and changes in the grain structure caused by the deformation done by the LSP induced shock wave.

The lack of uniformity and erratic behaviour in the results show that there is a certain degree of inaccuracy and uncertainty involved in the presented hardness data and results. From Figure 5.80 it can observed that the hardness near the surface for most ablative tapes fluctuates between 205 HV0.1 and 210 HV0.1 and decreases with gradients ranging between -1.6x and -1.8x, the fluctuating in the hardness can be attributed to errors which include both human and machining error.

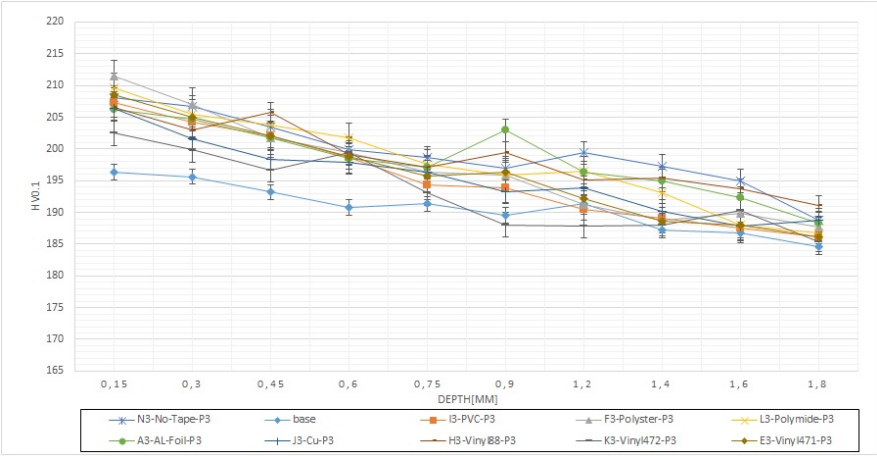


Figure 5.80: Microhardness Results for Samples Peened using 3 GW/cm^2.

The samples were machined across the peening region and therefore there is a certain degree of hardness that was introduced into the material during this process while the human error could have been contributed during the sample preparation phase, the sample were prepared by conducting three stages of grinding following three stages of polishing. Thus, these sample may have been prepared without sufficient care and therefore hardened the material during this process. Despite these errors the result certainly shows the effect the different ablative material has on the hardness. The hardness does decrease with increasing depth with most of the data falling within the allowable error.

Isolating the results for the vinyl tapes shown in Figure 5.81, illustrates the effect that the thickness of the ablative material has on the hardness of the material. The thinner V471 tape shows a maximum hardness of 208.62 HV0.1 near the surface while the V88 tape reflected a hardness of 206.58 HV0.1 near the surface. The thickest vinyl tape V472 achieved the lowest hardness between the tape, achieving a hardness of 202.5 HV0.1 near the surface. The gradient for the V471 sample data is -2.5x which is steeper than the -1.6x for V88 sample and -1.8x for the V472 tape

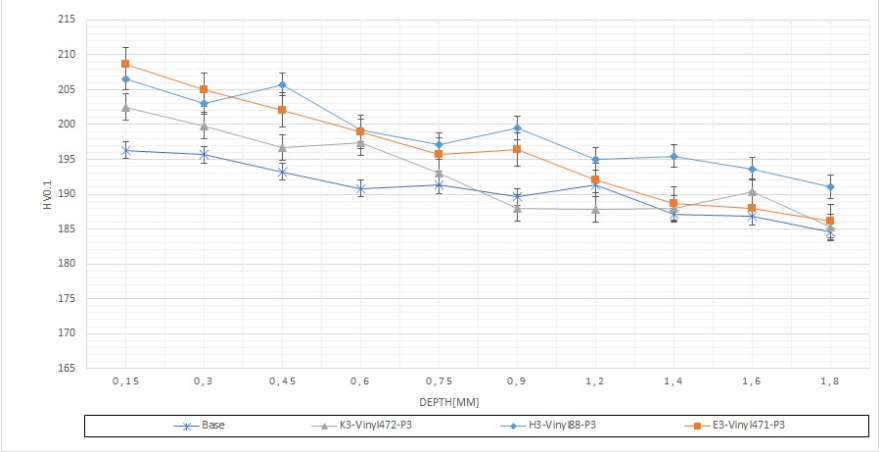


Figure 5.81: Microhardness Results for Vinyl Tape Samples.

The hardness result found show that the hardness does not only decrease with depth but the hardness in this case also decrease with increasing ablative thickness. Once again the effect of the ablative thickness does indeed influence the final peening results. However, in the case for hardness the degree of variation with depth between the different sample was not that significant with the only significant hardness being different near the surface, similarly it is expected that the residual stresses near the surface will be more compressive and gradually becoming less compressive with increasing depth. Similar hardness results were observed for the other power intensities, these results can be found in the appendix B.

5.16 Concluding Remarks

This chapter presented the surface structure and texture of the peened samples before and after the ablative tape was removed. The effect of using of the different ablative media for LSP can be seen by the unique results that were obtained for each individual ablative tape. A variety of results were obtained, some ablative tape performed better with LSP than the others.

The clear box sealing tape, the duct cloth fibre tape and the duct tape were found to be not compatible with LSP, whereas the vinyl backed tapes such as the vinyl 88, vinyl 471 and 472 showed high rates of compatibility with LSP. The variability and unpredictability for the performance of these tapes were described and highlighted with the use of a optical microscope, scanning electron microscopy and by mapping the 3-D surface structure of the samples by using the HOMMEL-ETAMIC T8000 surface roughness testing machine. The microhardness and surface roughness was also evaluated for the peened samples.

The chapter highlighted the importance of using an ablative medium with the LSP process. The results varied with both the power intensity and with different ablative adhesive tapes. The objectives that were set for characterising the laser induced damage on the surface and ablative medium and also evaluating the surface integrity of the peened samples.

The effect of the ablative thickness for LSP was found to be an important parameter, this was found by characterising and analysing the damage that was induced on the 3 different vinyl tapes. The ablative thickness also effected the performance of the aluminium and copper tapes.

The surface roughness of the peened samples was measured using two different machines, and it was found that the surface roughness of almost all samples increased with increasing power intensity. The other surface roughness parameters such as R_z and R_p provided further insight into the effect that LSP had on the surface integrity samples. The 3-D surface profile also helped to further characterise the surface features and provided the insight into the performance of the ablative tapes.

The SEM images of the surface showed that surface melting and re-solidification occurred and highlighted the different LSP impacts, craters and micro cracks for the different samples. These surface features contributed to the changes in the surface roughness of the samples.

The microhardness near the surface also increases with power intensity while the hardness also decreases with increasing depth. Even though the expected trend was observed through the depth, the results had large amounts of uncertainty, this may have been due to poor quality control that was used for the sample preparation.

Overall most of the finding with regards to the trends observed for the surface roughness and the microhardness confer well to the findings that were outlined in the literature. The results obtained from this study will be stored in the already growing South African LSP database.

5.17 Conclusions

The experiment of LSP was performed using 11 different ablative tape on Al 7075-T651 alloy using 4 different power intensities with a fixed coverage density. The conclusions are drawn from the surface roughness results, microhardness results and the observations made using both the optical microscopy and the scanning electron microscopy.

The conclusions for this phase of the project are as follows:

- The duct cloth fibre tape and the duct tape are not compatible as an ablative medium for LSP, as the fibre within these tape introduce numerous variables that work against the LSP treatment.
- The clear box seal tape is not compatible with LSP because of the uneven tape melting and the difficultly in removing the acrylic adhesive after LSP processing.
- The flame-retardant tape with polyester film provided inconsistent results and should not be used in conjunction with LSP.
- The polymide tape also provided inconsistent results, the tape experienced high degrees of melting and is not compatible with LSP.
- The 3 vinyl tapes and the PVC tape provided the best results and are compatible with LSP.
- The metallic tapes failed during the LSP process, only the copper tape remained intact but at low power intensities.
- The surface damage on the tape and the surface roughness increases with increasing power intensities.
- The hardness near the surface of the material increases with increasing power intensities and it gradually decreases with depth.
- The thickness of the ablative medium has an effect on the surface integrity and hardness of the material and needs to be studied further.
- The thickness of the ablative medium is an important parameter as the samples peened with the higher thickness provided lower roughness when compared to the less thicker ablative tapes.

5.18 Recommendations

The following recommendation should be considered for future projects:

- Thicker metallic tapes should be used to fully understand the effect metallic ablative tapes have on the surface integrity.
- The surface features could be studied using additional microscopy techniques to better understand the effect that LSP has on the surface.
- The sample preparation for the hardness testing should be performed with greater care so that differences in the properties can be evaluated with higher accuracy.
- The surface of the samples should be polished so that the features imparted by LSP can be easily identified.
- Future investigations could study a wider range of LSP parameters on different types alloys to show the effectiveness of ablative media for a wider range of applications. In particular the effect of changing spot size, peening strategy and coverage.
- Further studies can be conducted in to the effect that the thickness of the ablative medium has on the surface by using different types of ablative media such as paint for complex geometries.

6 | Phase I - Residual Stress Analysis

6.1 Incremental Hole Drilling Results

This chapter contains the incremental hole drilling results that were obtained for selected samples. The residual stress measurements were performed by using incremental hole drilling method at the University of the Witwatersrand, South Africa. Due to the large number of samples present only a select few were processed using IHD. The Laboratory X-Ray Diffraction (L-XRD) tests were conducted at the CSIR, South Africa.

The results for the first phase samples are discussed in this chapter. The majority of the hole drilling tests were conducted with the samples peened using the power intensity of 3 GW/cm^2 while only a few samples of interest for the other power intensities were tested using IHD. These choices were mainly influenced by the cost involved, additional factors such as the availability of the hole drilling machine and time involved in testing were considered.

Intermediate finding showed that the vinyl backed ablative medium provided results that well conferred to the objective set for this research project. Hence, hereafter a higher amount of focus will be placed on the samples processed using this ablative medium.

All samples processed with a power intensity of 1.5 GW/cm^2 were not considered residual stress analysis as certain ablative media did not show positive results at his power intensity. The focus will mainly be on samples peened with a power intensity of 3 GW/cm^2, because at this power intensity a variety of unique results were obtained. All IHD measurements were conducted following the ASTM E837 international standard.

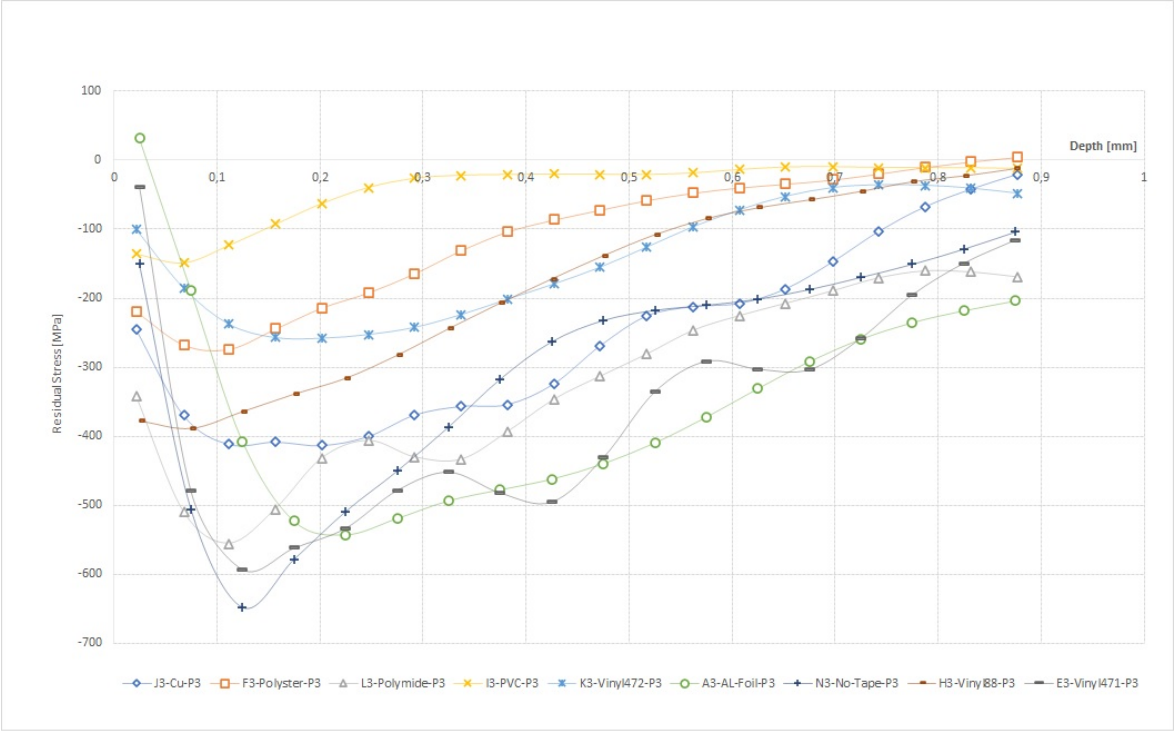


Figure 6.1: Residual Stress vs Depth for Samples Peened with PI = 3 GW/cm^2.

Figure 6.1 illustrates the effect of having different ablative media on IHD results for samples peened using power intensity of 3 GW/cm^2. For clarity purposes the x and y- directions error bars have been omitted in the figure. The figure shows a wide variety of results for samples peened using the same power intensity. The results have a good spread showing that by keeping power intensity the same and changing only the ablative material the residual stress can be engineered to a specific requirement, however additional factors such as the surface integrity have to also be considered.

The compressive residual stress peaks for all the sample occurs around a depth of 0.1 mm. The residual stress was most compressive for the sample peened without a coating, a compressive stress of -650 MPa and a depth of 0.125 mm. The vinyl 471 ablative medium achieved the second most compressive residual stress of -600 MPa at the same depth. The vinyl 471 tape introduced higher compressive residual stresses in near surface regions than the other ablative coatings. A peak compressive stress of -550 MPa was found for sample coated with the aluminium and polymide tapes. The copper and vinyl 88 tapes achieved a compressive peak of -400 MPa around a depth of 0.1 mm. The polyester and vinyl 472 tape showed a peak compressive stress of around -260 MPa near the surface region. While the PVC tape achieved the lowest compressive stress of -150 MPa at a depth of 0.075 mm.

The trend shown in the residual stress data confer well to the general trend outlined in literature. The residual stress peak occurs near the surface region and gradually decays with increasing depth. For all samples the residual stress is compressive, the results show that the ablative tapes have a significant impact on the final stress results.

In terms of penetration, a number of samples showed that the compressive residual stresses penetrated to a higher depth. The sample peened using the vinyl 471 tape showed that the stresses were significantly compressive even at the depth of 0.7 mm. Going further into the depth, the sample peened with the vinyl 471 tape, aluminium tape and polymide tape show stress that are consistently higher than the sample peened without any coating at depths higher than 0.3 mm. The stresses in certain areas for the vinyl 471 tape are 100-150 MPa higher in magnitude than that of the N3-No-tape-P3 sample, this increase in the magnitude for the slightly higher compression after 0.3 mm could be because of high compensating tensile stresses which were reducing the compressive stresses when using this vinyl ablative tape.

The results depicted in Figure 6.1 show that some ablative materials achieved higher magnitude for the residual stress than others. The error and inaccuracies in the data do not have a significant impact on the final results. The tests were conducted by strictly following the ASTM standard therefore the results depicted are the results that were obtained by LSP. Therefore, the low magnitude results obtained for the PVC ablative tape sample could be the result of factors such as: the hole drilling was conducted in a region that did not experience significant peening(refer to Figure 5.52 for the peened surface image), or the shock wave did not penetrate to the expected depth because of the properties of the ablative tape (i.e. most of the energy was absorbed by the tape before being ablated). A similar explanation can be used to characterise the results obtained for the sample peened using the polyester tape.

For the metallic coatings, the aluminium provided a higher magnitude residual stress than the copper coating. However, these metallic coating did not fully protect the surface when the peening was conducted (refer to section 5.2 and 5.10). The results for the non-metallic tapes showed that the vinyl 471 provided the highest magnitude residual stress while also keeping the surface integrity of the material intact.

The results show that using an ablative material decreases the magnitude of the overall residual stress, but this is an independent result because certain ablative coatings do not fully protect the surface and thus do not meet nor satisfy the research objectives. This is because even though the results for the polymide tape achieved a high magnitude residual stress near the surface, it did not keep the surface integrity intact (as discussed in section 5.12). The sample peened using aluminium tape also confers to this reasoning, the tape failed during peening and as a consequence did not protect the surface despite achieving high compressive stresses near the surface.

Overall the residual stresses results depicted for the samples peened using an ablative layer provided positive. The correlation in the trend of the results has reinforced the need to use an ablative coating to help achieve an acceptable surface integrity and compressive residual stress. The trend and nature of the data corresponds well to that found in the literature, thus showing that the IHD test were conducted and presented in the appropriate manner.

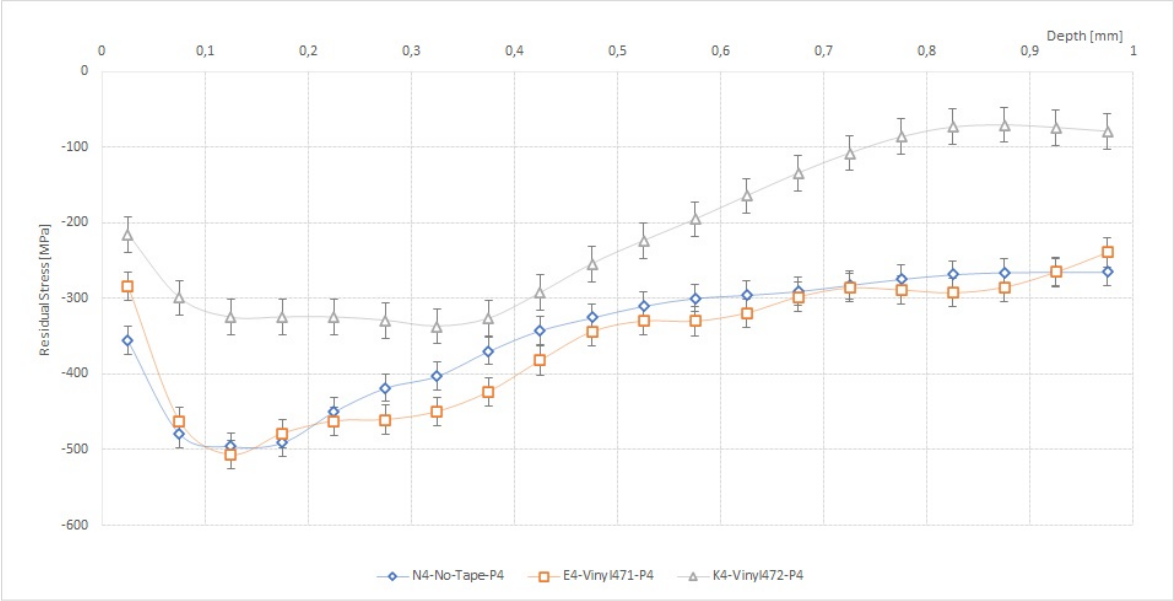


Figure 6.2: Residual Stress vs Depth for Samples Peened with PI = 4 GW/cm^2.

Figure 6.2 shows the residual stress as a function of distance from peened surface for samples peened using a power intensity of 4 GW/cm^2. The results are depicted for samples N4-No-Tape-P4, E4-Vinyl471-P4 and K4-Vinyl472-P4. At this power intensity, these samples were selected because they showed favourable results, particularly the vinyl tapes.

The results show that the stresses for all the samples penetrated deeper at this power intensity and were constant from depths of 0.1 mm to 0.4 mm. A peak compressive stress of -500 MPa at a depth of 0.125 mm was found for the N4-No-Tape-P4 sample and a peak compressive stress of -510 MPa at a depth of 0.125 mm was found for the sample E4-Vinyl471-P4 whereas a peak stress of -350 MPa at a depth of 0.3 mm was found for the sample K4-Vinyl472-P4.

Once again the samples peened using the ablative tape achieved a similar if not lower magnitude of residual stress when compared to the sample peened without a coating. The similarities between the results found for the vinyl 471 and the sample peened without a coating shows that when peening is conducted at high laser power intensities using an ablative coating that can be fully ablated and vaporised, shows that not only can the results be similar to peening without a coating but a better surface integrity can also be maintained.

The results obtained for the two vinyl tapes reinforce the idea that the thickness of the ablative material do indeed influence the final peening results. The effect of the increased thickness in the vinyl 472 tape shows that the magnitude of the residual stress is much lower than that obtained for the sample peened using the vinyl 472 tape. A brief reminder, from the previous section it was shown that the peening conducted at this power intensity showed that the vinyl 471 tape was fully ablated and vaporised whereas the vinyl 472 tape only partially ablated and mostly remained fully intact. From this, it can be noted that the vinyl 472 tape absorbed a considerable amount of energy whereas the vinyl 471 tape did not, the tape was

fully ablated and under the high coverage ratio allowed the consequent laser pulse to peen a partially protected surface. This reflects in the similarities in the residual stress data between the results found for the sample peened without a coating and the vinyl 471 results. Another factor to consider is the location the hole drilling was conducted on the sample, this is due to the laser pulse overlapping ratio, that is certain location on the peened area experienced a higher degree of peening as multiple laser pulses overlapped on that location, this has an influence on the final stress results.

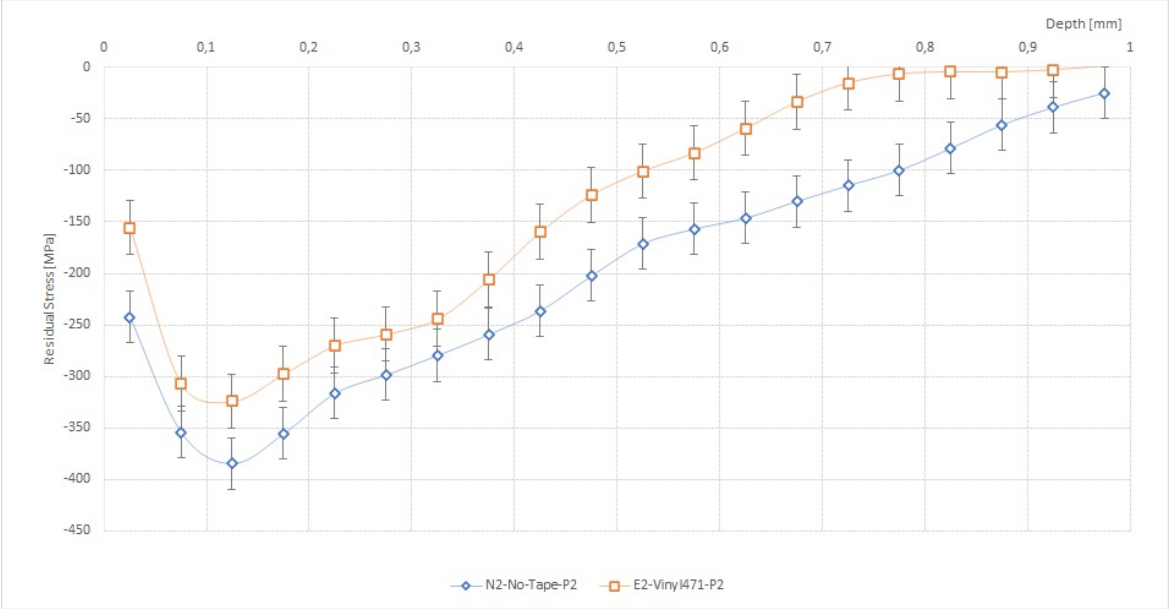


Figure 6.3: Residual Stress vs Depth for Samples Peened with PI = 2 GW/cm^2.

Figure 6.3 shows the residual stress as a function of distance from peened surface for samples peened using a power intensity of 2 GW/cm^2. Only two samples were tested at this power intensity mainly to investigate the effect of using an ablative coating has on the residual stress.

Once again the sample peened without a coating has a higher magnitude stress peak of -380 MPa while the sample coated with the vinyl 471 tape has a peak residual stress of -320 MPa. The residual stress for the two sample are relatively compressive from a depth of 0.07 mm to 0.3 mm.

The performance of the ablative tape with regards to the results for the compressive stresses is as expected, the usage of the ablative coating reduces the compressive residual stress while maintaining the surface integrity as found in chapter 5. The stresses found for the samples peened at this power intensity are approximately 80% lower than the stress found for samples peened with the power intensity of 3 GW/cm^2.

The depth of penetration is lower when compared to the samples peened with higher power intensities. While the depth of penetration is lower for the vinyl 471 when compared to the penetration depth achieved by the sample peened without a coating.

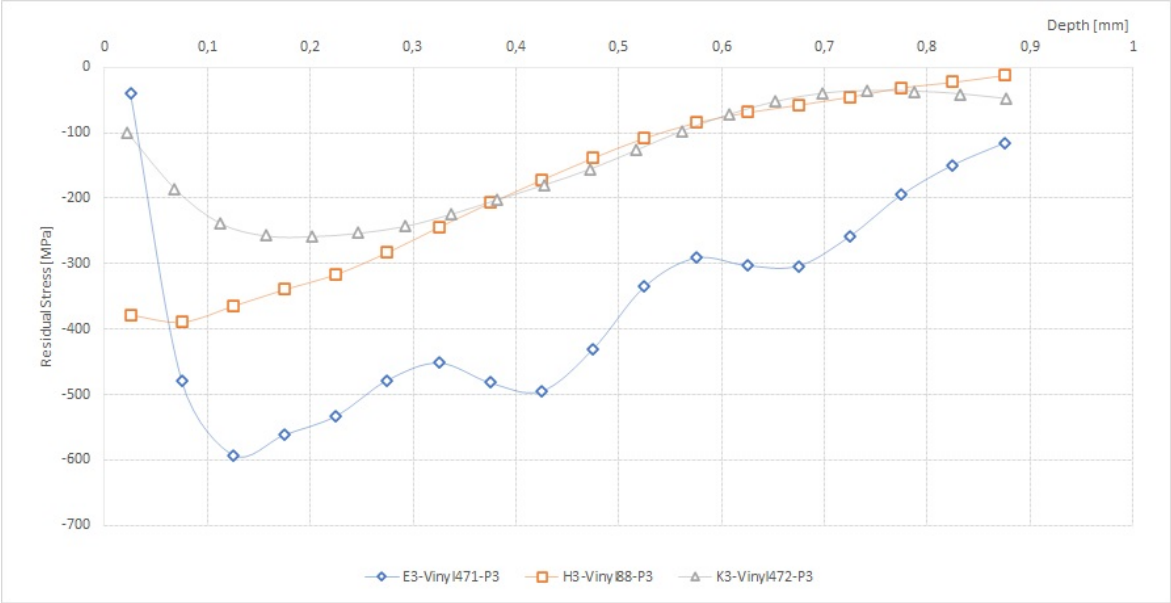


Figure 6.4: Residual Stress vs Depth for Samples Peened using the Vinyl Coating.

Figure 6.4 illustrates the isolated residual stress results as a function of depth for the samples solely peened using the vinyl ablative backing. The results depicted above show the effect that the thickness of the ablative material has on the compressive residual stress. It can be noted that an increase in the thickness of the ablative material result in a lower magnitude stress and a lower depth penetration.

The peak magnitude stress for all the samples occurs near the surface around 0.1 mm. These results illustrate that the thickness of the ablative material has a major influence on the final outcome on the stress results. This indicates that the thickness of the ablative material is another important parameter that should be considered in conjunction with the other laser parameters.

The thickness of the ablative layer is not necessarily dependent on the backing material, therefore if the aluminium tape had the thickness of the vinyl 472 tape than similar results would be obtained, because the larger thickness will significantly increase the resistance of the ablative tape but still allowing the surface integrity to be maintained while embedding the residual stresses into the material.

This same principle can be applied to other forms of ablative media such as paint, thus multiple paint coatings could be applied to the same material before peening and will yield lower residual stress result but will maintain the surface integrity of the material to a higher degree. The only negative effect this will have, is the increase in the preparation time required for the sample.

Figure 6.5 shows the residual stress as a function of depth for the vinyl 471 samples that were peened at 2 and 3 GW/cm^2. The effect of increasing the power intensity has the same

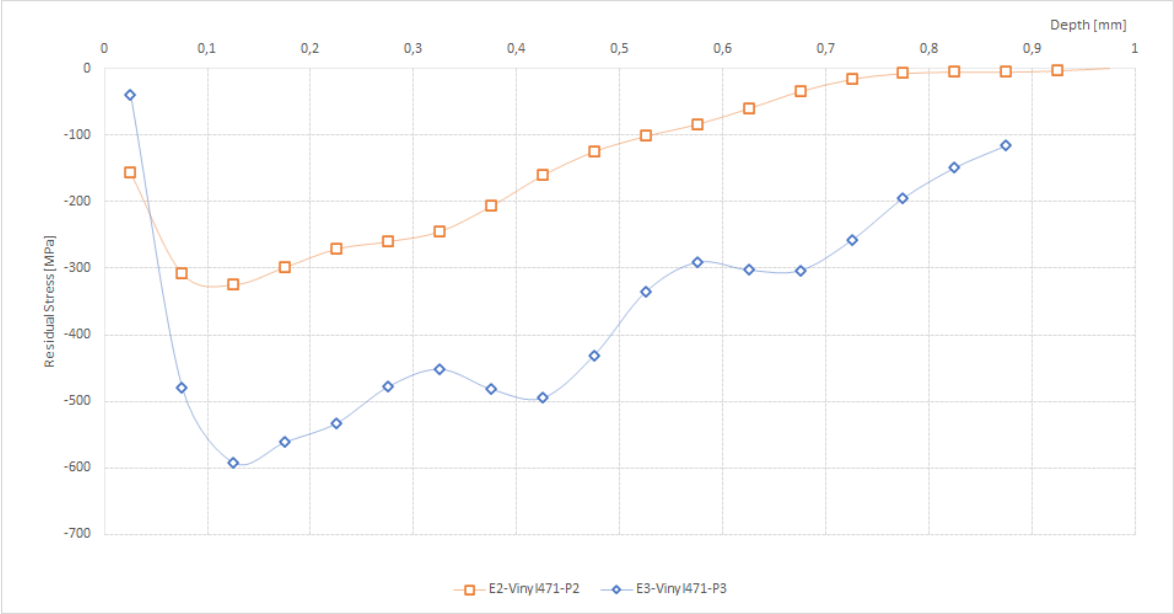


Figure 6.5: Residual Stress vs Depth for Samples Peened using the Vinyl 471 at Different PI.

effect that was outline in the literature. The peak compressive residual stress increases with increasing power intensity. The depth of penetration also increases with increasing power intensity. These results are not dependant on the type of ablative medium that is used with LSP.

6.2 Laboratory XRD

Figure 6.6 shows the L-XRD results for the LSPwC sample peened with a PI of 3 GW/cm^2. These L-XRD results are plotted against the IHD results for comparison. The L-XRD measurements were taken at an estimated depth of 0.026 mm whereas the first depth measurement for the IHD is at 0.025 mm thus a comparative study can be performed.

The minimum stress result for the L-XRD was -140,38 MPa and the IHD result was found to be -150,46 MPa and the maximum stress, the L-XRD result is -110,68 MPa whereas the IHD result is -95,216 MPa. The error bars for the L-XRD result are ±50 MPa. These large error bars are included because of the insufficient oscillations and counting times that were used for the LSPwC textured sample, this mean that higher textured samples have higher errors included in these results.

Even though the magnitude stress results for the two methods do not correspond exactly, they are however very similar and show that the stresses near the surface are significantly less compressive when compared to the stress results at a depth of 0.1 - 0.2 mm.

The advantage of XRD analysis is that the method is non-destructive whereas the IHD is semi-destructive but the depth of measurements for the two techniques are significantly different. The similar results that were obtained between these two methods confirm that the stresses are indeed compressive near the surface. The uncertainty in the results are not high as the results are quite similar, therefore the majority of the IHD results that were obtained in prior tests are acceptable. The only uncertainty involved with conducting IHD is the human and the handling error that can be imparted when physically conducting the test.

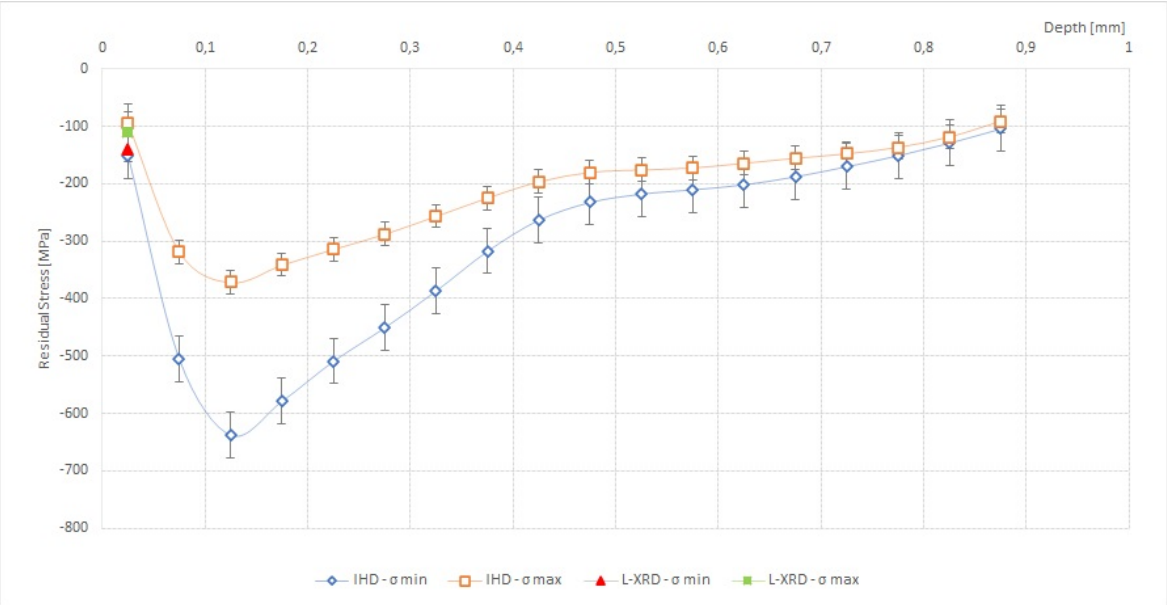


Figure 6.6: IHD and L-XRD Residual Stress vs Depth Results.

In terms of availability of the instrument and technician, time and cost: L-XRD had a lead-time of about 4 months. The equipment and apparatus was available located only 50 km from the University of the Witwatersrand and is not easily available for university students. The time per measurement was 2 hours, similar to IHD. The usage of the equipment is part of the CSIR Rental Pool Programme thus the cost was significantly reduced for academic research purposes. Due to these constraints only a few samples were tested using this technique.

6.3 Concluding Remarks

This chapter presented the residual stress results for the samples peened with the different ablative tapes using 4 different power intensities with a fixed SS and %Cv. The residual stress results were mainly obtained using IHD as the equipment and apparatus were readily available, L-XRD measurements were conducted for comparative purposes. The IHD results obtained for all samples showed the same trend that was observed in literature, this method was able to show the trend of the data near the surface and at intermediate depths.

The residual stress measurements were only performed on a selected set of samples. These samples were selected in such a way that the effect of the different ablative media, and laser parameters could be investigated. Unfortunately, some test did however did not capture the correct data and were deemed faulty and had to be re-drilled on a new location on the sample.

The IHD results obtained for all the sample follow the same intended trend that was found in literature, the residual stresses are most compressive near the surface and gradually become less compressive with increasing depth. The peak residual stress and the depth of penetration increase with increasing power intensity.

The highest compressive residual stress was obtained for the sample peened without any ablative coating, the second highest was found for the sample peened using vinyl 471 ablative tape.

The stress results for the 3 vinyl tapes showed that with increasing ablative thickness the peak residual stress and depth of penetration do decrease. These results verify that the thickness of the ablative tape is indeed an important parameter and should be taken into consideration when conducted LSP. The vinyl tape achieved the best results for both the surface integrity and for the residual stress analysis when compared to the results obtained for the other ablative tapes.

The L-XRD results were shown to be only suitable for measuring near surface residual stresses, the results corroborated well with the near surface results obtained by IHD.

Overall most of the residual stress finding with regards to the trends confer well to the findings that were outlined in the literature. The stress results obtained from this study will be stored in the already growing South African LSP database.

6.4 Conclusions

The conclusions for this part of the study are as follows

- The thickness of the ablative medium is an important parameter that should be considered when selecting ablative media for LSP.
- The vinyl 471 ablative tape achieved the highest compressive residual stress.
- The trends observed for the residual stress results obtained for all the samples correlated well to that found in literature.
- The non-metallic ablative tape provided higher depth penetration and magnitude stress results when compared to the metallic ablative tapes.

- Using an ablative medium with LSP lowers the peak magnitude stress and the depth of penetration.
- IHD was suitable for measurements at intermediate depths while L-XRD is suitable to evaluate near surface stresses.
- The depth of penetration increases with increasing power intensity and with decreasing ablative thickness.
- Due to the large quantity of peened samples and due to the different availability, time and cost for each residual stress method, a compromise was required when planning the testing.

6.5 Recommendations

The following recommendation should be considered for future projects:

- The depth-resolved residual stress measurements should be performed using multiple residual techniques, so a more in depth study can be performed.
- Use a less textured sample for L-XRD testing such that there can be higher oscillations and counting times to achieve more accurate results.
- Spare samples should be prepared since there is a chance that the IHD test could become faulty.
- Further investigations could be made into the residual stress by using different LSP parameters and alloys.
- Multiple stress measurement should be made in order to study to change that occur on the surface due to the unpredictable nature of the ablative media.

7 | Phase II Analysis

This chapter contains the experimental results, observations, discussion and conclusions pertaining to the final objectives outlined for the project which were to perform by varying the coverage ratio for the sample peened without a coating and sample peened using the vinyl 471 adhesive tape. The effect of the % coverage ratio was analysed by using:

- Optical microscopy.
- Surface roughness testing.
- The residual stress profile by using IHD and L-XRD.

The results obtained from the first phase showed that the surface finish left by the machining process was not adequate enough to fully outline the changes that were experienced by the surface of the material. Therefore, the samples used for this phase were first ground using the three stage outlined in the grinding process. This was done so that the effect the peening has on the material can be clearly seen. The final surface finish of the unpeened sample is shown in Figure 7.1. These sample were peened using a power intensity of 3 GW/cm^2 with coverage ratios starting for 30% to 90%. The reason the vinyl 471 tape was selected for this phase was due to the positive results obtained previous chapters and the cost of the material.

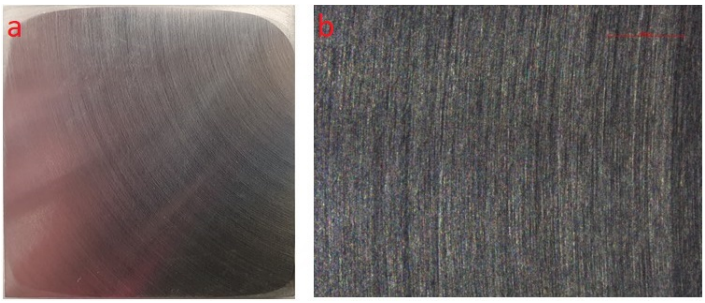


Figure 7.1: Unpeened Base Sample.

7.1 Surface Observations and Results

7.2 No Tape(LSPwC) Samples

Figure 7.2-Figure 7.8 illustrates the surface images taken using an optical microscope for the samples peened without a coating.

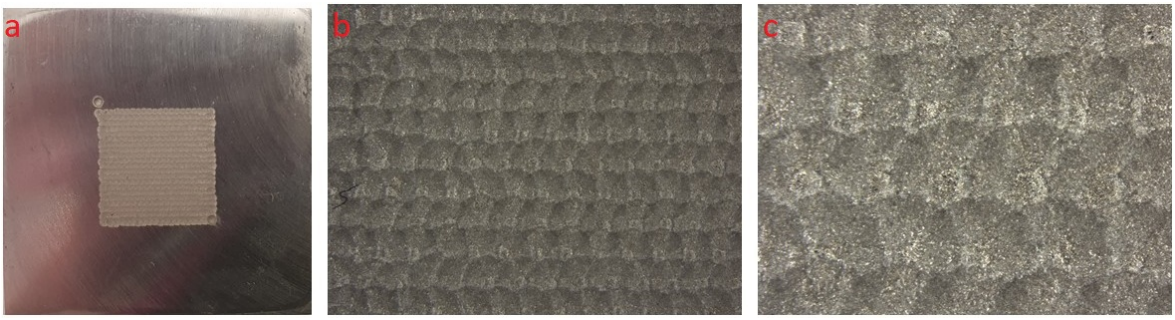


Figure 7.2: Surface Images for Sample: n1-No-Tape-30.

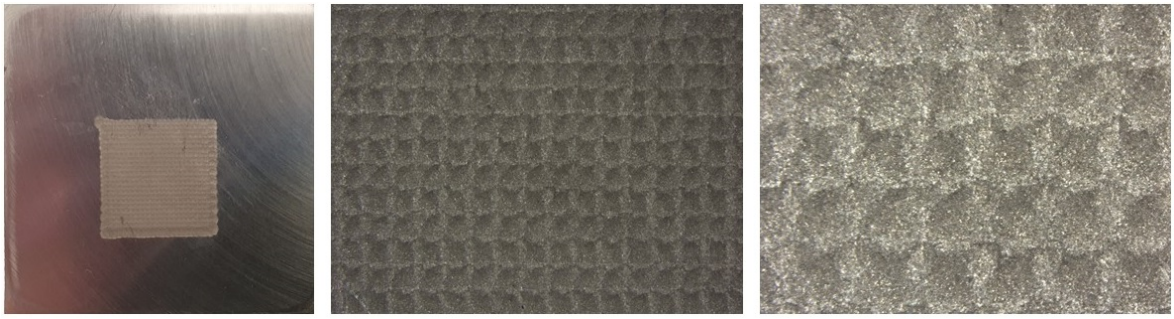


Figure 7.3: Surface Images for Sample: n2-No-Tape-40.

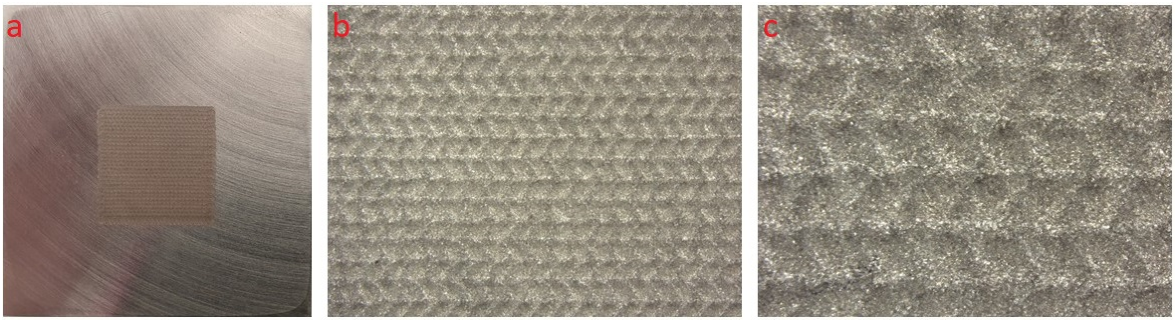


Figure 7.4: Surface Images for Sample: n3-No-Tape-50.



Figure 7.5: Surface Images for Sample: n4-No-Tape-60.



Figure 7.6: Surface Images for Sample: n5-No-Tape-70.



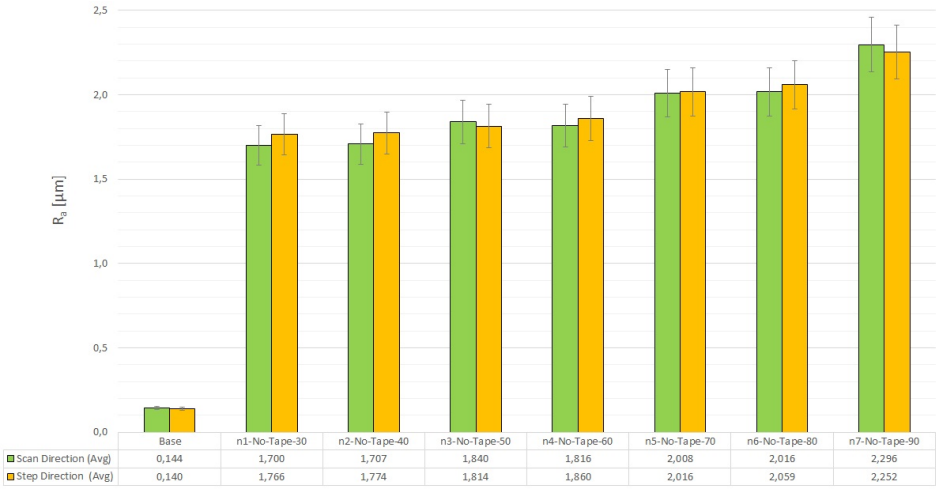
Figure 7.7: Surface Images for Sample: n6-No-Tape-80.



Figure 7.8: Surface Images for Sample: n7-No-Tape-90.

These 7 figures shown previously, clearly show the changes in the surface state with increasing coverage ratios at constant laser power intensity of 3 GW/cm^2. This nature and trend in the images confirms the finding that were outlined in the literature in section 2.6.

The surface features of the peened samples can be clearly seen, from Figure 7.2 the laser spot can be clearly identified, the impact and the resulting crater can be seen whereas with increasing coverage density these craters and laser impacts become visibly less noticeable. Surface roughness testing was conducted to further understand the effect the changing of coverage density has on the surface integrity of the material. The surface roughness testing was conducted using the portable SRT-6210 surface roughness testing unit.



	Base	n1-No-Tape-30	n2-No-Tape-40	n3-No-Tape-50	n4-No-Tape-60	n5-No-Tape-70	n6-No-Tape-80	n7-No-Tape-90
Scan Direction (Avg)	0,144	1,700	1,707	1,840	1,816	2,008	2,016	2,296
Step Direction (Avg)	0,140	1,766	1,774	1,814	1,860	2,016	2,059	2,252

Figure 7.9: Surface Roughness Results for LSPwC Samples

Figure 7.9 show the surface roughness results obtained for the samples peened without an ablative coating. These results represent the average of the multiple reading that were taken on each individual sample. A total of 18 readings were taken per sample, 9 in each direction. A 10% uncertainty and accuracy error is also represented in Figure 7.9.

The results obtained show a significant increase in the surface roughness for all peened samples from the unpeened base sample. Sample n1-No-Tape-30 was found to have mean average roughness of 1.733 μm which represent an increase of 1111.9%. The samples peened with a coverage density of 40% to 80% showed similar high percentage increases in the mean roughness. A maximum increase of 1490.2% was found for the sample peened with a 90% coverage ratio.

The changes in the surface state is not erratic, there is gradual increase in the surface roughness with the gradual increase in the coverage density. There is a 31.3% increase in the surface roughness for sample n7-No-Tape-90 from the surface roughness found for sample n1-No-Tape-30.

The changes in the surface integrity with respect to the increasing coverage density is gradual, and this confers to the results obtained in literature. The increase in the surface roughness is attributed to the changes that were observed in the surface craters that were induced by the laser impacts and the melting and re-solidifying of the surface under this power intensity.

7.3 Vinyl 471 Tape Samples

Figure 7.10-Figure 7.16 illustrates the surface images taken using an optical microscope for the samples peened without a coating.

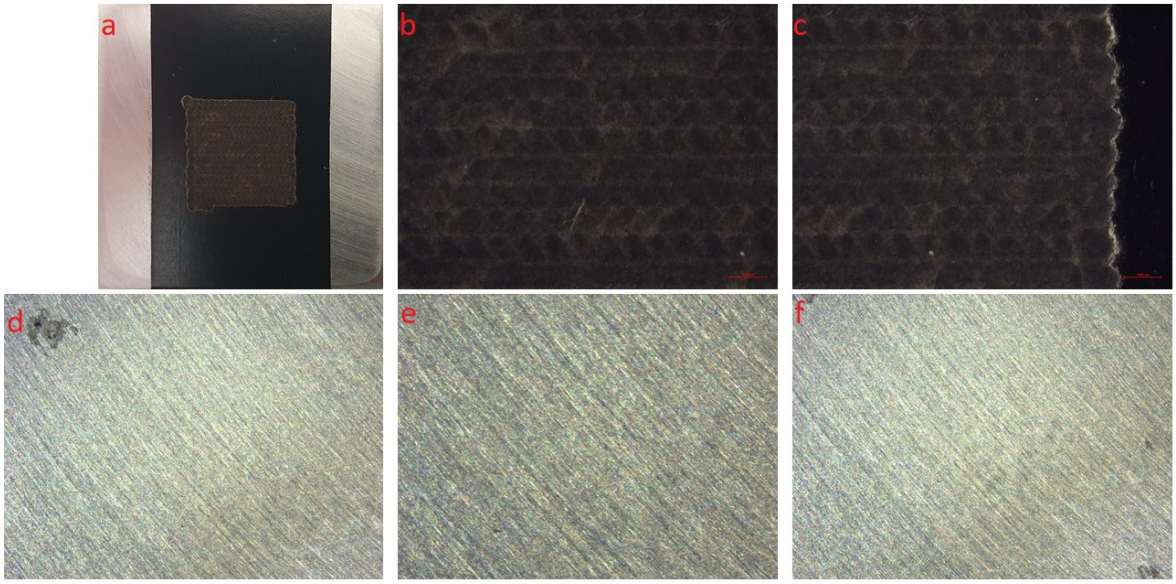


Figure 7.10: Surface Images for Sample: a1-Vinyl471-30.

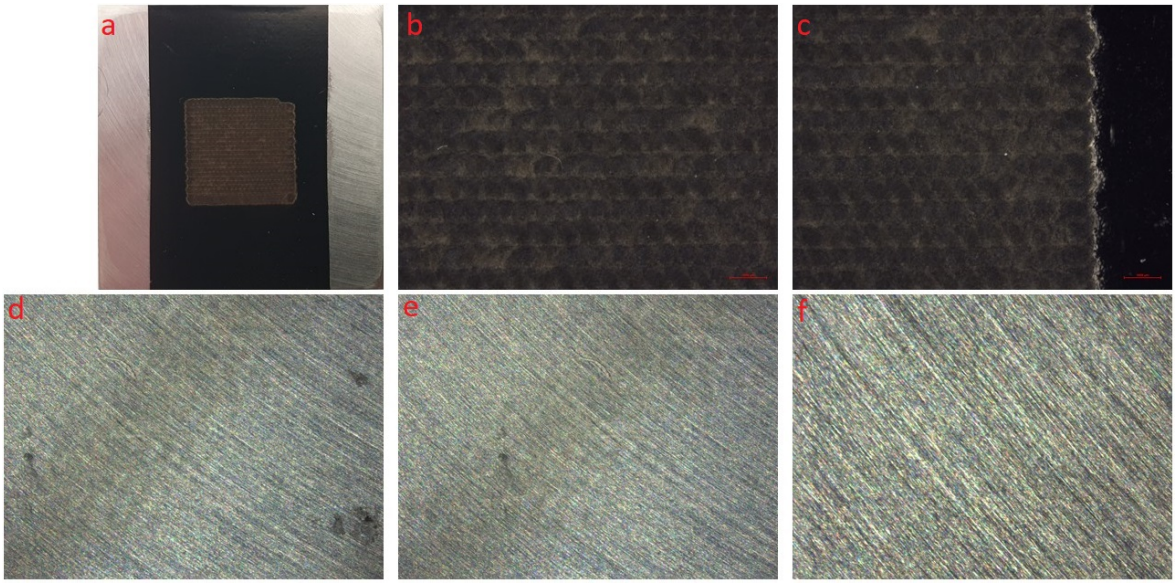


Figure 7.11: Surface Images for Sample: a2-Vinyl471-40.

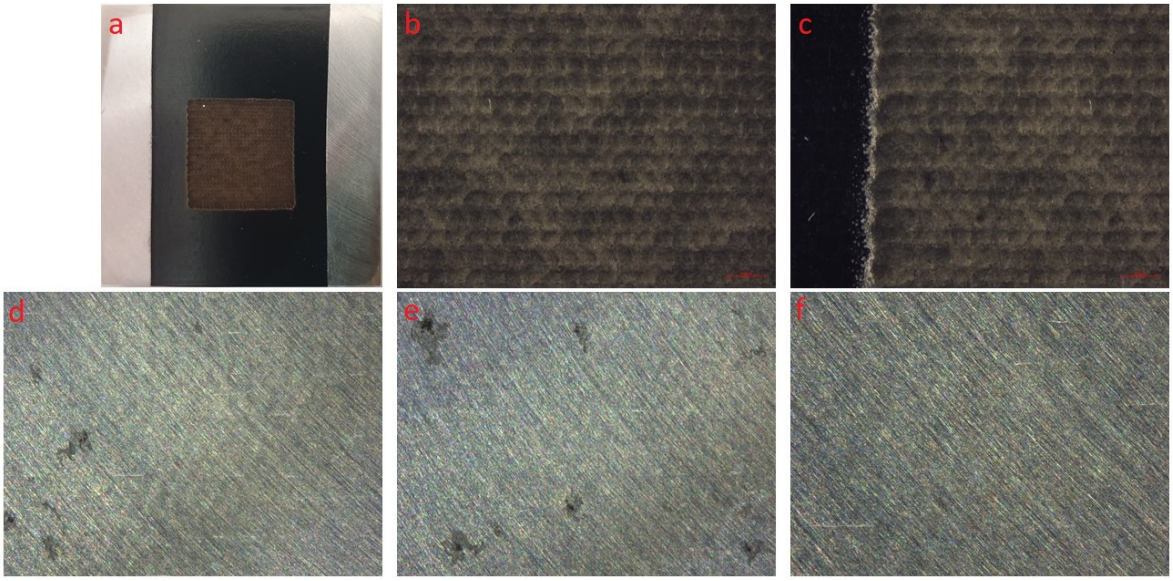


Figure 7.12: Surface Images for Sample: a3-Vinyl471-50.

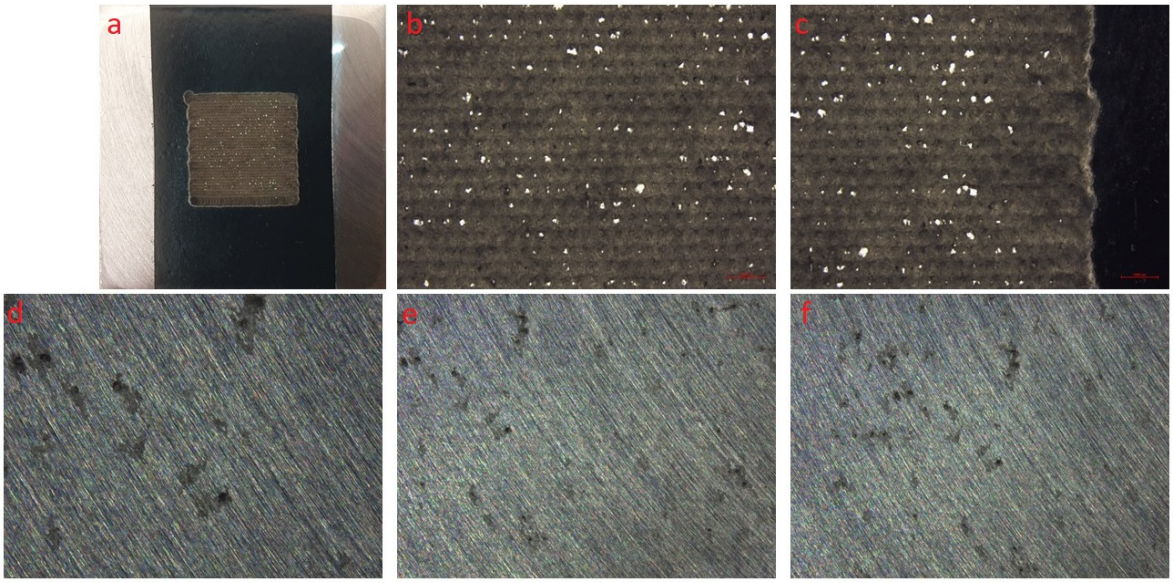


Figure 7.13: Surface Images for Sample: a4-Vinyl471-60.

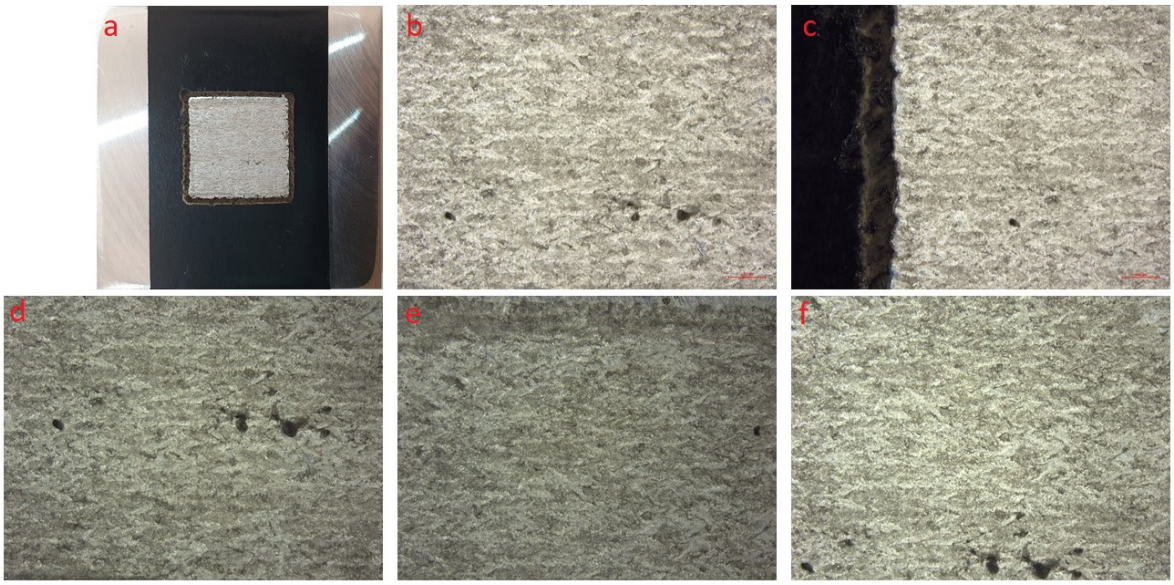


Figure 7.14: Surface Images for Sample: a5-Vinyl471-70.

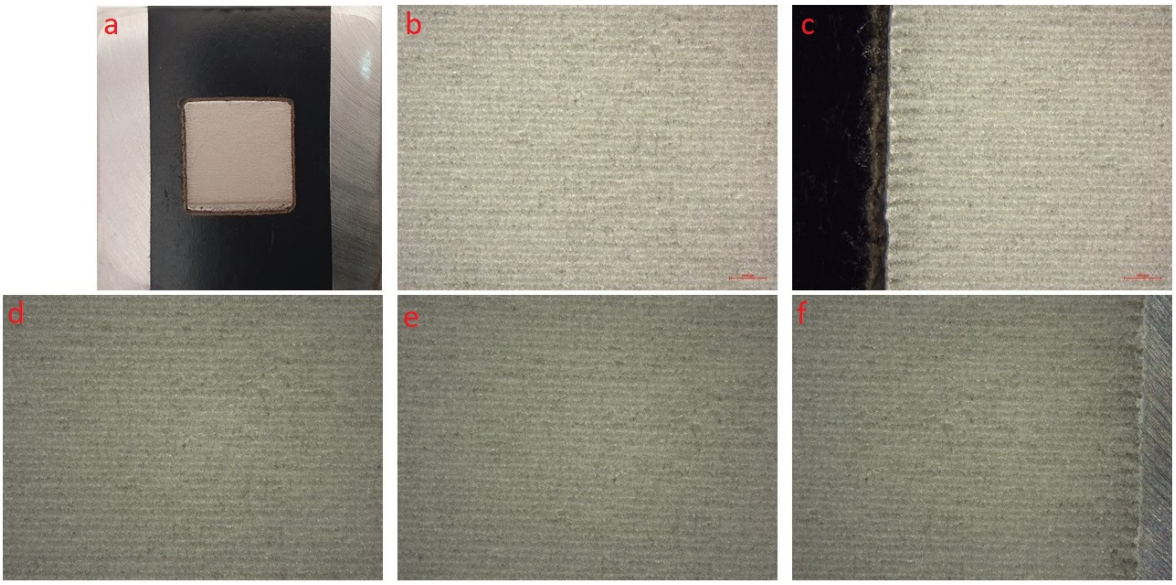


Figure 7.15: Surface Images for Sample: a6-Vinyl471-80.

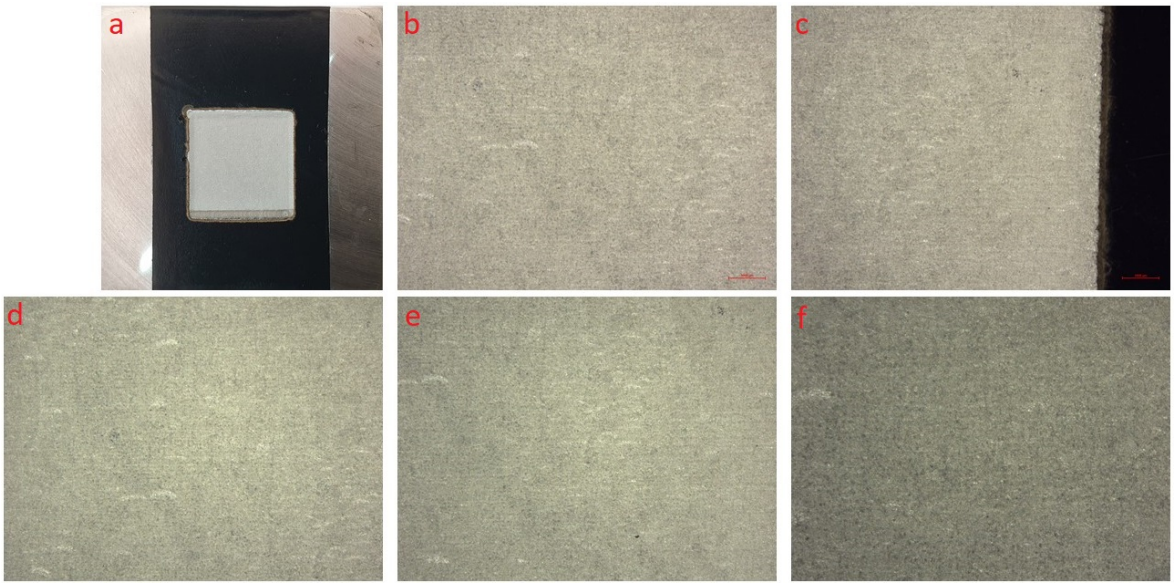


Figure 7.16: Surface Images for Sample: a7-Vinyl471-90.

The figures show previously show the surface state of the samples before and after the removal of the ablative tape. There are no visible changes that can be seen on the surface state of the peened samples, but the changes with respect to the coverage density can be clearly seen on the surface of the ablative tape itself.

The changes within the ablative tape increases with increasing coverage ratios, the ablative tape starts to show signs of laser penetration to the underlying surface from coverage ratio of 60% upwards. At the coverage of 70% and above the tape has been fully ablated and vaporised, however trace amounts of tape debris can be found on the peened surface.

The changes in the peened gradually increase, for sample a1-Vinyl471-30 there is no visible indication that represents peening, the surface texture mainly remains smooth with small areas that show some type of craters, this is however difficult to differentiate within the images shown in Figure 7.10.

As the coverage ratio is increased, more changes on the peened surface become visible. There are trace amount of residue and signs of peening can be seen on the surface for the a2-Vinyl471-40 sample and the a3-Vinyl471-50 sample. Sample a4-Vinyl471-60 shows high amounts of residue and shows a slightly better signs for peening. The change in the surface texture is quite significant from this coverage density onwards. This is because sample a5-Vinyl471-70 shows the effect that the total ablation of the tape has on the surface integrity, but at this coverage density the residue can be seen to be embedded into the material, this is after the removal of the tape and after the surface being cleaned using ethanol.

Sample a6-Vinyl471-80 and a7-Vinyl471-90 show that the tape has been completely vaporised under the effect of LSP, the final peened surface appears smooth and has very small if not any amounts of tape residue and debris left on the surface.

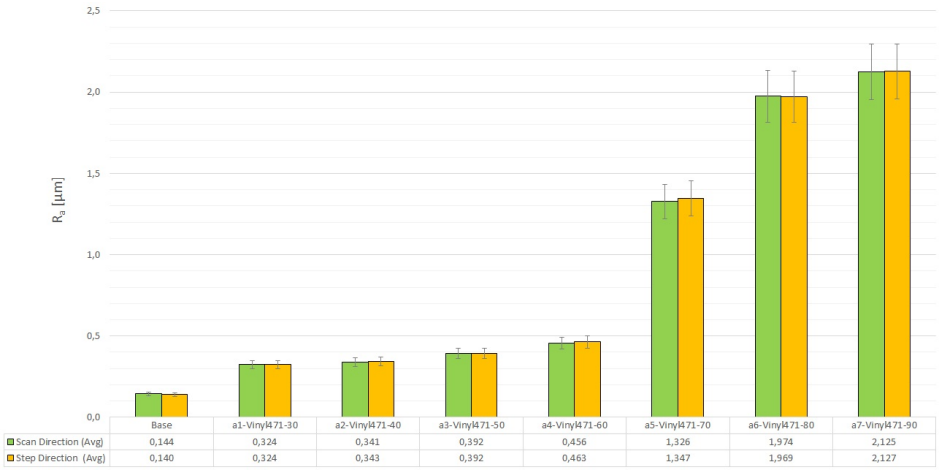


Figure 7.17: Surface Roughness Results for Vinyl 471 Tape Samples.

Figure 7.17 depicts the surface roughness results that were obtained for the 7 samples peened using the vinyl 471 ablative tape. The surface roughness results depicted in Figure 7.17 show that the roughness increases gradually with increasing %Cv up until the sample peened with the %Cv of 60%, thereafter the roughness increases significantly.

There is a 128.2% increase in the surface roughness for sample a1-Vinyl471-30 from the measured roughness for the unpeened base sample. While a 224.0% increase in the roughness was found for sample a4-Vinyl471-60, the samples peened with %Cv of 40% and 50% showed roughness increases of 140.8% and 176.1%. The change in the roughness between the sample a4-Vinyl471-60 and a5-Vinyl471-70 can be attributed to the fact that the ablative tape was fully ablated at the %Cv of 70% thus exposing the underlying surface, thus resulting in the surface roughness to increase by 840.9%. An increase of 1288.7% in the roughness was found for sample a6-Vinyl471-80 whereas for sample a7-Vinyl471-90 the increase in roughness was found to be 1397.2%.

An exponential type trend can be observed from the data displayed in Figure 7.17, the surface roughness increase with increasing coverage density. The results confirm that as the ablative medium experiences higher thermal damage with increasing coverage density, as a consequence the underlying surface experience additional shock waves thus modifying the surface. The rate of damage experienced by both the tape and the surface increase exponentially with higher coverage densities.

The surface roughness along both directions is very similar, this shows that grinding of the sample prior to peening does indeed help achieve better understanding of the surface. These results when compared to the finding from chapter 5, have a higher degree of accuracy and with lower uncertainty. The results represent the collective average of 9 measurement for each direction.

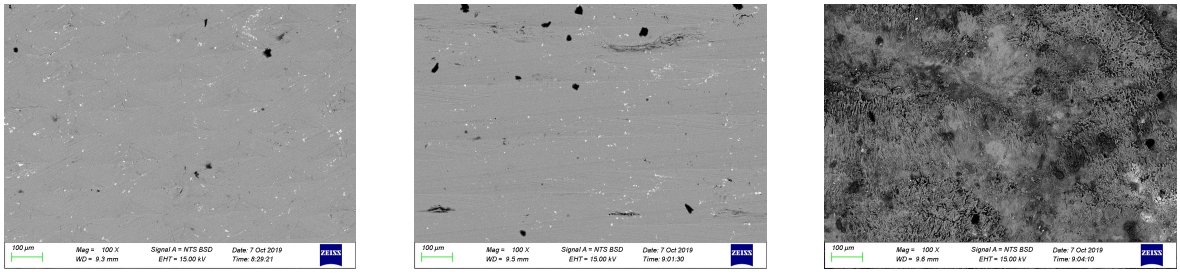


Figure 7.18: SEM results for Samples: a1-Vinyl471-30, a3-Vinyl471-50 and a5-Vinyl471-70.

Figure 7.18 show the BSD surface images that were obtained by using SEM for the samples peened using a coverage density of 30%, 50% and 70%. These surface image represent the changes that occurred in the chemical composition due to the effects of LSP. The changes in the surface once again increase with increasing coverage density. The remelting of the surface is quite evident for the sample peened with a coverage density of 70%, while there is no indication of remelting of the surface for the other two samples. The surface results are similar to that found by using the optical microscope.



Figure 7.19: Residual Stress vs Depth for Vinyl Tape Samples.

Figure 7.19 shows the compressive residual stresses as a function of depth that were found for samples a3-Vinyl471-50 and a5-Vinyl471-70. The sample peened with the higher coverage density achieved a higher peak compressive stress of 590 MPa and achieved a higher depth penetration while the sample peened with the lower coverage density achieved a peak magnitude stress of 400 MPa with a lower depth penetration. The peak residual stress occurs in the same region near the surface of the material.

These results confer well with the finding that were outlined in literature, the peak magnitude residual stress and the depth of penetration increase with increasing coverage density when using the same power intensity and laser spot size. Only two samples were tested to confirm the finding that were outlined in the literature, the findings are not dependent on the ablative material used because the finding outlined in literature were performed using LSPwC.

7.4 Concluding Remarks

This chapter presented the results into an investigation of using different coverage densities with an ablative medium. The surface integrity and the residual stresses were investigated using aluminium samples that were prepared meticulously by undergoing 3 stages of grinding.

The study of the surface showed that the damage induced by LSP increases with increasing coverage density. The ablative tape remained intact up until the coverage of 60% before begin completely vaporised at the higher coverage ratios. The surface roughness for the LSPwC samples showed a gradual linear increase with increasing coverage density but the samples peened using the vinyl 471 tape showed an exponential increase in the surface roughness. The SEM results showed that the chemical changes experienced by the surface also increase with increasing coverage density.

Using an ablative medium lower the surface roughness when compared to the findings for the LSPwC samples. The surface integrity is maintained and preserved to a higher degree when using lower coverage densities. The vinyl ablative tape is an excellent ablative medium as it is easy to apply and remove because of the rubber adhesive, the residue left behind post LSP is very small and insignificant.

The peak residual stress and the depth of penetration was to increase with increasing coverage density. The results obtained from this study correlated well with the finding that were outlined in the literature. The results obtained from this separate study will be stored in the South African LSP database.

7.5 Conclusions

The conclusions for this part of study is as follows:

- Increasing the coverage density for LSP increases the surface roughness of the material.
- The surface roughness increases exponentially with coverage density for material peened using an ablative medium.
- The peak residual stress and the depth of penetration increases with increasing coverage density.
- The surface integrity is maintained for sample peened using an ablative coating with low coverage densities.
- Using an ablative medium decreases the surface roughness of a material when compared to sample peened without an ablative coating using the same laser parameters.

7.6 Recommendations

The following recommendation should be considered for future projects:

- A similar study should be conducted using the different ablative media.
- Different microscopy analysis should be conducted for further study the changes that occur on the surface of the peened samples.
- The effect of LSP on additional factors such as the fatigue life and corrosion should be investigated.
- The residual stress should also be evaluated using different techniques.
- The surface of the sample should undergo three stages of polishing so that the feature imparted by LSP can be identified more clearly.

8 | Concluding Remarks

This chapter will offer final remarks for the work that has been performed and make recommendations for future projects that could be developed from this study. The current research programme was conducted in the context of developing the LSP based research in South Africa by investigating the effect that different ablative media have on the surface integrity, the depth resolved residual stress profile and the characteristics of the aluminium alloy 7075 samples. This grade of alloy was selected because it is locally available and is heavily used in the aeronautical industry and in high stress environments. The benefits provided by the LSP process greatly enhance the properties of this alloy and by using an ablative medium during the LSP process the surface integrity improves while still embedding beneficial compressive stress, thus a wider range of applications become available for the processed alloy due to the improved surface integrity.

The first part of the project was to investigate different ablative media and study their compatibility with the LSP process. 11 different ablative tapes were studied. The aluminium samples were machined to dimensions of 60 mm x 60 mm x 14 mm then were coated with the tapes and processed at the CSIR, using 4 different laser power intensities with a 1 mm spots size and 70% coverage density.

The surface of these peened samples and the effect of the ablative layer with LSP were studied and characterised in detail using optical microscopy, two different types of surface roughness testing and scanning electron microscopy, the microhardness of the samples were also evaluated. The residual stress was evaluated for selected samples using mainly, IHD to evaluate stress at intermediate depths and then L-XRD for near surface stresses.

The methods utilised had results that compared very favourably and provided significant insight into the effect of using an ablative medium with LSP, insight was also provided for the residual stress at different depths and highlighted the effect of using an ablative media.

A number of important lessons were learned for using the different ablative tapes. The clear box seal tape, the duct tape, and the cloth duct fibre tape were shown to be incompatible with LSP as the result obtained were unsatisfactory, because these tape did not completely satisfy the objectives that were set for this study. The two metallic tape that were studied

also provided unsatisfactory result, but the copper tape showed compatibility with LSP but only at low laser power intensities. The other tapes such as the polyester and polymide tape showed acceptable results but did not completely satisfy the objective for this study. The PVC tape showed acceptable result but only at high power intensities and did manage to satisfy some of the objectives.

The three vinyl tape showed the most promising results and showed a high degree of compatibility with LSP, these tape satisfied all the objectives and also showed that the thickness of the ablative material does indeed effect the final peening results and should be considered an important parameter for LSP. This is because the results showed that by increasing the ablative thickness the residual stress can be lowered, but as a consequence the surface integrity can be significantly improved.

The experiments that were performed for this study were done following strict intentional standards, thus the results obtained were accurate. The residual stress result found using IHD were done following the ASTM E837 standard and for the L-XRD method it was found that using a less textured sample will yield higher accurate results as the uncertainties and the fluctuations in the diffraction data will be less. The results obtained for this study using these two methods, showed that the vinyl 471 tape achieved the highest magnitude stress result with a high depth penetration when compared to the results obtained for the sample peened with the different ablative tapes.

The following are the key finding that were obtained the first part of the study:

- The surface roughness of the material increases with increasing power intensity.
- The SEM results showed that LSP modifies the surface of the material by imparting crater like shapes.
- The microhardness of the material increase with increasing power intensity, and the peak hardness occurs near the surface while gradually deceasing with depth through the material.
- The copper tape can be used as an ablative material at low power intensities.
- The vinyl tapes showed the best surface results and showed that the thickness of the ablative medium does have a major influence on LSP.
- The peak residual stress and the depth of penetration increase with increasing power intensity.
- Increasing the ablative thickness decreases the peak residual stress and the penetration depth but increases the surface integrity of the material.
- The IHD and the L-XRD showed results are similar near the surface.

This part of the study only looked at the effect different ablative media have on the surface integrity and on the residual stresses of the material by using 4 different power intensities at a fixed coverage density and laser spot size.

For the second part of the study, a new set of aluminium alloy 7075 with a thickness of 9 mm were used. The sample were machined to the dimensions of 40 mm x 40 mm, these samples were then ground to a surface finish of 18 μm by undergoing 3 separate stages of grinding, this was done so that the surface changes imparted by LSP could be easily identified. The samples were then coated using vinyl 471 tape and peened using a power intensity of 3 GW/cm^2, a spot size of 1 mm with coverage densities ranging from 30% to 90%. The surface of these samples were then analysed using optical microscopy, SEM and surface roughness testing and the residual stresses were evaluated using IHD. The effect of changing the % coverage were studied using an ablative medium.

The results found showed that the surface integrity and roughness changes with increasing coverage density. The surface roughness of the LSPwC samples showed a linear increase with increasing coverage density while the coated sampled showed an exponential increase in the roughness with increasing coverage density. The ablative tape experienced fully vaporisation from a coverage density of 70% and upwards and remained partially intact at 60% coverage and fully intact at 50% to 30% coverage. The peak residual stress and penetration depth was found to increase with increasing coverage density.

This part of the study only looked at the effect of changing coverage density when using an ablative media. The key finding from this study is that the surface roughness of the material increases exponential when an ablative medium is used.

This research project mainly looked at the surface integrity and residual stresses results for the sample coated with different ablative tape and some other material characteristics following the LSP treatment. Additional work that could be done to fully characterise the effect that the ablative layer has with the LSP process are the effects on the fatigue life and corrosion characteristics of different samples. This study is important because they show the benefits that the LSP process as a whole can contribute to the potential industrial partners as this is an essential part for the continued development of LSP process and for academic research.

The finding obtained from the current study will be stored in a LSP database for the 7075 aluminium alloy. This data can be used to optimise the LSP process in order to engineer a specific residual stress profile for future industrial process with the South African LSP group. These results can also be used for the development of simulation software such as Ansys for finite element models, this can be used as an additional tool for the selection of LSP parameters and will aid in using LSP for different applications.

The following are some of the recommendations that have been developed from this study.

- More ablative tapes should be studied as there is a large amount of tapes that are available and easily accessible.
- Additional ablative media such as paint should be studied as there are numerous types of paint that are available and easily accessible. Different amounts of layers of tape can be used to study the effect the thickness of the ablative material has on the surface integrity and on the compressive residual stresses.
- A vinyl ablative tape with a acceptable thickness can be engineered specifically for LSP to achieve an acceptable surface integrity and residual stress profile.
- More residual stress measurement techniques should be used to characterise the residual stresses at different depths while the existing methods should be improved upon so that the results obtained are more accurate.
- The parametric analysis should be performed with more alloys and with a wider variety of LSP parameters to broaden the knowledge base of the group.
- The effect of LSP using the different ablative tape on additional aspects such as corrosion and fatigue life should be investigated. This investigation will show the additional benefits that are provided by the LSP treatment.

9 | Contribution to Community

This chapter will outline the contribution made by the project to the scientific community.

The following is the abstract paper that was submitted for the 8th conference on Laser Peening and Related Phenomena (8thICLPRP) in Shanghai, China, 2020. The abstract paper can be found in Appendix C.

1. M. Mistry et al. *'Effect of Different Tape Overlays on the Surface Integrity and Mechanical Properties of 7075 Aluminum Alloy by Laser Shock Peening'*, 8th International Conference on Laser Peening and Related Phenomena, 2020.

References

[1] K. Ding & L. Ye. *"Laser Shock Peening: Performance and Process Simulation,"* Woodhead Publishing Ltd, 2006. **ISBN**: 13:978-1-84569-109-7.

[2] A. Azhari et al. *"A review on the application of peening processes for surface treatment,"* IOP Conference Series: Materials Science and Engineering, vol. 114, no. 1, 2016, issn: 1757899X. DOI: 10.1088/1757-899X/114/1/012002.

[3] Y. Sano et al. *"Laser Peening without Coating as a Surface Enhancement Technology,"* (2006) Journal of Laser Micro/Nano engineering

[4] A. Telang et al. *"Effect of Different Ablative Overlays on Residual Stresses Introduced in IN718 SPF by Laser Shock Peening,"*,(2018) International Journal of Peening Science and Technology, Vol. 1, pp. 75-86

[5] G Ivetic, V Ristori. *"Experimental campaign on Laser Shock Peening for thin Al specimen hole treatment,"*,(2010), Visiting Research Report.

[6] M. Sticchi et al. *"A Parametric Study of Laser Spot Size and Coverage on the Laser Shock Peening Induced Residual Stress in Thin Aluminium Samples,"*, (2015) The Journal of Engineering, no. 1.1 , pp. 1-9. issn: 2051-3305. DOI: 10.1049/joe.2015.0106.

[7] M.R. Hill et al. *"Laser Peening Technology,"*, (2003) Advanced Materials & Processes, Vol. 161, No. 8, ASM International Publication.

[8] M. Yoda, B. Newton. *"Underwater Laser Peening,"*(2008) Welding and Repair Technology for Power Plants, Eighth International EPRI Conference.

[9] R. Sundar et al. *"Studies on laser peening using different sacrificial coatings, Surface Engineering,"* p.564-568, 2012.

[10] T. Takata1 et al. *"Effect of Confinement Layer on Laser Ablation and Cavitation Bubble during Laser Shock Peening,"*(2016) Materials Transactions, Vol. 57, No. 10 (2016) pp. 1776 to 1783, The Japan Institute of Metals and Materials.

[11] C. Ziwen et al. *"Surface Defects Produced by Laser Shock Peening with Aluminium Foil Ablative Layer,"*(2013) Rare Metal Materials and Engineering, Vol. 42, Beijing Aeronautical Manufacturing Technology Research Institute

[12] R. Menig et al. *"Comparison Of Surface Characteristics And Thermal Residual Stress Relaxation Of Laser Peened And Shot Peened AISI 4140,"*(2002) Germany, University of Karlsruhe.

[13] R. Caslaru et al. *"Fabrication and Characterization of Micro Dents on Aluminum 6061-T6 Surface by Laser Shock Peening,"*(2009) University of Alabama Tuscaloosa, AL, USA.

[14] K. Eisner et al. *"Shock hardening as a novel technique for materials processing,"* Proc. SPIE 2789, High-Power Lasers: Applications and Emerging Applications, (23 September 1996).

[15] TL. Tseng et al. *"A novel approach to predict surface roughness in machining operations using fuzzy set theory,"* (2016) Journal of Computational Design and Engineering 3.

[16] Mitutoyo America Corporation *"QUICK GUIDE TO SURFACE ROUGHNESS MEASUREMENT,"*(2016) Reference guide for laboratory and workshop, 3M , USA.

[17] A. Salimianrizi et al. *"Effect of Laser Shock Peening on surface properties and residual stress of Al6061-T6,"* (2016) Optics and Lasers in Engineering 77, pp. 112âĂŞ117.

[18] A M. Mostafa et al. *"Effect of laser shock peening on the hardness of AL-7075 alloy,"* (2017) Journal of King Saud University - Science.

[19] K. Sowmya Joshi et al *"Optimization of Laser Shock Peening For Titanium,"* (2018) Materials Today: Proceedings 5, Elsevier Ltd.

[20] H. Wang et al *"The study of laser shock peening with side-water spraying and coaxial-water feeding technology,"* (2018) International Journal of Lightweight Materials and Manufacture.

[21] U. Sanchez-Santanaet al *"Wear and friction of 6061-T6 aluminum alloy treated by laser shock processing,"* (2005), Elsevier.

[22] I. Nikitin et al *" Comparison of the fatigue behavior and residual stress stability of laser-shock peened and deep rolled austenitic stainless steel AISI 304 in the temperature range 25 - 600* deg$C$ *,"*(2007) Materials Science and Engineering A465, Elsevier.

[23] J M. Yang et al *" Laser shock peening on fatigue behavior of 2024-T3 Al alloy with fastener holes and stop-holes ,"*(2001) Materials Science and Engineering A298, Elsevier.

[24] A H. Clauer *"Laser Shock Peening for Fatigue Resistance,"* (1996), The Metal Society of AIME, LSP Technologies Incorporated, Dublin.

[25] R A. Everett et al *"The Effects of Shot and Laser Peening on Fatigue Life and Crack Growth in 2024 Aluminum Alloy and 4340 Steel ,"*(2001) NASA Center for Aero-Space Information.

[26] P. Peyre et al *" Laser shock processing of aluminium alloys. Application to high cycle fatigue behaviour,"*(1996) Materials Science and Engineering A210, Elsevier.

[27] J E. Rankin and M R. Hill *" The effects of process variations on residual stress in laser peened 7049 T73 aluminum alloy,"*(2002) Materials Science and Engineering A, Elsevier.

[28] S H. Kosaraju *" Optimization of Laser Shock Peening Process Using Finite Element Modelling,"*(2018) All Theses 3252, Clemson University.

[29] J. L. Ocana et al *" Experimental assessment of the influence of irradiation parameters on surface deformation and residual stresses in laser shock processed metallic alloys,"*(2004) Applied Surface Science, vol. 238, p. 501-505.

[30] Proto *" X-ray Diffraction Residual Stress Measurement, AN INTRODUCTION,"* (2011) Proto Manufacturing Ltd. CANADA

[31] Los Almos National Laboratory - Comparison with other residual stress measurement methods. visited on 02/03/2019. 2019
url: https://www.lanl.gov/residual/compare.shtml

[32] ASTM, *" Standard Test Method for Determining Residual Stresses by the Hole-Drilling Strain-Gage Method,"* ASTM International, 2013.

[33] M. Fitzpatrick et al *" Determination of Residual Stresses by X-ray Diffraction - Issue 2,"*(2005) National Physics Laboratory. .

[34] Zwick Roell *" Indentec Hardness Testing Vickers Hardness Test ,"*Indentec Hardness Testing Machines Limited

[35] R. F. Muraca, J. S. Whittick *"MATERIALS DATA HANDBOOK: Aluminum Alloy 7075,"*(1972) WESTERN APPLIED RESEARCH & DEVELOPMENT INC.

[36] RS components. visited on 20/08/2018. 2018
url: https://za.rs-online.com/web/

[37] Nikon microscopy. visited on 21/07/2019. 2019
url: http://nikonmicroscopy.co.za/

[38] Sunpoc. material testing machine. visited on 28/07/2019. 2019
url: http://www.sunpoc.com/En/ProductView.Asp?ID=120

[39] Jenoptik Waveline. Stationary Roughness and Contour Measurement. visited 14/01/2020. 2020
url: https://www.jenoptik.com/products/metrology/

[40] Zeiss Technology. Field Emission Scanning Electron Microscope. visited on 01/02/2020. 2020
url: https://www.zeiss.com/microscopy/

[41] Struers: Metallographic products, knowledge and services. visited on 21/07/2019. 2019
url: https://www.struers.com/en/

[42] Innovatest. Falcon 500 Vickers Hardness Tester. visited on 27/02/2020. 2020
url: https://www.innovatest-europe.com/products/falcon-500/

[43] Sint Technology. Hole Drilling. visited on 20/01/2020. 2020
url: https://sint-technology.com/

[44] ProtoXRD. iXRD Portable - Residual Stress Measurements. visited on 02/03/2020. 2020
url: http://www.protoxrd.com/ixrd-portable.html

A | Supplementary Experimental Details

This section contains the images and specifications some of the equipment and apparatus during research project. The band-saw that was used to cut the material is shown in Figure A.1 and the specifications are listed below in Table A.1:

Model	30RWH
Serial No	115639
Voltage	380 V (3 phase)
Frequency	50 Hz
Power	1.1 kW

Table A.1: Startrite Band Saw: Machine Specifications.



Figure A.1: Startrite Band Saw.

A.1 Sample Preparation

The samples were prepared and cut at the laboratory workshop at the School of Mechanical, Industrial and Aeronautical Engineering at the University of the Witwatersrand. The procedure is as follows:

A.1.1 Cutting Procedure of Test Pieces

The following is a detailed procedure which was used to prepare the test pieces. This procedure applies to both the big and small test pieces from the two stock plates acquired for the supplier Nk Cutting.

1. Measure and cut the stock plate using a ruler, marker and the Startrite band-saw. Cut both of the stock plate into smaller plates measuring 260 mm x 520 mm for the CNC milling machine.
2. Machine the required 1 mm of the surface using the CNC milling machine to get the 14 mm thickness of the plate for the samples required for phase 1 of the experiment and to get a 9 mm thickness for the samples required for phase 2 of the experiment.
3. Measure the required dimensions for the test samples and mark them accordingly using a ruler and a marker. Allow at least 5 mm on either side before marking.
   (a) 48 specimens were segmented from two smaller plates into the required 60 mm x 60 mm square section.
   (b) 16 specimens were segmented from smaller plates into the required 40 mm x 40 mm square section.
4. Cut the smaller plate to the required dimensions by using the Startrite band-saw by following the guidelines drawn from the step 3.
5. Smooth all edges of the cut pieces by using milling machine then clean the samples.

A.1.1.1 Precautions

The following precautions should be taken when cutting the test pieces:

- When working with the band-saw and the milling machine, one should be fully protected by wearing the correct personal protective equipment (PPE) such as: a lab coat, safety boots, gloves, safety glasses and a hair net.

- The machines do vibrate when cutting or machining the samples therefore make sure that the samples are clamped correctly when machining and the right amount of pressure is used to keep the plate in place and steady when cutting.
- The material does get hot during cutting and machining process and may cause burn injuries, thus it is important to make sure that the appropriate PPE is worn at all times.
- Ensure that there is adequate supervision, or a technician is present when handling the machine.
- Make sure to switch the machine off before extracting of picking up the processed samples and the excess material.

Table A.2 below list the specifications for the Nikon SMZ1500 optical microscope that was used for the research project.

Optical System	Parallel-optics zoom system
Total Magnification	3.75x to 540x (Dependent on eye piece used)
Zoom range	0.75x-11.25x
Zoom ratio	15:1
Illumination system	Fibre-optic bifurcated Fluorescent ring Fibre-optic ring

Table A.2: Nikon Zoom SMZ1500 Stereo-microscope Specifications[37].

Table A.3 below list the specifications for the SRT-6210 roughness testing machine that was used for the research project.

Description	Specification
Display	4 digits, 10 mm LCD backlit(blue)
Parameters	R_a, R_z, R_q, R_t
Range	R_a, R_z:0.005-16.0 μm R_q, R_t:0.020-160.0 μm
Accuracy	10%
Data fluctuation	6%
Cut-off length	0.25/0.8/2.5 $[mm]$
Probe pin radius	5 μm

Table A.3: SRT-6210 Roughness Tester Specifications[38].

	Roughness measurement	
HOMMEL-ETAMIC	**T8000 R60-400**	**T8000 R120-400**
Measuring system	roughness pick-up TKU 300/600	roughness pick-up TKU 300/600
Measuring range	±300 µm or ±600 µm	±300 µm or ±600 µm
Min. resolution	1 nm or 2 nm[1]	1 nm or 2 nm[1]
Measurement force	1.6 mN	1.6 mN
Measuring stroke limitation	–	–
Pick-up/probe		
Length (standard)	34 mm	34 mm
Stylus tip	diamond 5 µm/90° or 2 µm/60°	diamond 5 µm/90° or 2 µm/60°
Mounting	standard: exchangeable optional: magnetic holder with collision protection	standard: exchangeable optional: magnetic holder with collision protection
Traverse unit		
Measuring range (traverse length)	60 mm	120 mm
Resolution	0.1 µm	0.1 µm
Tracing speed	0.1-3 mm/sec.	0.1-3 mm/sec.
Positioning speed	max. 3 mm/sec.	max. 3 mm/sec.
Straightness accuracy	≤0.2 µm/60 mm	≤0.4 µm/120 mm
Measuring column[2]		
Vertical travel	400 mm	400 mm
Auto-null- function	in Z-, programmable	in Z-, programmable
Travel speed	0.1-12 mm/sec.	0.1-12 mm/sec.
Positioning repeatability	≤50 µm	≤50 µm
Measuring station		
Granite plate (L x l x H)[3]	780 x 500 x 100 mm	780 x 500 x 100 mm
Damping	optional[4]	optional[4]
Instrument table (L x l x H)	optional[5]	optional[5]
Working table (L x l x H)	–	–

Table A.4: JENOPTIK waveline HOMMEL-ETAMIC T8000 Roughness Testing Machine[39].

Table A.3 list the specifications for the HOMMEL-ETAMIC T8000 roughness testing machine that was used for the research project.

A.2 Grinding and Polishing

The samples that were prepared for the microhardness had to undergo a grinding and polishing at the materials laboratory at the School of Mechanical, Industrial and Aeronautical Engineering at the University of the Witwatersrand.

The grinding and polishing was performed manually using the Struers LaboPol-21 Grinding and Polishing Table Machine shown in Figure A.2[41]. Additional specification and list of consumables can be found in the Appendix A.

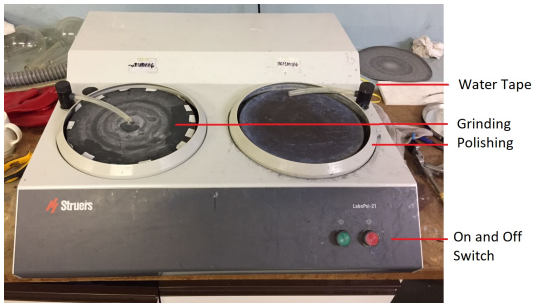


Figure A.2: Grinding and Polishing Table.

A.2.1 Apparatus and Instrumentation

The following is the additional apparatus and instruments that was required in order to grind and polish the samples.

1. LaboPol-21 Grinding and Polishing Table Machine - Used for placement and rotation of the grinding and polishing disks.
2. Struers Grinding Disks - Below are the different grinding disks that were used to achieve different surface finishes:
    - MD-Gekko SiC Foil # 320 - Coarse grinding disk used to achieve a grain size finish of 46 μm.
    - MD-Gekko SiC Foil # 500 - Medium grinding disk used to achieve a grain size finish of 30 μm
    - MD-Gekko SiC Foil # 1000 - Fine grinding disk used to achieve a grain size finish of 18 μm
3. Struers polishing Disks - Below are the different polishing disks that were used to achieve finer surface finishes after the grinding process:
    - MD-Largo - Coarse polishing disk used to achieve a grain size finish of 9 μm
    - MD-Mol - Medium polishing disk used to achieve a grain size finish of 3 μm

- MD-Chem - Fine polishing disk used to achieve a grain size finish of 1 μm

4. Diamond Polishing Suspension liquid - used in conjunction with the polishing disks to achieve the required grain size and surface finish, below are the different suspension liquids that were used:
    - Leco Ultra 9 μm Diamond Suspension liquid used in conjunction with the MD-Largo polishing disk
    - Leco Ultra 3 μm Diamond Suspension liquid used in conjunction with the MD-Mol polishing disk
    - Leco Ultra 1 μm Diamond Suspension liquid used in conjunction with the MD-Chem polishing disk
5. Ethanol and Pipette - The ethanol which was housed in the pipette was used as a cleaning agent between the polishing stages.

A.2.2 Grinding Procedure

Listed below is a detailed procedure used for the grinding process:

1. Place and secure edges of the MD-Gekko SiC Foil # 320 grinding disk.
2. Turn on the water tap on the machine and wet the surface of the disk then turn on the machine.
3. Take the sample and place it on top of the grinding disk, apply a light and even pressure on the sample so that the sample can be ground evenly.
4. After a minute of grinding check to see if the sample has been grounded sufficiently, If the sample does not pass inspection then repeat the previous step.
5. Once the sample has been grounded and has passed inspection then switch off the machine then remove the grinding disk and replace it with the MD-Gekko SiC Foil # 500 grinding disk then repeat step 1-4.
6. Once the sample has been grounded and has passed inspection then switch off the machine then remove the grinding disk and replace it with the MD-Gekko SiC Foil # 1000 grinding disk then repeat step 1-4.
7. Once the desired finish is achieved, turn off the LaboPol-21 machine and the water tap then take off the grinding disk.
8. Clean the test samples with ethanol and dry them using the hair dryer or by using a micro-fibre cloth and then store the sample in a sterile plastic bag.

A.2.2.1 Precautions

- Ensure that the water shield is placed securely on the machine before turning on the machine.
- Do not use excessive force as this may result in a possible injury or damage to the sample and machine.
- Ensure that one does not touch the surface of the rotating grinding disk as it can cause an injury.
- Ensure that the water is closed after completion as this can cause unwanted hazards such as electrical or slipping (wet floor).

A.2.3 Polishing Procedure

After grinding the sample, polishing can take place. The polishing is done so that a near mirror-like surface finish can be obtained. This fine surface finish will help distinguish the finer microscopic details and will help identify clearly, the indentions that are made during micro-hardness testing. The following are the steps taken for the polishing:

1. Place and secure the magnetic MD-Largo polishing disk on the turn table.
2. Turn on the machine and spray a slight amount of the 9 Micron Diamond Suspension in the centre to create a thin film on the surface of the polishing disk.
3. Hold and place the mounted test piece flat down on the rotating polishing disk, apply a light and even pressure on the sample.
4. Once the test piece has been placed down on the polishing disk spray the diamond suspension on the rotating disk every 20-30 second interval for a total duration of 2 minutes.
5. Lift the sample and conduct an inspection. If acceptable then turn off the machine, if not then repeat the previous step.
6. Rinse and clean the test pieces using water and then with ethanol, and blow dry using a hair dryer or by using a micro-fibre cloth and then store the sample in a sterile plastic bag.
7. Repeat steps 1 to 6 using the MD-Mol polishing disk using the 3 Micron Diamond suspension liquid.
8. Once the desired result obtained, repeat steps 1 to 6 by removing the MD-Mol polishing disk and replacing it with the MD-Chem polishing disk using 1 Micron Diamond suspension liquid

A.2.3.1 Precautions

- Ensure that all samples are cleaned thoroughly before proceeding to the next polishing stage, this will prevent cross contamination of suspension liquid and minimise errors.
- Do not touch the polished surface as this may lead to surface scratches
- Ensure that the polishing disks are free from contaminants as this could induce possible scratches during polishing.

Table A.5 lists the apparatus and consumables that were used for sample preparation.

Item	Name and Specifications	Supplier
Grinding Paper	Struers SiC Foil Grain Sizes 46, 30 and 18 μm	IMP Scientific Materialographic
Polishing Disk 1	Struers MD-Largo Grain Sizes 9 μm	IMP Scientific Materialographic
Polishing Suspension 1	Leco Ultra Diamond Suspension 812-509M 9 μm	Leco Africa
Polishing Disk 2	Struers MD-Mol Grain Sizes 3 μm	IMP Scientific Materialographic
Polishing Suspension 2	Leco Ultra Diamond Suspension 812-509M 9 μm	Leco Africa
Polishing Disk 3	Akasel Mag-Napal Grain Sizes 1 μm	IMP Scientific Materialographic
Polishing Suspension 3	Micro Diamant Magnum-Top-Duo 1 μm	Proscience Laboratory Solutions

Table A.5: Grinding and Polishing Apparatus and Consumables.

Table A.6 lists the apparatus and consumables that were used for the IHD process.

Item	Name and Specifications	Supplier
Strain Gauge Rosette	Micro-Measurements CEA-13-062UL-120	Elexsys
2 mm Diameter Drill Bit	SS White Carbide Burs SSW FG-38	Millners Dental Suppliers
De-greaser	Micro-Measurements CSM-2	Elexsys
Conditioner	Micro-Measurements MCA-1	Elexsys
Neutraliser	Micro-Measurements MN5A-1	Elexsys
Glue and Catalyst	Micro-Measurements M-Bond 200	Elexsys
Strain Gauge Installation Tape	Micro-Measurements PCT-2M	Elexsys

Table A.6: IHD Apparatus and Consumables.

Table A.7 list the specifications for the Falcon 500 hardness testing machine that was used for the research project. The model number for the machine is 507 and the serial number is 507D06172241.

FALCON 500	
Hardness scale	(Micro-) Vickers, Knoop & Brinell
Load application	Load cell, force feedback, closed loop system
Load range	1gf up to 62.5Kgf
Motorized turret	6 positions; 2 indentor positions, 4 objectives positions
Optical system	High definition, 5Mpx machine Vision system
Objectives	5x, 10x, 20x, 50x, 100x
Overview camera Cam 2	5Mpx optical ZOOM camera, field of view 50 x 37mm / 200 x 160mm
Electronic system	High performance embedded micro system controller, MS Windows®, 15" full color industrial touch screen, automatic and manual measurement
Test loads (depending model)	1gf, 2gf, 3gf, 4gf, 5gf, 6gf, 7gf, 8gf, 9gf, 10gf, 20gf, 25gf, 50gf, 100gf, 200gf, 300gf, 500gf, 1kgf, 2kgf, 2.5kgf, 3kgf, 4kgf, 5kgf, 6.25kgf, 10kgf, 15.625kgf, 20kgf, 25kgf, 30kgf, 31.25kgf, 50kgf, 62.5kgf
Vickers test range	HV0.001, HV0.002, HV0.003, HV0.004, HV0.005, HV0.006, HV0.007, HV0.008, HV0.009, HV0.010, HV0.015, HV0.020, HV0.025, HV0.050, HV0.1, HV0.2, HV0.3, HV0.5, HV1, HV2, HV2.5, HV3, HV4, HV5, HV10, HV20, HV25, HV30, HV40, HV50
Brinell test range	HB1/1kgf, HB1/1.25kgf, HB1/2.5kgf, HB1/5kgf, HB1/10kgf, HB1/30kgf; HB2.5/6.25kgf, HB2.5/7.8125kgf, HB2.5/15.625kgf, HB2.5/31.25kgf, HB2.5/62.5kgf HB5/25kgf, HB5/62.5kgf
Knoop	HK0.001, HK0.003, HK0.005, HK0.01, HK0.015, HK0.02, HK0.025, HK0.05, HK0.1, HK0.2, HK0.3, HK0.5, HK1, HK2, HK5
KiC Fracture	KC/1, KC/3, KC/5, KC/10, KC/15, KC/20, KC/25, KC/50, KC/100, KC/200, KC/300, KC/500
Indentors	Factory indentors or certified indentors (ISO / ASTM) (optional)
Test cycles	Fully automatic, automatic and manual
Standards	Complies to or exceeds, ISO, ASTM, JIS (Nadcap) standards
Test force tolerance	<0.5% for test force 100gr to 62.5kg, <1% for test force below 100gr
Display resolution	0.1 HV, HK, 0.5 HB
Hardness conversion	Rockwell, Rockwell Superficial, Vickers, Brinell, Knoop, Leeb & Tensile
Statistics	Total test, max, min, average, range, standard deviation, all in real time after each test
Data storage capacity	Dual SSD 80Gb, RAID system
Connectivity	5 USB ports, RJ45 Ethernet LAN, W-LAN, RS-232, Blue Tooth, 5 Axis CNC & motorized X-Y stage connector
Dwell time setting	Default 10 seconds, user defined 1 to 99 seconds (1 sec increments)
Printer	A4, A3 full colour laser printer (optional)
Manual stage dimensions	Stage 100mm x 100mm, Travel 25mm x 25mm, Reading 0.01mm
Motorized stage dimensions	See pag. 14
Operating temperature	10°C to 35°C, non-condensing
Humidity	10% to 90% non-condensing
Machine dimensions	525mm x 323mm x 773mm
Machine weight	75kg
Power consumption	100W
Power supply	100VAC to 240VAC, 50/60Hz, single phase

Table A.7: Falcon 500 Series Hardness Testing Machine[42].

B | Results and Data

The following are the microhardness results that were obtained for the sample peened using the different ablative tapes.

The results shown in Figure B.1 to Figure B.10 all confer to the results found in literature. That is the hardness decreases with increasing depth and the hardness increases with increasing power intensities. As explained previously, there is indeed a certain fluctuations in the observable results but the result do falling within the allowable range.

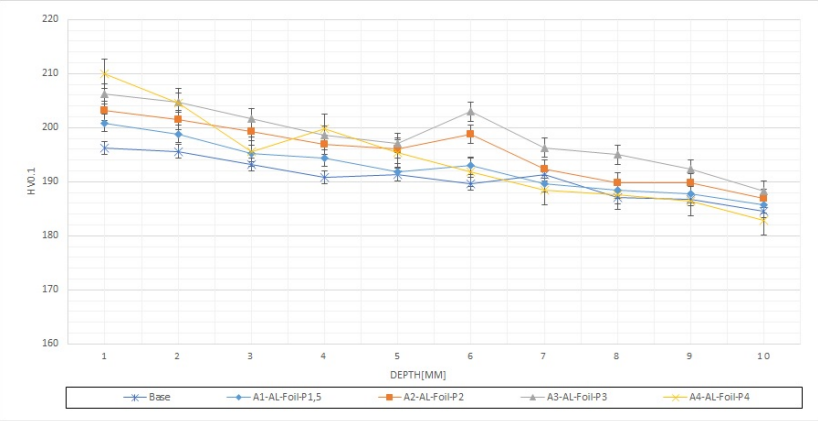


Figure B.1: Microhardness Results for Aluminium Tape Samples.

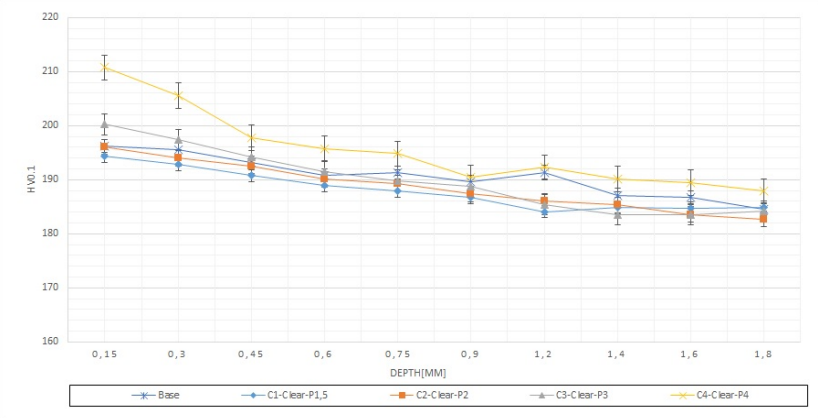


Figure B.2: Microhardness Results for Clear Box Sealing Tape Samples.

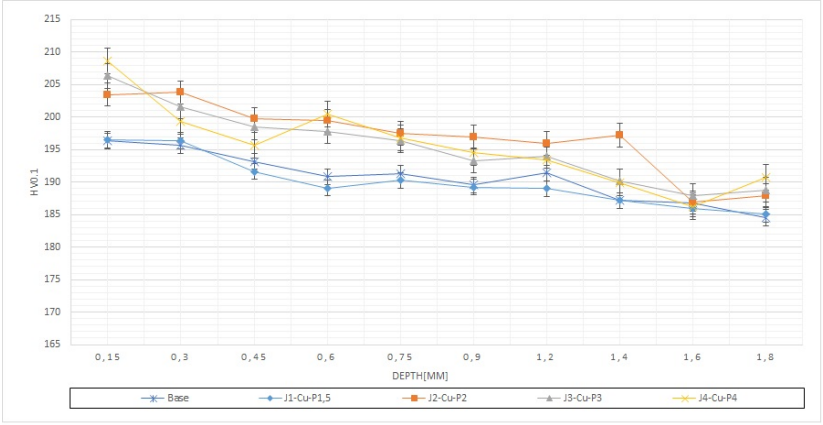


Figure B.3: Microhardness Results for Copper Tape Samples.

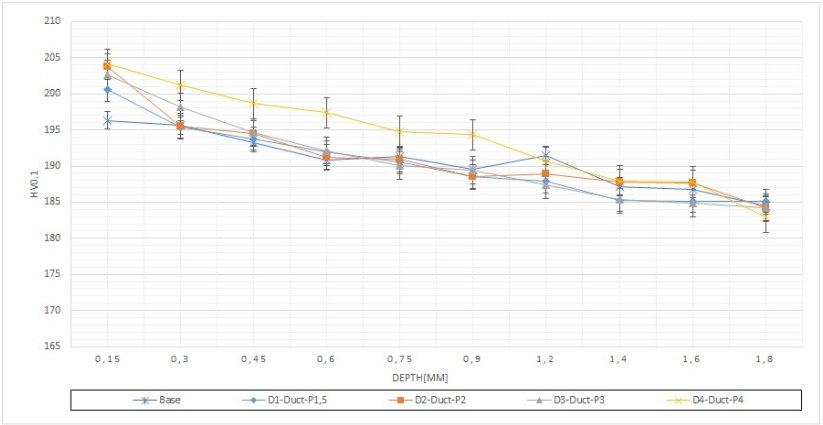


Figure B.4: Microhardness Results for Duct Tape Samples.

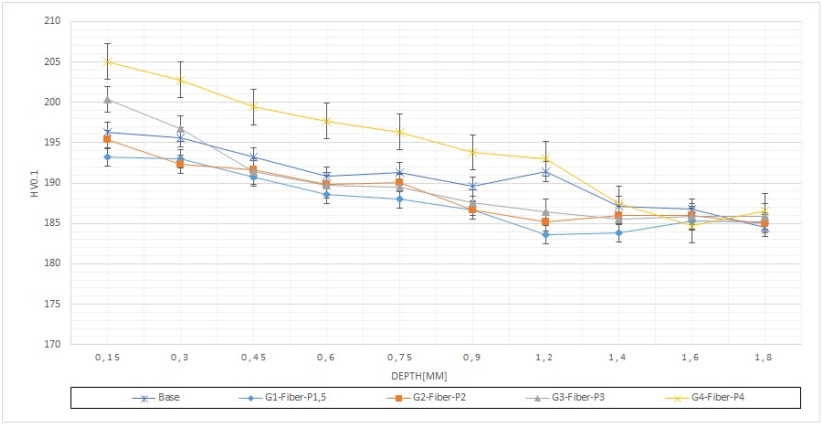


Figure B.5: Microhardness Results for Duct Cloth Fibre Tape Samples.

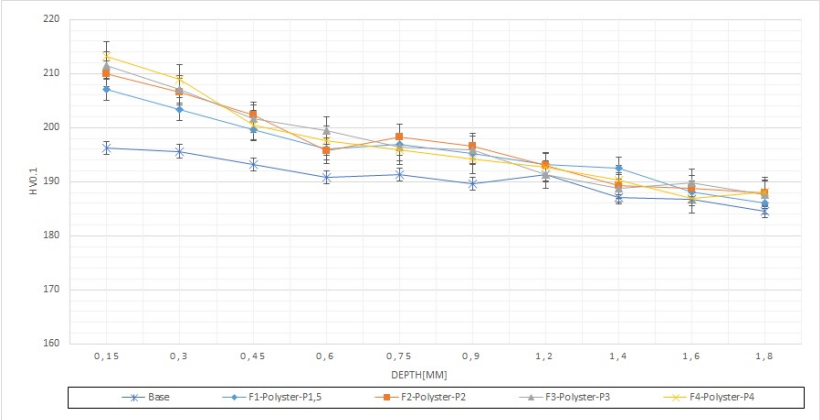


Figure B.6: Microhardness Results for Polyester Tape Samples.

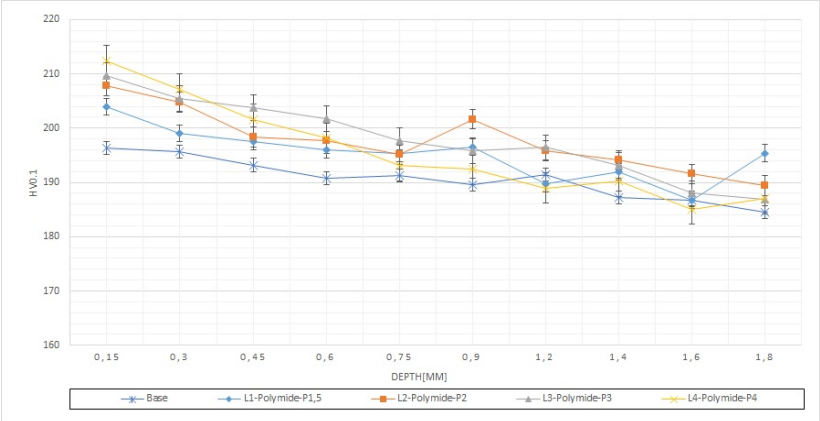


Figure B.7: Microhardness Results for Polymide Tape Samples.

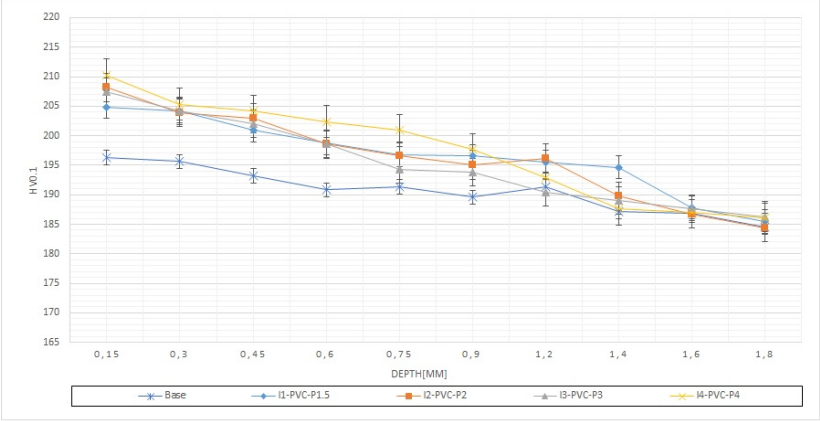


Figure B.8: Microhardness Results for PVC Tape Samples.

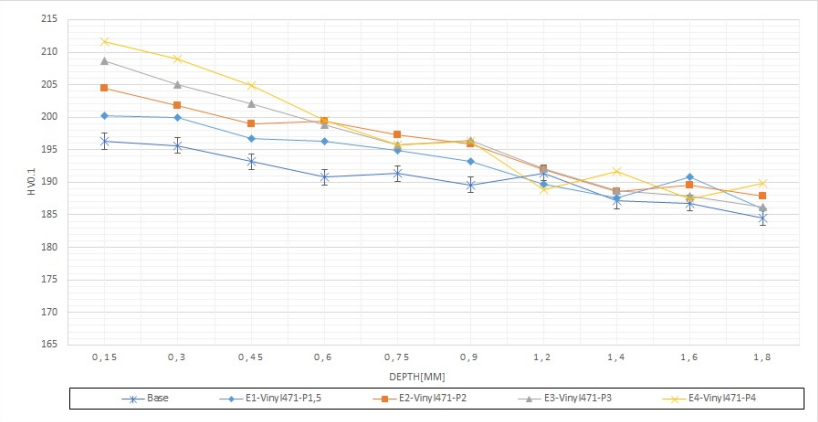


Figure B.9: Microhardness Results for Vinyl 471 Tape Samples.

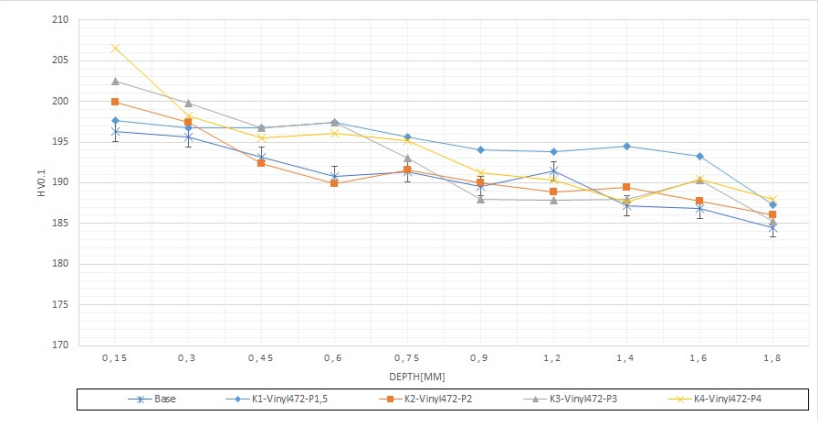


Figure B.10: Microhardness Results for Vinyl 472 Tape Samples.

C | Material Details

The following are the details for the material and ablative tape used in the experiments. These additional details were not provided in the main text.

INSPECTION CERTIFICATE № 12.39760

EN 10204 - 3.1

Certified by Russian Registe

Consigner: KAMENSK URALSKY METALLURGICAL WORKS JOINT STOCK COMPANY
5, Zavodskaya Str., Kamensk Uralsky, Sverdlovsk Region, 623405, Russia Tel: (3439) 39 52 22 Fax: (3439) 39 50 68

Consignee: NK Cutting cc	Quantity: 10
	Net Weight, kg.: 901
Contract number: V2779-S PO116105	Specification №: V2779
Article number: 3114	Lot №: 5
	Package №: 732168

Description of Goods: Plate

Grade of Product	Dimensions, inch/mm
-	10.000X1250.0X2500.0

Requirements on the Products:

Material conforms to quality of alloy: 7075 T651

Product conforms to all requirements of:
EN573-3,EN485-1,EN485-2,EN485-3

Mechanical Properties

The Condition of Tested Standards	Lot Number	Cast Number	Number of Tests	Tensile Strength MPa		Yield Strength (0,2% offset) MPa		Elongation, %		Hardness, HB
				min	max	min	max	min	max	
Required				540.0	-	460.0	-	8.0	-	160.00
-	717187	20-5586	1	586.0	586.0	529.0	529.0	14.0	14.0	-

Chemical Composition, %

Element	Silicon Si	Iron Fe	Copper Cu	Manganese Mn	Magnesium Mg	Chromium Cr	Nickel Ni	Zinc Zn	Titanium Ti	Zirconium Zr
Required	0.4	0.5	1.2-2.0	0.3	2.1-2.9	0.18-0.28	-	5.1-6.1	0.2	-
Contents	0.05	0.15-0.16	1.3-1.4	0.03	2.5-2.6	0.18-0.19	-	5.8-5.9	0.08	-

Element	Ti+Zr	Na	Tin Sn	Bismuth Bi	Plumbum Pb	Mn+Cr	Ca	Other Elements Each	Other Elements Total	Al
Required	-	-	-	-	-	-	-	0.05	0.15	remainder
Contents	-	-	-	-	-	-	-	0.05	0.15	remainder

Other Tests

Method	Macro-structure	Micro-structure	UT	Electro-conductivity	SCF	Contents H2 of metals cm3/100gr	
Result	-	-	-	-	-	-	-

On behalf: OAO KUMZ

Date: 30.12.12

Inspector: G.A.Ostanina

Inspection Department engineer: N.V. Alekhina

KAMENSK URALSKY METALLURGICAL WORKS J.S.C. QUALITY DEPARTMENT KUMZ

TEST CERTIFICATE

EN10204-3.1

Certificate No.: P-171218-7726

Customer				Standard	EN485-2008		
Adress							
Lot No.	7172309	Alloy/Temper	7075/T651	Order No.	120395921	Item No.	1000441
Product	Aluminium Alloy Plate	Specification mm	10*1520*3020	Quantity	26	Weight/kg	3454

Chemical Composition (%)														
Element	Si	Fe	Cu	Mn	Mg	Cr	Zn	Ti	Zr	Ni	-	Others		Al
												Each	Total	
Standard Min.	0.00	0.00	1.2	0.00	2.1	0.18	5.1	0.00	-	-	-	0.05	0.15	Remainder
Standard Max.	0.40	0.50	2.0	0.30	2.9	0.28	6.1	0.20	-	-	-			
Actual	0.10	0.23	1.55	0.07	2.69	0.22	5.76	0.03	-	-	-	≤0.05	≤0.15	

Item	Mechanical Properties					Corrosion		Nondestructive Testing	
	Tensile Strength Mpa	Yeild Strength Mpa	Elongation A_{50}/(%)	Bending	Hardeness (HB/HV/HRC)	Intrec.	Exfcor.	Ultrasonic	Conductance
Standard/Min.	540	460	8	90° /180°	-	-	-	-	-
Standard/Max.	-	-	-		-	-	-	-	-
Actual	581-592	544-554	12.5-13.0	-	-	-	-	-	-

Metallography		Cladding rate		Grain Size		Hydrogen Content (ml/100gAl)	
Macro.	Micro.	Standard	Actual	Standard	Actual	Standard	Actual
-	-	-	-	-	-	-	-
Note: -							

Quality have Certified as ISO9001.IRIS.AS9100C.GJB9001B.TS16949. Environment have Certified as ISO14001.Professional Health & Safety Management System have Certified as OHSAS18001.Level 3 confidential.The Classification Society have Certified as per DNVGL.ABS.BV.CCS.The pressure vessel material have Certified as TÜV-PED4.3&AD2000W0.

We hereby certify that the material described above has been tested and complies with the terms of the order contract.
The inspection results indicated in the chemical composition have been obtained from cast analysis.

Issued by Quality Inspector: QA55 Reviewed by: QA53

NO.: 20184028

20670

CERTIFIED TEST REPORT

PRIME ALUMINIUM ALLOY PLATE

(EN 10204:2004 3.1)

SERIAL NO.: 20160517G6404914254

DATE: May 17th,2016

PRODUCT	ALLOY & TEMPER	LOT NO.	DIMENSION(MM)		
PLATE	7075T651	G64049	15×1520×3020		
CONTRACT NO.	PALLETS NO.		NET WEIGHT (KG/PIECES)		
120310520	14254		LOT NO.	G64049	1206/6
TECHNICAL STANDARD			SURFACE		
EN 485/515/573			UNIFORM BRUSHED FINISH		

Chemical Composition(WT%)

ELEMENT		Si	Fe	Cu	Mn	Mg	Cr	NI
SPECIFIED VALUE		≤0.4	≤0.5	1.2~2.0	≤0.30	2.1~2.9	0.18~0.28	
LOT NO.	G64049	0.11	0.31	1.67	0.11	2.63	0.21	
ELEMENT		Zn	Ti	Zr		Each	Total	Al
SPECIFIED VALUE		5.1~6.1	≤0.20			≤0.05	≤0.15	Rest
LOT NO.	G64049	5.66	0.03			≤0.05	≤0.15	Rest

Physical Test

LOT NO.		UTS(MPa)	YTS(MPa)	ELONG(%)	HARDNESS	CONDUCT	BEND
STANDARD VALUE	Min Max	540	470	6			
G64049		580~586	526~532	10.0~11.5			

hereby certifies that each lot has been sampled,tested and inspected in accordance with applicable requirements described herein.MELTED AND MANUFACTURED Material meets requirements of REACH Rev. 6-16-14 and RoHS 2 Rev. 2011/65/EU.

Scotch®

Vinyl Electrical Tape Super 88

Data Sheet **July 2011**

Description	Scotch® Vinyl Electrical Tape Super 88 is a premium grade, 8.5-mil thick, all-weather vinyl insulating tape. It is designed to perform continuously in ambient temperatures up to 105°C (220°F). The tape is conformable for cold weather applications down to -18°C (0°F). It has excellent resistance to abrasion, moisture, alkalies, acids, corrosion and varying weather conditions. The combination of elastic backing and aggressive adhesive provides moisture-tight electrical and mechanical protection with minimum bulk. Scotch® Tape Super 88 is an Underwriters' Laboratories Listed and Canadian Standards Association Certified "Insulating Tape."
Agency Approvals & Self Certifications	UL Listed; UL 510 Standard "Insulating Tape" (product category OANZ), File E129200 CSA Certification; Standard C22.2 No. 197-M1983 "PVC Insulating Tape," File LR48769 RoHS 2002/95/EC RoHS Compliant 2002/95/EC" means that the product or part ("Product") does not contain any of the substances in excess of the maximum concentration values in EU Directive 2002/95/EC, as amended by Commission Decision 2005/618/EC, unless the substance is in an application that is exempt under RoHS. This information represents 3M's knowledge and belief, which may be based in whole or in part on information provided by third party suppliers to 3M.
Tape Features	• Polyvinyl chloride (PVC) backing • Pressure-sensitive rubber-based adhesive • Compatible with solid dielectric cable insulations • Compatible with rubber and synthetic splicing compounds, as well as epoxy and polyurethane resins • Inhibits corrosion of electrical conductors • For indoor or outdoor applications
Applications	• Primary electrical insulation for all wire and cable splices rated up to 600 volts and 105°C (220°F) • Primary electrical insulation for 600-volt bus applications, and protective jacketing for high- and low-voltage bus • Protective jacketing for high-voltage cable splices and repairs • Harnessing of wires and cables

3M

Scotch® Vinyl Electrical Tape Super 88

Typical Properties

Not for specifications. Values are typical, not to be considered minimum or maximum. Properties measured at room temperature 73°F (23°C) unless otherwise stated.

Physical Property (Test Method ASTM D-1000*)	**Typical Value** US units (metric)
Color	Black
Thickness*	8.5 mils (0,22 mm)
Adhesion to Steel*	
22ºC (72ºF)	28 oz./in. (3,0 N/10 mm)
-18ºC (0ºF)	60 oz./in. (6,5 N/10 mm)
Adhesion to Backing*	
22ºC (72ºF)	28 oz./in. (3,0 N/10 mm)
-18ºC (0ºF)	60 oz./in. (6,5 N/10 mm)
Breaking Strength*	
22ºC (72ºF)	20 lbs./in. (35 N/10 mm)
Ultimate Elongation*	
22ºC (72ºF)	250%
-18ºC (0ºF)	100%
Flagging*	< 0.1 in. (2,5 mm)
Telescoping	
24 hrs. W 50ºC (120ºF)	< 0.1 in. (2,5 mm)
Flammability (Maximum)	
UL 510	Pass

Electrical Property (Test Method ASTM D-1000*)	**Typical Value** US units (metric)
Dielectric Breakdown*	
Standard condition	10,000 volts
High Humidity Condition	90% of Standard
Insulation Resistance*	
(High Humidity Method)	> 1x 10^6 Megohms

Product Specifications

Scotch® Vinyl Electrical Tape Super 88 is based on polyvinyl chloride (PVC) and/or its copolymers, and has a rubber-based, pressure-sensitive adhesive. The tape shall be 8.5 mils thick, and be UL Listed and marked per UL Standard 510 as “Flame-Retardant and Cold Resistant.” The tape must be applied at temperatures ranging from 0°F through 100°F (-18°C through 38°C), without loss of physical properties. It shall be compatible with synthetic cable insulations, jackets and splicing compounds. Scotch® Tape Super 88 will remain stable and will not telescope more than 0.1 inches when maintained at temperatures below 120°F (50°C).

Scotch® Vinyl Electrical Tape Super 88

Engineering/ Architectural Specifications	Primary electrical insulation (branch wiring in wet or dry locations): All splices 600-volt wire rated 105°C (220°F) and below shall be insulated with a minimum of two half-lapped layers of Scotch® Vinyl Electrical Tape Super 88. All connectors having irregular surfaces shall be padded with 3M™ Scotchfil™ Electrical Insulation Putty or Scotch® Linerless Rubber Splicing Tape 130C prior to insulating with this tape. **Mechanical Protection (outer jacketing)** All rubber and thermoplastic insulating high voltage power cable tape splices and repairs shall be over wrapped with at least two half-lapped layers of Scotch® Tape Super 88.
Installation Techniques	Scotch® Tape Super 88 shall be applied in half-lapped layers with sufficient tension to produce a uniform wind (for most applications this tension will reduce the tape's width to approximately 5/8 of its original width). On pigtail splices, the tape shall be wrapped beyond the end of the wires and then folded back, leaving a protective cushion to resist cut-through. Wrap tape up-hill, taping from a smaller diameter surface to a larger diameter surface. Apply the tape with no tension on the last wrap to prevent flagging.
Availability	Please contact your local distributor; available from 3M.com/electrical [Where to Buy] or call 1.800.245.3573.
Shelf Life & Storage	This product has a 5-year shelf life from date of manufacture when stored in a humidity controlled storage (10°C/50ºF to 27°C/80ºF and <75% relative humidity).

Important Notice	All statements, technical information, and recommendations related to 3M's products are based on information believed to be reliable, but the accuracy or completeness is not guaranteed. Before using this product, you must evaluate it and determine if it is suitable for your intended application. You assume all risks and liability associated with such use. Any statements related to the product, which are not contained in 3M's current publications, or any contrary statements contained on your purchase order, shall have no force or effect unless expressly agreed upon, in writing, by an authorized officer of 3M.
Warranty; Limited Remedy; Limited Liability	This product will be free from defects in material and manufacture at the time of purchase. 3M MAKES NO OTHER WARRANTIES INCLUDING, BUT NOT LIMITED TO, ANY IMPLIED WARRANTY OF MERCHANTABILITY OR FITNESS FOR A PARTICULAR PURPOSE. If this product is defective within the warranty period stated above, your exclusive remedy shall be, at 3M's option, to replace or repair the 3M product or refund the purchase price of the 3M product. Except where prohibited by law, 3M will not be liable for any indirect, special, incidental or consequential loss or damage arising from this 3M product, regardless of the legal theory asserted.

3M, Scotch and Scotchfil are trademarks of 3M Company.

3M

Electrical Markets Division
6801 River Place Blvd.
Austin, TX 78726-9000
800.245.3573
FAX: 800.245.0329
www.3M.com/electrical

Please recycle
© 3M 2011 All rights reserved

78-8124-4857-5 G

Value Duct Tape

1900

Technical Data **June, 2011**

Product Description

3M™ Value Duct Tape 1900 is a conformable cloth duct tape made with polyethylene film over cloth scrim and rubber adhesive. A good choice for non-critical applications.

Product Construction

Backing	Adhesive	Color	Standard Roll Length	Standard Width
Polyethylene over cloth scrim	Synthetic rubber	Silver	60 yds. (54.9 m)	1.88 in. (48 mm) 2.83 in. (72 mm)

Typical Physical Properties

Note: The following technical information and data should be considered representative or typical only and should not be used for specification purposes.

		ASTM Test Method
Adhesion to Steel:	62 oz./in. width (67.9 N/100 mm)	D-3330
Tensile Strength:	19 lbs./in. width (332.7 N/100 mm)	D-3759
Elongation at Break:	15%	D-3759
Thickness:	5.8 mils (0.147 mm)	D-3652
Temperature Use Range:	Up to 200°F (93°C)	

Features

- Polyethylene backing provides moisture resistance to tape applications.
- Rubber adhesive sticks well to many surfaces.
- Easy tear.
- Low profile.
- Individual roll wrap for easy identification.

Application Ideas

- Tool box tape for non-critical uses.
- Light duty sealing and holding.
- Marking.

3M™ Value Duct Tape

1900

Storage

Store under normal conditions of 60° to 80°F (16° to 27°C) and 40 to 60% R.H. in the original carton.

Shelf Life

To obtain best performance, use this product within 12 months from date of manufacture.

Technical Information

The technical information, recommendations and other statements contained in this document are based upon tests or experience that 3M believes are reliable, but the accuracy or completeness of such information is not guaranteed.

Product Use

Many factors beyond 3M's control and uniquely within user's knowledge and control can affect the use and performance of a 3M product in a particular application. Given the variety of factors that can affect the use and performance of a 3M product, user is solely responsible for evaluating the 3M product and determining whether it is fit for a particular purpose and suitable for user's method of application.

Warranty, Limited Remedy, and Disclaimer

Unless an additional warranty is specifically stated on the applicable 3M product packaging or product literature, 3M warrants that each 3M product meets the applicable 3M product specification at the time 3M ships the product. 3M MAKES NO OTHER WARRANTIES OR CONDITIONS, EXPRESS OR IMPLIED, INCLUDING, BUT NOT LIMITED TO, ANY IMPLIED WARRANTY OR CONDITION OF MERCHANTABILITY OR FITNESS FOR A PARTICULAR PURPOSE OR ANY IMPLIED WARRANTY OR CONDITION ARISING OUT OF A COURSE OF DEALING, CUSTOM OR USAGE OF TRADE. If the 3M product does not conform to this warranty, then the sole and exclusive remedy is, at 3M's option, replacement of the 3M product or refund of the purchase price.

Limitation of Liability

Except where prohibited by law, 3M will not be liable for any loss or damage arising from the 3M product, whether direct, indirect, special, incidental or consequential, regardless of the legal theory asserted, including warranty, contract, negligence or strict liability.

ISO 9001:2008

This Industrial Adhesives and Tapes Division product was manufactured under a 3M quality system registered to ISO 9001:2008 standards.

3M

Industrial Adhesives and Tapes Division
3M Center, Building 225-3S-06
St. Paul, MN 55144-1000
800-362-3550 • 877-369-2923 (Fax)
www.3M.com/industrial

Recycled Paper
40% pre-consumer
10% post-consumer

3M is a trademark of 3M Company.
Printed in U.S.A.
©3M 2011 70071101771 (6/11)

Scotch®
Box Sealing Tape
313

Technical Data **January, 2011**

Product Description

Scotch® Box Sealing Tape 313 is designed for easy handling and smooth dispensing. The high coating weight of acrylic adhesive makes it ideal for wide temperature swings and applications where it is applied. It adheres well to recycled liner paper and will maintain its performance and appearance better than most products when exposed to UV light.

Construction

Backing	Adhesive	Colors
Biaxially oriented polypropylene film	Pressure sensitive acrylic. Requires no moisture, heat or solvent for activation.	Clear and tan

Typical Physical Properties

Note: The following technical information and data should be considered representative or typical only, and should not be used for specification purposes.

		ASTM Test Method
Adhesion to Steel:	32 oz./in. width (35 N/100 mm width)	D-3330
Tensile Strength:		
Machine Direction:	35 lbs./in. width (613 N/100 mm width)	D-3759
Cross Direction:	56 lbs./in. width (981 N/100 mm width)	D-3759
Elongation at Break:	125%	D-3759
Thickness - Backing:	1.6 mil (0.041 mm) nominal	D-3652
Total:	2.55 mil (0.065 mm) nominal	D-3652

Features

- Adheres instantly to a variety of surfaces.
- Conformable backing.
- Edge tear and split resistant.
- Good aging in sunlight or fluorescent lighting.
- Reliable closures.
- Long life in use.

Available Sizes

Standard Widths:	48 mm, 72 mm
Core Size (ID):	3 in.
Lengths:	50 m, 100 m, 914 m

Scotch® Box Sealing Tape
313

Storage Conditions

Store in a clean, dry place. Temperature of 40-80°F (4-26°C) and 40 to 50% relative humidity are recommended.

Shelf Life

To obtain best performance, use this product within 18 months from date of manufacture.

Technical Information

The technical information, recommendations and other statements contained in this document are based upon tests or experience that 3M believes are reliable, but the accuracy or completeness of such information is not guaranteed.

Product Use

Many factors beyond 3M's control and uniquely within user's knowledge and control can affect the use and performance of a 3M product in a particular application. Given the variety of factors that can affect the use and performance of a 3M product, user is solely responsible for evaluating the 3M product and determining whether it is fit for a particular purpose and suitable for user's method of application.

Warranty, Limited Remedy, and Disclaimer

Unless an additional warranty is specifically stated on the applicable 3M product packaging or product literature, 3M warrants that each 3M product meets the applicable 3M product specification at the time 3M ships the product. 3M MAKES NO OTHER WARRANTIES OR CONDITIONS, EXPRESS OR IMPLIED, INCLUDING, BUT NOT LIMITED TO, ANY IMPLIED WARRANTY OR CONDITION OF MERCHANTABILITY OR FITNESS FOR A PARTICULAR PURPOSE OR ANY IMPLIED WARRANTY OR CONDITION ARISING OUT OF A COURSE OF DEALING, CUSTOM OR USAGE OF TRADE. If the 3M product does not conform to this warranty, then the sole and exclusive remedy is, at 3M's option, replacement of the 3M product or refund of the purchase price.

Limitation of Liability

Except where prohibited by law, 3M will not be liable for any loss or damage arising from the 3M product, whether direct, indirect, special, incidental or consequential, regardless of the legal theory asserted, including warranty, contract, negligence or strict liability.

ISO 9001:2008

This Industrial Adhesives and Tapes Division product was manufactured under a 3M quality system registered to ISO 9001:2008 standards.

3M

Industrial Adhesives and Tapes Division
3M Center, Building 225-3S-06
St. Paul, MN 55144-1000
800-362-3550 • 877-369-2923 (Fax)
www.3M.com/industrial

Recycled Paper
40% pre-consumer
10% post-consumer

Scotch is a registered trademark of 3M.
Printed in U.S.A.
©3M 2011 70071002953 (1/11)

3M Vinyl Tape 472

Technical Data **February, 2011**

Product Description

3M™ Vinyl Tape 472 is comprised of a heavy duty black vinyl backing with a black pigmented rubber adhesive. The thick vinyl backing makes it ideal for applications requiring both abrasion resistance and the inherent conformability of vinyl. The rubber adhesive has good instant adhesion and sticks well to a variety of surfaces.

Product Construction

Backing	Adhesive	Color	Standard Roll Length
Vinyl	Pigmented rubber	Black	36 yds. (33 m)

Typical Physical Properties

Note: The following technical information and data should be considered representative or typical only and should not be used for specification purposes.

		ASTM Test Method
Adhesion to Steel:	23 oz./in. width (25 N/100 mm)	D-3330
Tensile Strength at Break:	32 lbs./in. width (560 N/100 mm)	D-3759
Elongation at Break:	270%	D-3759
Backing Thickness:	9.0 mils (0.23 mm)	D-3652
Total Tape Thickness:	10.4 mils (0.26 mm)	D-3652
Temperature Use Range:	Up to 225°F (107°C)	

Features

- Best results are attained when applied to clean, dry surface at temperatures between 60° to 80°F (16° to 27°C).
- Thick backing is ideal where heavy abrasion is anticipated.
- Temperature resistance to 225°F (107°C).
- Pigmented adhesive will stain some surfaces. Testing by the user is recommended to determine suitability in the proposed application.
- Resists most common solvents, care should be taken to avoid ketones, chlorinated hydrocarbons, and esters, found in lacquer thinners, degreasers, paint strippers, etc. which may cause the backing to swell or curl.
- Can be used in outdoor applications with clean removal from many surfaces up to 6 months.
- Stays on outdoors for up to a year.

3M™ Vinyl Tape
472

Application Ideas

- Heavy duty protection and abrasion resistance.
- Splicing and patching.
- Outdoor sealing, protecting, and marking.
- Dissimilar metal separation.
- Sealing barrier films and containers.
- Sand blast and bead blast overspray protection.

Storage

Store under normal conditions of 60° to 80°F (16° to 27°C) and 40 to 60% R.H. in the original carton.

Shelf Life

To obtain best performance, use this product within 18 months from date of manufacture.

Technical Information

The technical information, recommendations and other statements contained in this document are based upon tests or experience that 3M believes are reliable, but the accuracy or completeness of such information is not guaranteed.

Product Use

Many factors beyond 3M's control and uniquely within user's knowledge and control can affect the use and performance of a 3M product in a particular application. Given the variety of factors that can affect the use and performance of a 3M product, user is solely responsible for evaluating the 3M product and determining whether it is fit for a particular purpose and suitable for user's method of application.

Warranty, Limited Remedy, and Disclaimer

Unless an additional warranty is specifically stated on the applicable 3M product packaging or product literature, 3M warrants that each 3M product meets the applicable 3M product specification at the time 3M ships the product. 3M MAKES NO OTHER WARRANTIES OR CONDITIONS, EXPRESS OR IMPLIED, INCLUDING, BUT NOT LIMITED TO, ANY IMPLIED WARRANTY OR CONDITION OF MERCHANTABILITY OR FITNESS FOR A PARTICULAR PURPOSE OR ANY IMPLIED WARRANTY OR CONDITION ARISING OUT OF A COURSE OF DEALING, CUSTOM OR USAGE OF TRADE. If the 3M product does not conform to this warranty, then the sole and exclusive remedy is, at 3M's option, replacement of the 3M product or refund of the purchase price.

Limitation of Liability

Except where prohibited by law, 3M will not be liable for any loss or damage arising from the 3M product, whether direct, indirect, special, incidental or consequential, regardless of the legal theory asserted, including warranty, contract, negligence or strict liability.

ISO 9001:2008

This Industrial Adhesives and Tapes Division product was manufactured under a 3M quality system registered to ISO 9001:2008 standards.

3M

Industrial Adhesives and Tapes Division
3M Center, Building 225-3S-06
St. Paul, MN 55144-1000
800-362-3550 • 877-369-2923 (Fax)
www.3M.com/industrial

Recycled Paper
40% pre-consumer
10% post-consumer

3M is a trademark of 3M Company.
Printed in U.S.A.
©3M 2011 70070950178 (2/11)

TECHNICAL DATA

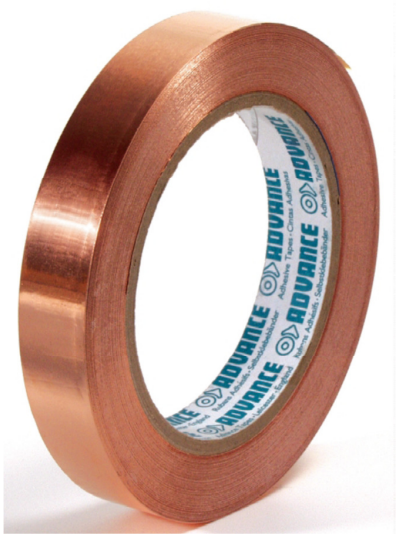
Version 3

AT525 35 Micron Copper Foil Shielding Tape

General Description
35 micron copper foil coated with a non-conductive acrylic adhesive supplied on a removable silicone release liner.

- Non-conductive acrylic adhesive
- Good high and low temperature resistance
- Can be easily soldered
- Easy unwind

Specification*
Tested in accordance with ASTM D-1000 latest issue,
BS EN 60454 - Part 2 test methods (formerly VDE 0340, BS 3924).
Tested and meets Flame Retardency requirements of UL 510
(UL guide OANZ 2, File number E 86214 (M)



Technical Details

Typical values	BS value	ASTM value
Foil thickness	0.035mm	1.4 mil
Adhesive thickness	0.030mm	1.2 mil
Total thickness	0.065mm	2.6 mil
Adhesion to steel	4.5 N/cm	41 oz/in.
Tensile strength	40 N/cm	23 lbs/inch
Temperature resistance	-20℃ to +155℃	Up to +311℉
RoHS compliant	Yes	
Storage Temperature	+12℃ to +25℃	

*Standard charge for certificate: £25.00.

NOTE
Except where indicated otherwise, the figures stated are average values and should not be regarded as MAXIMUM or MINIMUM values for specification purposes. The Company reserves the right to improve products and any change in specification will result in a re-issue of the relevant 'Technical Data Sheet'. Customers should satisfy themselves that the tape is suitable for their requirements whether after such modifications or otherwise. Please check that you have the latest issue of the 'Technical Data Sheet'. All slitting and length tolerances are to British Standards. Before use the customer is advised to consult the Health & Safety Data Sheet produced by the company for this product, which is available on request.

STORAGE
Tapes stored below the minimum recommended temperature will require warming up to that level before use. Up to 24 hours may be required for this to take place.

AFERA
Association des Fabricants Européens de Rubans Auto-Adhésifs.

Adding more to adhesive tape

Registered in England No. 929843
Vat No. 115-6143-00

Advance Tapes International Limited
Westmoreland Avenue
Thurmaston
Leicester LE4 8PH
England

Tel. +44 (0)116 251 0191
Fax. +44 (0)116 265 2046
contact@advancetapes.com

www.advancetapes.com

bsi. ISO 9001 Quality Management
Q05026

Scotch® Duct Cloth Tape 2903

Product Data Sheet

June 2016
Supersedes: New

Product Description

3M™ Scotch® Duct Cloth Tape 2903 is a general purpose conformable cloth duct tape made with polyethylene film over cloth scrim and a synthetic rubber adhesive. A good choice for general maintenance, bundling, wrapping, attaching, sealing, protecting, and colour coding.

Key Features

- Aggressive synthetic rubber adhesive provides instant adhesion to a wide variety of surfaces
- Cloth scrim tears straight in both directions.
- Cloth scrim has high tensile strength, ideal for bundling materials
- Conformable and can be applied to irregular surfaces

Physical Properties

Thickness AFERA 5006) Tape Liner	 0,15 mm None
Adhesive Type	Synthetic rubber and resin
Tape Colour	Black, White and Silver

Performance Characteristics

Adhesion to Stainless Steel (AFERA 5001 TM A)	8 N / cm
Tensile Strength (AFERA 5004 MD)	100 N / 25cm
Elongation at Break (AFERA 5004 MD)	30%

Storage & Shelf Life	Store at 16 °C – 25 °C and 40-65 % relative humidity in its original box. The product can be stored up to 12 months after production.
For Additional Information	To request additional product information or to arrange for sales assistance, call…… Address correspondence to: 3M
Important Notice	All statements, technical information and recommendations contained in this document are based upon tests or experience that 3M believes are reliable. However, many factors beyond 3M's control can affect the use and performance of a 3M product in a particular application, including the conditions under which the product is used and the time and environmental conditions in which the product is expected to perform. Since these factors are uniquely within the user's knowledge and control, it is essential that the user evaluate the 3M product to determine whether it is fit for a particular purpose and suitable for the user's method or application. All questions of liability relating to this product are governed by the terms of the sale subject, where applicable, to the prevailing law.

Values presented have been determined by standard test methods and are average values not to be used for specification purposes. Our recommendations on the use of our products are based on tests believed to be reliable but we would ask that you conduct your own tests to determine their suitability for your applications. This is because 3M cannot accept any responsibility or liability direct or consequential for loss or damage caused as a result of our recommendations.

3M is a trademark the 3M Company.

3M United Kingdom PLC
3M Centre, Cain Road Bracknell
Berkshire, RG12 8HT
0870 60 800 50

3M Ireland Ltd
The Iveagh Building The Park,
Carrickmines Dublin 18
00353 (01) 280 3555

Vinyl Tape

471 • 4712 (Linered)

Technical Data **February, 2011**

Product Description

3M™ Vinyl Tape 471 and 4712 are a conformable colored (9 colors plus transparent) tapes made from vinyl backing with rubber adhesive. They are ideal for many lane and safety markings, color coding, abrasion protection, masking, sealing, splicing and other general purpose applications.

3M vinyl tape 4712 is a linered version of 3M vinyl tape 471 that may be used for die cutting or large area applications.

Product Construction

Product	Adhesive	Color	Standard Roll Length
3M™ Vinyl Tape 471	Rubber	Yellow, white, red, black, brown, green, orange, purple, blue and transparent	36 yds. (33 m)
3M™ Vinyl Tape 4712	Rubber	Yellow, white, red, black, brown, green, orange, purple, blue and transparent	36 yds. (33 m)

Typical Physical Properties

Note: The following technical information and data should be considered representative or typical only and should not be used for specification purposes.

		ASTM Test Method
Properties for all colors except transparent:		
Adhesion to Steel:	23 oz./in. width (25 N/100 mm)	D-3330
Tensile Strength at Break:	14 lbs./in. width (270 N/100 mm)	D-3759
Elongation at Break:	130%	D-3759
Backing Thickness:	4.1 mils (0.10 mm)	D-3652
Total Tape Thickness:	5.2 mils (0.14 mm)	D-3652
Liner Thickness: (3M™ Vinyl Tape 4712)	2.5 mils (0.6 mils)	D-3652
Temperature Use Range:	40° to 170°F (4° to 77°C)	
Low Leachable Halogen and Sulfur:	Passes	MIL-STD-2041D(SH)
Properties for transparent:		
Adhesion to Steel:	26 oz./in. width (28 N/100 mm)	D-3330
Tensile Strength at Break:	14 lbs./in. width (270 N/100 mm)	D-3759
Elongation at Break:	150%	D-3759
Backing Thickness:	4.1 mils (0.10 mm)	D-3652
Total Tape Thickness:	5.2 mils (0.14 mm)	D-3652
Liner Thickness: (3M™ Vinyl Tape 4712)	2.5 mils (0.6 mils)	D-3652
Temperature Use Range:	40° to 170°F (4° to 77°C)	

3M™ Vinyl Tape

471 • 4712 (Linered)

Features

- Pigmented backings maintain their vivid colors even when exposed to heavy abrasion.
- Can be sold to Commercial Item Description A-A-1689 Type I & II
- Conformability and dead stretch properties are ideal for taping, wrapping or sealing many curved, convex, or irregular surfaces.
- Rubber adhesive provides good adhesion to many surfaces for easier application and excellent holding strength.
- Sharp colors for color coding or marking systems, draw attention and help enhance plant safety.
- Clean removal from many surfaces which helps reduce clean-up and labor costs.
- Abrasion resistant and longer potential application life.
- Good solvent resistance for application protection and longer product life.
- 3M™ Vinyl Tape 4712 can be printed using the thermal printing process.

Application Ideas

- Excellent for many lane and safety marking applications. When used with an applicator like the M-77 dispenser, 3M™ Vinyl Tape 471 can be quickly applied to define storage and safety areas. The fact that 3M tape 471 tape is quickly and cleanly removed in most cases makes it a faster, more versatile and less costly option than painting. Using tape for lane marking instead of painting also eliminates the need to ventilate paint solvents from an open area.
- Because they have low leachable halogens and sulfur, 3M™ Vinyl Tapes 471 and 4712 can be used in corrosion sensitive applications like the nuclear and stainless steel industries.
- 3M tape 4712 is great for die cuts and large area masking.
- Printed 3M tape 4712 can extend the range of 3M tape 471 for color coding by allowing multiple colors or identification on one tape.
- 3M tapes 471 and 4712 stretch to seal canisters and other storage containers that require a tight seal.
- Vivid colors of the tapes make them ideal for color, coding and decorating.

Application Techniques

- Best results are attained when applied to a clean, dry surface at temperatures between 60° to 85°F (16° to 27°C).

Note: While 3M tapes 471 and 4712 resist many common solvents, they should not be exposed to ketones, chlorinated hydrocarbons and esters found in lacquer thinner, degreasers, paint strippers, etc., which may cause the backing to swell or curl.

3M™ Vinyl Tape

471 • 4712 (Linered)

Storage

Store under normal conditions of 60° to 80°F (16° to 27°C) and 40 to 60% R.H. in the original carton.

Shelf Life

To obtain best performance, use this product within 18 months from date of manufacture.

Technical Information

The technical information, recommendations and other statements contained in this document are based upon tests or experience that 3M believes are reliable, but the accuracy or completeness of such information is not guaranteed.

Product Use

Many factors beyond 3M's control and uniquely within user's knowledge and control can affect the use and performance of a 3M product in a particular application. Given the variety of factors that can affect the use and performance of a 3M product, user is solely responsible for evaluating the 3M product and determining whether it is fit for a particular purpose and suitable for user's method of application.

Warranty, Limited Remedy, and Disclaimer

Unless an additional warranty is specifically stated on the applicable 3M product packaging or product literature, 3M warrants that each 3M product meets the applicable 3M product specification at the time 3M ships the product. 3M MAKES NO OTHER WARRANTIES OR CONDITIONS, EXPRESS OR IMPLIED, INCLUDING, BUT NOT LIMITED TO, ANY IMPLIED WARRANTY OR CONDITION OF MERCHANTABILITY OR FITNESS FOR A PARTICULAR PURPOSE OR ANY IMPLIED WARRANTY OR CONDITION ARISING OUT OF A COURSE OF DEALING, CUSTOM OR USAGE OF TRADE. If the 3M product does not conform to this warranty, then the sole and exclusive remedy is, at 3M's option, replacement of the 3M product or refund of the purchase price.

Limitation of Liability

Except where prohibited by law, 3M will not be liable for any loss or damage arising from the 3M product, whether direct, indirect, special, incidental or consequential, regardless of the legal theory asserted, including warranty, contract, negligence or strict liability.

ISO 9001:2008

This Industrial Adhesives and Tapes Division product was manufactured under a 3M quality system registered to ISO 9001:2008 standards.

3M

Industrial Adhesives and Tapes Division
3M Center, Building 225-3S-06
St. Paul, MN 55144-1000
800-362-3550 • 877-369-2923 (Fax)
www.3M.com/industrial

Recycled Paper
40% pre-consumer
10% post-consumer

3M is a trademark of 3M Company.
Printed in U.S.A.
©3M 2011 70070944528 (2/11)

1350-1, 1350-2 Tape

Flame-Retardant Tape with Polyester Film and Acrylic Pressure-Sensitive Adhesive

Data Sheet

Product Description

3M™ 1350 Tape is an electrical insulating polyester film tape, which meets the flame-retardancy requirements of UL 510. It consists of materials that are represented in many UL Recognized Insulation Syatems and has a Ul 130˚C temperature rating. It also offers excellent flagging and solvent resistance; good wet grab; smooth, even unwind and is suitable for use on automated equipment.

- UL Recognized flame retardant
- UL Recognized Class 130˚C/CSA
- Excellent Flagging Resitant
- Printable
- Solvent resistant without thermosetting
- Excellent shelf life

Colors

3M 1350 Tape is available in yellow, white and black.

Applications

3M 1350 Tape is especially suited for applications such as wrapping coils, capacitors, wire harnesses, transformers, shaded pole motors and fractional horsepower motors.

UL and CSA Component Recognition

UL Recognized for use at temperature not exceeding 130˚C, flame retardant per UL Standard 510, UL File Number E17385, Product Category AOANZ2. Underwriters Laboratories (UL) Recognized products are evaluated for use as components of end-product equipment that is Listed or Classified by UL. To achieve Underwriters Laboratories Recognition, component construction must meet UL specifications and conditions of acceptability for proper and safe use of the component products, 3M Flame Retardant Tape with Polyester Film and Acrylic Pressure Sensitive Adhesive.

Typical Properties	1-mil Film	2-mil Film
Adhesive	Acrylic	Acrylic
Backing	Polyester Film	Polyester Film
Backing Thickness[1]	One mil (25 micron)	Two mils (50 micron)
Total Thickness[1]	2.5 mils / 0,063 mm	3.5 mils / 0,088 mm
Colors	Yellow, White, Black	Yellow, White, Black
Temperature Class	130˚C (266˚F)	130˚C (266˚F)
Dielectric Breakdown[1]	5500 Volts	7,000 Volts
Insulation Resistance[1] (megohms)	>1 x 10^6	>1 x 10^6
Breaking Strength[1]	25 lbs. / in (44 N/10mm)	50 lbs. / in(88N/10mm)
Elongation[1] (% at break)	100	110
Electrolytic Corrosion Factor[3]	1.0	1.0
Adhesion to Steel[1]	30 oz/in (3,3N/10mm)	30 oz/in (3,3N/10mm)
UL 510 Flame Retardant[2]	Yes	Yes
Printable	Yes	Yes

Note: Typical properties are not recommended for specification purposes. Product specifications will be provided upon request.

Footnote: 1 Test Method ASTM D 1000
2 UL-recognized for flame retardancy per UL510, Product Category OANZ2, File E17385
3 3M Test Method-Available on request

3M is a trademark of 3M

IMPORTANT NOTICE

Before using this product, you must evaluate it and determine if it is suitable for your intended application. You assume all risks and liability associated with such use.

Warranty; Limited Remedy; Limited Liability. This product will be free from defects in material and manufacture as of the date of purchase. **3M MAKES NO OTHER WARRANTIES INCLUDING, BUT NOT LIMITED TO, ANY IMPLIED WARRANTY OF MERCHANTABILITY OR FITNESS FOR A PARTICULAR PURPOSE.** If this product is defective within the warranty period stated above, your exclusive remedy shall be, at 3M's option, to replace or repair the 3M product or refund the purchase price of the 3M product. **Except where prohibited by law, 3M will not be liable for any loss or damage arising from this 3M product, whether direct, indirect, special, incidental or consequential regardless of the legal theory asserted.**

3M

Electrical Products Division

6801 River Place Blvd.
Austin, TX 78726-9000
http://www.3M.com/elpd/oem

Litho in USA.
© 3M IPC 2000 78-8124-4751-0-B

1436 Aluminium Foil Tape

Product Data Sheet

Updated : June 2000
Supersedes : July 1999

Product Description

An aluminium foil combined with a rubber adhesive and an easy release liner designed for holding and sealing on a variety of surfaces. 1436 meets low flammability rating according to DIN 4102B1.

Physical Properties
Not for specification purposes

Adhesive Type	Rubber
Backing	Soft Aluminium Foil
Liner	White Silicone Paper (Possible alternative : PE Film)
Shelf Life	12 months from date of despatch by 3M when stored in the original carton at 21°C (70°F) & 50 % Relative Humidity

Performance Characteristics
Not for specification purposes

Adhesion to Steel AFERA 4001	12 N/10mm	
Tensile Strength AFERA 4001	18 N/10mm	
Elongation at Break AFERA 4005	3.1 %	
Total Tape Thickness	0.075 mm	
Water Vapour Transmission Rate	<1.0 g/m² x 24 h	
Flammability Rating DIN 4102B1, Reference PA-111 2-216	B1	

Date : June 2000
1436 Aluminium Foil Tape

Additional Product Information

- Foil backing provides an excellent reflective surface for both heat and light
- Rubber adhesive bonds to many surfaces.
- Low water vapor transmission rate offers excellent sealing and patching performance.
- Best results obtained when applied to clean dry surfaces above 0 °C.
- Performance range –25 °C to +70 °C; short term +100 °C.

Storage

Store in a dry location, out of direct sunlight and away from all sources of heat. Ideal conditions are 20 °C and 50% relative humidity. Storage in roll form for more than 12 months is not recommended.

3M is a trademark of the 3M Company.

Values presented have been determined by standard test methods and are average values not to be used for specification purposes. Our recommendations on the use of our products are based on tests believed to be reliable but we would ask that you conduct your own tests to determine their suitability for your applications.
This is because 3M cannot accept any responsibility or liability direct or consequential for loss or damage caused as a result of our recommendations.

Tapes & Adhesives

© 3M United Kingdom PLC 1996

3M United Kingdom PLC
3M House,
28 Great Jackson Street,
Manchester,

Product Information :
Tel 0870 60 800 50
Fax 0870 60 700 99

3M Ireland
3M House, Adelphi Centre,
Upper Georges Street,
Dun Laoghaire,Co. Dublin,

Customer Service :
Tel (01) 280 3555
Fax (01) 280 3509

Bondplus Electrical Tapes

The Bondplus +- range of high performance electrical tapes feature high quality films and foils coated to precise coat-weights with silicone, acrylic and electrically conductive adhesives.

These tapes are suitable for the most demanding of applications within the electronics industries with a wide range of uses, suitable for die- cutting to precise tolerances for intricate surface protection and masking application.

HB 830,HB 830FL,HB 930, HB 833

High temperature masking, no adhesive residue. Masking terminals on PCB. Very High temperature resistance 250 °C surface protection applications. High temperature clamping, 200 °C, heat resistance, clean removable.

	HB 830	**HB 830FL**	**HB 930**	**HB 833**
Carrier	Polyimide	Polyimide	Polyimide	Polyimide
Adhesive	Silicone	Silicone	Silicone Double Sided	Silicone
Colour	Amber	Amber	Amber	Amber
Thickness Carrier	25	25	25	25
Thickness Total	70	70	100	40
Peel Adhesion (g/25mm)	700	700	600	40
Tensile Strength (kg/mm2)	≥ 7	≥ 7	≥ 7	≥ 7
Elongation %	≥ 50	≥ 50	≥ 50	≥ 50
Temperature Resistance °C	250 °C	250 °C	200 °C	250 °C
Dielectric Breakdown (kv) Electric Resistance (‰CM)			8	

Applications

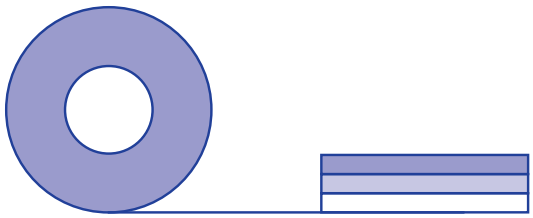
- Electrical insulation
- E.M.I. / R.F.I. shielding
- Fixing Static laminators
- Clamping at high temperatures
- Membrane switch and keypad applications
- Anti-static applications
- P.C.B. Masking
- Surface protection
- Splicing of silicone-coated films, papers etc.
- Bonding to high temperature surfaces.
- Bonding to low energy surfaces.
- Conductive connection & fixing
- Powder coating masking
- Metal process masking (electroplating)

Product:	**PVC 21**
Product group:	**Insulating Tapes**

General description

Nitto PVC 21 is a premium grade PVC tape coated with a rubber-based pressure sensitive adhesive. PVC 21 is accepted as a top quality general use vinyl tape.

Construction



- Rubber-based pressure sensitive adhesive
- Primer
- Plasticized PVC film

Characteristics

Nitto PVC 21 is a genuine “soft” tape. No fillers of any kind are used to guarantee excellent physical properties.

A good balance between adhesion strength, unwind force and film flexibility assures outstanding workability, high conformability and good sealing properties.

The tape has a good resistance against moisture, oils and solutions with acids and alkaline.
Nitto PVC 21 is a 190 micron thick insulating tape and is suitable for a wide range of applications.

The PVC tape is suited for outside use thanks to the good ageing and weatherability properties

Application

Nitto PVC 21 is a heavy duty general purpose tape which is ideal for wire and cable harnessing, color coding, duct sealing, corrosion preventing, holding and protection.

Features

- pure plasticized PVC (no fillers)
- non-sticky sides
- good weatherability
- good sealing properties
- high conformability
- excellent workability
- WEEE compliant (2002/96/CE)
- RoHS compliant (2002/95/CE)
- good moisture and chemical resistant

Properties

	Typical Value	Test Method
Total thickness	0.19 mm	IEC 60454-2 §4
Tensile strength LD*	220 N/10 mm² (section) 42 N/10 mm width	IEC 60454-2 §8
Elongation LD	250%	IEC 60454-2 §8
Adhesion to BA steel	1.92 N/10 mm	IEC 60454-2 §11 (Dwelling time 15 min.)
Adhesion to backing		
at room temperature	1.75 N/10 mm	IEC 60454-2 §11
at low temperature (-10°C)	4.50 N/10 mm	IEC 60454-2 §12
Electrical strength		
at room temperature	11.0 kV	IEC 60454-2 §17
after humid conditioning	10.7 kV	IEC 60454-2 §18
Electrolytic corrosion (23°C)	1x1012 Ohm/25mm width	IEC 60454-2 §7.6 (IEC 60167)
Low temperature properties (-10°C)	no cracking no unwinding, no breakdown	IEC 60454-2 §9
Penetration at elevated temperature	68 °C	IEC 60454-2 §10
Shear adhesion to backing after water immersion	33.0 N	IEC 60454-2 §13
Flammability	Flammable	IEC 60454-2 §19
Max. Operating Temperature	+90 °C	IEC 60454-2 §21

* LD = Length Direction

Warranty

The product is guaranteed to be free from defect in material and workmanship at the time of delivery and will be suitable for use for a period of 12 months thereafter, subject to the conditions set out herein.

Availability

Colours: transparent, black, blue, green, red, grey, yellow, white, brown, isogene-grey, light blue, orange, yellow-green
Widths: 12, 15, 19, 25, 30, 38, 50 and 100 mm Lengths: 10 and 20 m
Core diameter: 31.5 mm
* Please contact us for other dimensions and/or colors

Application guidelines

- The tape should be applied on a clean and dry surface.
- Apply the tape with a moderate tension and with an overlap of 50%.

If you require additional information on technical properties and application as well as product sampling or testing, please contact your local Nitto Europe sales office.

General conditions of use and precautions:
The properties of the product might be adversely affected by various elements such as composition, condition and surface of and impurities in or on the substrate, temperature and humidity during storage, the surrounding environment at and after application and time of exterior use. When the product is used in combination with another material or process, the user shall assure the compatibility of the product in such combination and whether this combination results in the expected performance. The same principle applies in the event of product use in extreme conditions or circumstances, whether at or after the moment of application, including extended exposure to sunlight or extreme temperatures and pressure.

Packaging, transport and storage:
During transport and storage the product should always be protected against direct sunlight and extremes in temperature and humidity and contained in its original packaging. Once removed from its packaging, it should be promptly applied and remain shielded from direct sunlight and extreme temperature as well as protected against dust and other impurities.

Liability:
Except for its wilful misconduct, Nitto Europe's liability shall be limited to a replacement, a reimbursement or an additional delivery of the product, and shall not exceed the purchase price of the products. In no event shall Nitto be liable in respect of any indirect or consequential damages, including loss of profits.
The above limitations of liability shall equally apply if Nitto Europe has assisted in any manner with the selection, treatment or application of the product.

Product information:
This datasheet provides a general description of the product properties and application scope. Full technical details in connection with this product are presented in the customer product specification, which is available upon request.

The information reflected in this datasheet is subject to change and the product described herein may be modified or discontinued without notice.

Edition: September 2013
Code: DS/04.08/B PVC 21 ENG
This datasheet replaces all previous versions

Nitto Europe NV has obtained following certificates:

- ISO 9001
- ISO 14001
- ISO/TS 16949

Please check our website for applicable scope

For your local Nitto Europe sales office, please visit our web site:
www.nitto.com

Copyright © 2013 NITTO EUROPE NV. All rights reserved.

Effect of Different Tape Overlays on the Surface Integrity and Mechanical Properties of 7075 Aluminum Alloy by Laser Shock Peening

M. Mistry[1, 2] and C. Polese [1, 2]

[1]*School of Mechanical, Aeronautical and Industrial Engineering, University of the Witwatersrand, South Africa*
[2]*DSI-NRF Centre of Excellence in Strong Materials, University of the Witwatersrand, South Africa*

e-mail address: Claudia.Polese@wits.ac.za

The Laser Shock Peening (LSP) treatment introduces beneficial compressive residual stresses by irradiating laser pulses on to the surface of metallic alloys under an aqueous environment. [1] The process however, modifies the surface integrity which in certain applications is not desired, thus there is a need to protect the surface of material when conducting LSP. [1] LSP can be conducted with and without an ablative coating; the ablative coating applied to the surface of the material has two roles: to protect to surface from thermal effects and to enhance the formation of plasma. [2] The use of an ablative coating creates a pure mechanical effect in the material with no thermal effects. [2] The current activity was aimed at investigating the effect of the LSP process on 7075 aluminium alloy by using different adhesive tape ablative coatings. The AA7075 samples were coated with the tape overlays and processed with four different laser Power Intensities (PI) of 1.5 GW/cm^2, 2.0 GW/cm^2, 3.0 GW/cm^2 and 4.5 GW/cm^2, with a fixed laser spot size of 1mm in diameter using a raster scanning strategy. A total of twelve different types of ablative tape overlays were selected for LSP processing, these commercial tapes were selected with different properties, adhesive layer and backing material such as Vinyl, Polyester, Polymide, Copper and Aluminium Tape. The surface integrity of the processed samples was studied and benchmarked against LSP without coating. The surface roughness for non-metallic tapes was found to be lower when compared to metallic tape coatings as shown in Figure 1a. An interesting point regarding the relationship between the ablative thickness and surface roughness was found when using non-metallic tapes with the same properties but different thicknesses. It was found that an increase in ablative thickness resulted in lower surface roughness values when using constant LSP parameters as depicted in Figure 1b.

Currently the research activity is in its final phase, the residual stresses introduced by LSP is being measured using laboratory X-ray diffraction (XRD) and by using Incremental Hole Drilling (IHD). The microhardness and the microstructure of the cross section will be investigated in detail. The results obtained from these experiments will aid in investigating the mechanical properties of the alloy and in providing an optimised solution using ablative media for industry.

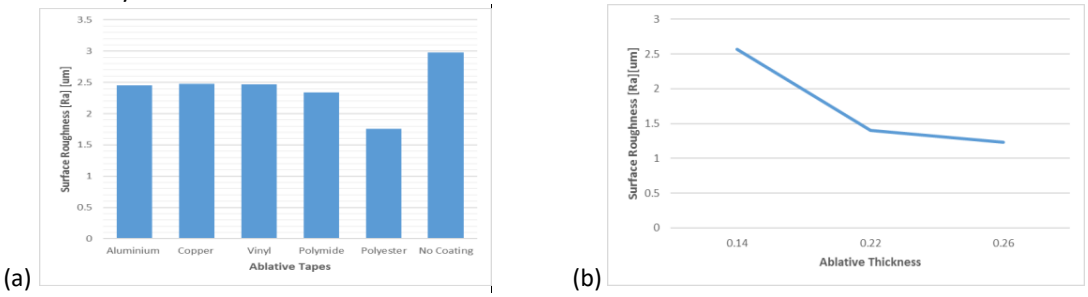


Fig. 1. Surface Roughness Variations for AA7075. (a) Surface Roughness vs Ablative Thickness. (b) Surface Roughness vs Ablative Tapes

[1] A. Azhari et al. "A review on the application of peening processes for surface treatment ", IOP Conference Series: Material Science and Engineering, Vol. 114, no. 1 (2016).
[2] A. Telang et al. "Effect of Different Ablative Overlays on Residual Stresses Introduced in IN718 SPF by Laser Shock Peening", International Journal of Peening Science and Technology, Vol. 1, pp. 75–86 (2018).